

AD_____

Award Number: DAMD17-04-1-0365

TITLE: Mechanism for prenatal LPS-induced DA neuron loss

PRINCIPAL INVESTIGATOR: Paul M. Carvey, Ph.D.

CONTRACTING ORGANIZATION: Rush University Medical Center
Chicago, IL 60612

REPORT DATE: September 2006

TYPE OF REPORT: Final

PREPARED FOR: U.S. Army Medical Research and Materiel Command
Fort Detrick, Maryland 21702-5012

DISTRIBUTION STATEMENT: Approved for Public Release;
Distribution Unlimited

The views, opinions and/or findings contained in this report are those of the author(s) and should not be construed as an official Department of the Army position, policy or decision unless so designated by other documentation.

REPORT DOCUMENTATION PAGE				<i>Form Approved</i> OMB No. 0704-0188	
Public reporting burden for this collection of information is estimated to average 1 hour per response, including the time for reviewing instructions, searching existing data sources, gathering and maintaining the data needed, and completing and reviewing this collection of information. Send comments regarding this burden estimate or any other aspect of this collection of information, including suggestions for reducing this burden to Department of Defense, Washington Headquarters Services, Directorate for Information Operations and Reports (0704-0188), 1215 Jefferson Davis Highway, Suite 1204, Arlington, VA 22202-4302. Respondents should be aware that notwithstanding any other provision of law, no person shall be subject to any penalty for failing to comply with a collection of information if it does not display a currently valid OMB control number. PLEASE DO NOT RETURN YOUR FORM TO THE ABOVE ADDRESS.					
1. REPORT DATE (DD-MM-YYYY) 01/09/06		2. REPORT TYPE Final		3. DATES COVERED (From - To) 1 Mar 2004 – 31 Aug 2006	
4. TITLE AND SUBTITLE Mechanism for prenatal LPS-induced DA neuron loss				5a. CONTRACT NUMBER	
				5b. GRANT NUMBER DAMD17-04-1-0365	
				5c. PROGRAM ELEMENT NUMBER	
6. AUTHOR(S) Paul M. Carvey, Ph.D. E-Mail: pcarvey@rush.edu				5d. PROJECT NUMBER	
				5e. TASK NUMBER	
				5f. WORK UNIT NUMBER	
7. PERFORMING ORGANIZATION NAME(S) AND ADDRESS(ES) Rush University Medical Center Chicago, IL 60612				8. PERFORMING ORGANIZATION REPORT NUMBER	
9. SPONSORING / MONITORING AGENCY NAME(S) AND ADDRESS(ES) U.S. Army Medical Research and Materiel Command Fort Detrick, Maryland 21702-5012				10. SPONSOR/MONITOR'S ACRONYM(S)	
				11. SPONSOR/MONITOR'S REPORT NUMBER(S)	
12. DISTRIBUTION / AVAILABILITY STATEMENT Approved for Public Release; Distribution Unlimited					
13. SUPPLEMENTARY NOTES					
14. ABSTRACT: (familial Parkinson's disease). The etiologies of the majority of patients are still unknown. Recent advance in our laboratories suggests that prenatal exposure to bacterial toxin, lipopolysaccharide (LPS), could be an important etiology for some PD patients. A key finding is that animals exposed to LPS prenatally display fewer than normal number of dopamine (DA) neuron in the midbrain, the hallmark pathology in human patients. The mechanism for such DA neuron loss is not known. The preliminary data suggested that prenatal LPS may interfere DA neuron precursor cells (progenitor cells) migration to substantia nigra or DA neuron process outgrowth and therefore reduce the number of DA neurons in the midbrain. We proposed to use both in vivo and in vitro approaches to investigate these possibilities. Significant progress has been made in the last eleven months. Implementation of this proposal has resulted in three major findings: 1. Prenatal bacterial LPS induce loss of BrdU positive cells in the midbrain. 2. The toxicity of prenatal LPS requires removal of mitotic signal (s) to the dividing progenitor (stem) cells. 3. Prenatal LPS reduced dopamine neuron process total length that prevents dopamine neurons to reach trophic-rich striatal target tissue, a positive mechanism underlying the dopamine neuron loss in the prenatal LPS model.					
15. SUBJECT TERMS LPS, prenatal, Parkinson's disease, cytokine, dopamine, etiology					
16. SECURITY CLASSIFICATION OF:			17. LIMITATION OF ABSTRACT	18. NUMBER OF PAGES	19a. NAME OF RESPONSIBLE PERSON
a. REPORT U	b. ABSTRACT U	c. THIS PAGE U			USAMRMC
			UU	142	19b. TELEPHONE NUMBER (include area code)

Table of Contents

Cover.....	1
SF 298.....	2
Table of Contents.....	3
Introduction.....	4 - 5
Body.....	6 - 16
Key Research Accomplishments.....	17
Reportable Outcomes.....	18 - 19
Conclusions.....	19
References.....	20
Appendices..... with 10 articles	21 - 142

Introduction:

The cause of non-familial Parkinson's disease (PD) is currently unknown, although numerous environmental toxins have been implicated. To date, all studies evaluating the role of environmental toxins in PD have assumed exposure to toxin during adult life. In contrast, studies in our laboratory suggest that prenatal exposure may be just as important. We have shown that treating gravid female rats with the bacteriotoxin lipopolysaccharide (LPS) produces offspring born with fewer dopamine (DA) neurons. This DA neuron reduction persists throughout adulthood and progresses with age. These animals exhibit reductions in striatal DA, increased DA activity, increases in pro-inflammatory cytokines (that remain elevated through 16 months), increased levels of oxidized proteins, and the development of α -synuclein aggregates. We have proposed, the pre-natal LPS-exposed rat, as a new animal model of PD. The relevance of this model to PD is supported by the fact that LPS is known to enter the human chorioamniotic environment of the fetus in women with bacterial vaginosis (BV). BV increases pro-inflammatory cytokines, including tumor necrosis factor (TNF α) and interleukin 1 beta (IL-1 β), and induces several teratogenic effects. Unfortunately, the mechanisms responsible for the LPS-induced changes in the DA system are unknown. Preliminary *in vivo* studies using BrdU (marker incorporated into dividing cells) suggest that LPS may reduce the mitotic activity in the ventricular area of the mesencephalon, which could lead to reduced migration of DA progenitors into the nigra. *In vitro* studies, using our newly developed 2-dimensional (2D) micro-island culture system, which allows us to evaluate the very early stages of development of the nigro-striatal pathway, suggest that LPS may interfere with the extension of DA processes to the trophic-rich striatum. This could lead to loss of DA neurons due to inadequate trophic support. We will evaluate these two possibilities in the following specific aim.

Specific Aim: Rat fetal brains exposed to LPS at E10.5 will have reduced numbers of DA neurons in their mesencephalons due to reduced progenitor cell activity or inhibited process extension. **Experimental series 1:** Gravid rats will be injected (i.p.) with 10,000 EU/kg LPS or Hank's Balanced Salt Solution (HBSS) at E10.5. The animals will also receive BrdU (70 mg/kg) at E10.5 and E11.0 to label dividing cells in the midbrain. The fetuses will be harvested at E18.5 and the brains assessed for the number of TH immuno-reactive (THir)/BrdU cells, NeuNir (neuronal marker)/BrdU cells, GFAPir (astrocyte marker) and Ox-42ir cells (microglia marker) in the substantia nigra. The density of the THir staining in the striatum and medial forebrain bundle (MFB) will be used as an index of process extension. If the LPS-induced DA neuron loss is the result of reduced development/conversion of progenitor cells to DA neurons, we should then see reduced numbers of THir/BrdU double-labeled cells. However, if alterations in process extension are responsible, we would observe reduced striatal THir density with normal cell counts in the nigra. **Experimental Series 2:** Gravid female rats will be treated with BrdU as above. At E10.5, the abdomen will be reflected and LPS (800 EUs) will be injected into each amniotic sac in one uterine horn (HBSS in the other). The abdomen will be sutured closed. At E14.5 the rostral mesencephalic tegmentums (nigra) and lateral ganglionic eminences (striata) will be harvested from each uterine horn, pooled, and assessed using 2D micro-island cultures. Various combinations of the LPS exposed (affected) and unaffected nigras and striata will be co-cultured together and immunostained after 96 hrs. Evaluation of these combinations should reveal which tissue is more affected (nigra or striatum). Other pups from this treatment protocol will be taken by C-section at E21, and cross fostered until sacrificed at P5 or P15 (4 days after the 2 phases of apoptotic culling, respectively). These animals will be assessed for THir/BrdU

and NeuNir/BrdU cell counts, striatal DA biochemistry (HPLC) and GSH/GSSG, striatal and mesencephalic trophic activity, and striatal TH density and cytokine protein levels (ELISA). These studies should reveal whether progenitor cells convert normally into DA neurons or alternatively, do these cells die off during development because of inadequate access to trophic support, and therefore as a result undergo excess culling at P1 or P15.

Reason for delays in completing this project:

There are two fundamental reasons why we have been delayed in completing this work. First, when we discovered the prenatal LPS model several years ago, we submitted several proposals like any research group would and fortunately four of the grants funded successively (this proposal being the 4th). We looked at the workload, which appeared daunting, but we felt as though we could complete the work on time. We were able to accomplish all of the specific aims of all the proposals, but were delayed in completing two of the proposals (this being one of them). The second reason this work has been delayed is that my primary co-investigator (Dr. Ling) was offered an associate directorship in an overseas program. His departure in January was further complicated by illness that markedly curtailed his productivity. We have proceeded in completing the BrdU counting assessments here with limited staff. Thus, we were delayed approximately 9 months in completing the studies.

Specific Aim 1:

In the first specific aim, we planned to assess the supposition that prenatal LPS interferes with progenitor cells destined to become DA neurons [either through interfering with mitotic activity in the developing ventricular zone or their subsequent migration to the substantia nigra (SN)]. The concept was that if LPS interfered with the development of DA neurons the result would be fewer DA neurons in the SN suggesting a very early event. Therefore we planned to pulse the proliferating cells with bromodeoxyuridine (BrdU: a nucleotide substitution that replaces thymidine with uridine in the DNA structure of dividing cells) when developmentally the DA cells are at their peak, and follow their migration into the SN. We would then evaluate cells, throughout the horizontal sections of the brain, labeled for BrdU, THir, and double-labeled BrdU/THir cells. These studies have been completed.

Methods:

Gravid Sprague-Dawley rats (n=13) were used in this study (Zivic Miller, Zeneopolis, PA). Rats were divided into two conditions, those that received LPS and BrdU and those that received saline and BrdU. Gravid rats at E10.5 were injected (i.p.) with either 10,000 EU of LPS (1 mg/ml = 1×10^6 EU) (n=8) or saline (n=5). Both treatment groups were then administered 70 mg/kg of BrdU (i.p) two hours later, at E11.5 and again at E12. On E18, gravid rats were anesthetized with pentobarbital (60mg/kg) and a careful incision was made from the anterior to posterior of the abdomen to expose the lateral uterus sacs containing the fetuses. The fetuses were removed and the whole brain of the fetuses were quickly removed, placed immediately in cold 4% paraformaldehyde for post-fixation, then stored at 4°C for 48 hours to ensure complete penetration, and then stored in 20% sucrose in 0.1M PO₄ buffer solution at 4°C for 5 days. Brains were then sectioned on a sliding microtome at 60µm on a horizontal plane. Free-floating sections were stored in cryoprotectant (0.05 M PBS with 30% sucrose and 30% ethylene glycol) at 4°C until processed for immunohistochemistry.

While the brains of all fetuses were taken, only one fetus' brain from each gravid rat was used for each dependent measure. During this study, one dam in the saline/BrdU condition was not pregnant and one dam in the LPS/BrdU group at E18 had only 3 fetuses that were unusually small and the others appeared to have been reabsorbed, therefore they were not used. This left 7 fetus brains for the LPS/BrdU condition and 4 in the saline/BrdU condition. In addition, we encountered the anticipated challenges associated with sectioning the fetal brains (very difficult to cut because of its high water content). After experimenting with a number of different techniques on practice brains, we settled on frozen brains (on dry ice) and sliced horizontally on a cold sliding microtome at 60 µm thickness. Normally, we have the luxury of multiple series through a structure, but because of the reduced size of the brain, we had to commit to only three series so that we could perform the BrdU, THir, and BrdU-THir immunohistochemistry.

Immunohistochemistry

The entire sectioned brains from fetuses in both conditions (LPS/BrdU and saline/BrdU) were processed for either tyrosine hydroxylase (TH, a DA neuron marker), bromodeoxyuridine (BrdU: a nucleotide substitution that replaces thymidine with uridine in the DNA structure of dividing cells) or THir/BrdU double labeled for immunohistochemistry. Briefly, for anti-THir labeling, sections were washed (3 x 10 mins) in 0.1M PBS buffer (pH 7.4), incubated in endogenous blocking solution to block peroxidase activity (1% hydrogen peroxide in methanol)

for 10 to 15 mins, and then incubated in 10% serum from host secondary antibody (goat) with 0.03% Triton X-100 in 0.1M PBS for 1 hour. Sections were then incubated for 24 hours at 4°C with 2% goat serum and 0.03 % Triton X-100 in 0.1M PBS with the primary antibody to TH (rabbit:anti-mouse, Chemicon, 1:1,000 dilution). After 24 hours, the sections were washed in 0.1M PBS (3 x 10 mins) and incubated for 1 hour with biotinylated secondary antibody (goat:anti-rabbit, Vector Laboratories, 1:200), 0.03 % Triton X-100 in 0.1M PBS. The antibody complex was amplified using an avidin-biotin kit (ABC-Elite kit; Vector) and visualized with 3,3' -diaminobenzidine (DAB; ImmunoPure Metal enhanced DAB; Pierce, Rockford, IL) with and without nickel enhancement. For control sections, the primary antibody was omitted. Once sections were mounted onto slides and rinsed in 0.1 M PBS, pH 7.4, they were cover-slipped with 95% glycerol and examined by standard epi-illumination microscopy.

In processing sections for BrdU labeling, the first part of the methods used are unique for anti-BrdU labeling. Briefly, sections were washed in 0.1M PBS (pH 7.4; 3 x 10 mins) and incubated in 2N HCl (2 x 15 mins), which is used to denature the DNA structure of the labeled cells. Tissue sections were then neutralized in 0.1M borate buffer (2 x 15 mins), after which sections are washed (3 x 10 mins, 0.1M PBS, pH 7.4). From this point forward, the methods are identical to those used for THir staining, except the primary antibody is BrdU (mouse:anti-BrdU, Ab8039-100 lot 118010; from Abcam; at 1:50).

Stereological assessment of cell counts

The estimation of the total number of THir cells, BrdU cells, and THir/BrdU labeled cells throughout the entire brain was performed using the computerized optical dissector method (MicroBrightField software) as described previously (Vu et al., 2000). Briefly, a 10X objective lens was used to define the contour around the area of interest and the 100X oil immerge objective lens was used for the cell count assessments. The total number (N) of THir, BrdU or THir/BrdU labeled cells in each area of interest from each fetus brain was estimated using the formula $N = NV \cdot VAI$, where NV is the numerical density and VAI is the volume of the area of interest, as determined by Cavalieri's principle.

Descriptions of Figures

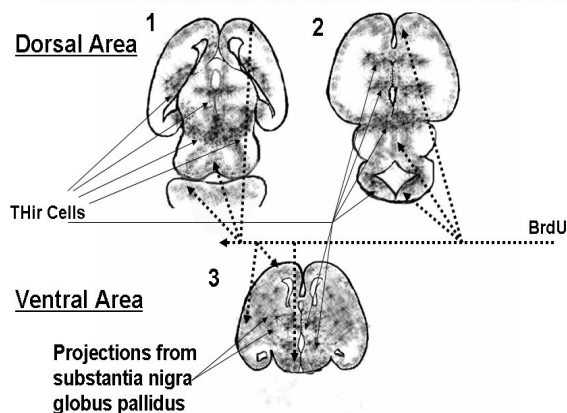
The diagrams (Figures 1 & 2) of the horizontal plane depict the level of brain sections that represent areas where cell counts were performed, along with where the majority of THir and BrdU cells were located. To assist as a reference tool, these diagrams correspond to the graphs in that the numbering on the axis of the graph matches those on the diagrams with the most dorsal section equaling number 1 on the graph, followed by number 2, and the most ventral section which is number 3. These numbers have been included on the actual pictures to further assist in establishing the photographed area.

Results SAI

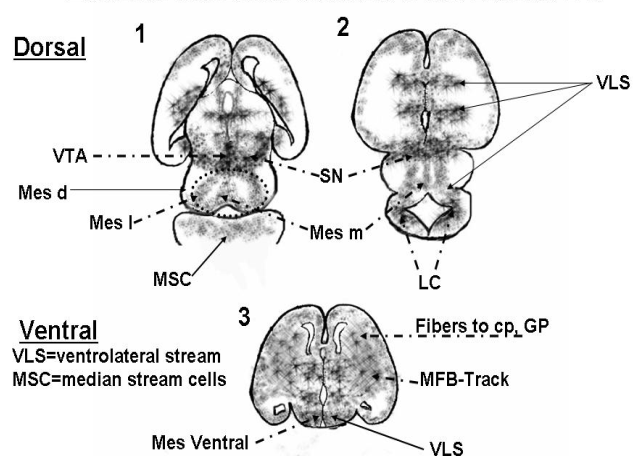
The study has been completed as planned. The diagrams of the brain sections are included to assist in identifying the sections that were examined/counted along with labels identifying the areas that correspond to this discussion (Figures 1 & 2). One of the major difficulties encountered in this study was identifying where the origin of DA cells of the SN emerge from (this was recognized as a caveat in the original application and has not changed). The origin of DA progenitor cells is believed to be the isthmus and mesencephalic flexure. To

the best of our knowledge, this very restricted area of the developing neural tube consists of the midbrain directly anterior to the isthmus, directly posterior to the mesencephalic tegmentum, and posterior to the ventricular and subventricular zones from which DA cells migrate to form the SN and VTA (Luskin, 1993*; Menezes *et al.*, 1995; Erlandsson, 2003). Therefore, the first DA progenitor cells are observed at the most ventral rim of the neuroepithelium, lining up along the mesencephalic flexure of the ventral mesencephalon and migrating rostral and ventrally (Figure 1 and 2). The establishment of neuroepithelial centers in the neural tube is required for two adjacent, but separate cell populations. The isthmus separates the fore- and midbrain from the hindbrain anatomically and molecularly and is believed to be the origin of the DA progenitor cells (Figure 5, c – dotted line). Receiving signals from the floor plate, the isthmus divides the midbrain and the diencephalon into dorsal and ventral regions, in which each area has their own developmental objective. Although for the adult brain the progenitor/stem cells from the subventricular zone migrate through the rostral migratory stream (RMS), this is not so for the developing brain. Originally, one primary migratory pathway for DA cells was believed to exist, which occurred in two distinct waves with the first set of cells migrating from the ventricular zone and the second from the subventricular zone (Monk *et al.*, 2001). Thus, progenitors of DA cells would migrate from the mesencephalic flexure, medially and rostrally, through the medial part of the raphe, to the subventricular area, and too the ventral mesencephalic tegmentum. However, by the time DA cells of the SN reached the age of E18 there appears to be two migratory streams that are theorized to compose the developing SN cells, one which has just been discussed and the other is called the ventrolateral stream (VLS) (Marchand & Poirier, 1983). This stream of cells originates more laterally along the basal plate and at the same level of the MSC. The VLS follows the radial course through the tegmentum of the isthmus and downwards to the ventrolateral surface of the cephalic flexure. By E18 the cells within the ventral mesencephalon acquire a more adult morphology. While cells remain ventrolaterally to the surface of the mesencephalon, extend more rostrally, and the RMS of cells moves more rostrally and laterally towards the lateral sides (wings) of the SN (Figures 1 & 2). This pattern of migration was apparent in the labeled sections we observed (Figure 5) and illustrated (Figure 1).

Figure 1
Horizontal Sections of Rat Brain at E18 THir and BrdU



Labels of Horizontal Sections of Rat Brain at E18

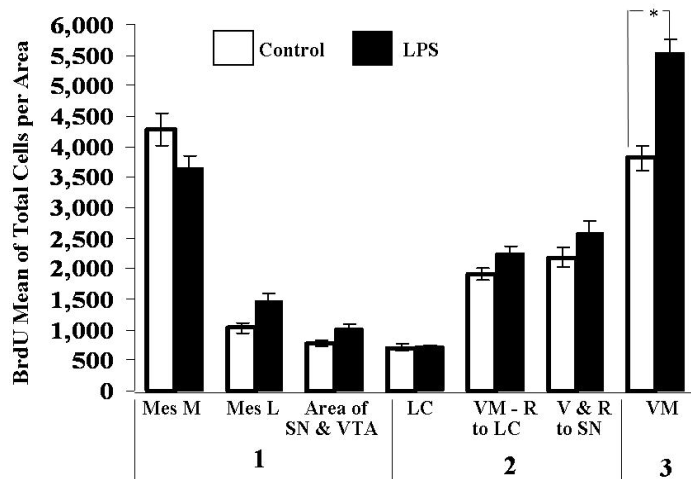


MFB= medial forebrain bundle pathway, cp= caudatus putamen, GP= Globus pallidus
 Mes l= Mesencephalon lateral, Mes m= Mes medial, Mes d= Mes LC= Locus ceruleus,
 AVT= Area ventralis tegmenti, SN= Substantia nigra, SNL=SN lateral, SNv= SN ventral

The BrdU labeled cells showed no significant differences between LPS and the saline condition except in the ventral mesencephalon (VM) area. This was the only area of BrdU staining that showed significantly more LPS BrdU labeled cells (Figures 2a & 5). Given that this region (VM), may be the primary migratory channel for DA cells this would seem within reason. One of the major limitations of this approach is the inability to know whether these cells will eventually become DA neurons and it is therefore difficult for us to draw conclusions about the BrdU labeled cells. However, staying with our original hypothesis, we would have expected to see a decrease in the number of LPS – BrdU cells. However we observed an increased trend in the LPS-BrdU cells in the dorsal medial and lateral mesencephalon, plus the region of the SN and VTA (Figure 2a).

Figure 2a.

BrdU Labeled Cells at E18 Prenatal Rat Brain

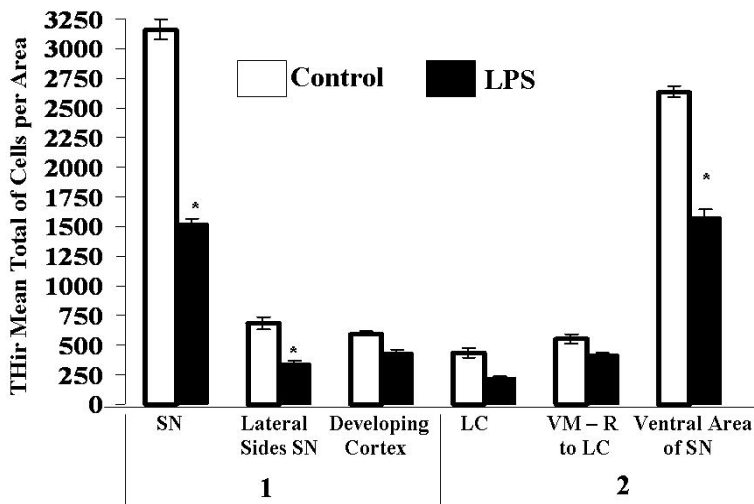


SN=Substantia Nigra, LC=Locus Coeruleus, Mes=Mesencephalon, VM=Ventral Mesencephalon, R=Rostral, D=Dorsal, L=Lateral, M=medial, and V=Ventral

The THir cell counts, were as expected, reduced 32 to 40% in the LPS condition compared to the saline control condition (Figure 2b), which is well within the limits that we obtained previously studying early postnatal animals. The SN and the more ventral area of the SN exhibited significantly fewer TH cells compared to their saline condition counterpart (Figure 4). This reduction is consistent with our earlier published work where we demonstrated that mesencephalic cultures established from fetuses in which the pregnant rat was exposed to LPS at E10.5 had reduced numbers of TH cells relative to cultures established from unexposed-LPS pregnant rats at E10.5.

Figure 2b.

THir Labeled Cells at E18 Prenatal Rat Brain



In a previous study, we also performed THir cell counts of the SN from fetuses exposed to LPS or saline over time. These results replicated the findings from this study such that the THir cells were reduced in fetuses from mothers exposed to LPS relative to the THir cell counts observed in fetuses from saline treated mothers (in regards to the reduction of

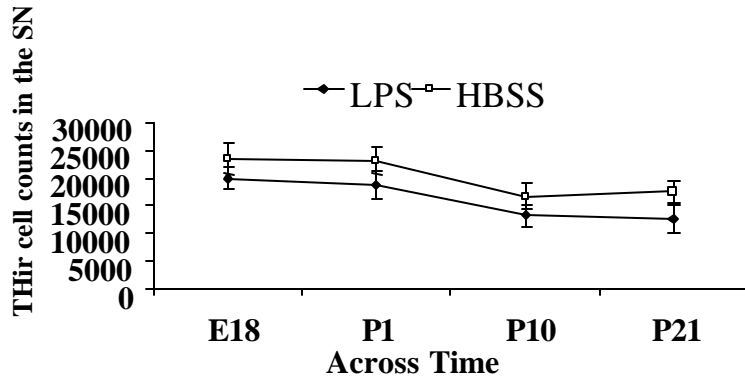
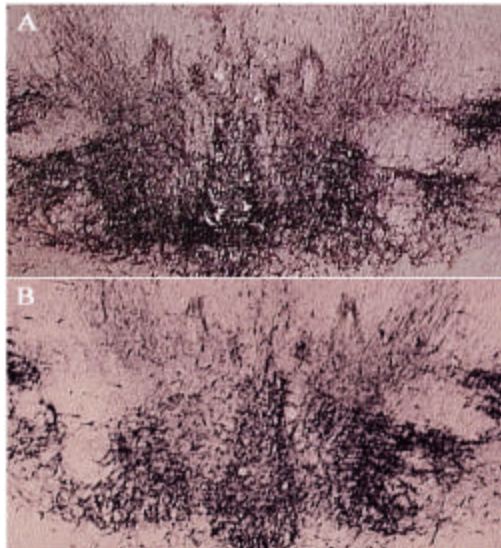
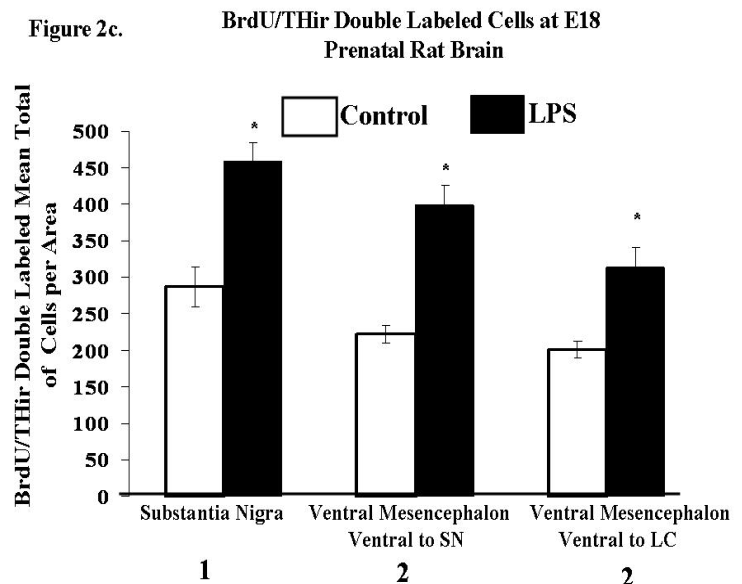


Figure 3 THir cell counts in the SN at E18, P1, P10, and P21. Prenatal LPS exposure produced a significant decrease of THir cell counts at each time point ($P < 0.05$). In addition, THir cell counts were significantly decreased between P10 and P1

occur in rats between E21 and P3. Given that the reductions in both the LPS and the saline exposed animals were parallel in the amount of THir cells decreased during the culling phase, this suggests that the reduction in THir cell counts seen in the young animals (non culling phase time) is not the consequence of changes in the apoptotic culling. Rather, apoptotic culling proceeds normally; it is just that there are fewer cells overall present. As a whole, the data is consistent with the notion that THir cell counts are already

THir cells, we have observed this phenomenon in more than 10 studies). Moreover, when we examined the THir cells over time, it was clear that the reductions in THir cell counts seen at E18 were still present at P1, P10, and P21 and the differences between the LPS exposed and saline exposed fetuses were parallel (Figure 3). Within this data set, there was also a significant reduction in THir cell counts between P1 and P10 coinciding with the major apoptotic culling phase known to

Figure 2c.



reduced at a very early stage of development probably between E11 and E14, and these cells undergo normal apoptotic culling thereafter.

Figure 4. Microphotographs representing sections of the SN on a horizontal plane. Both sections are immune labeled with TH (dark black) and with BrdU (brown to red). (A) Shows a full and vital nigra from the prenatal saline control condition, in which health DA neurons are present with extended processes. (B) Pregnant mothers were treated with LPS and the SN from fetus at E18 had significantly fewer THir cells with broken and degenerating processes. (5x). The SN sections here correspond to the dorsal level on the brain diagrams.

Overall, the results of the double-labeled immunohistochemistry indicated an increase in BrdU/THir positive cells, from fetuses exposed to LPS at E10.5 and counted at E18 (Figure 2c.). The substantia nigra had the highest number of double-labeled cells (Figures 2c & 1-tissue section 1), followed by a more ventral area of SN (Figures 2c & 1-tissue section 2) and then by the VM area around the LC and 4th ventricle (Figures 2c & 1-tissue section 2). The BrdU/THir positive cells were also present in control brains indicating normal progression of DA neurons. We are assuming that these BrdU/TH cells will become cells belonging to either the SN or LC, depending on the anatomical location and their microenvironment. This is especially true because the floor plate and the isthmus, by E9 in the rat fetus, have released both sonic hedgehog (SHH) and fibroblast growth factor-8 (FGF8), which are required proteins in the development of DA neurons (Hynes et al., 1995b; Hynes and Rosenthal, 1999; Lin and Rosenthal, 2003). While the floor plate spans the rostral to caudal neuroaxis and releases FGF-8, the isthmus will release the majority of FGF-8 to the midbrain and hindbrain by E9 with only scant amounts released thereafter. This supports the supposition that the majority of the DA phenotypic cells are induced by or at E10.5.

Additionally, even though the extent of double-labeled BrdU/TH cells is not uniform across sections of brains, there is congruence within a given section of the brains in the number of appropriate cells present. For example, the area within the brain that should have decreased numbers of THir cells, because of the prenatal LPS exposure, are reduced compared to the same area in the saline control condition. The reverse of this also holds true. Therefore, we believe the results are accurate and reflect that which is occurring in the developing SN of the brain when the pregnant mother is exposed to LPS at E10.5.

The most valid means of ascertaining alterations in TH cells or progenitor cells proliferation or migration as a result of prenatal LPS exposure was to examine the BrdU/THir double-labeled cells (Figures 2c, 4 & 5). At the time of BrdU, administration (E10.5-E12) cells are in a state of active proliferation under normal conditions. However, if the LPS caused a decrease in cell proliferation, migration, or the TH phenotype, these factors would have been apparent at E18 when the brains were harvested.

While there was a significant decrease in THir cells of the SN (Figures 2b & 4), this was not so for the BrdU cells overall (Figure 2a). These cells, attributed to their morphology, are more than likely progenitor cells with small round bodies and no processes. Based on our original

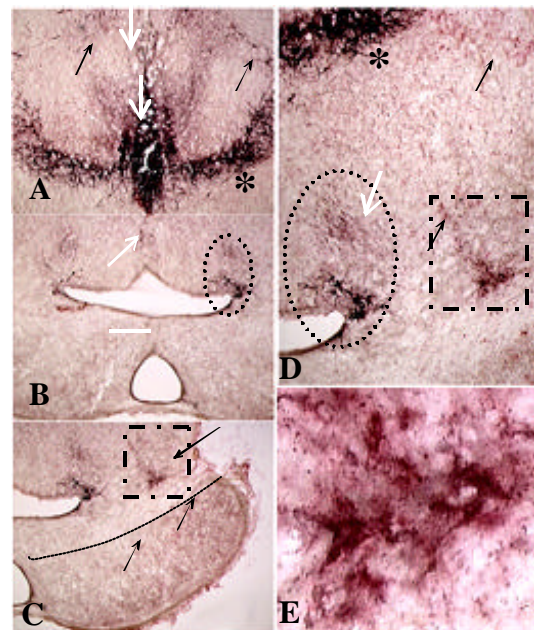


Figure 5. Microphotograph of double-labeled BrdU/THir horizontal section of LPS brain. (A,B,C) Represents a dorsal section showing the SN, LC, 4th ventricle and the cerebral aqueduct (5x). D is the same area as A-C, but taken at 10x. (E) Shows an aggregation of proliferating BrdU labeled cells (40x), which was consistently present in sections at this level in both conditions. These cells are identified on the photo by the black square. The circle highlights the LC THir cells. The MSC is demarcated by the white arrows and the black arrows indicate the VLS. In C the dotted line identifies the isthmus fovea.

hypothesis, we assumed that the BrdU/THir cells would be reduced suggesting that there was a deficiency in proliferation and or migration, because of the prenatal LPS exposure. However, the exact opposite was true. The increase in double-labeled cells (Figure 2c) occurred despite the fact that there were significant reductions in the numbers of THir cells. These unanticipated results suggest a compensatory role in the progenitor cells that must recognize a defect in TH cell production/existence consequently from the LPS prenatal exposure.

At this time, it is unknown whether the BrdU/THir cells are compensating for the decrease in THir cells resulting in an increase of DA neurons in the SN/mesencephalon area. Thus, because there are reduced numbers of DA neurons, the system may compensate by generating signals (see below) that lead to greater conversion of cells to DA neurons. Given there remained a significant reduction in THir cells, it appears that if compensation did occur, it was not adequate to overcome the overall reductions in THir cells suggesting that had this compensation not occurred, the deficit in DA neurons would be even more pronounced. Thus the results indicate that prenatal LPS exposure does not interfere with the progenitor cell production in producing DA neurons. However, still unknown is the mechanism by which LPS induces the loss of DA neurons.

Specific Aim 2:

Initial Problems: The intent here was to examine the brains of animals exposed to prenatal LPS for trophic activity. We originally proposed unilateral LPS injections on one side of the uterine horn and saline injections on the other side. Although this was technically possible and we were able to perform the injections, there were a significant number of embryos absorbed. Therefore, we moved to simple injections of LPS and HBSS in individual animals since it proved to be more economical in terms of numbers of animals lost. We also encountered a second problem with this specific aim. We had originally intended to perform a 2-dimensional micro-island technique to assess trophic activity. Devised by Dr. Ling, this procedure utilized micro-islands of 5 μ L of striatal and mesencephalic cells lying next to one another in a culture well. When the tissue is positioned correctly, the fibers from the mesencephalic cultures would extend into the striatum enabling us to assess process extension. Although this procedure on the surface appears powerful, it is fraught with variability. What we discovered was that depending on the distance between the two micro-islands, we would get variability in cell growth, independent of the actual trophic conditions. We attempted to use different coatings on the plates to control this, but again we could not get repeatable results, probably due to a variety of factors associated with guidance and strength of signaling. We eventually abandoned this technique and went to simple co-cultures. In the absence of distance and extracellular matrix issues, these studies proved reliable and provided excellent data that was immediately interpretable. The results can be summarized as follows.

Methods: Sprague-Dawley gravid rats (Zivic Miller, Zeneopolis, PA) were obtained at E7 and housed in a 12 hour lights on-off cycle, temperature and humidity controlled environment, and allowed free access to food and water. At E 10.5, the pregnant rats were injected (i.p) with 10,000 endotoxin units of lipopolysaccharide or 0.9% saline. At E14.5 animals from both groups were anesthetized with pentobarbital (60 mg/kg, i.p.) followed by removal of the uterus via cesarean section and stored in dissecting media (HBSS, 1% penicillin, 1% glutamine-D) on ice. The mesencephalic region (SN) and the lateral ganglionic eminence (ST) were dissected from each fetus and pooled by treatment group. The tissue was then centrifuged for two minutes followed by incubation in 0.25% trypsin for 30 minutes at room temperature. The tissue was then centrifuged for two minutes followed by incubation in DNAase for ten minutes at 37°C. After centrifuging the tissue for two minutes, complete media (DMEM with high glucose, F-12 HAMS, 10% FBS, and 1% penicillin) was added and the tissue was triturated until a single cell suspension was seen. Cells (5×10^4) from the ST region were plated into 96 well poly-lysine coated tissue culture plates and allowed to adhere to the plates for ten minutes at 37°C. Cells (5×10^4) from the SN region were then plated on top of the ST according to the following scheme: SAL –SN /SAL-ST; SAL – SN /LPS-ST; LPS-SN/SAL-ST; LPS-SN/LPS-ST. All conditions were repeated four times (4 plates or 4 wells). The

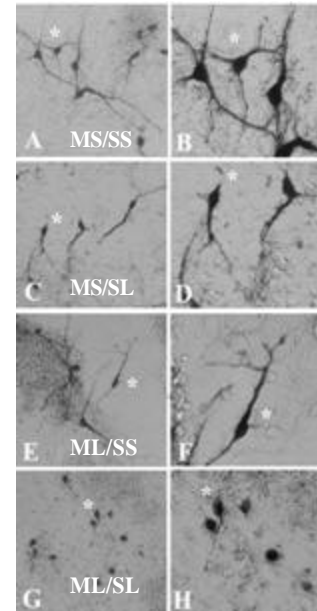


Figure1.

- A. Saline ST co-cultured with saline treated SN 20X
- B. Saline treated ST co-cultured with saline treated SN 40X
- C. LPS treated ST co-cultured with saline treated SN 20X
- D. LPS treated ST co-cultured with saline treated SN 40X
- E. Saline treated ST co-cultured with LPS treated SN 20X
- F. Saline treated ST co-cultured with LPS treated SN 40X
- G. LPS treated ST co-cultured with LPS treated SN 20 X
- H. LPS treated ST co-cultured with LPS treated SN 40 X

co-cultures were then incubated at 37°C with 5% CO₂ for 7 days. The cultures were then fixed with 4% paraformaldehyde for 10 minutes followed by a 0.01M PBS rinse times three. The cells were then stained for rat anti-TH, followed by secondary biotinylated horse anti-rat and visualized using VECTA Stain and DAB. The TH labeled cells in each well were then counted using a crisscross cell counting method covering 38% of the area.

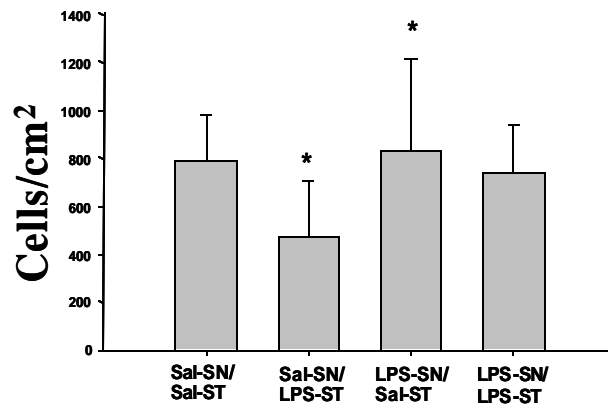


Figure. 2: THir cell counts from co-cultures of various combinations of striatal and mesencephalic tissues from Saline and LPS treated mothers.

Results: Overall, the results were striking. Examination of the cultures demonstrated two overt effects. First and most obvious was the effect on process extension (Figure 1). Cultures established from animals exposed to LPS had less process extension. This was obvious in the THir cells in mesencephalic cultures taken from saline treated controls and co-cultured with striatal cells established from LPS treated mothers [i.e. MS/SL (mesencephalon-saline/striatal-LPS) in photomicrograph] and was most obvious in co-cultures where both the mesencephalon and striatum were harvested from LPS exposed mothers (i.e. ML/SL). (Note: we are in the process of quantifying

fiber process length for publication).

As we originally proposed, it appears that one of the effects of prenatal LPS is to reduce process extension, which could then lead to

reduced access to target derived trophic factors and reduced number of cells. When the THir cell counts were assessed (Figure 2), the LPS had a profound effect when the counts were made in co-cultures established from mesencephalic cultures established from Saline treated mothers with striatal cells from LPS treated

	TH			GDNF		
	Cerebellum	SN	Striatum	Cerebellum	SN	Striatum
HBSS	2.26±1.23	0.67±0.29	0.98±0.22	0.36±0.59	0.59±0.24	6.29±3.47
LPS	2.67±1.39	0.63±0.29	1.01±0.33	0.31±0.17	0.46±0.25	10.45±6.58

Table I: The mRNA levels of TH and GDNF in the striatum, SN, and cerebellum. No significant differences were found.

	Nurr-1			Ptx-3		
	Cerebellum	SN	Striatum	Cerebellum	SN	Striatum
HBSS	2.23±2.74	0.90±0.31	0.72±0.18	n.d.	1.02±1.70	n.d.
LPS	2.59±1.95	0.66±0.26	0.56±0.14	n.d.	0.93±1.04	n.d.

	Shh			FGF8		
	Cerebellum	SN	Striatum	Cerebellum	SN	Striatum
HBSS	0.73±0.52	0.91±0.45	0.84±0.17	9.29±6.31	1.27±0.36	0.87±0.23
LPS	0.98±0.44	0.60±0.28	0.63±0.33	6.44±1.78	0.84±0.61	0.78±0.47

mothers.

Table II: mRNA levels of Nurr-1, Ptx-3, Shh, and FGF-8 in various structures gathered from E-18 fetuses of mothers treated with Saline and HBSS.

Interestingly, the profound effects on process extension seen in the ML/SL co-cultures did not translate into significant reductions in cell counts. (These cultures combinations are scheduled for another replication in early December 2006 to verify the later results since we would assume that the ML/SL cultures would also exhibit reduced cell counts). Since we have observed these effects which suggest alterations in trophic activities, we collected the media conditioned by each of four possible mono-cultures (i.e., striatal cells from saline and LPS mothers and mesencephalic cultures from saline and LPS mothers). This media will be used in conditioned media transfer studies (see below for future studies).

Given the reduced process extensions and reduced cell counts observed in the co-cultures of MS/SL it could be argued that there is a reduction in striatal derived trophic activity. Thus, there could be reductions in GDNF known to be the most potent trophic factor for DA neurons. These results could also suggest reductions in other neurotrophic factors including bFGF, BDNF and neurturin. However, we evaluated the effects of prenatal LPS on GDNF mRNA (Table I) and bFGF at E18 and found no significant changes (Qin et al, in preparation). Moreover, we evaluated several other factors that could affect the development of DA neurons including Nurr-1, Ptx-3 and sonic hedgehog (Shh) and similarly found no changes (Table II). Taken together, these data suggest that GDNF and FGF-8 are not involved with the loss of DA neurons seen. Moreover, other transcription factors that could be involved with DA neuron development including Nurr-1 and Ptx-3 are similarly not affected.

The reductions in trophic activity could reflect alterations in other trophic factors including BDNF or other unknown factors. Our group as well as two others has characterized a so-called striatal derived neurotrophic activity (SdNTF); a factor that has yet to be identified (see Carvey et al., 1993). Changes in this unknown neurotrophic factor(s) could account for the results seen and conditioned media transfer studies are planned to assess this possibility.

One of the elements of the prenatal LPS that has emerged as we have studied the model further, was the fact that these in-utero exposed LPS animals are more sensitive to the effects

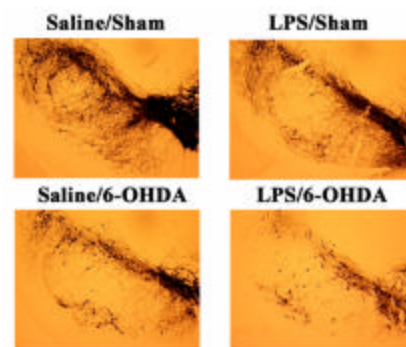


Figure 3: These photomicrographs reveal the typical prenatal LPS effect of reducing THir cells in the SN. 6OHDA also reduced the THir cell counts. However, 6OHDA into animals exposed to LPS prenatally produced greater DA neuron loss although the magnitude of the loss was additive and not synergistic.

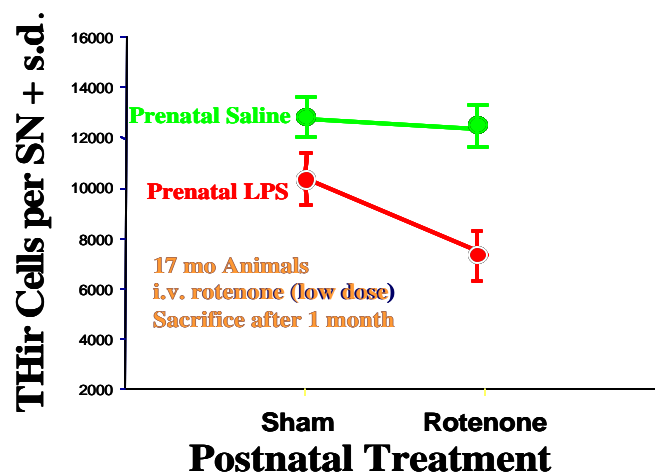


Figure 4. Animals exposed to LPS prenatally and then a subthreshold dose of rotenone exhibit synergistic DA neuron loss.

of DA neurotoxins later in life (Figure 3). When young, the animals do not exhibit increased sensitivity to 6OHDA (Ling et al., 2004a). However, when the animals are older, we did demonstrate increased sensitivity to subsequent exposure to LPS (Ling et al., 2006) and rotenone (Figure 4) (Ling et al., 2004b). We have argued that these changes are consistent with the so-called multiple hit hypothesis (Carvey et al., 2006). Thus, the long-lived increases in neuroinflammation seen in these animals renders them more susceptible to the effects of exposure to a second neurotoxin because the additional increases in inflammation produced by the second exposure overwhelms the anti-inflammatory compensatory capacity of the CNS leading to further increases, or more likely longer lived inflammation (see Ling et al., 2006). Although this hypothesis is supported by the data, this new data may suggest that neurotrophism is involved as well. Thus, we previously demonstrated that compensatory changes in neurotrophic activity were a function of age (Ling et al., 200; Collier et al., 2005). If *in-utero* exposure to LPS in some way reduces the overall levels of trophic activity, it is possible that as animals age, they show greater DA neuron losses from DA neurotoxins, that could potentially convert into progressive DA neuron loss due to the combined effects of greater neuroinflammation (second hit concept) and reduced compensatory neurotrophism. This intriguing possibility will be pursued in future studies.

Specific Aim 2 Future Studies:

Based on the results, the following studies need to be performed. First, we need a replication of the co-culture conditions described above. These are already scheduled for early December. These studies will complete the statement of work, given that the process extension assessment, currently underway, will also be completed by then. Unrelated to the statements of work, but needed to for our understanding of the mechanisms involved in the prenatal LPS effects, we need to perform two additional sets of experiments. First, as these experiments were emerging from pilot to working studies, it became apparent that changes in trophic activity were involved. As a result, we began to mono-culture cells left over from the co-culture experiments. Thus, when we had extra cells from a striatal-mesencephalic co-culture, we grew these cultures out separately for 14 days and collected the media every 3 days. We thus now have 4 sets of conditioned media from striatal cultures from mothers exposed to Saline and LPS as well as their counterparts from the mesencephalon. We can now use these conditioned medias to assess trophic activity in both the striatum (as we have done in the past for striatal conditioned medias (see Carvey et. al, 1993 for review) and mesencephalon (i.e. DA autotrophic activity; see Ling et al., 1993 for review)). These medias are added to normal mesencephalic cultures growing in defined media for trophic factor assessments and are compared with heat-inactivated conditioned media. These studies will tell us if there is a quantitative change in trophism during development. The second set of studies would be to perform trophic studies in animals at various ages following prenatal LPS and prenatal saline treatment. Using striatal and mesencephalic extracts in a fashion similar to the conditioned media transfer studies described above would tell us if tissues from LPS-exposed offspring have less trophic activity. If this were found to be the case, we could then determine if the compensatory changes in this trophic activity that accompanies DA neuron loss normally, is also compromised. This would add another level of understanding to the evolution of the multiple hit hypotheses.

Key Research Accomplishments:

Several conclusions can be drawn from this study.

1. It is clear that the DA neuron loss observed in animals exposed to LPS prenatally occurs in the earliest phases of development (i.e. prior to E14.5 where there is already a reduction in THir cells).
2. These reductions are not a consequence of alterations in the homeobox genes Shh or Ptx3, the nuclear receptor Nurr1 gene, or the FGF8 gene since they were normal in all animals exposed to LPS. This suggests that LPS does not alter the expression of these genes leading to the reductions in DA cells seen in LPS exposed animals.
3. The loss of DA neurons following *in utero* exposure to LPS is also not likely a consequence of LPS' effect on progenitor cell proliferation. Although it was difficult at best to identify which BrdU labeled cells would eventually go on to develop into DA neurons since the region of origin of these cells could not be identified without the ability to determine what their actual cell fate would be, it was clear that there were not significant decreases in the numbers of these cells. Thus, LPS does not appear to interfere with subventricular proliferation in the mesencephalic region.
4. Prenatal exposure also does not appear to interfere with the normal phases of apoptotic culling that occurs at P1-P3 since the cell counts in both the LPS and saline exposed animals decreased equivalently and in parallel across the developmental period through P10.
5. It does appear that prenatal LPS interfered with the trophic environment of the nigro-striatal pathway. Striatal tissue from LPS exposed fetuses was less able to grow DA neurons in co-cultures and the process extension from these cells was markedly reduced.
6. Prenatal LPS exposure may also affect DA autotrophic activity since cells harvested from LPS exposed animals had diminished cell processes (although cell counts were normal) and when combined with striatal cultures from LPS exposed animals, very few cells had processes at all.
7. Taken together, it is hypothesized that *in utero* LPS leads to alterations in the trophic environment that compromise process extension leading to trophic restriction by the developing DA neurons with associated cell loss. Despite these reductions in trophic activity, the apoptotic culling occurs normally since it is likely that the overall levels of target derived trophic activity were reduced, but not completely absent. This hypothesis will be tested in future studies where levels of trophic activity will be assessed in conditioned media transfer studies.
8. Our group is closer to developing an understanding of the mechanisms responsible for the reduced numbers of DA neurons reliably observed in animals exposed to LPS prenatally. If we are able to confirm reductions in trophic activity in future studies, these results might aid in our understanding of the increased sensitivity adult animals exhibit following prenatal LPS exposure and exposure to a second neurotoxin during adulthood.

Reportable Outcomes:

The following is a list of publications that came out during the period of funding from the DoD in which they are thanked for their support. The primary outcome from this work will be likely one and perhaps two manuscripts discussing the data reported here. These manuscripts will be in preparation until the results of the culture replicates are completed and the conditioned media transfer studies are complete. Although the manuscripts below are not directly related to the specific aims of this proposal, they are all indirectly related including the work on the blood brain barrier (BBB) since it was the life-long neuroinflammation associated with the prenatal LPS model that first got us thinking about the ramifications of inflammation on the parenchymal side of the barrier and its impact on BBB integrity. The published works during the funding period are as follows:

1. Ling, Z.D., Lipton, J.W., Chin, Q. Chong, C.W., Carvey, P.M. Combined Toxicity of Prenatal Bacterial Endotoxin Exposure and Postnatal 6-Hydroxydopamine in the Adult Rat Midbrain. *Neuroscience*. 2004;124(3):619-28.
2. Ling Z, Chang QA, Tong CW, Leurgans SE, Lipton JW, Carvey PM. Rotenone potentiates dopamine neuron loss in animals exposed to lipopolysaccharide prenatally. *Exp Neurol*. 2004 190(2):373-83.
3. Carvey, P.M., Chen, E-Y, Lipton, J.W., Tong C., Chang, Q.A., and Ling, Z.D. Intra-parenchymal injection of TNF- α and IL-1- β produces dopamine neuron loss in the rat. *J Neural Transm*. 2005;112(5):601-12.
4. Collier, Timothy J, Zao Dung Ling, Paul M. Carvey, Anita Fletcher-Turner, David M. Yurek, John R. Sladek Jr., and Jeffrey H. Kordower. Striatal trophic factor activity in aging monkeys with unilateral MPTP-induced parkinsonism *Exp Neurol*. 2005 Feb;191 Suppl 1:S60-7
5. Carvey, PM C.H. Zhao, B. Hendey, H. Lum, J. Trachtenberg, B.S. Desai, J. Snyder, Y.G. Zhu and Z.D. Ling. 6-hydroxydopamine-induced Alterations in Blood Brain Barrier Permeability. *Eur J Neurosci*. 2005 Sep;22(5):1158-68.
6. Chen L, Cagniard B, Mathews T, Jones S, Koh HC, Ding Y, Carvey PM, Ling Z, Kang UJ, Zhuang X. Age-dependent motor deficits and dopaminergic dysfunction in DJ-1 null mice. *J Biol Chem*. 2005 Jun 3;280(22):21418-26.
7. Ling Z, Zhu Y, Tong CW, Snyder JA, Lipton JW, Carvey PM. Progressive dopamine neuron loss following supra-nigral lipopolysaccharide (LPS) infusion into rats exposed to LPS prenatally. *Exp Neurol*. 2006 199(2):499-512
8. Carvey, PM, Punati A, and Newman, MB. Progressive dopamine neuron loss in Parkinson's disease: the multiple hit hypothesis. *Cell Transplant*. 2006; 15(3) 239-250.

9. Zhu, Y, Carvey PM, and Ling Z. Age-related changes in glutathione and glutathione-related enzymes in rat brain. *Brain Res.* 2006 May 23;1090(1):35-44.
10. Zhao C, Ling ZD, Newman MB, Bhatia A, and Carvey PM. TNF-Alpha Knockout and Minocycline Treatment Attenuates Blood Brain Barrier Leakage in MPTP-Treated Mice. In revision, *Neurobiology of Disease*.

In addition to these publications, we have presented work yearly at the Society for Neurosciences and the American Society for Neural Therapeutics and Repair where several posters were presented and oral presentations were made acknowledging the support of the DoD.

Conclusions:

The results suggest that prenatal exposure to LPS leads to loss of DA neurons in the early phases of development of the nigro-striatal pathway. LPS does not appear to interfere with homeobox genes or other nuclear receptors or some trophic factors (GDNF or FGF8) known to be involved with the development of the DA system. Moreover, LPS does not appear to interfere with proliferation of cells in the subventricular zones that potentially are destined to become DA neurons. However, analysis of BrdU-THir double labeled cells appears to indicate that there are greater numbers of these cells in the SN of E18 animals. This might suggest that the reduced numbers of THir cells in the SN at E18 in same way signals the progenitor cell population to increase their phenotypic conversion to DA neurons. However, this potential compensatory response is inadequate since the overall number of THir cells in the SN is still reduced relative to normal. Moreover, analysis of co-cultures of mesencephalic DA neurons and striatal tissues suggest that there are alterations in growth potential and most importantly, the extension of DA neuron processes which are consistent with altered neurotrophic support. Given there were no changes in mRNA for FGF8 and GDNF, it is possible that the trophic factors involved are the yet to be identified Striatal-Derived Neurotrophic factor described by our group and several others and the DA Neuron autotrophic factor. If indeed, the loss of DA neurons is a consequence of these factors, this would explain why DA neurotoxins administered to aged animals produced greater DA neuron losses in animals exposed to LPS prenatally than animals exposed to saline since reduced trophic support would render the animals more susceptible to toxic insult. Overall, the negative data provided by this project as well as the potential involvement of neurotrophic factors provides greater insight into the mechanism(s) underlying the prenatal LPS effect and represents the first mechanistic clues for this potentially important new animal model of PD.

References

- Carvey, P.M., et al., *Striatal extracts from patients with Parkinson's disease promote dopamine neuron growth in mesencephalic cultures*. Exp Neurol, 1993. **120**(1): p. 149-52.
- Carvey, P.M., A. Punati, and M.B. Newman, *Progressive dopamine neuron loss in Parkinson's disease: the multiple hit hypothesis*. Cell Transplant, 2006. **15**(3): p. 239-50.
- Collier, T.J., et al., *Striatal trophic factor activity in aging monkeys with unilateral MPTP-induced parkinsonism*. Exp Neurol, 2005. **191 Suppl 1**: p. S60-7.
- Hynes, M., et al., *Control of neuronal diversity by the floor plate: contact-mediated induction of midbrain dopaminergic neurons*. Cell, 1995. **80**(1): p. 95-101.
- Hynes, M., et al., *Induction of midbrain dopaminergic neurons by Sonic hedgehog*. Neuron, 1995. **15**(1): p. 35-44.
- Hynes, M. and A. Rosenthal, *Specification of dopaminergic and serotonergic neurons in the vertebrate CNS*. Curr Opin Neurobiol, 1999. **9**(1): p. 26-36.
- Lin, J.C. and A. Rosenthal, *Molecular mechanisms controlling the development of dopaminergic neurons*. Semin Cell Dev Biol, 2003. **14**(3): p. 175-80.
- Ling, Z., et al., *Rotenone potentiates dopamine neuron loss in animals exposed to lipopolysaccharide prenatally*. Exp Neurol, 2004. **190**(2): p. 373-83.
- Ling, Z.D., et al., *Combined toxicity of prenatal bacterial endotoxin exposure and postnatal 6-hydroxydopamine in the adult rat midbrain*. Neuroscience, 2004. **124**(3): p. 619-28.
- Ling, Z., et al., *Progressive dopamine neuron loss following supra-nigral lipopolysaccharide (LPS) infusion into rats exposed to LPS prenatally*. Exp Neurol, 2006. **199**(2): p. 499-512.
- Luskin, M.B., *Restricted proliferation and migration of postnatally generated neurons derived from the forebrain subventricular zone*. Neuron, 1993. **11**(1): p. 173-89.
- Marchand, R. and L.J. Poirier, *Isthmic origin of neurons of the rat substantia nigra*. Neuroscience, 1983. **9**(2): p. 373-81.
- Menezes, J.R., et al., *The division of neuronal progenitor cells during migration in the neonatal mammalian forebrain*. Mol Cell Neurosci, 1995. **6**(6): p. 496-508.
- Monk, C.S., S.J. Webb, and C.A. Nelson, *Prenatal neurobiological development: molecular mechanisms and anatomical change*. Dev Neuropsychol, 2001. **19**(2): p. 211-36.
- Vu, T.Q., et al., *Pramipexole attenuates the dopaminergic cell loss induced by intraventricular 6-hydroxydopamine*. J Neural Transm, 2000. **107**(2): p. 159-76.

COMBINED TOXICITY OF PRENATAL BACTERIAL ENDOTOXIN EXPOSURE AND POSTNATAL 6-HYDROXYDOPAMINE IN THE ADULT RAT MIDBRAIN

Z. D. LING,^{a,b*} Q. CHANG,^a J. W. LIPTON,^b C. W. TONG,^a T. M. LANDERS^a AND P. M. CARVEY^{a,b}

^aDepartment of Pharmacology, 1735 West Harrison Street, Room 410, Rush University Medical Center, Chicago, IL 60612, USA

^bDepartment of Neurological Sciences, Rush University Medical Center, Chicago, IL 60612, USA

Abstract—We previously reported that injection of the Gram (–) bacteriotoxin, lipopolysaccharide (LPS), into gravid females at embryonic day 10.5 led to the birth of animals with fewer than normal dopamine (DA) neurons when assessed at postnatal days (P) 10 and 21. To determine if these changes continued into adulthood, we have now assessed animals at P120. As part of the previous studies, we also observed that the pro-inflammatory cytokine tumor necrosis factor α (TNF α) was elevated in the striatum, suggesting that these animals would be more susceptible to subsequent DA neurotoxin exposure. In order to test this hypothesis, we injected (at P99) 6-hydroxydopamine (6OHDA) or saline into animals exposed to LPS or saline prenatally. The results showed that animals exposed to prenatal LPS or postnatal 6OHDA alone had 33% and 46%, respectively, fewer DA neurons than controls, while the two toxins combined produced a less than additive 62% loss. Alterations in striatal DA were similar to, and significantly correlated with ($r^2=0.833$) the DA cell losses. Prenatal LPS produced a 31% increase in striatal TNF α , and combined exposure with 6OHDA led to an 82% increase. We conclude that prenatal exposure to LPS produces a long-lived THir cell loss that is accompanied by an inflammatory state that leads to further DA neuron loss following subsequent neurotoxin exposure. The results suggest that individuals exposed to LPS prenatally, as might occur had their mother had bacterial vaginosis, would be at increased risk for Parkinson's disease. © 2004 IBRO. Published by Elsevier Ltd. All rights reserved.

Key words: Parkinson's disease, TNF α , IL-1 β , dopamine, prenatal, lipopolysaccharide.

Although genetic factors account for some cases of Parkinson's disease (PD; Gasser, 1998; Polymeropoulos et al., 1997), the vast majority of PD is considered idiopathic.

*Correspondence to: Z. Ling, Department of Pharmacology, 1735 West Harrison Street, Room 410, Chicago, IL 60612, USA. Tel: +1-312-563-2556; fax: +1-312-563-3552. E-mail address: zling@rush.edu (Z. D. Ling).

Abbreviations: BV, bacterial vaginosis; DA, dopamine; E, embryonic day; EDTA, ethylenediaminetetraacetic acid; ELISA, enzyme-linked immunosorbent assay; EU, endotoxin unit; HBSS, Hanks' balanced salt solution; HPLC, high performance liquid chromatography; HVA, homovanillic acid; IL-1 β , interleukin 1 β ; ir, immunoreactive; LPS, lipopolysaccharide; P, postnatal; PD, Parkinson's disease; SN, substantia nigra; TH, tyrosine hydroxylase; TNF α , tumor necrosis factor α ; VTA, ventral tegmental area; 6OHDA, 6-hydroxydopamine.

0306-4522/04/\$30.00+0.00 © 2004 IBRO. Published by Elsevier Ltd. All rights reserved.
doi:10.1016/j.neuroscience.2003.12.017

Several environmental factors, including chemical neurotoxins, such as rotenone, dieldrin, and paraquat have been proposed as risk factors (Brooks et al., 1999; Thiruchelvam et al., 2000; Betarbet et al., 2000; Jenner, 2001). Although these known dopamine (DA) neurotoxins have been widely discussed, their potential roles as PD risk factors are suspect because of the large dosages that would be needed. However, if exposure were to occur in an individual that already had fewer than normal DA neurons, and especially if that hypo-dopaminergic condition was associated with a pro-inflammatory state, then lower dosages of neurotoxins would be needed. Recent studies in animals from our laboratory suggest that this is possible.

We previously demonstrated that rat fetuses exposed to the Gram(–) bacteriotoxin, lipopolysaccharide (LPS) at embryonic day (E) 10.5 were born with fewer than normal DA neurons (Ling et al., 2002a,b). Assessment of tyrosine hydroxylase (TH) immunoreactive (ir) neuron counts (used as an index of DA neurons) in the substantia nigra (SN) of postnatal day (P) 10 and P21 rat pups revealed losses of 25 and 31%, respectively. Similar reductions in striatal DA and increases in DA activity ([homovanillic acid (HVA)]/[DA]) were also seen. In addition, increased levels of the pro-inflammatory cytokine tumor necrosis factor α (TNF α), were seen in the SN of these animals, indicating a pro-inflammatory state. These changes in DA and increases in TNF α are consistent with the well-established effects of LPS. Thus, LPS, acting through the CD14 and toll-like receptor-4, is a well known inducer of pro-inflammatory cytokines and has been shown to kill DA neurons both *in vitro* and *in vivo* by several investigators (Castano et al., 1998, 2002; Gayle et al., 2002). Taken together, these studies suggested that LPS and infections that increase pro-inflammatory cytokines prenatally, may be involved in the etiology of PD. We hypothesized that individuals born to mothers with bacterial vaginosis (BV), a well known inducer of LPS and pro-inflammatory cytokines in the chorioamniotic environment (Fortunato et al., 1996; Menon et al., 1995), would be at increased risk for PD. Moreover, if prenatal LPS led to a continued pro-inflammatory state, then subsequent exposure to DA neurotoxins would produce a more pronounced DA cell loss. This would then support the notion that PD is a consequence of the combined effects of multiple environmental factors with a prenatal factor representing an entirely new exposure paradigm.

We set out to assess this possibility in rats exposed to LPS prenatally followed by postnatal neurotoxin exposure. We chose the well-known DA neurotoxin, 6-hydroxydopa-

mine (6OHDA) as the postnatal toxin for several reasons. First, it has been shown to increase $\text{TNF}\alpha$ in brain, suggesting that it would further increase proinflammatory cytokine(s) in animals prenatally exposed to LPS (Mogi et al., 2000). Second, i.c.v. injection of 6OHDA kills DA cells bilaterally, which is similar to the effects of prenatal LPS (Vu et al., 2000). Third, when injected i.c.v., 6OHDA kills DA neurons in a dose-dependent manner (Carvey et al., 1994).

EXPERIMENTAL PROCEDURES

Animals

Forty-nine timed-gravid female Sprague–Dawley rats (Zivic-Miller, Allison Park, PA, USA) were delivered to Rush's animal facility at gestational day 9 ± 12 h. Two additional male and two non-gravid female Sprague–Dawley rats were also studied. All animals were maintained in an environmentally regulated animal facility for the duration of the study (lights on 06:00–18:00 h). The protocols and procedures used in these studies were approved by the Institutional Animal Care and Utilization Committee (IACUC) of Rush University and met the guidelines of the Council on Accreditation of the Association for Assessment and Accreditation of Laboratory Animals Care (AAALAC, international). Minimal number of animals was used in the study and all survival surgeries were performed under pentobarbital anesthesia (40 mg/kg body weight) to minimize pain.

Prenatal treatment and body temperature study

LPS was purchased from Sigma Chemical Co. (St. Louis, MO, USA; L-8274; prepared from *Escherichia coli* 026:B6) and dissolved in saline (Hanks' balanced salt solution [HBSS]; Gibco-Invitrogen) at 10,000 endotoxin units (EU)/ml. At E10.5, each gravid female received a single injection (i.p.) of either 10,000 EU/kg LPS or HBSS (1 ml/kg; $n=18$ for each group). This dosage was chosen based on previous studies where it was shown to be well tolerated and did not produce fetal demise (Ling et al., 2002a). E10.5 was used because it is just prior to the birth of DA neurons at E11–E11.5 (Specht et al., 1981; Sinclair, 1999; Cohen and Sladek, 1997; Bouvier and Mytilineou, 1995) and previous studies showed it to produce the most profound DA neuron loss while earlier injections and later injections (E12.5 and greater) produced no loss at all (Ling et al., 2002b). All the animals were monitored daily for obtundation or other signs of distress, and were allowed to deliver their pups normally. The pups were weaned at P21 and housed two per cage with same-sex partners.

Increased maternal body temperature has been previously hypothesized to produce teratogenic effects in offspring (Colado et al., 1999; Albers and Sonsalla, 1995). Although the dosage of LPS used in the present study was considerably lower than those known to produce hyperthermia (Miller et al., 1997; Meszaros et al., 1991) we needed to rule out the possibility that the THir cell loss seen was simply a consequence of hyperthermia. Rectal temperature was measured in separate groups of animals treated with the same protocol (prenatal saline [$n=6$]; prenatal LPS [$n=7$]) prior to, and following i.p. LPS injection, at 30 min intervals for 5.5 h, and again at 24 h. In order to determine if the effect of LPS on body temperature was influenced by gender or gravidity, we also assessed rectal temperature in two males and two, non-gravid females.

Treatment groups, postnatal treatment, and kill protocol

One male pup from each of the 24 litters was chosen (12 LPS and 12 saline) and randomly assigned to one of two postnatal treat-

ment groups (i.c.v. Sham Control [vehicle] or 6OHDA) creating a 2×2 design (LPS/Sham; LPS/6OHDA; Saline/Sham; and Saline/6OHDA).

At P99 the animals were subjected to the postnatal treatment protocol. One hour prior to surgery, every animal received an i.p. injection of desipramine HCl (25 mg/kg) to reduce the uptake of 6OHDA into noradrenergic terminals (Carvey et al., 1994). The animals were anesthetized with pentobarbital (40 mg/kg; i.p.) and placed in a stereotaxic frame. 5 μl of a 6OHDA solution containing 150 μg 6OHDA as the HBr salt (Research Biochemicals Inc.) in an ascorbate vehicle (0.02% ascorbate/saline) or 5 μl ascorbate vehicle was delivered into the right lateral ventricle (anterior/posterior = -3.8 mm, medial/lateral = -4.8 mm, dorsal/ventral = -6.8 mm, relative to bregma) as described previously (Carvey et al., 1994). This dose was chosen because our previous studies have demonstrated that it was likely to produce a 50% DA neuron depletion in the SN (Vu et al., 2000). The animals were allowed to recover under a heating lamp, returned to their home cages, and perfused transcardially 21 days later at P120 with ice-cold saline. The brains were quickly removed and processed for subsequent assessments as described previously (Vu et al., 2000). Briefly, the frontal part of the brain (4 mm from the apex) was isolated using a coronal knife cut, and kept for biochemistry and cytokine studies. The posterior part of brain was submerged in Zamboni's fixative (7.5% saturated picric acid, 12 mM NaH_2PO_4 , 88 mM Na_2HPO_4 , and 4% paraformaldehyde) for immunocytochemistry studies. Two sets of tissue punches were taken from the center of the left and right striatum, pooled and passed to high performance liquid chromatography (HPLC) assessment of DA and DA activity, or enzyme-linked immunosorbent assay (ELISA) for assessment of $\text{TNF}\alpha$ and interleukin 1β (IL- 1β). IL- 1β was assessed because it is also a pro-inflammatory cytokine, and because our previous studies revealed that it was elevated in animals exposed to LPS prenatally and killed at P10, but was not elevated in animals killed at P21 (Ling et al., 2002a,b).

DA biochemistry

DA and its metabolite HVA were assessed using HPLC with electrochemical detection in pooled (left and right) tissue punches taken from the center of each striatum as previously described (Vu et al., 2000). DA and HVA were expressed as ng/mg tissue protein (assessed using the Biorad Protein Assay Kit), and the ratio of [HVA]/[DA] was used as an index of DA activity.

ELISA for cytokine protein assessments

The pooled tissue punches from each striatum destined for cytokine assessment were submerged in 200 μl homogenate buffer (Trizma/HCl, pH 7.2, 0.1 M, sodium chloride 0.9%, EDTA 1 mM, Aprotinin 2%, leupeptin 0.5 $\mu\text{g}/\text{ml}$, pepstatin 0.7 $\mu\text{g}/\text{ml}$, phenylmethanesulfonyl fluoride 200 μM ; all reagents obtained from Sigma) and homogenized as described previously (Lipton et al., 1999). To each tube, 200 μl homogenate buffer containing 0.5% NP-40 (Sigma) was then added. The tubes were shaken, centrifuged (10,000 $\times g$ for 15 min), and the supernatants collected. The levels of $\text{TNF}\alpha$ and IL- 1β were assessed in each supernatant by an ELISA run according to the manufacturer's instructions (R & D Systems, Minneapolis, MN, USA). The plates were read in a Dynatech ELISA plate reader (Dynatech Laboratories, Chantilly, VA, USA) and the concentrations of the cytokines were determined against a six-point standard curve. The protein content of each supernatant was determined using the Bio-Rad Protein Assay kit and the quantity of the cytokines was expressed as pg/mg protein.

THir and NeuNir immunocytochemistry

The number of THir and NeuNir cells (a nuclear marker expressed in most post-mitotic neurons (Mullen, 1992) were assessed using

a stereological procedure (Vu et al., 2000). The entire mesencephalon was sliced on a cryostat into consecutive 40 μm sections. Every sixth section was immunohistochemically processed for TH as described previously (Vu et al., 2000; Ma et al., 1997) using mouse anti-rat TH antibody (Immunostars, Stillwater, MN, USA; 1:20,000). The immunohistochemical procedure was continued by using a biotinylated horse anti-mouse IgG (0.5%; Vector Laboratories, Burlingame, CA, USA) for 1 h then peroxidase conjugated avidin–biotin complex (Vector Laboratories) for 1 h. The chromogen solution used to complete the reaction consisted of 0.05% 3,3'-diaminobenzidine, 0.5% nickel sulfate, and 0.003% H_2O_2 in I/A solution (10 mM imidazole/50 mM sodium acetate) to obtain a jet-black stain. The NeuN antibody (1:5000; Chemicon, Temecula, CA, USA) immunohistochemistry was performed in the same series of sections, only the chromogen was developed without nickel sulfate to generate a brown color. The sections were washed, mounted on gelatin-coated slides, dehydrated through graded alcohols, cleared in xylenes, and coverslipped with Permount.

Stereology assessments

The estimation of the total number of THir and NeuNir neurons in the SN and ventral tegmental area (VTA) was performed using the computerized optical disector method. This method allowed for the stereological estimation of THir cells in the entire structure, independent of size, shape, orientation, tissue shrinkage or anatomical level using MicroBrightField software (Ling et al., 2002a). Since the compacta region of the SN cannot be easily distinguished from the reticulata, the two regions were combined for stereological assessment and designated SN. The VTA was identified as the region medial to the accessory optic tract and lateral to the midline. In regions where the accessory optic tract was not readily seen, the line connecting the most inferior point on the dorsal curvature between the THir cells of the SN and the VTA and the most superior point of the ventral curvature, represented the lateral boundary of the VTA (see Fig. 3).

The antibody penetration throughout the whole tissue section was assessed by dissectors using the imaging capture technique (Emborg et al., 1998; Kordower et al., 1996; Ma et al., 1999a,b). The total number (N) of SN or VTA neurons was calculated using the formula $N = N_V V_{\text{SN or VTA}}$, where N_V is the numerical density and $V_{\text{SN or VTA}}$ is the volume of the SN or VTA respectively, as determined by Cavalieri's principle (Cavalieri et al., 1966). The MicroBrightField software was also used to determine the total area of the SN and VTA as outlined by the blinded investigator (volume in mm^3), the density of the cells in that volume (cell counts/ mm^3), and the size of the cell bodies chosen for assessment (μm^2 ; Ling et al., 2002a). After immunostaining and dehydration, the thickness of sections varied from 18 to 20 μm . The thickness of each section was measured and this reading was entered as a counting parameter. The upper and lower forbidden layers (4 μm) were eliminated from counting, leaving a 10–12 μm thick section as the final thickness for stereological assessment. This procedure ensures that cells layered on top of one another within a section are accurately assessed.

Statistical analysis

The various measures were assessed using two-way ANOVA. Differences between treatment groups were assessed using Tukey's post hoc analysis run following one-way ANOVA for that particular group. Pearson's two-tailed test was used to statistically correlate the cell count data with the biochemistry values. The temperature data were analyzed using a repeated measures ANOVA.

We have repeatedly shown that despite unilateral i.c.v. injection of 6OHDA, it produces equivalent bilateral effects on DA cell counts and DA biochemistry (Vu et al., 2000). Similarly, as also

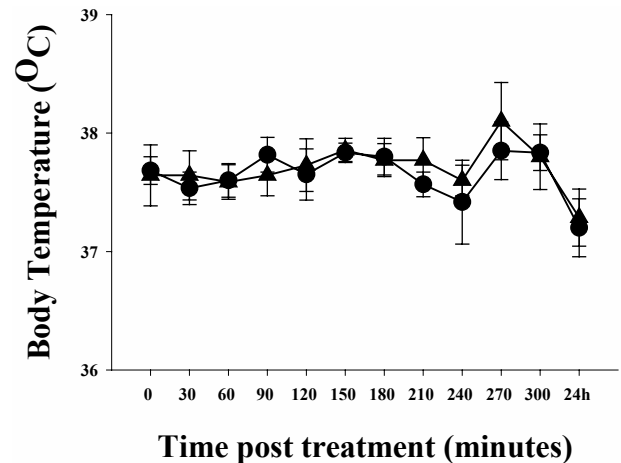


Fig. 1. Rectal body temperature in LPS- and HBSS-treated gravid rats. The rectal temperature of each group is depicted prior to (0) and following i.p. HBSS (circles) or LPS treatment (triangles) at E10.5.

reported previously (Ling et al., 2002a) prenatal LPS leads to equivalent THir cell losses on both sides of the brain. As a result, all results from the left and right sides were pooled (DA biochemistry and cytokine assessments) or combined (cell counts) for statistical analysis.

RESULTS

Overall, the gravid dams tolerated the treatment protocol without difficulty. A total of 13 dams were monitored for rectal temperature fluctuations within the 24 h following injection at E10.5. No significant alterations in body temperature were noted (Fig. 1; $F_{1,12}=0.589$, $P=0.459$). Non-gravid females and males injected with 10,000 EU/kg LPS also failed to exhibit significant alterations in rectal temperature (data not shown). Only animals giving birth at approximately E21.5–22, which was 9.5–10 days after initial treatment (suggesting that the injection of LPS into the gravid females occurred at approximately E10.5) were accepted into the protocol. Neither the pup body weights nor the litter sizes in the LPS- or saline-treated groups were significantly different from one another (data not shown). In the 6OHDA lesion studies, one animal died within 24 h of i.c.v. injection of 6OHDA in the LPS/6OHDA group. One of the ELISA determinations from the Saline/Sham group had an unusually low protein content and the sample was dropped from analysis. All other values were used.

SN cell counts

The sections from the animals were immuno-stained for TH and NeuN in an effort to determine if the THir cell loss seen was a consequence of phenotypic suppression of TH or actual cell loss. If prenatal LPS or postnatal 6OHDA suppressed TH expression, but did not actually kill THir cells, then loss of THir cells would be associated with increases in NeuNir cells and the two sets of cell counts would be inversely correlated. If, on the other hand, THir cell loss reflected death of cells, there would be a reduction

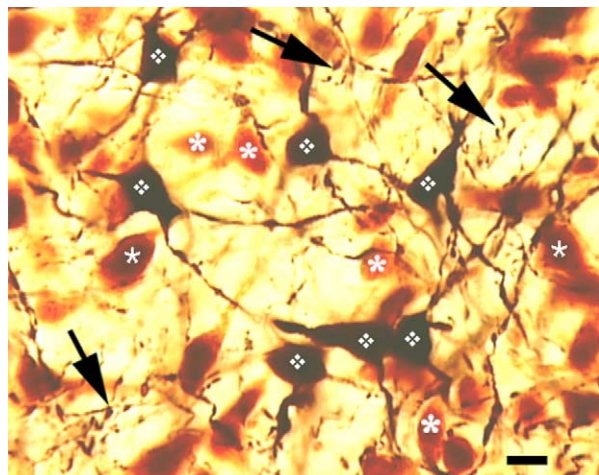


Fig. 2. Double stain of THir and NeuNir neurons in the SN compacta. This photomicrograph of the compacta region of the SN depicts the typical staining pattern seen. Numerous large THir neurons were observed (black cells with white \diamond) that had numerous processes with varicosities typical of DA neurons (black arrows). Cells reacting to NeuN were not developed with nickel enhancement and therefore appear brown. The NeuN reacted primarily with the cell bodies of non-dopaminergic cells (sampled cells are labeled with white *). (Magnification Bar=15 μ m).

in THir cells, no change in NeuNir cells, and the reduction in THir cells would be positively correlated with the changes seen in total cells.

The double stains of the mesencephalic sections revealed clear segregation of the two different cell types that readily allowed for stereological assessment (Fig. 2). THir cells were jet black and exhibited fine, thread-like, extensive processes with varicosities typical of DA neurons in the compacta region of the SN. In contrast, the NeuNir cells were rich brown, and since the NeuN immunoreacts only with neuronal nuclei, there was no confusion between cell types. The sum of the THir and NeuNir cell counts thus generated the total neuron cell counts. In the compacta and reticulata regions of the SN in the Saline/Sham control animals, THir cells represented 33.17% of the total cell counts.

Both prenatal LPS exposure and postnatal treatment had significant effects on the apparent THir immunoreactivity (Fig. 3) as well as the THir cell counts (Fig. 4). The photomicrographs of the SN clearly revealed that the most pronounced THir cell loss was present in the lateral regions of the nigra, as well as the ventral regions of the compact and within the reticulata. Both prenatal LPS and postnatal 6OHDA had this effect. However, postnatal treatment with 6OHDA in animals exposed to LPS prenatally, produced a more profound THir cell loss. Statistically, the effects of pre- and postnatal treatments were both highly significant (prenatal exposure: $F_{1,22}=35.036$, $P<0.001$; postnatal treatment: $F_{1,22}=92.246$, $P<0.001$). In addition, the pre- vs. postnatal treatment interaction was also statistically significant ($F_{3,22}=7.36$, $P=0.014$). This, together with an examination of the means, suggested that the combined effects of prenatal LPS exposure and postnatal toxin treatment produced a less than additive effect, albeit

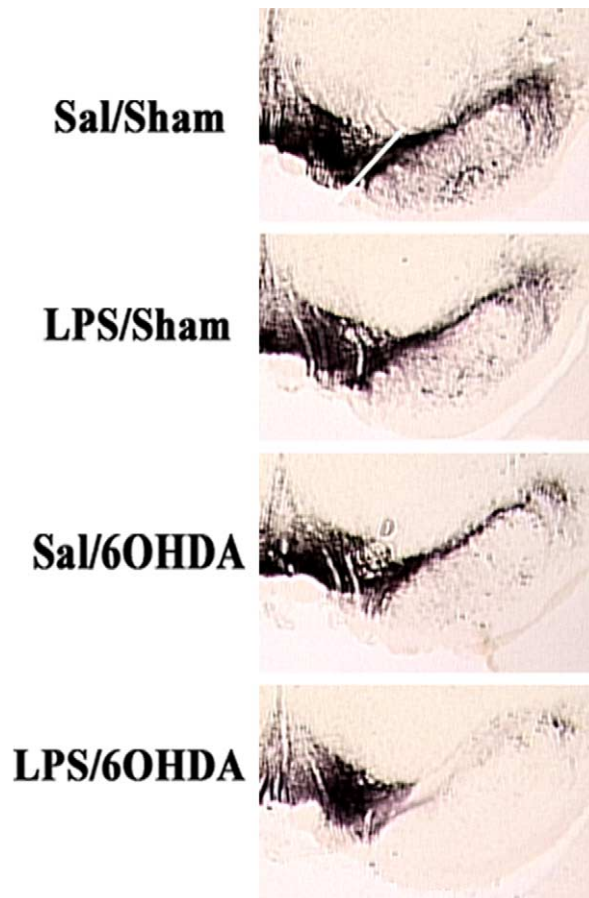


Fig. 3. Photomicrographs of the mesencephalons. Representative photomicrographs (20 \times) of the right side of the mesencephalon of animals exposed to the various combinations of treatments (Sal=saline; Sham=Vehicle treatment). The sections depicted were immunostained for TH only and were adjacent to those used to generate the data in Figs. 4 and 5. The white line transecting the stained area in the Sal/Sham photomicrograph depicts the dividing point between the VTA (medial to) and the SN (lateral to).

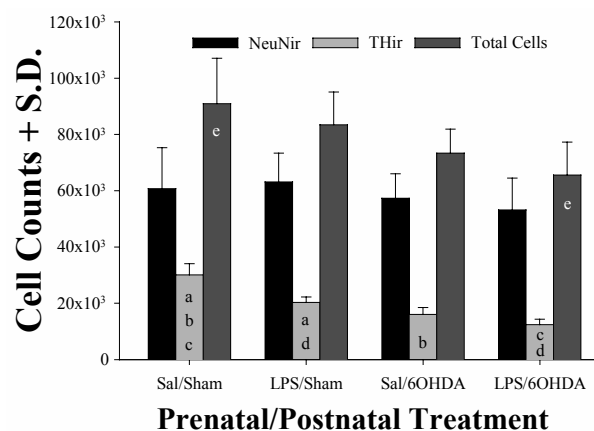


Fig. 4. Stereological cell counts from the SN. The mean THir, NeuNir, and Total Cells (THir+NeuNir) cell counts from the four different treatment groups are shown. Bars which share the same letter are significantly different from one another ($P<0.05$). Sal=saline; LPS=lipopolysaccharide; 6OHDA=6-hydroxydopamine.

Table 1. Stereology data on THir cells in the SN

Prenatal/postnatal	Cell counts	Density	Volume (mm ³)	Cell size (μm ²)
Saline/Sham	30,152±3,916 ^{abc}	9,683±1,150 ^{ab}	3.13±0.39*	180.77±13.51
LPS/Sham	20,293±2,005 ^{ad}	7,734±1,118 ^a	2.64±0.23	174.43±16.00
Saline/6OHDA	16,084±2,443 ^b	8,819±920 ^b	2.36±0.23	189.45±24.67
LPS/6OHDA	12,423±1,933 ^{cd}	5,299±934 ^a	2.35±0.16	227.70±22.10*

Values which share a common letter are significantly different from one another in the same column. * = $P < 0.05$ relative to all other treatment groups in the same column. LPS=lipopolysaccharide; 6OHDA=6-hydroxydopamine.

significantly greater than either of the two treatments alone (Fig. 4). The LPS/Sham animals exhibited a 32.7% decrease in THir cells, which was significantly reduced relative to control animals. The Saline/6OHDA animals similarly exhibited a statistically significant 46.7% THir cell count reduction, which was in excellent agreement with the 50% cell loss anticipated from the 150 μg dose of 6OHDA injected. However, the combined effects of prenatal LPS and postnatal 6OHDA resulted in further statistically significant cell loss (58.8% decrease). As anticipated, the density of the THir cells decreased proportionately with cell loss (Table 1). Interestingly, the cross-sectional cell size of the THir cells was dramatically increased ($P < 0.05$) in the animals exposed to LPS prenatally and injected with 6OHDA postnatally. No other pair-wise comparisons were statistically significant.

In contrast to the effects of pre- and postnatal treatment on THir cell counts, neither of these treatments produced significant changes in the SN NeuNir cell counts (prenatal exposure: $F_{1,22}=0.034$; postnatal treatment: $F_{1,22}=1.971$). Prenatal treatment did not affect total cell counts (i.e. THir+NeuNir: $F_{1,22}=2.188$, $P=0.156$), while postnatal treatment did reduce the total number of cells slightly ($F_{1,22}=11.697$, $P=0.003$) probably reflecting the significant loss of THir cells. The only statistically significant pair-wise comparison for total cells was between the control animals and the LPS/6OHDA animals. Pearson's two-tailed test revealed that the THir cell counts and NeuNir were not significantly correlated ($r^2=0.162$), whereas the THir and the total cell counts were ($r^2=0.622$; $P=0.001$), suggesting that the THir cell loss seen was not simply phenotypic suppression, but actual cell loss.

VTA cell counts

Cell counts in the VTA were assessed in an effort to determine if the prenatal or postnatal treatments produced similar effects to those seen in the SN. Although cell losses were seen in the VTA, the overall effects were significantly less obvious than those seen in the SN (Fig. 3). In the VTA, the average THir cell count was 18,723 in the Saline/Sham group which was 37.8% lower than that seen in the SN. However, the number of THir cells represented 70.75% of the total cells. This percentage is significantly higher than that seen in the SN (33.17%), and likely reflects the fact that the total cell counts for the SN were combined from the THir-rich compacta and THir-poor reticulata region. Regardless, approximately 30% of the cells in the VTA were non-dopaminergic.

Both pre- ($F_{1,22}=4.884$; $P=0.04$) and postnatal ($F_{1,22}=6.081$; $P=0.024$) treatments had a statistically significant effect on the VTA THir cells counts, although the magnitudes of the effects were less than those seen in the SN (Fig. 5). THir cell counts were only reduced by 10.97% by prenatal LPS exposure and 12.2% by 6OHDA, neither of which was significantly reduced relative to controls. The combined effects of both treatments led to a THir cell reduction of only 22.4%, although pair-wise comparisons revealed that this value was significantly reduced relative to the Saline/Sham group. Unlike the effects seen in the SN, the interaction between pre- and postnatal treatments was not statistically significant ($F_{3,22}=0.006$), suggesting that both pre- and postnatal treatment contributed equally to the cell loss seen. Prenatal treatment did not alter NeuNir cell counts, although the effect of postnatal treatment was statistically different ($F_{1,22}=11.26$; $P=0.004$). Total cells were similarly affected only by postnatal treatment ($F_{1,22}=10.997$; $P=0.004$), while no other statistically significant effects were seen.

Striatal DA biochemistry

Striatal DA measurements were made in order to determine if any changes in mesencephalic cell counts were associated with biochemical changes in this target structure. The mean striatal DA content of 221 ng/mg protein in the Saline/Sham group was in excellent agreement with

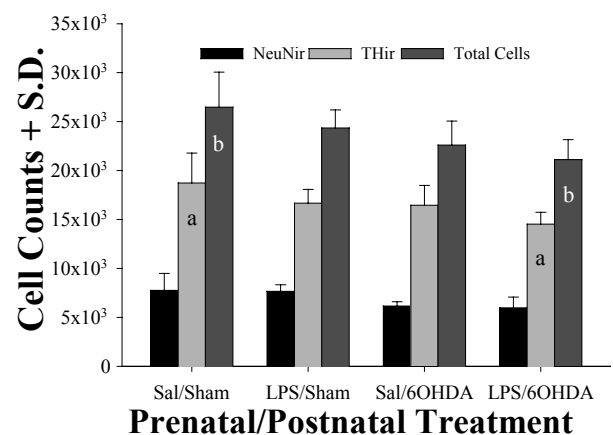


Fig. 5. Stereological cell counts from the VTA. The mean THir, NeuNir, and Total Cells (THir+NeuNir) cell counts from the four different treatment groups are shown. Bars which share the same letter are significantly different from one another ($P < 0.05$). Sal=saline; LPS=lipopolysaccharide; 6OHDA=6-hydroxydopamine.

Table 2. Striatal biochemistry and TNF α levels in the four treatment groups

Prenatal/postnatal	DA (ng/mg protein)	HVA (ng/mg protein)	HVA/DA ratio	Mean striatal TNF α (pg/mg protein)
Saline/Sham	211.51 \pm 9.96 ^a	21.93 \pm 1.63 ^a	0.099 \pm 0.007 ^a	71.49 \pm 6.26 ^a
LPS/Sham	186.70 \pm 18.13 ^a	19.79 \pm 2.18 ^b	0.107 \pm 0.014 ^c	92.65 \pm 4.85 ^a
Saline/6OHDA	116.05 \pm 9.45 ^a	16.33 \pm 0.76 ^a	0.141 \pm 0.008 ^{ac}	86.81 \pm 20.13 ^b
LPS/6OHDA	73.65 \pm 34.52 ^a	13.31 \pm 3.73 ^{ab}	0.193 \pm 0.040 ^{ac}	129.90 \pm 23.62 ^{ab}

Values which share a common letter are significantly different from one another ($P < 0.05$ relative to all other treatment groups in the same column). The mean striatal levels for each of the measures were determined from pooled (left and right) tissue punches taken from each of the four treatment groups. LPS=lipopolysaccharide; 6OHDA=6-hydroxydopamine.

normal levels seen in several previous studies from our laboratory (Vu et al., 2000). Similar to the results seen for the cell counts in the SN, both prenatal ($F_{1,22}=21.998$; $P < 0.001$) and postnatal treatments ($F_{1,22}=176.18$; $P < 0.001$) had statistically significant effects on striatal DA, but unlike the SN cell count data, the interaction term was not significantly altered (Table 2). DA levels in the striatum of the animals exposed to LPS prenatally were reduced 11.7%, while postnatal 6OHDA treatment led to a more pronounced 45.16% DA loss. The combined effects of prenatal LPS exposure and postnatal 6OHDA led to a 65.1% DA loss. All four treatment groups were significantly different from one another. The DA levels in the striatum were highly correlated with the THir cell counts in the SN ($r^2=0.833$; $P < 0.001$). Similar reductions were seen in HVA levels (Table 2).

DA activity (i.e. [HVA]/[DA]) is a widely used index of DA release (Thiblin et al., 1999; D'Astous et al., 2003; Yurek et al., 1998) with increases in this ratio ostensibly reflecting increased DA release and metabolism to HVA. The effects on DA activity were opposite to those seen on DA (Table 2). The ratio in the Saline/Sham animals was 0.099, while the effects of prenatal LPS increased the ratio only 7.7% ($P > 0.05$), yet the overall effects of prenatal treatment were significantly altered ($F_{1,22}=12.066$; $P=0.003$). Postnatal 6OHDA increased the ratio by 42.3% ($F_{1,22}=56.29$; $P < 0.001$), while the combined effects of both treatments increased the ratio dramatically (95.15%) yielding a significant interaction term ($F_{3,22}=6.733$; $P=0.017$) consistent with a super-additive effect of prenatal and postnatal treatments on this index.

Striatal cytokine protein levels

Cytokine levels were assessed in the striatum to determine if prenatal LPS was associated with long-term elevations in TNF α , and if the combined effects of prenatal LPS and postnatal 6OHDA produced further increases in this pro-inflammatory cytokine. IL-1 β levels were also assessed in striatal tissue punches. However, ELISA determinations revealed that all IL-1 β levels were below the lower level of quantification (lower level of quantification=5 pg/ml lysate) for the cytokine kit. In contrast, levels of TNF α were not only detected in all samples studied, but significantly increased by the respective treatments (Table 2). Thus, prenatal LPS exposure led to a statistically significant increase of 29.61% ($F_{1,21}=16.41$; $P < 0.001$), and while TNF α levels in the striatum of animals treated with 6OHDA

were only 21.4% increased ($P > 0.05$), postnatal treatment overall was statistically significant ($F_{1,21}=24.51$; $P < 0.001$). The combined effects of prenatal LPS exposure and postnatal 6OHDA led to a 81.71% increase in TNF α although the interaction term between pre- and postnatal treatments was not statistically significant ($F_{3,21}=2.85$), suggesting that both pre- and postnatal treatments contributed equally to the overall increases seen.

DISCUSSION

Overall, the effects seen in the present study confirm those seen at P10 and P21 in that the prenatal LPS-induced THir cell losses reported in younger animals were still present in P120 animals. This suggests that prenatal LPS treatment produces long-lived effects in the mesencephalon. Similarly, the reductions in DA and increases in DA activity seen at P10 and P21 were still present at P120 as would be suggested by the THir cell losses seen at all time points. TNF α protein levels were also statistically elevated in animals prenatally treated with LPS as was also seen in animals killed at P10 and P21. This later point is significant given the fact that TNF α is known to be increased in the brains of patients with PD (Boka et al., 1994; Hunot et al., 1999). In contrast, IL-1 β levels were elevated in the striatum of P10 animals, but not in P21 animals. In animals killed at P120, these levels were not even detectable, suggesting that the IL-1 β elevations seen in younger animals in response to prenatal LPS exposure were transient.

THir cell loss vs phenotype suppression

The THir and NeuNir cell count data supports our previous assertion that LPS produces actual DA neuron cell loss, and not just phenotypic suppression. Prior studies have shown that neurotrophic factors can rescue THir cells in the SN of animals treated with 6OHDA (Bowenkamp et al., 1995, 1996; Kearns and Gash, 1995; Winkler et al., 1996). These studies suggested that simply assessing THir cell counts can give the false impression that THir cell loss is indicative of DA neuron death. However, combining TH staining with NeuN staining, as was done in the present study, circumvents this problem. So, if the effect of prenatal LPS was simply to suppress TH expression and not kill the cell, the number of THir cell counts would have decreased while the NeuNir cell counts in that same animal would have increased proportionately. This was clearly not the case, and therefore argues that the decreases in the

THir cell counts seen in the P10, P21 and P120 animals reflect the birth of animals with fewer than normal DA neurons.

Pattern of cell loss

The current findings demonstrate that the pattern of LPS-induced DA cell loss is not only preferentially in the lateral nigra, its ventral tier, and in the reticulata, but that the cells of the VTA are relatively spared. Thus, despite the fact that prenatal LPS produced a 33% DA cell loss in the SN, the magnitude of the DA cell loss in the VTA was only 11%. The pattern of cell loss in the SN together with the apparent reduced sensitivity of the VTA is significant because it is similar to the cell loss pattern seen in the mesencephalon of PD patients (Javoy-Agid et al., 1981; Hornykiewicz and Kish, 1987). Furthermore, the decreases in striatal DA and HVA, and increases in DA activity in the animals exposed to LPS prenatally, are similar to those seen in PD patients. This is significant since an increase in the DA activity ratio implies increased DA metabolism, which is thought to lead to increased free radical production and further compromises in DA neuron function (Jenner, 1998). This, together with the increases in the $\text{TNF}\alpha$ seen in these animals, could lead to further DA neuron loss over time.

Absolute THir cell counts in control animals

In the current study, the average number of THir cells in the SN of control animals was 30,152 and in the VTA, 18,732. Previously, Banrezes et al. (2001) reported numbers of 13,518 and 20,372, respectively, while German and Manaye (1993) reported 20,912 and 20,418, respectively. Our average total THir cell count of 48,500 is not dramatically different from that of German and Manaye (1993), but significantly larger than that reported by Banrezes et al. (2001). These differences could reflect differences in animal strain, counting techniques, antibody penetration, and sampling issues. However, a major discrepancy occurs in the cell numbers of cells in the SN relative to the VTA. In the present study we designated the SN as the stained cells lateral to the accessory optic track or, when this landmark was not present, lateral to a line connecting the most inferior point on the dorsal curvature between the THir cells of the SN and the VTA and the most superior point of the ventral curvature. This could under and over-estimate SN cells in some sections which could have contributed to the differences in the cell counts seen. In addition, and of greatest importance, is that we routinely included the lateral regions of the parabrachial pigmented nucleus with our SN assessments. Located immediately dorsal to the compacta (Rodriguez et al., 2001), including this cell-rich, probable A10 region could easily lead to over-estimation of the THir cell counts. Regardless, it was still noteworthy that in both structures, a large percentage of the cells were not THir. This was particularly true in the SN where the non-THir cells counted in the reticulata likely contributed to the low percentage of THir cells. However, even in the compacta where Fig. 2 was taken, it was clear that a large number of cells (NeuNir) in the compacta region were not dopaminergic and likely GABA neurons.

Regardless, statistical analysis revealed that the number of NeuNir cells was not affected by any of the treatments employed suggesting that the toxicity of both prenatal LPS and postnatal i.c.v. 6OHDA were specific to the DA neuron.

Effects of pre- and postnatal toxin exposures on THir cells

The elevations in $\text{TNF}\alpha$ seen in P10 and P21 animals as a result of prenatal LPS exposure, together with the reduced numbers of THir cells, suggested that such animals would be more susceptible to the effects of DA neurotoxins. Since 6OHDA is thought to induce THir cell loss, at least in part, through increased $\text{TNF}\alpha$ (Nagatsu et al., 2000; Cicchetti et al., 2002), we hypothesized that inflammatory synergy between the effects of prenatal LPS and postnatal neurotoxin exposure would produce a greater THir cell loss than LPS or 6OHDA exposure alone. Interestingly, the results from the present study do not support this hypothesis. Although 6OHDA treatment led to DA cell loss in the SN and decreased DA in the striatum, the combined effects of prenatal LPS exposure and postnatal 6OHDA treatment did not lead to greater than expected THir cell loss. The interaction term for THir cell loss and examination of the group means argued that the combined effects of the two toxins were less than additive. This might suggest that prenatal LPS exposure conferred partial resistance to subsequent 6OHDA exposure. Thus, DA neurons within the mesencephalon remaining after prenatal LPS exposure might be less susceptible to 6OHDA, or represent a different subtype of DA neuron that is more resistant to this neurotoxin (e.g. calbindin ir; Rodriguez, 2003). However, although the combined effects of LPS and 6OHDA on DA cell counts were less than additive, the effects on DA and $\text{TNF}\alpha$ were additive, and the effects on DA activity were synergistic. Thus, further studies on the interactions between prenatal LPS and postnatal toxin exposure are warranted in order to adequately characterize the true nature of multiple toxin exposures. These should include time-course studies as well as studies in older animals, both of which could influence the nature of the interaction. Regardless, the data clearly show that animals born with fewer than normal DA neurons will exhibit further loss of DA neurons following exposure to a second toxin like 6OHDA in adult life. This suggests that animals born with fewer than normal DA neurons are at greater risk for compromised DA function in response to subsequent neurotoxin exposure. This is consistent with the often considered notion that several factors might contribute to PD (multifactorial), but that cell loss sufficient to produce PD may require multiple exposures ("multiple hit" concept; Di Monte et al., 2002). Therefore, whether the effect of multiple exposures to environmental toxins is additive or synergistic, the end result is greater compromise to DA function and subsequent increased risk for PD. A study by Gao and colleagues (2003) demonstrated that combining the effects of LPS and the DA neurotoxin rotenone produced synergistic DA neuron loss in tissue culture. They also demonstrated that whether or not an additive or synergistic

effect was produced, was a consequence of dosage and duration of treatment with optimal synergistic effects being seen at low dosages for longer durations (Gao et al., 2003). Thus it is possible that had the animals been exposed to a lower dosage of 6OHDA or had the kill interval been extended longer than three weeks, a synergism may have been seen.

Interestingly, the cell body sizes of the DA neurons in the combined treatment group were significantly enlarged relative to all other treatment groups. We interpret this increase to indicate compensatory increases in neuronal activity and function of remaining neurons, since we have also seen it previously in response to DA depletion-induced increased trophic activity (Vu et al., 2000). If so, then had a larger dosage of 6OHDA been used, or had exposure occurred in older animals where compensatory capacity is attenuated (Ling et al., 2000), a more profound cell loss might have occurred. Regardless, the data clearly shows that animals born with fewer than normal DA neurons will exhibit further loss of DA neurons following exposure to a second toxin like 6OHDA in adult life.

Effects of pre- and postnatal toxin exposures on striatal TNF α levels

The striatal TNF α levels were not increased statistically in the group treated with 6OHDA alone. Previous studies (Mogi et al., 1999, 2000) showed that 6OHDA led to increased levels of striatal TNF α . Failure to detect changes in TNF α in response to 6OHDA in the present study could simply reflect differences in dosage and the time to kill between the two studies. Regardless, the combined effects of both prenatal LPS and postnatal 6OHDA did produce a dramatic 82% increase in TNF α within the striatum. Again, however, this increase was at best additive. Despite this lack of synergism, it is remarkable that a single injection of LPS into a gravid female at E10.5 produced increases in TNF α in her offspring that lasted 132 days. If this increase were to continue into advanced age, it is possible that the combined effects of reduced compensatory activity associated with aging (Yurek and Fletcher-Turner, 2001; Calne and Peppard, 1987) together with the reduced anti-inflammatory environment seen in the aged brain (Saurwein-Teissl et al., 2000) might then combine to produce synergistic DA cell losses.

Body temperature of LPS-exposed gravid females

The mechanism(s) responsible for the LPS induced DA cell loss are unknown at this time, although the data from the P21 animals (Ling et al., 2002b) suggested that the DA neuron loss seen was likely not a consequence of alterations of programmed cell death (apoptotic culling) during development. However, since LPS is a well known inducer of hyperthermia, it was possible that the DA neuron loss seen in the animals was a consequence of hyperthermia, which is a known generalized teratogen (Edwards, 2003) and known to alter neurotransmitter systems (Colado et al., 1999) including DA (Albers and Sonsalla, 1995). However, the results indicated only transient body temperature fluctuations in some LPS-treated gravid dams that were

short-lived and not statistically significant. The inability of LPS to alter body temperature was not a function of gender or gravidity, since neither male rats nor non-gravid females, respectively, exhibited alterations in rectal temperature in response to LPS. The failure of LPS to induce the expected increases in body temperature has been described previously (Fraifeld and Kaplanski, 1998), and was likely a consequence of the very low dosage used in the present study relative to those typically used to produce hyperthermia. Other factors associated with the LPS-induced DA neuron loss that are currently being considered are alterations in the DA neuron progenitor cell population and alterations in fetal TNF α transcription in glia within the developing brain. Regardless, prenatal LPS does appear to produce long-lived reductions in DA cell counts in the mesencephalon coupled with DA biochemical alterations and increases in TNF α that are similar to those seen in patients with PD.

Implications for PD

The current results suggest that prenatal LPS exposure may serve as a risk factor for PD. That prenatal LPS could be a potential risk factor for PD becomes more plausible given that a common condition of pregnancy, BV, leads to fetal LPS exposure. Approximately 14% of pregnant women have BV (Thorsen et al., 1998). Numerous studies have consistently shown that BV leads to increased levels of IL-1 α/β , IL-6, and TNF α in the chorioamniotic environment (Dammann and Leviton, 1997; Purwar et al., 2001; Haefner, 1999; Romero et al., 1989). Moreover BV is known to affect the CNS and has been associated with white matter damage (periventricular leukomalacia), intraventricular hemorrhage, and cerebral palsy (Dammann and Leviton, 1997, 1998; Dammann et al., 2002; Yoon et al., 1997). Thus, it is likely that the brains of many patients who reach adult age will have been exposed to LPS prenatally, and the results from the present study suggest that even mild exposure can disrupt normal DA neuron development when that exposure occurs just prior to the development of the DA neuron. Although it is intriguing to speculate that such patients might exhibit progressive loss of DA neurons which could lead to PD in advanced age, it seems more likely that such individuals would be at increased risk to the DA-depleting effects of DA neurotoxin exposure encountered in later life. This would support the notion that PD is a consequence of exposure to multiple environmental toxins, and further suggests that prenatal toxin exposure should be considered in the pathogenesis of PD. If prenatal LPS exposure is taken into consideration, it could then be argued that the adult toxin dosages needed to produce clinically significant DA depletion in later life might not need to be as large as previously thought, elevating the potential role of environmental DA toxins in the etiopathogenesis of PD.

Acknowledgements—This work was supported by ES10776, NS045316, ES012307, DAMD 17-01-1-0771, The Michael J. Fox Foundation, and the American Parkinson's Disease Association.

REFERENCES

- Albers DS, Sonsalla PK (1995) Methamphetamine-induced hyperthermia and dopaminergic neurotoxicity in mice: pharmacological profile of protective and nonprotective agents. *J Pharmacol Exp Ther* 275:1104–1114.
- Banrezes B, Maurin Y, Verney C (2001) Intrauterine growth retardation does not alter the distribution of tyrosine hydroxylase-immunoreactive neurons of A8, A9 and A10 groups in the rat: a three-dimensional reconstruction study. *Brain Res Dev Brain Res* 126:13–20.
- Betarbet R, Sherer TB, MacKenzie G, Garcia-Osuna M, Panov AV, Greenamyre JT (2000) Chronic systemic pesticide exposure reproduces features of Parkinson's disease. *Nat Neurosci* 3:1301–1306.
- Boka G, Anglade P, Wallach D, Javoy-Agid F, Agid Y, Hirsch EC (1994) Immunocytochemical analysis of tumor necrosis factor and its receptors in Parkinson's disease. *Neurosci Lett* 172:151–154.
- Bouvier MM, Mytilineou C (1995) Basic fibroblast growth factor increases division and delays differentiation of dopamine precursors in vitro. *J Neurosci* 15:7141–7149.
- Bowenkamp KE, David D, Lapchak PL, Henry MA, Granholm AC, Foffer BJ, Mahalik TJ (1996) 6-Hydroxydopamine induces the loss of the dopaminergic phenotype in substantia nigra neurons of the rat: a possible mechanism for restoration of the nigrostriatal circuit mediated by glia cell line-derived neurotrophic factor. *Exp Brain Res* 111:1–7.
- Bowenkamp KE, Hoffman AF, Gerhardt GA, Henry MA, Biddle PT, Hoffer BJ, Granholm AC (1995) Glial cell line-derived neurotrophic factor supports survival of injured midbrain dopaminergic neurons. *J Comp Neurol* 355:479–489.
- Brooks AI, Chadwick CA, Gelbard HA, Cory-Slechta DA, Federoff HJ (1999) Paraquat elicited neurobehavioral syndrome caused by dopaminergic neuron loss. *Brain Res* 823:1–10.
- Calne DB, Peppard RF (1987) Aging of the nigrostriatal pathway in humans. *Can J Neurol Sci* 14:424–427.
- Carvey PM, Terrence J, Maag, Donghui Lin (1994) Injection of biologically active substances into the brain. In: *Methods in neurosciences*, pp 214–234. Academic Press, Inc.
- Castano A, Herrera AJ, Cano J, Machado A (1998) Lipopolysaccharide intranigral injection induces inflammatory reaction and damage in nigrostriatal dopaminergic system. *J Neurochem* 70:1584–1592.
- Castano A, Herrera AJ, Cano J, Machado A (2002) The degenerative effect of a single intranigral injection of LPS on the dopaminergic system is prevented by dexamethasone, and not mimicked by rh-TNF-alpha, IL-1beta and IFN-gamma. *J Neurochem* 81:150–157.
- Cavalleri U, Tammaro AE, Quadri A, Baldoli C, Bonaccorso O (1966) A new approach to the pathogenesis of osteoporosis. *G Gerontol* 14:1187–1189.
- Cicchetti F, Brownell AL, Williams K, Chen YI, Livni E, Isacson O (2002) Neuroinflammation of the nigrostriatal pathway during progressive 6-OHDA dopamine degeneration in rats monitored by immunohistochemistry and PET imaging. *Eur J Neurosci* 15:991–998.
- Cohen BR, Sladek CD (1997) Expression of floor plate in dispersed mesencephalic cultures: role in differentiation of tyrosine hydroxylase neurons. *Exp Neurol* 147:525–531.
- Colado MI, Granados R, O'Shea E, Esteban B, Green AR (1999) The acute effect in rats of 3,4-methylenedioxymethamphetamine (MDA, "eve") on body temperature and long term degeneration of 5-HT neurones in brain: a comparison with MDMA ("ecstasy"). *Pharmacol Toxicol* 84:261–266.
- D'Astous M, Morissette M, Tanguay B, Callier S, Di Paolo T (2003) Dehydroepiandrosterone (DHEA) such as 17beta-estradiol prevents MPTP-induced dopamine depletion in mice. *Synapse* 47:10–14.
- Dammann O, Kuban KC, Leviton A (2002) Perinatal infection, fetal inflammatory response, white matter damage, and cognitive limitations in children born preterm. *Ment Retard Dev Disabil Res Rev* 8:46–50.
- Dammann O, Leviton A (1997) Does prepregnancy bacterial vaginosis increase a mother's risk of having a preterm infant with cerebral palsy? *Dev Med Child Neurol* 39:836–840.
- Dammann O, Leviton A (1998) Infection remote from the brain, neonatal white matter damage, and cerebral palsy in the preterm infant. *Semin Pediatr Neurol* 5:190–201.
- Di Monte DA, Lavasani M, Manning-Bog AB (2002) Environmental factors in Parkinson's disease. *Neurotoxicology* 23:487–502.
- Edwards MJRSK (2003) Effects of heat on embryos and fetuses. *Int J Hyperthermia* 19:295–324.
- Emborg ME, Ma SY, Mufson EJ, Levey AI, Taylor MD, Brown WD, Holden JE, Kordower JH (1998) Age-related declines in nigral neuronal function correlate with motor impairments in rhesus monkeys. *J Comp Neurol* 401:253–265.
- Fortunato SJ, Menon RP, Swan KF, Menon R (1996) Inflammatory cytokine (interleukins 1, 6 and 8 and tumor necrosis factor-alpha) release from cultured human fetal membranes in response to endotoxic lipopolysaccharide mirrors amniotic fluid concentrations. *Am J Obstet Gynecol* 174:1855–1861.
- Fraifeid V, Kaplanski J (1998) Brain eicosanoids and LPS fever: species and age differences. *Prog Brain Res* 115:141–157.
- Gao HM, Hong JS, Zhang W, Liu B (2003) Synergistic dopaminergic neurotoxicity of the pesticide rotenone and inflammogen lipopolysaccharide: relevance to the etiology of Parkinson's disease. *J Neurosci* 23:1228–1236.
- Gasser T (1998) Genetics of Parkinson's disease. *Ann Neurol* 44:S53–S57.
- Gayle DA, Ling Z, Tong C, Landers T, Lipton JW, Carvey PM (2002) Lipopolysaccharide (LPS)-induced dopamine cell loss in culture: roles of tumor necrosis factor-alpha, interleukin-1beta, and nitric oxide. *Brain Res Dev Brain Res* 133:27–35.
- German DC, Manaye KF (1993) Midbrain dopaminergic neurons (nuclei A8, A9, and A10): three-dimensional reconstruction in the rat. *J Comp Neurol* 331:297–309.
- Haefner HK (1999) Current evaluation and management of vulvovaginitis. *Clin Obstet Gynecol* 42:184–195.
- Hornykiewicz O, Kish SJ (1987) Biochemical pathophysiology of Parkinson's disease. *Adv Neurol* 45:19–34.
- Hunot S, Dugas N, Faucheux B, Hartmann A, Tardieu M, Debre P, Agid Y, Dugas B, Hirsch EC (1999) FcepsilonRII/CD23 is expressed in Parkinson's disease and induces, in vitro, production of nitric oxide and tumor necrosis factor-alpha in glial cells. *J Neurosci* 19:3440–3447.
- Javoy-Agid F, Ploska A, Agid Y (1981) Microtopography of tyrosine hydroxylase, glutamic acid decarboxylase, and choline acetyltransferase in the substantia nigra and ventral tegmental area of control and Parkinsonian brains. *J Neurochem* 37:1218–1227.
- Jenner POC (1998) Understanding cell death in Parkinson's disease. *Ann Neurol* 44:S72–S84.
- Jenner P (2001) Parkinson's disease, pesticides and mitochondrial dysfunction. *Trends Neurosci* 24:245–246.
- Kearns CM, Gash DM (1995) GDNF protects nigral dopamine neurons against 6-hydroxydopamine in vivo. *Brain Res* 672:104–111.
- Kordower JH, Rosenstein JM, Collier TJ, Burke MA, Chen YE, LJM, Martel L, Levey AE, Mufson EJ, Freeman TB, Olanow W (1996) Functional fetal nigral grafts in a patient with Parkinson's disease: chemoanatomic, ultrastructural and metabolic studies. *J Comp Neurol* 370:203–230.
- Ling ZD, Collier TJ, Sortwell CE, Lipton JW, Vu TQ, Robie HC, Carvey PM (2000) Striatal trophic activity is reduced in the aged rat brain. *Brain Res* 856:301–309.
- Ling ZD, Gayle DA, Lipton JW, Carvey PM (2002b) Prenatal lipopolysaccharide alters postnatal dopamine in the laboratory rat. In: *Catecholamine research: from molecular insights to clinical medicine* (Nagatsu T, Nabeshima T, McCarty R, Goldstein D, eds), pp 209–212. New York: Kluwer Academic/Plenum Publishers.

- Ling Z, Gayle DA, Ma SY, Lipton JW, Tong CW, Hong JS, Carvey PM (2002a) In utero bacterial endotoxin exposure causes loss of tyrosine hydroxylase neurons in the postnatal rat midbrain. *Mov Disord* 17:116–124.
- Lipton JW, Ling Z, Vu TQ, Robie HC, Mangan KP, Weese-Mayer DE, Carvey PM (1999) Prenatal cocaine exposure reduces glial cell line-derived neurotrophic factor (GDNF) in the striatum and the carotid body of the rat: implications for DA neurodevelopment. *Brain Res Dev Brain Res* 118:231–235.
- Ma SY, Ciliax BJ, Stebbins G, Jaffar S, Joyce JN, Cochran EJ, Kordower JH, Mash DC, Levey AI, Mufson EJ (1999a) Dopamine transporter-immunoreactive neurons decrease with age in the human substantia nigra. *J Comp Neurol* 409:25–37.
- Ma SY, Roytta M, Collan Y, Rinne JO (1999b) Unbiased morphometrical measurements show loss of pigmented nigral neurones with ageing. *Neuropathol Appl Neurobiol* 25:394–399.
- Ma SY, Roytta M, Rinne JO, Collan Y, Rinne UK (1997) Correlation between neuromorphometry in the substantia nigra and clinical features in Parkinson's disease using disector counts. *J Neurol Sci* 151:83–87.
- Menon R, Swan KF, Lyden TW, Rote NS, Fortunato SJ (1995) Expression of inflammatory cytokines (interleukin-1 beta and interleukin-6) in amniochorionic membranes. *Am J Obstet Gynecol* 172:493–500.
- Meszaros K, Bojta J, Bautista AP, Lang CH, Spitzer JJ (1991) Glucose utilization by Kupffer cells, endothelial cells, and granulocytes in endotoxemic rat liver. *Am J Physiol* 260:G7–12.
- Miller AJ, Luheshi GN, Rothwell NJ, Hopkins SJ (1997) Local cytokine induction by LPS in the rat air pouch and its relationship to the febrile response. *Am J Physiol* 272:R857–R861.
- Mogi M, Togari A, Tanaka K, Ogawa N, Ichinose H, Nagatsu T (1999) Increase in level of tumor necrosis factor (TNF)-alpha in 6-hydroxydopamine-lesioned striatum in rats without influence of systemic L-DOPA on the TNF-alpha induction. *Neurosci Lett* 268:101–104.
- Mogi M, Togari A, Tanaka K, Ogawa N, Ichinose H, Nagatsu T (2000) Increase in level of tumor necrosis factor-alpha in 6-hydroxydopamine-lesioned striatum in rats is suppressed by immunosuppressant FK506. *Neurosci Lett* 165–168.
- Mullen RJBSCA (1992) NeuN, a neuronal specific nuclear protein in vertebrates. *Development* 116:201–211.
- Nagatsu T, Mogi M, Ichinose H, Togari A (2000) Changes in cytokines and neurotrophins in Parkinson's disease. *J Neural Transm Suppl* 60:277–290.
- Polymeropoulos MH, Lavedan C, Leroy E, Ide SE, Dehejia A, Dutra A, Pike B, Root H, Rubenstein J, Boyer R, Stenroos ES, Chandrasekharappa S, Athanassiadou A, Papapetropoulos T, Johnson WG, Lazzarini AM, Duvoisin RC, Di Iorio G, Golbe LI, Nussbaum RL (1997) Mutation in the alpha-synuclein gene identified in families with Parkinson's disease. *Science* 276:2045–2047.
- Purwar M, Ughade S, Bhagat B, Agarwal V, Kulkarni H (2001) Bacterial vaginosis in early pregnancy and adverse pregnancy outcome. *J Obstet Gynecol Res* 27:175–181.
- Rodriguez M, Barroso-Chinea P, Abdala P, Obeso J, Gonzalez-Hernandez T (2001) Dopamine cell degeneration induced by intraventricular administration of 6-hydroxydopamine in the rat: similarities with cell loss in Parkinson's disease. *Exp Neurol* 169:163–181.
- Romero R, Manogue KR, Mitchell MD, Wu YK, Oyarzun E, Hobbins JC, Cerami A (1989) Infection and labor: IV Cachectin-tumor necrosis factor in the amniotic fluid of women with intraamniotic infection and preterm labor. *Am J Obstet Gynecol* 161:336–341.
- Saurwein-Teissl M, Blasko I, Zisterer K, Neuman B, Lang B, Grubeck-Loebenstein B (2000) An imbalance between pro- and anti-inflammatory cytokines, a characteristic feature of old age. *Cytokine* 12:1160–1161.
- Sinclair SR, Fawcett JW, Dunnett SB (1999) Dopamine cells in nigral grafts differentiate prior to implantation. *Eur J Neurosci* 11:4341–4348.
- Specht LA, Pickel VM, Joh TH, Reis DJ (1981) Light-microscopic immunocytochemical localization of tyrosine hydroxylase in prenatal rat brain: I. Early ontogeny. *J Comp Neurol* 199:233–253.
- Thiblin I, Finn A, Ross SB, Stenfors C (1999) Increased dopaminergic and 5-hydroxytryptaminergic activities in male rat brain following long-term treatment with anabolic androgenic steroids. *Br J Pharmacol* 126:1301–1306.
- Thiruchelvam M, Richfield EK, Baggs RB, Tank AW, Cory-Slechta DA (2000) The nigrostriatal dopaminergic system as a preferential target of repeated exposures to combined paraquat and maneb: implications for Parkinson's disease. *J Neurosci* 20:9207–9214.
- Thorsen P, Jensen IP, Jeune B, Ebbesen N, Arpi M, Bremmelgaard A, Moller BR (1998) Few microorganisms associated with bacterial vaginosis may constitute the pathologic core: a population-based microbiologic study among 3596 pregnant women. *Am J Obstet Gynecol* 178:580–587.
- Vu TQ, Ling ZD, Ma SY, Robie HC, Tong CW, Chen EY, Lipton JW, Carvey PM (2000) Pramipexole attenuates the dopaminergic cell loss induced by intraventricular 6-hydroxydopamine. *J Neural Transm* 107:159–176.
- Winkler C, Sauer H, Lee CS, Bjorklund A (1996) Short-term GDNF treatment provides long-term rescue of lesioned nigral dopaminergic neurons in a rat model of Parkinson's disease. *J Neurosci* 16:7206–7215.
- Yoon BH, Jun JK, Romero R, Park KH, Gomez R, Choi JH, Kim IO (1997) Amniotic fluid inflammatory cytokines (interleukin-6, interleukin-1beta, and tumor necrosis factor-alpha), neonatal brain white matter lesions, and cerebral palsy. *Am J Obstet Gynecol* 177:19–26.
- Yurek DM, Fletcher-Turner A (2001) Differential expression of GDNF, BDNF, and NT-3 in the aging nigrostriatal system following a neurotoxic lesion. *Brain Res* 891:228–235.
- Yurek DM, Hipkens SB, Hebert MA, Gash DM, Gerhardt GA (1998) Age-related decline in striatal dopamine release and motoric function in brown Norway/Fischer 344 hybrid rats. *Brain Res* 791:246–256.

(Accepted 15 December 2003)

Rotenone potentiates dopamine neuron loss in animals exposed to lipopolysaccharide prenatally

Zaodung Ling^{a,b,*}, Qin A. Chang^a, Chong Wai Tong^a, Susan E. Leurgans^b,
Jack W. Lipton^b, Paul M. Carvey^{a,b}

^aDepartment of Pharmacology, Rush University Medical Center, Chicago, IL 60612, United States

^bDepartment of Neurological Sciences, Rush University Medical Center, Chicago, IL 60612, United States

Received 3 March 2004; revised 26 July 2004; accepted 12 August 2004

Available online 30 September 2004

Abstract

We previously demonstrated that treating gravid female rats with the bacteriotoxin lipopolysaccharide (LPS) led to the birth of offspring with fewer than normal dopamine (DA) neurons. This DA neuron loss was long-lived and associated with permanent increases in the pro-inflammatory cytokine tumor necrosis factor alpha (TNF α). Because of this pro-inflammatory state, we hypothesized that these animals would be more susceptible to subsequent exposure of DA neurotoxins. We tested this hypothesis by treating female Sprague–Dawley rats exposed to LPS or saline prenatally with a subtoxic dose of the DA neurotoxin rotenone (1.25 mg/kg per day) or vehicle for 14 days when they were 16 months old. After another 14 days, the animals were sacrificed. Tyrosine hydroxylase-immunoreactive (THir) cell counts were used as an index of DA neuron survival. Animals exposed to LPS prenatally or rotenone postnatally exhibited a 22% and 3%, respectively, decrease in THir cell counts relative to controls. The combined effects of prenatal LPS and postnatal rotenone exposure produced a synergistic 39% THir cell loss relative to controls. This loss was associated with decreased striatal DA and increased striatal DA activity ([HVA]/[DA]) and TNF α . Animals exposed to LPS prenatally exhibited a marked increase in the number of reactive microglia that was further increased by rotenone exposure. Prenatal LPS exposure also led to increased levels of oxidized proteins and the formation of α -Synuclein and eosin positive inclusions resembling Lewy bodies. These results suggest that exposure to low doses of an environmental neurotoxin like rotenone can produce synergistic DA neuron losses in animals with a preexisting pro-inflammatory state. This supports the notion that Parkinson's disease (PD) may be caused by multiple factors and the result of "multiple hits" from environmental toxins.

© 2004 Elsevier Inc. All rights reserved.

Keywords: Parkinson's diseases; LPS; Rotenone; Prenatal; Environment; Lewy body; Dopamine

Introduction

Environmental factors are thought to contribute to the development of nonfamilial Parkinson's disease (PD). Von Economo's pan encephalitis (Casals et al., 1998) and manganese (Zheng et al., 1998) are considered long-standing members of a growing list of risk factors, while more recent additions include pesticides and fungicides such as dieldrin (Corrigan et al., 2000) and maneb

(Thiruchelvam et al., 2000), respectively (see Adams and Odunze, 1991; Dawson et al., 1995; Di Monte, 2003; for reviews). That environmental factors serve as risk factors for PD was formalized by Calne and Langston (1983). They proposed that exposure to an environmental toxin such as 1-methyl, 4-phenyl, 1,2,3,6 tetrahydropyridine (MPTP) killed a portion of the DA neurons; but not enough cells were lost to produce PD. However, additional age-related DA neuron losses eventually produced sufficient cell losses to cause clinical symptoms. Unfortunately, the vast majority of PD patients cannot identify a specific exposure in their past that was sufficient enough to produce their disease. Although this might suggest that environmental factors are not responsible, it might also

* Corresponding author. Departments of Pharmacology and Neurological Sciences, Cohn Building, Room 410, 1735 West Harrison Street (Cohn 406), Chicago, IL 60612. Fax: +1 312 563 3552.

E-mail address: zling@rush.edu (Z. Ling).

imply the involvement of low doses of toxins acting synergistically. This latter possibility is consistent with the emerging hypothesis that the cause of PD is multifactorial and a result of interacting “multiple hits” involving different toxins (Di Monte, 2003) or gene–toxin interactions (Greenamyre et al., 2003; Le Couteur et al., 2002).

The multiple hit hypothesis is attractive because it raises the possibility of synergistic interactions. This would imply that toxin exposure levels could be low or sporadic, and therefore difficult to detect epidemiologically. It has been widely assumed that these exposures occurred during adult life. However, we previously demonstrated that exposure to a low dose of the bacteriotxin lipopolysaccharide (LPS) during a critical window of vulnerability during fetal development led to the birth of rat pups with fewer than normal DA neurons (Ling et al., 2002a,b). This suggests toxin exposure relevant to PD can also occur in utero. Such exposure frequently occurs in humans as a result of bacterial vaginosis (Dammann and Leviton, 1998; Paige et al., 1998), which is known to complicate approximately 14% of normal births (Thorsen et al., 1998). Interestingly, animals born following prenatal exposure to LPS have long-lived elevations in the pro-inflammatory cytokine tumor necrosis factor alpha (TNF α). This is potentially significant because TNF α can kill DA neurons (McGuire et al., 2001), is increased by several DA neurotoxins (Hornykiewicz and Kish, 1987; Nagatsu et al., 2000), and is elevated in the brains of patients with PD (Boka et al., 1994; Mogi et al., 2000a). If animals exposed to LPS prenatally were exposed as adults to a neurotoxin that increased TNF α or other pro-inflammatory factors, synergistic DA neuron loss might occur.

We previously tested this hypothesis in vivo. Four-month-old male rats exposed to LPS prenatally received a moderate dose of the DA neurotoxin 6-hydroxydopamine (6OHDA; icv) (Ling et al., 2004). Both prenatal LPS exposure and postnatal 6OHDA produced significant DA neuron losses, although the combined effects of both factors were, at best, additive. Although the results supported the hypothesis that “multiple hits” to the DA system can combine to produce significant DA neuron loss, synergism was not seen. The young age of animals and the toxin used were discussed as possible reasons why synergistic cell losses were not seen. In the present study, we evaluated a different DA neurotoxin, the complex I inhibitor rotenone (Fiskum et al., 2003; Sherer et al., 2003), and evaluated it in aged female rats (17 months old) to explore the possibility of synergistic cell loss further. Rotenone is a pesticide that is found naturally in the environment and has been distributed even more widely by man (Gosalvez, 1983; Soloway, 1976). It selectively kills DA neurons in rats (Betarbet et al., 2000, 2002). Here we show that synergistic DA neuron losses do result from exposure to rotenone in animals treated with LPS prenatally.

Materials and methods

Animals

Thirty-six timed-gravid, Sprague–Dawley (Zivic-Miller, Allison Park, PA) female rats were delivered to Rush’s animal facility at gestational day nine \pm 12 h. All animals and their offspring were allowed access to food and water ad libitum and were maintained in an environmentally regulated animal facility for the duration of the study (lights on 0600–1800). The survival surgery was carried out under ketamine and xylazine anesthesia to minimize pain. The protocols and procedures used in these studies were approved by the Institutional Animal Care and Utilization Committee (IACUC) of Rush University.

Prenatal treatments and postnatal groupings

LPS was purchased from Sigma (St. Louis) and dissolved in saline (Hank’s balanced salt solution (HBSS)) at 10,000 endotoxin units (EU)/ml. At embryonic day (E) 10.5, each gravid female received a single injection (intraperitoneal) of either 10,000 EU/kg LPS or HBSS (1 ml/kg; $n = 18$ for each group). This very low dose of LPS was chosen based on prior studies where it was shown to be well tolerated, did not produce fetal demise (Ling et al., 2000), and did not increase the gravid female’s body temperature (Ling et al., 2004). All the animals were monitored daily for obtundation or other signs of distress, and were allowed to deliver their pups normally. The pups were weaned at P21 and housed two per cage with same-sex partners.

The offspring from these gravid females were used in several studies. In the present study, 32 female offspring were used. Fourteen of the 32 animals were from seven different litters that had been exposed to saline (Sal) prenatally and litter pairs were randomly assigned to one of two postnatal treatment groups. One group received rotenone (Rot) infusion (Sal/Rot; $n = 7$) and the other group received vehicle (Veh) infusion (Sal/Veh; $n = 7$). Fourteen animals from seven different litters that had been exposed to LPS prenatally were similarly randomly assigned to the two postnatal treatment groups (LPS/Rot; $n = 7$) or vehicle infusions (LPS/Veh; $n = 7$). Additional two female littermates from each prenatal treatment group were sacrificed and assessed using OxyBlot analysis when they were 16 months old.

Intrajugular rotenone infusion

Rotenone (Sigma) was dissolved in a dimethyl sulphoxide and polyethylene glycol vehicle [DMSO/PEG (1:1)]. Jugular cannulation (right side in all animals) was performed as described previously (Betarbet et al., 2000) under ketamine (100 mg/kg) and xylazine (5 mg/kg) anesthesia. The cannulae were attached to Alzet osmotic

minipumps (2ML1, Alzet Osmotic Pumps, Cupertino, CA) implanted subcutaneously in the napes of the neck. The pumps were designed to deliver 1.25 mg rotenone/kg per day or vehicle for 14 days. At the end of 14 days, the pumps were removed and the skin was sutured. Animals were allowed to recover for an additional 14 days to provide time for development of a stable lesion. After 14 days they were injected with pentobarbital (65 mg/kg; Sigma). Once fully anesthetized, the abdomens were opened, the chests invaded, and the brains perfused with ice-cold saline following insertion of a standard feeding tube (attached to a saline reservoir) into the left common carotid with the vena cava and aorta clamped. Following perfusion, the brains were removed and frozen immediately by immersion in dry ice-cooled 2-methylbutane. Once frozen, the frontal part of the brain (containing the striatum) was cut off and passed to enzyme-linked immunosorbent assay (ELISA) and DA biochemistry. The posterior part of brain (containing the mesencephalon) was immediately submerged in Zamboni's fixative (7.5% saturated picric acid, 12 mM NaH₂PO₄, 88 mM Na₂HPO₄, and 4% paraformaldehyde) for stereology studies. Animals destined for assessment using OxyBlot were sacrificed using the same protocol and perfused. However, the entire brain was frozen.

Tyrosine hydroxylase and microglia immunohistochemistry

Tyrosine hydroxylase (TH) is the rate-limiting, DA-producing enzyme in DA neurons and is widely used as an index of DA neurons (Fishell and Van Der, 1989). The number of TH immunoreactive (THir) cells was assessed using a stereological procedure described in detail elsewhere (Ma et al., 1997; Vu et al., 2000). Briefly, the entire mesencephalon was sliced on a cryostat into consecutive 40- μ m sections. Every sixth section was immunohistochemically processed for TH using mouse anti-rat TH antibody overnight (Immunostar, Stillwater MN; 1:20,000). The endogenous peroxidase activity was eliminated using a 1-h incubation with 0.1% periodate. The immunohistochemical procedure was continued by using a biotinylated horse anti-mouse IgG (0.5%; Vector Laboratories, Burlingame CA) for 1 h and peroxidase conjugated avidin–biotin complex (Vector Laboratories) for 1 h. The chromogen solution used to complete the reaction consisted of 0.05% 3,3'-diaminobenzidine (DAB), 0.5% nickel sulfate, and 0.003% H₂O₂ in I/A solution (10 mM imidazole/50 mM sodium acetate) to obtain a black stain. The sections were washed, mounted on gelatin-coated slides, dehydrated through graded alcohols, cleared in xylenes, and cover-slipped with Permount.

Reactive microglia were revealed using the major histocompatibility complex class II (MHC II) immunoreactivity marker (Ox-6) (Ng and Ling, 1997; Shigematsu et al., 1992). MHC II immunohistochemistry was performed using a primary antibody purchased from NOVUS Biologicals

(Littleton, CO). Mesencephalic sections were immunostained overnight using Ox-6 (diluted 1:5,000). The sections were then processed using the secondary antibody as described above for TH.

Stereology

The estimation of the total number of THir neurons in the SN was determined using the computerized optical dissector method, which allows for the stereological estimation of THir cells in the entire structure independent of size, shape, orientation, tissue shrinkage, or anatomical level using MicroBrightField software (Ling et al., 2004). The antibody penetration throughout the whole tissue section was assessed by dissectors using an imaging capture technique (Kordower, 1996; Ma et al., 1999). The total number (N) of SN neurons was calculated using the formula $N = N_V \cdot V_{SN}$, where N_V is the numerical density and V_{SN} is the volume of the SN, as determined by Cavalieri's principle. The MicroBrightField software was also used to determine the total volume of the SN (in mm³), the density of the cells in that volume (cell counts/mm³), and the cell body size (μ m²).

The SN was segregated from the ventral tegmental area for stereology as described previously (Ling et al., 2004). Briefly, the cells lateral to the accessory optic track were designated as SN, while those medial to the track were considered part of the ventral tegmental area (see Fig. 2).

Biochemistry

DA and its metabolite homovanillic acid (HVA) were measured using HPLC (Lipton et al., 2002) with electrochemical detection in pooled (left and right) tissue punches taken from the center of each striatum as previously described (Vu et al., 2000). DA and HVA were expressed as ng/mg tissue protein (assessed using the Bio-Rad Protein Assay Kit) and the ratio of [HVA]/[DA] was used as an index of DA activity.

Cytokine assessments using ELISA

The cytokine levels were determined as previously described (Ling et al., 2000). Briefly, pooled tissue punches from the left and right striata were submerged in 200 μ l homogenate buffer (Trizma/HCl pH 7.2, 0.1 M, sodium chloride 0.9%, Aprotinin 2%, leupeptin 0.5 μ g/ml, pepstatin 0.7 μ g/ml, and PMSF 200 μ M; all reagents were purchased from Sigma) and homogenized. To each tube, 200- μ l homogenate buffer containing 0.5% NP-40 (Sigma) was then added. The tubes were shaken, centrifuged (10,000 \times g), and the supernatants collected. The levels of TNF α were assessed in each supernatant by an ELISA that was run according to the manufacturer's instructions (R&D Systems, Minneapolis, MN). The plates were read in a Dynatech ELISA plate reader (Dynatech Laboratories, Chantilly, VA) and the concentrations of the cytokines were determined

against a six-point standard curve. The total protein content of each homogenate was determined using the Bio-Rad Protein Assay kit and the quantity of TNF α was expressed as pg/mg total protein.

OxyBlot

Four females, two exposed to LPS prenatally and two exposed to saline, were left in the colony after assigning the other animals to their respective treatment groups. Even though we did not have sufficient animals to perform a formal study, we evaluated the relative levels of oxidized protein in the striata and mesencephalons of these animals using the Oxyblot technique. The OxyBlot technique assesses total protein oxidation and was performed according to the manufacturer's instructions (Intergen, Purchase, NY). Briefly, the striata and mesencephalons from each animal were dissected out and homogenized in lysis buffer containing NP-40 detergent, 2-Me, and proteinase inhibitors. The homogenate was adjusted to 2 μ g/ μ l of protein concentration. Protein was derivatized in a 2,4-dinitrophenylhydrazine (DNPH) solution or control solution for 20 min and neutralized. The samples were loaded onto a 12% polyacrylamide gel. Upon completion of electrophoresis, the protein was blotted overnight onto a piece of nitrocellulose membrane. The membranes then were blocked with a 2% fat-free dry milk/TBS solution followed by sequential incubations with primary and secondary antibodies that were conjugated with horseradish peroxidase enzyme. The protein bands were visualized in a dark room following exposure of X-ray films to the membranes incubated with chemiluminescent reagent (Pharmigen).

α -Synuclein immunohistochemistry and H and E staining

The protocol used for α -Synuclein immunohistochemistry was the same as that used for THir immunohistochemistry except anti- α -Synuclein (1:1,000; Pharmingen) was used as a primary antibody and the DAB was not nickel enhanced. For hematoxylin and eosin (H and E; Sigma) staining, tissue sections were mounted onto coated slides and sequentially stained in hematoxylin and eosin according to the manufacturer's protocol (Sigma). All sections were covered with Permount and cover slips.

Statistics

All data were expressed as the mean \pm SD. Initial examination of the data revealed that the variances across groups were not homogeneous and therefore the raw data were transformed using a log scale after which homogeneity was achieved. The data were then analyzed using two-way ANOVA with prenatal treatment (LPS vs. HBSS) and postnatal treatment (Rot vs. Veh) as factors. Individual differences between treatment groups were determined

using Tukey's HSD post hoc test following one-way ANOVA with significance accepted if $P < 0.05$. Because the biochemical and cell count data were gathered from the same brains, it was possible to determine the relationship, if any, between these two variables. Pearson correlation of striatal DA and THir cell count data was assessed using two-tailed test.

Results

Animals

Overall, the animals tolerated the LPS treatments without difficulty. At birth, the female pups were all full-term and no differences in birth weights were detected (data not shown). The animals developed normally and did not exhibit overt behavioral effects. We had performed a study similar to the current experiment except that 6-month-old males were used and 2.5 mg rotenone/kg per day was used. Unfortunately, at the dosage used, the animals became very sick, several died, and the experiment had to be terminated early. We tested additional animals and eventually chose a dosage of 1.25 mg/kg per day. Overall, the animals tolerated this dosage reasonably well, although one Sal/Veh and one LPS/Rot animal became sick immediately after surgery and another two animals became sick after 10 days and were dropped from the study. The remaining animals (Sal/Veh, $n = 5$; Sal/Rot, $n = 6$; LPS/Veh, $n = 7$; and LPS/Rot, $n = 6$) survived the protocol with no adverse effects or no overt behavioral changes until sacrifice (28 days after surgery) when they were 17 months old. At that time there were no significant differences in their body weights ($F(1,23) = 0.052$).

SN THir cell counts

Overall, the effects of prenatal LPS and postnatal rotenone treatment had a profound and highly significant effect on THir cell counts ($F(3,23) = 15.04$; $P < 0.001$). Prenatal LPS exposure produced a significant reduction in THir cell counts ($F(1,23) = 34.842$; $P < 0.0001$) reducing the average THir cell counts by 22% (Fig. 1; Table 1). In contrast, postnatal rotenone treatment did not statistically alter THir cell counts (3% decrease; $F(1,23) = 3.005$; $P = 0.098$). However, the combined effects of prenatal exposure to LPS together with postnatal exposure to rotenone produced a further, dramatic significant THir cell loss of 39%. The interaction term between the pre- and postnatal treatments was significant ($F(1,23) = 5.717$; $P < 0.05$), suggesting that the effects of LPS and rotenone were synergistic. In addition to alterations in cell counts, the prenatal and postnatal treatments had a similar, statistically significant effect on the density of THir cells (Table 1), but had no significant effects on the volume of the nigra or the size of the individual THir cell bodies.

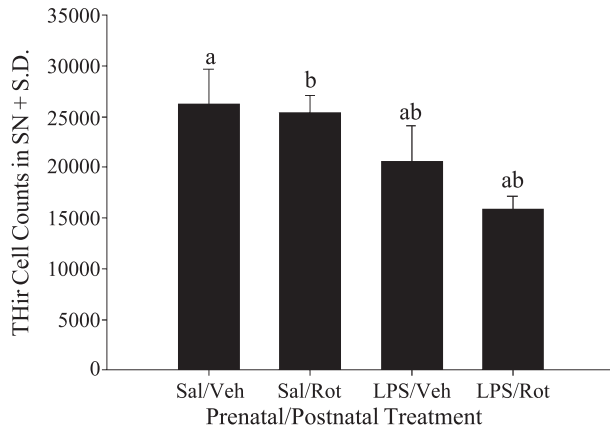


Fig. 1. Tyrosine hydroxylase-immunoreactive (THir) cell counts in the substantia nigra (SN). Stereological cell counts were gathered from animals exposed to lipopolysaccharide (LPS) or Hank's balanced salt solution (Sal) prenatally at E10.5. When they were 16 months old, they were infused for 14 days with rotenone (Rot) or vehicle (Veh). (Bars that share a common letter are significantly different from one another ($P < 0.05$).)

As we have reported in previous studies, the THir cell loss appeared to be primarily in the lateral regions of the substantia nigra and its ventral tier (Fig. 2). This cell loss pattern was similar in animals exposed only to prenatal LPS and those exposed to both prenatal LPS and postnatal rotenone. Interestingly, the apparent intensity of the TH immunoreactivity in the animals treated only with rotenone was decreased, although few cells were lost. This might suggest that rotenone treatment reduced expression of TH without killing the cells. No apparent loss of cells was seen in the ventral tegmental area in any of the treatment groups (data not shown).

Striatal biochemistry

Like the cell count data, the overall effect of treatments had a significant effect on DA levels in the striatum ($F(3,23) = 10.196$; $P < 0.001$). However, unlike the cell count data, two-way ANOVA revealed that both factors (prenatal LPS; $F(1,23) = 8.78$; $P < 0.01$; postnatal Rot exposure; $F(1,23) = 16.76$; $P < 0.001$) significantly reduced striatal DA levels (Fig. 3). Prenatal LPS reduced striatal DA by 12% from that seen in the Sal/Veh group (204.63 ng/mg), while rotenone reduced levels by 22%. Post hoc analysis revealed that these two treatment groups were not significantly different from controls. However, the combined effects of both treatments reduced levels to 47% of normal.

Yet, despite the magnitude of this change, the two-way ANOVA interaction term was not statistically significant ($F(1,23) = 3.309$), suggesting that the change in DA was not synergistic. Regardless, the striatal DA levels were highly correlated with the SN THir cell counts ($r^2 = 0.855$; $P < 0.001$), verifying the relationship between striatal DA loss and reductions in THir cell counts in the SN.

Striatal HVA levels were not statistically different among the four groups ($F(1,23) = 2.203$; data not shown). As expected, as THir cells decreased, DA activity increased proportionately (Fig. 3) and the overall effect on DA activity was highly significant ($F(3,23) = 9.633$; $P < 0.001$). As was true with DA, both prenatal ($F(1,23) = 20.281$; $P < 0.001$) and postnatal treatments ($F(1,23) = 7.034$; $P < 0.05$) significantly increased DA activity, although again, the interaction term was not statistically significant. Post hoc analysis of the ratio of [HVA]/[DA] revealed that the 67.5% increase seen in the LPS/Veh group was significantly elevated relative to that seen in the Sal/Veh group. Although the 40% increase in DA activity seen in postnatal rotenone animals was not statistically significant, the combined effects of both treatments were significantly increased by 85%. Interestingly, the 0.04 DA activity ratio seen in the control females (Sal/Veh) is significantly lower than that normally seen in males, which generally runs around 0.09. Thus, in our previous studies using 4-month-old males, the DA activity ratio was 0.099 (Ling et al., 2004). Because the DA levels in females (204.63 ng/mg protein) were similar to those seen in 4-month-old males (211.51 ng/mg protein), the reduction in DA activity was primarily a consequence of reduced HVA.

Striatal $TNF\alpha$

Overall, the combined effects of prenatal LPS and postnatal Rot produced significant alterations in striatal TNF levels ($F(3,23) = 19.17$; $P < 0.0001$; Fig. 3). However, only the prenatal effects reached statistical significance ($F(1,23) = 51.02$; $P < 0.001$), and while the effects of Rot on TNF α levels were minimal and not statistically significant ($F(1,23) = 3.459$; $P = 0.075$), the combined effects of pre- and postnatal treatments were 91% increase.

Reactive microglia

Reactive microglia were recognized using the OX-6 monoclonal antibody. Microscopic examination of the brain

Table 1
The effect of prenatal LPS and postnatal rotenone on stereological measures in the substantia nigra

Group	Cell count	Density (cells/mm ³)	Volume (mm ³)	Size (μ m ³)
Sal/Veh	26,202.64 \pm 3501.01 ^a	10,666.27 \pm 1659.55 ^a	2.47 \pm 0.12	157.04 \pm 11.16
Sal/Rot	25,394.31 \pm 1677.72 ^b	10,177.67 \pm 837.86 ^b	2.50 \pm 0.15	184.32 \pm 17.50
LPS/Veh	20,527.72 \pm 3613.72 ^{ab}	8347.35 \pm 1267.30 ^{ab}	2.45 \pm 0.13	170.54 \pm 17.49
LPS/Rot	15,901.04 \pm 1286.86 ^{ab}	6307.88 \pm 452.97 ^{ab}	2.53 \pm 0.20	177.08 \pm 22.87

Values that share the same letter are significantly different from one another at the $P < 0.05$ level.

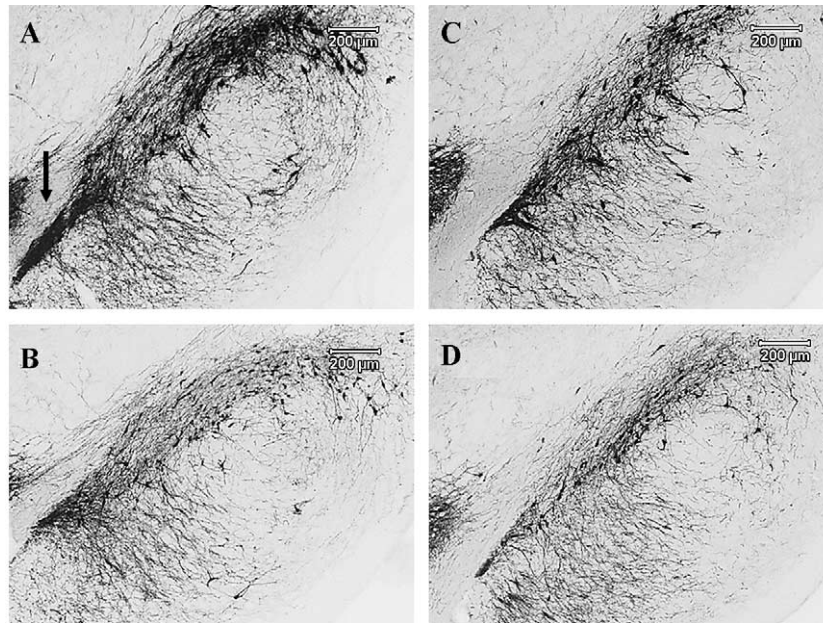


Fig. 2. Photomicrographs of TH immunocytochemistry from the right SN of the four treatment groups. (A) Sal/Veh; (B) Sal/Rot; (C) LPS/Veh; (D) LPS/Rot. Note the reduced intensity of immunostaining in the B and D sections due to exposure to postnatal rotenone infusion. The arrow in A identifies the accessory optic track that defined the medial demarcation point separating the SN from the ventral tegmental area. Scale bar = 200 µm.

sections from animals exposed to saline prenatally and sham treatment postnatally revealed an occasional OX-6ir cell such that in most sections no activated microglia could be seen (Fig. 4). In contrast, the numbers of microglia were markedly elevated in animals exposed to LPS prenatally. These cells were rod shape and possessed numerous reactive processes indicative of activated microglia. Although the numbers of OX-6ir cells were more common than controls

throughout the LPS brains, their numbers were markedly elevated in the SN, and to a lesser extent, in the striatum. A similar pattern was seen in saline animals exposed postnatally to rotenone, although the magnitude of increase was not as profound. However, in animals exposed to LPS prenatally and rotenone postnatally, the number of OX-6ir cells was so markedly increased in the SN that it was visible on gross inspection of the sections (Fig. 4). Again, although

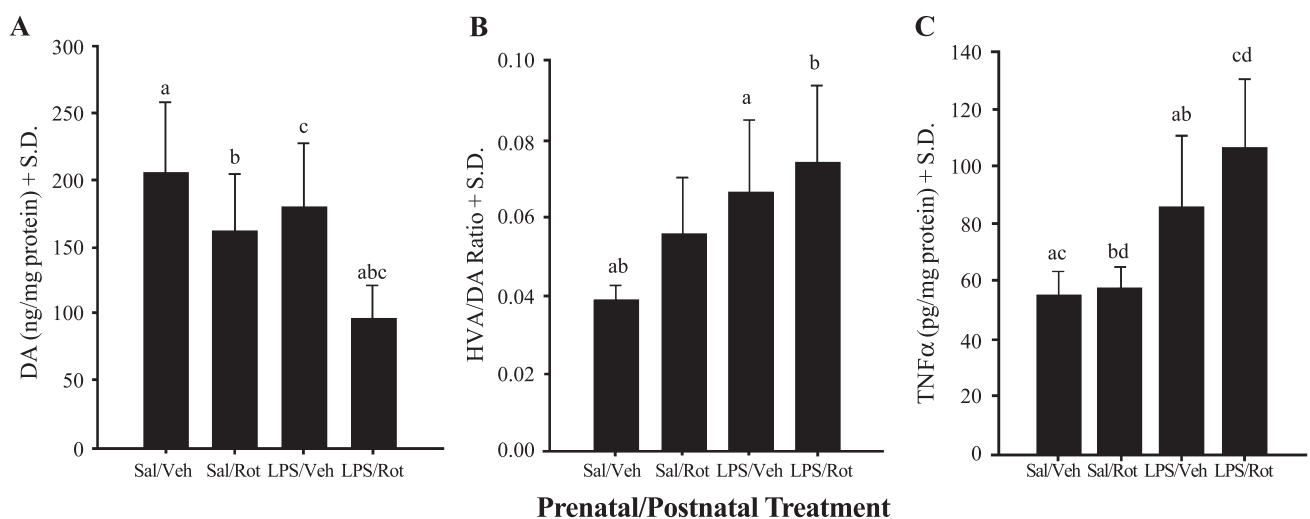


Fig. 3. Dopamine (DA), DA activity, and tumor necrosis factor alpha (TNFα) levels in the striata of the four treatment groups. Animals were exposed to lipopolysaccharide (LPS) or saline (Sal) prenatally and rotenone (Rot) or vehicle (Veh) when they were 16 months old. Striatal DA (A) and DA activity ([HVA]/[DA]) (B) were assessed using HPLC. Striatal TNFα (C) was assessed using ELISA. (Bars that share the same letter are statistically different from one another ($P < 0.05$).)

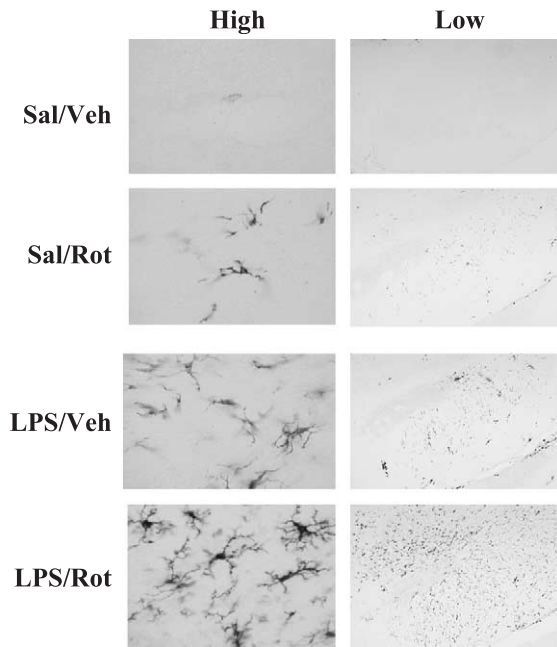


Fig. 4. OX-6-immunoreactive cells in the substantia nigra histochemistry. This photomicrograph represents typical sections in the SN of the four treatment groups. Low: low power magnification ($\times 10$); High: high power magnification ($\times 100$). Sal/Veh: prenatal saline exposure and postnatal vehicle infusion; Sal/Rot: prenatal saline exposure and postnatal rotenone infusion; LPS/Veh: prenatal LPS exposure and postnatal vehicle infusion; LPS/Rot: prenatal LPS exposure and postnatal rotenone infusion. Note that in LPS-exposed animals treated with rotenone, the number of reactive microglia was so pronounced they were overtly visible upon gross inspection.

OX-6ir cells were found throughout the brain in these animals, the density was profoundly elevated in the SN with significant increases also seen in the striatum.

OxyBlot

Two separate sets of animals were assessed using the OxyBlot technique to evaluate the overall oxidation status of animals exposed to LPS or HBSS prenatally just before rotenone treatment. The idea here was that the level of oxidized protein in the 16-month-old animals would be indicative of the overall accumulated protein damage arising from oxidant stress. Overall, there was a dramatic increase in the density of, and number of, protein bands in both the mesencephalons and the striata of the females exposed to LPS prenatally compared with controls (Fig. 5). This suggested that in both structures, the accumulated level of oxidant stress was such that it led to extensive protein oxidation.

α -Synuclein and H and E-positive inclusions

α -Synuclein immunostains of the tissue sections revealed a diffuse, mottled background staining with occasional deep-brown, rounded immunopositive intracellular objects in animals prenatally exposed to LPS (Fig. 6B). These α -

Synuclein-ir objects were similarly present in animals exposed to LPS prenatally and rotenone postnatally. However, these objects were not seen in any of the control animals, although the mottled background staining typical of the treated animals was seen (Fig. 6A).

The H and E sections revealed numerous eosin-positive inclusions in animals exposed to LPS prenatally (Figs. 6D–F). These inclusions were seen in numerous brain regions including cortex, hippocampus, and SN. However, inspection of the sections revealed that the inclusions were more abundant in the SN than in other regions. Interestingly, their distribution appeared to parallel that of microglia. Many of these inclusions were clearly located intracellularly (Fig. 6F). They were smaller than typical Lewy bodies seen in human brain, and did not have the traditional halo often seen around Lewy bodies. Animals exposed to prenatal LPS and postnatal rotenone infusion also exhibited these Lewy-like bodies. Interestingly, the number of inclusion bodies was not noticeably increased in any of brains of animals exposed to both toxins. These inclusions were not seen in any of the control animals.

Discussion

Results from the present study showed that exposure to rotenone, at a dose that failed to alter THir cell counts and had minimal effects on striatal DA in control animals, produced a synergistic loss of THir cells in animals exposed to LPS prenatally. This loss was accompanied by and was correlated with striatal DA losses. The combination of both treatments also increased DA activity and TNF α . This study extends those reported previously in that the DA cell losses and increases in TNF α seen in young animals perinatally (P10 and 21; Ling et al., 2000, 2004) and in young adults (P120; Ling et al., 2004) are still present in aged adults (P510). In addition, the effects of prenatal LPS are not

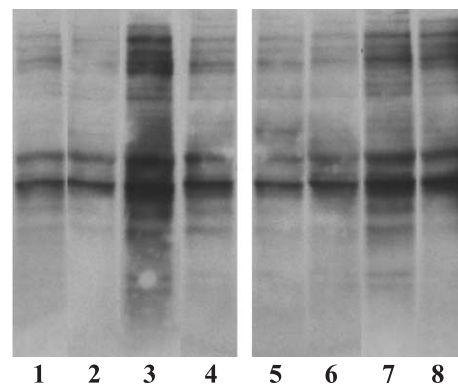


Fig. 5. Chemiluminescence patterns of oxidized protein in animals exposed to Sal (1–2; 5–6) or LPS (3–4; 7–8) prenatally. Gels were loaded with equal amounts of protein from the striata (lanes 1–4) and SN (lanes 5–8), and then exposed to X-ray film. Striata and SNs from animals exposed to LPS prenatally have more oxidized proteins as indicated by the apparent darker bands.

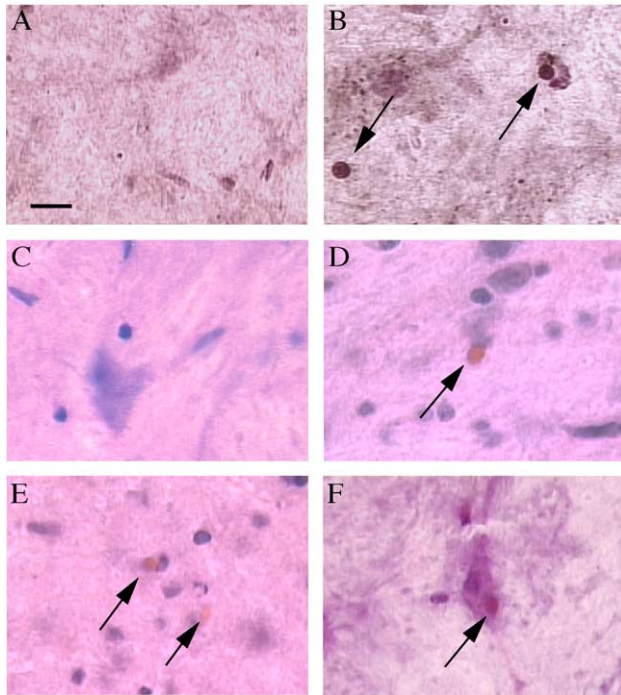


Fig. 6. The α -Synuclein (A and B) and H and E stained sections (C–F) of the SN. α -Synuclein immunoreactivity produced a mottled background staining in control sections (A). In animals exposed to LPS prenatally, deep-brown, spheroid α -Synuclein inclusions were often seen (arrows in B). Hematoxylin and eosin (H and E) processed sections revealed typical backgrounds of reddish-gray interrupted by bluish-black nuclei typical of normal tissue (C). In animals exposed to LPS prenatally (D and F) or LPS and rotenone (E), numerous reddish inclusions were detected (arrows in D and E) and were sometimes seen inside of cells (arrow in F) (scale bar = 5 μ m).

restricted to males, but can be seen in females as well. Furthermore, prenatal LPS exposure was associated with increases in oxidized proteins in both the striatum and mesencephalon, significant increases in microglia activation, and the formation of Lewy-like bodies.

We previously examined animals exposed to LPS prenatally for possible synergistic cell losses following icv 6OHDA treatment. However, in that study, the THir cell loss seen was additive. We suggested that the failure to produce synergistic toxicity was, in part, a consequence of the young age of the animals studied. The present results support this contention. A recent study by Thiruchelvam et al. (2003) further supports this argument. Thus, they showed that the combined neurotoxicity of paraquat and maneb produced greater DA neuron losses in aged mice than in young animals. They also showed that this synergistic toxicity was associated with an attenuated compensatory response to DA neuron loss (i.e., increased DA activity). We have shown that several compensatory responses to DA cell loss including increased DA activity and trophic factor production are reduced in aged animals (Ling et al., 2000). Moreover, pro-inflammatory cytokines such as interleukin-1 and TNF α increase in the aged brain (Kyrkanides et al., 2001; Terao et al., 2002). Indeed, Kalehua et al. (2000)

demonstrated that the pro-inflammatory response of the aged brain to LPS was greater than in young animals. Thus, it is possible that a synergistic response was seen at 17 months, but not after 4 months, because the aged brain is more sensitive to toxins due to reduced compensation coupled with an increased pro-inflammatory response.

It is also possible that differences in toxicity were a consequence of the toxin used. Thus, 6OHDA might not be capable of producing a synergistic response regardless of the age of the animals it is used in, and studies are currently underway to assess this possibility. Another explanation involves dosage. Gao et al. (2003a,b) demonstrated in tissue cultures pretreated with LPS that synergistic THir cell loss was more readily produced when lower concentrations of MPTP or rotenone were used. Interestingly, low dosages of paraquat and maneb were used in studies by Thiruchelvam et al. (2000), and a low dosage of rotenone was used in the present study. Using lower dosages, preferably ones that do not produce overt toxicity, clearly allows greater room for additive and synergistic effects.

As part of the 6OHDA study, we stereologically assessed the loss of THir cells as well as other neurons in the mesencephalon. Those results clearly showed that prenatal LPS, as well as adult exposure to 6OHDA, produced actual DA cell loss and not simply a suppression of the DA neuron phenotype. In addition, the cell loss was almost exclusively in the lateral regions of the substantia nigra and its ventral tier, sparing the ventral tegmental area. This is significant because this pattern of cell loss mimics that seen in PD patients (Hornykiewicz and Kish, 1987; Javoy-Agid et al., 1981). Although not specifically assessed here, the pattern of cell loss was similar to that in the 4-month-old study, and we further assume that the decrease in THir cell counts seen here represents true DA cell loss.

The timing of exposures in the current study differs from the more traditional exposure paradigms where two toxins are often co-administered or administered close together during adulthood. Thus, exposure to the first toxin (LPS) occurred in utero while exposure to the second toxin (rotenone) occurred 17 months later. The prenatal LPS model used here assumes that some type of permanent alteration was produced by exposure to LPS in utero that rendered the animal more susceptible to a toxin exposure that occurred 17 months later. Thiruchelvam et al. (2002) showed a similar effect in mice. They exposed mice to paraquat or maneb perinatally and showed that the mice exhibited a greater than expected DA cell loss to a subsequent challenge to the same toxin during adulthood several months later. They referred to this as a “silent toxicity”. Thus, in their study, as was true in the LPS animals studied here, early exposure did not produce an overtly affected animal, but nonetheless, an animal that exhibited synergistic DA losses following low dose toxin treatment during adulthood. The mechanism(s) responsible for the silent toxicity in the paraquat/maneb model, unfortunately, remains unknown. However, we are beginning to gain

insight into the potential mechanisms involved in the LPS model.

In the present model, prenatal LPS exposure increased DA activity that is known to produce significant free radical production and DA cell death (Jenner, 2003; Spina and Cohen, 1988). Thus, it is possible that the life-long increases in DA activity seen in animals exposed to LPS prenatally perpetuates a cycle of continuous free-radical production that was elevated even further by exposure to a low dose of rotenone. This was not only supported by the significant increases in DA activity seen in animals exposed to LPS alone, but by the increased levels of oxidized proteins seen in the striata and mesencephalons of animals exposed to LPS prenatally. However, it is hard to envision this type of feed-forward inflammatory process lasting for 17 months. An alternative hypothesis involves pro-inflammatory cytokines.

LPS is a known inflammogen and inducer of pro-inflammatory cytokines (Gayle et al., 2002; Paludan, 2000). It is thus possible that elevated levels of TNF α are responsible for, or at least involved with the DA neuron loss, because the levels of this pro-inflammatory cytokine remain elevated for life following prenatal LPS exposure. This hypothesis is particularly attractive because TNF α kills DA neurons (McGuire et al., 2001), is increased by several DA neurotoxins (Hebert et al., 2003; Nagatsu et al., 2000), and is elevated in the brains of patients with PD (Boka et al., 1994; Mogi et al., 2000b). However, one again has to determine how such a phenomenon could occur for life. One potential mechanism involves epigenetic alterations in the genes responsible for TNF α production (Li et al., 2003; Sutherland and Costa, 2003). Thus, if LPSs were able to alter the methylation status of the TNF α promoter in utero, protein levels of TNF α would remain elevated for the life of the animal. Such an elevation would be particularly interesting if it were present in microglia given that their numbers were markedly elevated in LPS animals and that these cells are also the primary source of TNF α in brain (Kielian et al., 2002; Kim et al., 2000). Moreover, because rotenone also appeared to activate microglia, it is possible that microglial activation already present in animals exposed to LPS prenatally produced further increases in TNF α resulting in further DA neuron loss. We are currently exploring this possibility.

Regardless of the cause of the DA cell loss in the animals exposed to LPS prenatally and the synergism associated with subsequent exposure to rotenone, it is clear that the animals described in this study share many characteristics with patients with PD. We examined the sections to determine whether these toxins also induced formation of Lewy-like bodies seen in similar animal model (Betarbet et al., 2000). Alpha-Synuclein-immunoreactive inclusions were detected in the animals exposed to prenatal LPS or animals exposed to prenatal LPS and postnatal rotenone. Moreover, traditional H and E stains of the sections from the LPS animals also revealed the

presence of inclusion bodies resembling Lewy bodies in LPS-exposed animals as well as the animals exposed to LPS and rotenone. Many of these inclusions were present in cell bodies, were found in several brain regions including cortex (although they were more prevalent in the SN), but lacked the halo traditionally seen in human Lewy bodies (Forno, 1996). Rotenone infusion alone was reported to be able to induce Lewy-like inclusion in rat (Betarbet et al., 2000). Therefore, a synergism of prenatal LPS and postnatal rotenone in the inclusion formation was originally predicted. A careful evaluation had demonstrated that this was not the case. The absence of such synergism was believed due to the lower dose of rotenone (1.25 mg/kg per day) and shorter infusion duration (14 days) being used in our current study compared to higher dose (2.5 mg/kg per day) and longer infusion duration (28 days) by other group (Betarbet et al., 2000). The presence of Lewy-like and other inclusion bodies like these was once considered very rare, but is becoming more common in a variety of animal models (Betarbet et al., 2000; Chapman et al., 2003; Fornai et al., 2004; Song et al., 2004). Regardless, they represent an important finding that further validates the animal model. The presence of alpha-Synuclein inclusions and Lewy-like bodies might suggest an abnormality in proteosomal processing (Chung et al., 2003) secondary to increased oxidant stress present in these animals (Jenner and Olanow, 1996). Regardless, the presence of alpha-Synuclein inclusions and Lewy-like bodies suggests that prenatal LPS produces numerous characteristics in animals that are similar to those seen in human PD patients.

Taken together, these studies are consistent with the notion that exposure to multiple DA neurotoxins can combine to produce synergistic DA cell loss supporting the idea that the etiology of PD may be multifactorial and a result of multiple “hits” from environmental toxins. From the perspective of the patient, the notion of synergistic cell losses makes it easier to understand how a cell loss of the magnitude needed to produce PD can occur from environmental events. A synergistic response between two or more toxins, especially resulting from low, subthreshold dosages, could produce the heterogeneous cell loss typical of PD, but not be sufficient enough to produce clinical symptoms. Such an event would be difficult to detect epidemiologically and likely not be recalled by the patient. Homogeneous age-related DA neuron losses could then bring the patient to the symptom threshold as originally proposed by Calne and Langston (1983). Alternatively, exposure to low doses of a second toxin as described in the present study could produce synergistic DA neuron loss that starts 4–7 years before actual symptom expression, and thereby produce the exponential pattern of DA neuron loss predicted by imaging studies of PD patients (Calne et al., 1997; Morrish et al., 1998; Nurmi et al., 2000). Regardless, it is clear that synergistic cell losses resulting from multiple hits with environmental toxins as proposed here or genetic–environ-

mental interactions are consistent with the current clinical phenomenology of PD and are likely to be relevant to our understanding of its pathogenesis.

Acknowledgments

This work was supported by ES10776, NS045316, and The Michael J. Fox Foundation.

References

- Adams Jr., J.D., Odunze, I.N., 1991. Oxygen free radicals and Parkinson's disease. *Free Radical Biol. Med.* 10, 161–169.
- Betarbet, R., Sherer, T.B., Mackenzie, G., Garcia-Osuna, M., Panov, A.V., Greenamyre, J.T., 2000. Chronic systemic pesticide exposure reproduces features of Parkinson's disease. *Nat. Neurosci.* 3, 1301–1306.
- Betarbet, R., Sherer, T.B., Di Monte, D.A., Greenamyre, J.T., 2002. Mechanistic approaches to Parkinson's disease pathogenesis. *Brain Pathol.* 12, 499–510.
- Boka, G., Anglade, P., Wallach, D., Javoy-Agid, F., Agid, Y., Hirsch, E.C., 1994. Immunocytochemical analysis of tumor necrosis factor and its receptors in Parkinson's disease. *Neurosci. Lett.* 172, 151–154.
- Calne, D.B., Langston, J.W., 1983. Aetiology of Parkinson's disease. *Lancet* 2, 1457–1459.
- Calne, D.B., Fuente-Fernandez, R., Kishore, A., 1997. Contributions of positron emission tomography to elucidating the pathogenesis of idiopathic parkinsonism and dopa responsive dystonia. *J. Neural Transm., Suppl.* 50, 47–52.
- Casals, J., Elizan, T.S., Yahr, M.D., 1998. Postencephalitic parkinsonism—A review. *J. Neural Transm.* 105, 645–676.
- Chapman, G., Beaman, B.L., Loeffler, D.A., Camp, D.M., Domino, E.F., Dickson, D.W., Ellis, W.G., Chen, I., Bachus, S.E., Lewitt, P.A., 2003. In situ hybridization for detection of nocardial 16S rRNA: reactivity within intracellular inclusions in experimentally infected cynomolgus monkeys—And in Lewy body-containing human brain specimens. *Exp. Neurol.* 184, 715–725.
- Chung, K.K., Dawson, V.L., Dawson, T.M., 2003. New insights into Parkinson's disease. *J. Neurol.* 250 (Suppl. 3), III15–III24.
- Corrigan, F.M., Wienburg, C.L., Shore, R.F., Daniel, S.E., Mann, D., 2000. Organochlorine insecticides in substantia nigra in Parkinson's disease. *J. Toxicol. Environ. Health* A 59, 229–234.
- Dammann, O., Leviton, A., 1998. Infection remote from the brain, neonatal white matter damage, and cerebral palsy in the preterm infant. *Semin. Pediatr. Neurol.* 5, 190–201.
- Dawson Jr., R., Beal, M.F., Bondy, S.C., Di Monte, D.A., Isom, G.E., 1995. Excitotoxins, aging, and environmental neurotoxins: implications for understanding human neurodegenerative diseases. *Toxicol. Appl. Pharmacol.* 134, 1–17.
- Di Monte, D.A., 2003. The environment and Parkinson's disease: is the nigrostriatal system preferentially targeted by neurotoxins? *Lancet Neurol.* 2, 531–538.
- Fishell, G., Van Der, K.D., 1989. Pattern formation in the striatum: developmental changes in the distribution of striatonigral projections. *Brain Res., Dev. Brain Res.* 45, 239–255.
- Fiskum, G., Starkov, A., Polster, B.M., Chinopoulos, C., 2003. Mitochondrial mechanisms of neural cell death and neuroprotective interventions in Parkinson's disease. *Ann. N. Y. Acad. Sci.* 991, 111–119.
- Fornai, F., Lenzi, P., Gesi, M., Soldani, P., Ferrucci, M., Lazzeri, G., Capobianco, L., Battaglia, G., De Blasi, A., Nicoletti, F., Paparelli, A., 2004. Methamphetamine produces neuronal inclusions in the nigrostriatal system and in PC12 cells. *J. Neurochem.* 88, 114–123.
- Forno, L.S., 1996. Neuropathology of Parkinson's disease. *J. Neuropathol. Exp. Neurol.* 55, 259–272.
- Gao, H.M., Hong, J.S., Zhang, W., Liu, B., 2003a. Synergistic dopaminergic neurotoxicity of the pesticide rotenone and inflammogen lipopolysaccharide: relevance to the etiology of Parkinson's disease. *J. Neurosci.* 23, 1228–1236.
- Gao, H.M., Liu, B., Zhang, W., Hong, J.S., 2003b. Synergistic dopaminergic neurotoxicity of MPTP and inflammogen lipopolysaccharide: relevance to the etiology of Parkinson's disease. *FASEB J.* 17, 1957–1959.
- Gayle, D.A., Ling, Z., Tong, C., Landers, T., Lipton, J.W., Carvey, P.M., 2002. Lipopolysaccharide (LPS)-induced dopamine cell loss in culture: roles of tumor necrosis factor-alpha, interleukin-1beta, and nitric oxide. *Brain Res., Dev. Brain Res.* 133, 27–35.
- Gosalvez, M., 1983. Carcinogenesis with the insecticide rotenone. *Life Sci.* 32, 809–816.
- Greenamyre, J.T., Betarbet, R., Sherer, T.B., 2003. The rotenone model of Parkinson's disease: genes, environment and mitochondria. *Parkinsonism Relat. Disord.* 9 (Suppl. 2), S59–S64.
- Hebert, G., Arsaut, J., Dantzer, R., Demotes-Mainard, J., 2003. Time-course of the expression of inflammatory cytokines and matrix metalloproteinases in the striatum and mesencephalon of mice injected with 1-methyl-4-phenyl-1,2,3,6-tetrahydropyridine, a dopaminergic neurotoxin. *Neurosci. Lett.* 349, 191–195.
- Hornykiewicz, O., Kish, S.J., 1987. Biochemical pathophysiology of Parkinson's disease. *Adv. Neurol.* 45, 19–34.
- Javoy-Agid, F., Ploska, A., Agid, Y., 1981. Microtopography of tyrosine hydroxylase, glutamic acid decarboxylase, and choline acetyltransferase in the substantia nigra and ventral tegmental area of control and Parkinsonian brains. *J. Neurochem.* 37, 1218–1227.
- Jenner, P., 2003. Oxidative stress in Parkinson's disease. *Ann. Neurol.* 53 (Suppl. 3), S26–S36.
- Jenner, P., Olanow, C.W., 1996. Oxidative stress and the pathogenesis of Parkinson's disease. *Neurology* 47, S161–S170.
- Kalehua, A.N., Taub, D.D., Baskar, P.V., Hengemihle, J., Munoz, J., Trambadia, M., Speer, D.L., De Simoni, M.G., Ingram, D.K., 2000. Aged mice exhibit greater mortality concomitant to increased brain and plasma TNF-alpha levels following intracerebroventricular injection of lipopolysaccharide. *Gerontology* 46, 115–128.
- Kielian, T., Mayes, P., Kielian, M., 2002. Characterization of microglial responses to *Staphylococcus aureus*: effects on cytokine, costimulatory molecule, and Toll-like receptor expression. *J. Neuroimmunol.* 130, 86–99.
- Kim, W.G., Mohney, R.P., Wilson, B., Jeohn, G.H., Liu, B., Hong, J.S., 2000. Regional difference in susceptibility to lipopolysaccharide-induced neurotoxicity in the rat brain: role of microglia. *J. Neurosci.* 20, 6309–6316.
- Kordower, J.H., 1996. Functional fetal nigral grafts in a patient with Parkinson's disease: chemoanatomic, ultrastructural, and metabolic studies. In: Rosenstein, J.M., Collier, T.J., Burke, M.A., Chen, Y.E.L.J.M., Martel, L., Levey, A.E., Mufso, E.J., Freeman, T.B., Olanow, W. (Eds.), *The Journal of Comparative Neurology*, vol. 370, pp. 203–230.
- Kyrkanides, S., O'banion, M.K., Whiteley, P.E., Daeschner, J.C., Olschowka, J.A., 2001. Enhanced glial activation and expression of specific CNS inflammation-related molecules in aged versus young rats following cortical stab injury. *J. Neuroimmunol.* 119, 269–277.
- Le Couteur, D.G., Muller, M., Yang, M.C., Mellick, G.D., Mclean, A.J., 2002. Age-environment and gene-environment interactions in the pathogenesis of Parkinson's disease. *Rev. Environ. Health* 17, 51–64.
- Li, S., Hursting, S.D., Davis, B.J., McLachlan, J.A., Barrett, J.C., 2003. Environmental exposure, DNA methylation, and gene regulation: lessons from diethylstilbestrol-induced cancers. *Ann. N. Y. Acad. Sci.* 983, 161–169.
- Ling, Z.D., Collier, T.J., Sortwell, C.E., Lipton, J.W., Vu, T.Q., Robie, H.C., Carvey, P.M., 2000. Striatal trophic activity is reduced in the aged rat brain. *Brain Res.* 856, 301–309.

- Ling, Z., Gayle, D.A., Ma, S.Y., Lipton, J.W., Tong, C.W., Hong, J.S., Carvey, P.M., 2002a. In utero bacterial endotoxin exposure causes loss of tyrosine hydroxylase neurons in the postnatal rat midbrain. *Mov. Disord.* 17, 116–124.
- Ling, Z.D., Gayle, D.A., Lipton, J.W., Carvey, P.M., 2002b. Prenatal lipopolysaccharide alters postnatal dopamine in the laboratory rat. In: Nagatsu, T., Nabeshima, T., McCarty, R., Goldstein, D. (Eds.), *Catecholamine Research: From Molecular Insights to Clinical Medicine*. Kluwer Academic/Plenum Publishers, New York, pp. 209–212.
- Ling, Z.D., Chang, Q., Lipton, J.W., Tong, C.W., Landers, T.M., Carvey, P.M., 2004. Combined toxicity of prenatal bacterial endotoxin exposure and postnatal 6-hydroxydopamine in the adult rat midbrain. *Neuroscience* 124, 619–628.
- Lipton, J.W., Vu, T.Q., Ling, Z., Gyawali, S., Mayer, J.R., Carvey, P.M., 2002. Prenatal cocaine exposure induces an attenuation of uterine blood flow in the rat. *Neurotoxicol. Teratol.* 24, 143–148.
- Ma, S.Y., Roytta, M., Rinne, J.O., Collan, Y., Rinne, U.K., 1997. Correlation between neuromorphometry in the substantia nigra and clinical features in Parkinson's disease using dissector counts. *J. Neurol. Sci.* 151, 83–87.
- Ma, S.Y., Roytt, M., Collan, Y., Rinne, J.O., 1999. Unbiased morphometrical measurements show loss of pigmented nigral neurones with ageing. *Neuropathol. Appl. Neurobiol.* 25, 394–399.
- McGuire, S.O., Carvey, P.M., Ling, Z.D., 2001. Tumor necrosis factor is toxic to mesencephalic dopamine neurons. *Exp. Neurol.* 169, 219–230.
- Mogi, M., Togari, A., Kondo, T., Mizuno, Y., Komure, O., Kuno, S., Ichinose, H., Nagatsu, T., 2000a. Caspase activities and tumor necrosis factor receptor R1 (p55) level are elevated in the substantia nigra from parkinsonian brain. *J. Neural Transm.* 107, 335–341.
- Mogi, M., Togari, A., Tanaka, K., Ogawa, N., Ichinose, H., Nagatsu, T., 2000b. Increase in level of tumor necrosis factor- α in 6-hydroxydopamine-lesioned striatum in rats is suppressed by immunosuppressant FK506. *Neurosci. Lett.* 165–168.
- Morrish, P.K., Rakshi, J.S., Bailey, D.L., Sawle, G.V., Brooks, D.J., 1998. Measuring the rate of progression and estimating the preclinical period of Parkinson's disease with [18F]dopa PET. *J. Neurol., Neurosurg., Psychiatry* 64, 314–319.
- Nagatsu, T., Mogi, M., Ichinose, H., Togari, A., 2000. Changes in cytokines and neurotrophins in Parkinson's disease. *J. Neural Transm., Suppl.*, 277–290.
- Ng, Y.K., Ling, E.A., 1997. Induction of major histocompatibility class II antigen on microglial cells in postnatal and adult rats following intraperitoneal injections of lipopolysaccharide. *Neurosci. Res.* 28, 111–118.
- Nurmi, E., Ruottinen, H.M., Kaasinen, V., Bergman, J., Haaparanta, M., Solin, O., Rinne, J.O., 2000. Progression in Parkinson's disease: a positron emission tomography study with a dopamine transporter ligand [18F]CFT. *Ann. Neurol.* 47, 804–808.
- Paige, D.M., Augustyn, M., Adih, W.K., Witter, F., Chang, J., 1998. Bacterial vaginosis and preterm birth: a comprehensive review of the literature. *J. Nurse-Midwifery* 43, 83–89.
- Paludan, S.R., 2000. Synergistic action of pro-inflammatory agents: cellular and molecular aspects. *J. Leukocyte Biol.* 67, 18–25.
- Sherer, T.B., Betarbet, R., Testa, C.M., Seo, B.B., Richardson, J.R., Kim, J.H., Miller, G.W., Yagi, T., Matsuno-Yagi, A., Greenamyre, J.T., 2003. Mechanism of toxicity in rotenone models of Parkinson's disease. *J. Neurosci.* 23, 10756–10764.
- Shigematsu, K., McGeer, P.L., Walker, D.G., Ishii, T., McGeer, E.G., 1992. Reactive microglia/macrophages phagocytose amyloid precursor protein produced by neurons following neural damage. *J. Neurosci. Res.* 31, 443–453.
- Soloway, S.B., 1976. Naturally occurring insecticides. *Environ. Health Perspect.* 14, 109–117.
- Song, D.D., Shults, C.W., Sisk, A., Rockenstein, E., Masliah, E., 2004. Enhanced substantia nigra mitochondrial pathology in human alpha-Synuclein transgenic mice after treatment with MPTP. *Exp. Neurol.* 186, 158–172.
- Spina, M.B., Cohen, G., 1988. Exposure of striatal [corrected] synaptosomes to L-dopa increases levels of oxidized glutathione [published erratum appears in *J. Pharmacol. Exp. Ther.* 1989 (Jan);248(1):478]. *J. Pharmacol. Exp. Ther.* 247, 502–507.
- Sutherland, J.E., Costa, M., 2003. Epigenetics and the environment. *Ann. N. Y. Acad. Sci.* 983, 151–160.
- Terao, A., Apte-Deshpande, A., Dousman, L., Morairty, S., Eynon, B.P., Kilduff, T.S., Freund, Y.R., 2002. Immune response gene expression increases in the aging murine hippocampus. *J. Neuroimmunol.* 132, 99–112.
- Thiruchelvam, M., Richfield, E.K., Baggs, R.B., Tank, A.W., Cory-Slechta, D.A., 2000. The nigrostriatal dopaminergic system as a preferential target of repeated exposures to combined paraquat and maneb: implications for Parkinson's disease. *J. Neurosci.* 20, 9207–9214.
- Thiruchelvam, M., Richfield, E.K., Goodman, B.M., Baggs, R.B., Cory-Slechta, D.A., 2002. Developmental exposure to the pesticides paraquat and maneb and the Parkinson's disease phenotype. *Neurotoxicology* 23, 621–633.
- Thiruchelvam, M., McCormack, A., Richfield, E.K., Baggs, R.B., Tank, A.W., Di Monte, D.A., Cory-Slechta, D.A., 2003. Age-related irreversible progressive nigrostriatal dopaminergic neurotoxicity in the paraquat and maneb model of the Parkinson's disease phenotype. *Eur. J. Neurosci.* 18, 589–600.
- Thorsen, P., Jensen, I.P., Jeune, B., Ebbesen, N., Arpi, M., Bremmelgaard, A., Moller, B.R., 1998. Few microorganisms associated with bacterial vaginosis may constitute the pathologic core: a population-based microbiologic study among 3596 pregnant women. *Am. J. Obstet. Gynecol.* 178, 580–587.
- Vu, T.Q., Ling, Z.D., Ma, S.Y., Robie, H.C., Tong, C.W., Chen, E.Y., Lipton, J.W., Carvey, P.M., 2000. Pramipexole attenuates the dopaminergic cell loss induced by intraventricular 6-hydroxydopamine. *J. Neural Transm.* 107, 159–176.
- Zheng, W., Ren, S., Graziano, J.H., 1998. Manganese inhibits mitochondrial aconitase: a mechanism of manganese neurotoxicity. *Brain Res.* 799, 334–342.

Intra-parenchymal injection of tumor necrosis factor- α and interleukin 1- β produces dopamine neuron loss in the rat

**P. M. Carvey^{1,2}, E.-Y. Chen², J. W. Lipton^{1,2}, C. W. Tong¹,
Q. A. Chang¹, and Z. D. Ling^{1,2}**

¹ Department of Pharmacology, and

² Department of Neurological Sciences, Rush University Medical Center,
Chicago, IL, USA

Received May 10, 2004; accepted July 31, 2004

Published online December 7, 2004; © Springer-Verlag 2004

Summary. Inflammatory processes are thought to underlie the dopamine (DA) neuron loss seen in Parkinson's disease (PD). However, it is not known if the inflammation precedes that loss, or is a consequence of it. We injected tumor necrosis factor alpha (TNF α) and interleukin 1 beta (IL-1 β) into the median forebrain bundle to determine if these pro-inflammatory cytokines could induce DA neuron loss in the substantia nigra (SN) by themselves. The magnitude of the DA cell loss as well as the decreases in striatal DA, were both dose and time to sacrifice dependent. Injecting both cytokines together produced greater cell losses and DA reductions than that seen when the cytokines were injected alone. The DA neuron loss seen was more pronounced in the lateral nigra and its ventral tier and similar to that seen when other toxins are injected. These data suggest that TNF α and IL-1 β can induce DA neuron loss by themselves and could produce DA neuron loss independent of other inflammatory events.

Keywords: Inflammation, cytokine, Parkinson's disease, rat, infusion.

Introduction

Parkinson's disease (PD) is a progressive neurodegenerative disorder characterized by loss of the dopamine (DA) producing cells in the Substantia Nigra (SN). Although a genetic basis for the disease has been identified for some, the etiology in the majority of the affected patients remains unknown. Regardless of cause, the DA neuron loss and reductions in striatal DA that characterize all patients with PD are accompanied by increases in several pathological indices (Hunot and Hirsch, 2003; Jenner, 2003). Thus, increased levels of cyclooxygenase 2 (Knott et al., 2000), nitrite (Qureshi et al., 1995), oxidized protein (Floor and Wetzel, 1998), oxidized DNA (Zhang et al., 1999), and lipid peroxidation (Yoritaka et al., 1996) as well as decreased levels of the reduced

form of glutathione (Sofic et al., 1992) and impaired mitochondrial Complex I function (Schapira et al., 1990) have all been reported. Some of these changes strongly implicate the involvement of neuroinflammation. Although the central question as to whether these changes are a consequence of DA neuron loss, are the cause of the degenerative process itself, or contribute to the progression of PD remains, there is little controversy about the need to better understand the role of inflammation in this disease process.

The brains of patients with PD also exhibit elevations in proinflammatory cytokines. Thus, Nagatsu et al. (2000) and Boka et al. (1994) have reported elevations in Tumor Necrosis Factor- α (TNF α) and Interleukin 1 beta (IL-1 β) in the brains of patients with PD. These two cytokines in particular, are centrally involved in inflammatory processes, are a product of microglia activation which has also been noted in PD patients (McGeer and McGeer, 1998), and can support many of the inflammatory events known to be increased in PD patients. In addition to studies in patients, animal models of PD and culture systems have also demonstrated that increases in TNF α and IL-1 β are associated with DA neuron loss (Castano et al., 1998; Bronstein et al., 1995; Jarskog et al., 1997; Kabiersch et al., 1998; McGuire et al., 2001; Gayle et al., 2002; Sriram et al., 2002; Ferger et al., 2004; Rousselet et al., 2002). Taken together, these data might suggest that elevations in proinflammatory cytokines lead to DA neuron loss, or at the very least, contribute to further DA neuron loss once the degenerative process has started.

Previous studies have demonstrated that injection of the bacteriotoxin lipopolysaccharide (LPS) directly into the brains of rodents leads to the loss of DA neurons (Castano et al., 1998; Herrera et al., 2000; Kim et al., 1995, 2000; Gao et al., 2002). LPS is a potent inducer of TNF α and IL-1 β (Gayle et al., 2002; Paludan, 2000), and it is possible that the DA cell death seen following LPS may arise as a consequence of increased levels of either of these two cytokines. We have further shown that offspring from gravid rats exposed to LPS during development are born with fewer than normal DA neurons and have life-long increases in TNF α (Carvey et al., 2002; Ling et al., 2002, 2004). In order to ascertain whether or not elevations in TNF α and/or IL-1 β contribute directly to DA cell loss independently of other LPS induced factors, we infused these two pro-inflammatory cytokines alone and in combination into the SN of young adult rats. The results show that these two pro-inflammatory cytokines can indeed produce DA neuron loss suggesting that they are not only associated with the disease process by themselves, but could actually contribute to the DA neuron loss seen in PD.

Materials and method

Animals

Male Sprague-Dawley rats (250–300 g) were purchased from Zivic-Miller (Allison Park, PA), and were allowed to acclimate to the animal facility for a period of at least 5 days before the onset of the experiments. All animals were housed in a temperature and humidity controlled environment, allowed free access to food (Agway Rat Chow; Prolab, Syracuse, NY) and water, and were kept on a 12 hour lights-on/12 hour lights-off cycle (lights on 0600). The protocols and

procedures used in these studies were approved by the Institutional Animal Care and Utilization Committee (IACUC) for Rush University Medical Center.

Cytokine concentrations

Recombinant rat cytokines were purchased from R and D System (Minneapolis, MN), and dissolved in Hank's Balanced Salt Solution (HBSS) with 1% rat serum albumin (vehicle) (Sigma-Aldrich Co.). For control injections the cytokines were heat-inactivated for 1 hr at 65°C in a water bath and dissolved in vehicle (HBSS with 1% rat serum albumin) prior to injection.

The two cytokines were injected at various concentrations alone and in combination. IL-1 β was injected at 100, 200, and 10,000 pg in 3 μ L vehicle. TNF α was injected at 10, 50, and 200 ng in 3 μ L vehicle. 100 pg IL-1 β and 10 ng TNF α concentrations were injected alone and in combination into animals that were sacrificed 14 days later. 10,000 pg IL-1 β and 200 ng TNF α were injected alone and in combination and sacrificed 14 days later. 200 pg IL-1 β and 50 ng TNF α were injected alone and in combination into two groups that were sacrificed 7 and 14 days later, respectively.

Cytokine injections

The rats were anesthetized with pentobarbital (40 mg/kg; Sigma-Aldrich Co.), and placed into a stereotaxic frame. A mid-cranial incision was made and the skin was reflected. A burr hole was then made on the right side of the cranium in all animals using a flexible drill (Foredom Electric Co., Bethel CT) fixed to a micro manipulator. The cytokines or inactivated cytokines were injected over five minutes into the right medial forebrain bundle (AP = -4.3; ML = -1.2; DV = -7.5) using a Hamilton syringe. The needle was left in place for an additional five minutes and then slowly withdrawn. The burr hole was filled with surgical foam and skin sutured. The animals were allowed to recover in their home cages under a heating lamp for 5 hours and then returned to the animal facility. Their general health was monitored daily for the duration of the study.

Perfusion and tissue preparation

At the end of the study, the animals were anaesthetized using an overdose of pentobarbital (65 mg/kg). The chest was invaded and each animal was perfused transcardially using 300 ml ice-cold saline. During perfusion, the descending aorta was clamped to increase perfusion to the brain.

The brains were divided into rostral and caudal sections. The rostral part of the brain (4 mm from the apex) was frozen in the cold 2-methylbutane and sectioned into 1 mm slabs on a cold slate block. The right (ipsilateral to injection) and left (contralateral to the injection) striata were isolated separately. The striatal pieces ipsilateral and contralateral to the cytokine injection were immediately placed in 200 μ l of ice cold antioxidant (0.4 N perchlorate, 0.05% EDTA, and 0.1% bis-metabisulfite). These pieces were then homogenized for 3 secs. using a Polytron GmbH homogenizer (setting 6; Kinematica; Luzern, Switzerland), and centrifuged (30,000 \times G for 30 minutes). The total protein was measured in the pellet using a Protein Assay Kit (Bio-Rad, CA). The supernatants were assessed in duplicate for DA and homovanillic acid (HVA) using High Performance Liquid Chromatography (HPLC) as previously described (Vu et al., 2000) by comparison to 6 point standard curves run daily. The levels were expressed as ng/mg protein. The ratio of [HVA]/[DA] was also computed and served as an index of DA activity.

The caudal part of brain was immediately submerged in Zamboni's fixative (7.5% saturated picric acid, 12 mM NaH₂PO₄, 88 mM Na₂HPO₄, and 4% paraformaldehyde) for immunohistochemistry studies. After three days, Zamboni's fixative was removed and the brains were submerged through two changes of 30% sucrose. The caudal pieces were then sectioned (40 μ m) on a sliding microtome and divided into six series. Sections were kept in cryoprotectant (Glycerol, 30%; Ethylene glycol, 30%; PBS 40%) until processed. Sections were immunostained for tyrosine hydroxylase (TH) as described previously (Ling et al., 2002). The endogenous peroxidase activity was eliminated with a 20-minute incubation in 0.1 M sodium periodate (Sigma Chem. Co.). Sections were then incubated at room temperature for 24 hours with a monoclonal mouse

anti-TH (1:20,000 [Immunostar, MN]; with PBS and 0.25% triton). The staining was followed by incubation with biotinylated horse anti-mouse IgG (Vector Laboratories) and avidin biotin complex (ABC) conjugated with peroxidase (Vector Laboratories). The TH immunoreactive (THir) cells were visualized with I/A solution containing nickel sulfate (2.5%, Sigma), 3,3'-diaminobenzidine (DAB, 0.05%, Sigma), and H₂O₂ (0.003%, Sigma) for a period of 5 minutes followed by 3 washes with I/A. Finally, the slides were dehydrated through graded alcohols and xylene. The slides were eventually cover-slipped (Stephens Scientific) and allowed to dry overnight.

Stereological assessment

The number of THir cell bodies in the SN area were counted by an observer blinded to treatment history using a stereological procedure described previously (Ling et al., 2002). The system used for stereological counting was an Olympus BX-50 microscope that was hard-coupled with a Prior H128 computer-controlled x-y-z motorized stage, a high sensitive Hitachi 3CCD video camera system (Hitachi, Japan), and a PC computer. THir cell counts were carried out using MicroBrightField stereological software. The SN was outlined under a low magnification (10 X) lens and approximately 10% of the outlined region was measured with a systematic, random design using dissector counting frames. Total THir neurons were estimated using the optical dissector method employing a 100 X planapo oil immersion objective with a 1.4 numerical aperture. Under the dissector principle, about 200 THir neurons were sampled by optical scanning using a uniform, systematic and random designed procedure for all measurements. Once the top of the section was in focus, the z-plane was lowered 2.5 μ m (forbidden plane which was not included in the analysis). The total number of THir cells (N) within the SN was calculated using the following formula: $N = N_v \bullet V_{sn}$ where the N_v was the density and V_{sn} was the volume of the SN determined by the Cavalieri principle. THir neurons within the ventral tegmental area (medial to the accessory optic tract (Ling et al., 2004) were excluded from dissector analysis.

Statistical analysis

Two-way ANOVA was performed with treatment and side as factors. Individual group differences within a study were assessed using Tukey's *post hoc* comparison following One-way ANOVA. SN THir cell counts were compared with striatal DA levels using Pearson's correlation.

Results

Overall, the ipsilateral injections did not alter the measures in the contralateral hemisphere (Two-Way ANOVAs on all studies revealed a statistically significant effect of side). In addition, regardless of dose, cytokine, cytokine combination, or time to sacrifice, no statistically significant changes were observed in DA levels or cell counts on the side contralateral to the injection. In contrast, the injections had a profound effect on the measures on the ipsilateral side of the brain.

Striatal biochemistry

In general, injection of IL-1 β and/or TNF α reduced striatal DA and increased DA activity on the side ipsilateral to the injection. In addition, this effect was dose-dependent for both cytokines. The highest combined doses of IL-1 β and TNF α produced the most dramatic changes (Table 1). Thus, DA levels were reduced by both IL-1 β and TNF α injection and the combined injection of both produced further striatal DA loss (Fig. 1; $F_{3,31} = 3.884$; $p < 0.05$). IL-1 β (10 ng) reduced ipsilateral DA 29.9% whereas TNF α (200 ng) reduced levels 54.3%. Although the combined effect of both dosages produced a greater DA decrease (61.2%),

Table 1. Effect of 100 pg, 200 pg, and 10 ng IL-1 β (low, medium, and high dose, respectively) and 10, 50 and 100 ng TNF α (low, medium, and high dose, respectively) on striatal biochemistry and tyrosine hydroxylase immunoreactive (THir) cell counts in the substantia nigra (SN) (Data that shares a common letter within group is significantly different from one another at $p < 0.05$)

Infusion		Low dose	Medium dose (MD)	MD (7 days)	High dose
Dopamine					
Vehicle	Ipsi-	212.12 \pm 22.49	207.36 \pm 29.99 ^{ab}	204.33 \pm 17.19 ^a	201.11 \pm 20.48 ^{ab}
	Contra-	206.73 \pm 19.44	197.26 \pm 25.25	215.51 \pm 25.44	200.73 \pm 12.19
IL-1 β	Ipsi-	199.79 \pm 17.49	178.76 \pm 21.42	206.50 \pm 29.82	140.77 \pm 14.12 ^{ab}
	Contra-	191.83 \pm 25.09	194.88 \pm 30.99	215.51 \pm 25.44	217.13 \pm 19.06
TNF α	Ipsi-	182.34 \pm 14.13	154.46 \pm 53.98 ^a	191.24 \pm 19.73	91.69 \pm 15.29 ^a
	Contra-	218.41 \pm 30.02	204.99 \pm 38.02	202.34 \pm 20.95	242.46 \pm 37.90
IL-1/TNF	Ipsi-	176.11 \pm 16.39	130.03 \pm 7.75 ^b	153.41 \pm 33.44 ^a	77.51 \pm 14.31 ^b
	Contra-	192.86 \pm 20.64	231.74 \pm 24.26	212.44 \pm 23.64	239.10 \pm 51.06
HVA					
Vehicle	Ipsi-	15.66 \pm 5.01	18.74 \pm 4.57	18.76 \pm 4.00	18.62 \pm 2.35 ^{ab}
	Contra-	18.21 \pm 3.02	17.77 \pm 4.46	19.55 \pm 3.54	16.78 \pm 5.31
IL-1 β	Ipsi-	17.31 \pm 4.51	17.20 \pm 4.15	17.94 \pm 4.55	17.91 \pm 2.84 ^{cd}
	Contra-	19.34 \pm 5.82	16.07 \pm 4.80	18.05 \pm 3.73	24.51 \pm 6.10
TNF α	Ipsi-	20.04 \pm 5.27	17.59 \pm 7.86	17.02 \pm 2.95	12.32 \pm 1.66 ^{ac}
	Contra-	18.73 \pm 6.05	22.11 \pm 7.17	19.20 \pm 3.42	24.88 \pm 6.42
IL-1/TNF	Ipsi-	16.42 \pm 4.98	16.82 \pm 4.40	15.43 \pm 3.12	13.20 \pm 0.83 ^{bd}
	Contra-	17.07 \pm 3.96	25.74 \pm 7.81	20.23 \pm 1.98	25.16 \pm 5.28
HVA/DA					
Vehicle	Ipsi-	0.075 \pm 0.026	0.090 \pm 0.017	0.092 \pm 0.022	0.092 \pm 0.007 ^a
	Contra-	0.089 \pm 0.022	0.091 \pm 0.026	0.093 \pm 0.023	0.083 \pm 0.021
IL-1 β	Ipsi-	0.087 \pm 0.022	0.097 \pm 0.024	0.088 \pm 0.023	0.128 \pm 0.025
	Contra-	0.099 \pm 0.021	0.082 \pm 0.017	0.091 \pm 0.019	0.112 \pm 0.018
TNF α	Ipsi-	0.109 \pm 0.020	0.121 \pm 0.065	0.096 \pm 0.030	0.136 \pm 0.024
	Contra-	0.085 \pm 0.025	0.106 \pm 0.016	0.094 \pm 0.008	0.105 \pm 0.030
IL-1/TNF	Ipsi-	0.095 \pm 0.035	0.144 \pm 0.040	0.104 \pm 0.029	0.175 \pm 0.035 ^a
	Contra-	0.089 \pm 0.019	0.110 \pm 0.024	0.096 \pm 0.009	0.138 \pm 0.021
SN THir cell counts					
Vehicle	Ipsi-	12800 \pm 2590	12348 \pm 784 ^{ab}	12212 \pm 1080	12468 \pm 760 ^{ac}
	Contra-	13060 \pm 1731	13968 \pm 4625	12727 \pm 1798	12281 \pm 1568
IL-1 β	Ipsi-	12754 \pm 740	11030 \pm 1413	12920 \pm 245	10720 \pm 813 ^b
	Contra-	11957 \pm 1672	12619 \pm 791	11705 \pm 1333	12486 \pm 972
TNF α	Ipsi-	10372 \pm 1283	10235 \pm 944 ^a	11176 \pm 1683	9620 \pm 2195 ^c
	Contra-	12648 \pm 910	12444 \pm 503	12823 \pm 1354	12964 \pm 1033
IL-1/TNF	Ipsi-	10144 \pm 2030	9423 \pm 1318 ^b	10265 \pm 1502	7524 \pm 1011 ^{ab}
	Contra-	12853 \pm 630	12507 \pm 568	12833 \pm 751	12008 \pm 904

this change was at best additive. The effects on DA activity ([HVA]/[DA]) were similar, although the effects were statistically not as profound (Fig. 1). Thus, the effects of IL-1 β (10 ng) or TNF α (200 ng) injection on [HVA]/[DA] were significantly altered ($F_{3,31} = 6.38$; $p < 0.01$) although the combined effects of both cytokines only increased DA activity 85.1%. Again, the effects of combined cytokines on DA activity was, at best, characterized as additive.

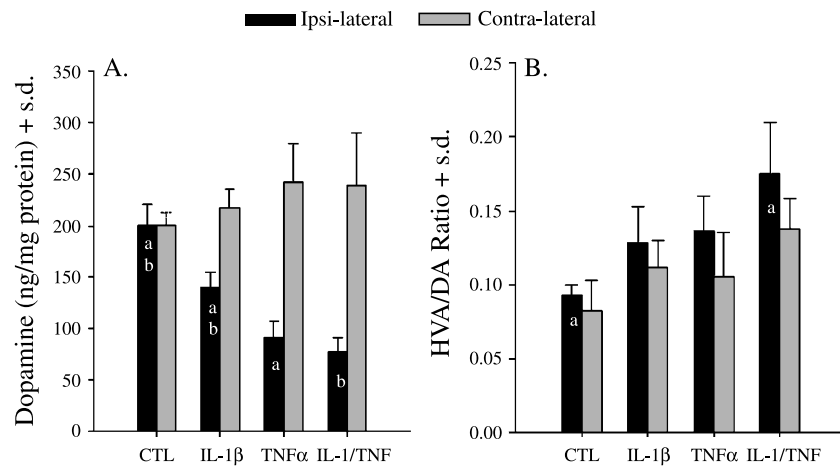


Fig. 1. The effects of IL-1 β (10 ng) and TNF α (200 ng) injected into the medial forebrain bundle (MFB) alone and together on striatal DA content (left) and DA activity (right). Animals were sacrificed 14 days following injection. Bars sharing a common letter are statistically different from one another at $p < 0.05$

Substantia nigra THir cell counts

As was true for the DA biochemical results, the effects on THir cell counts were also dose-dependent (Table 1) and statistically significant (Fig. 2; $F_{3,35} = 3.206$; $p < 0.05$) although the magnitude of the effects was not as profound.

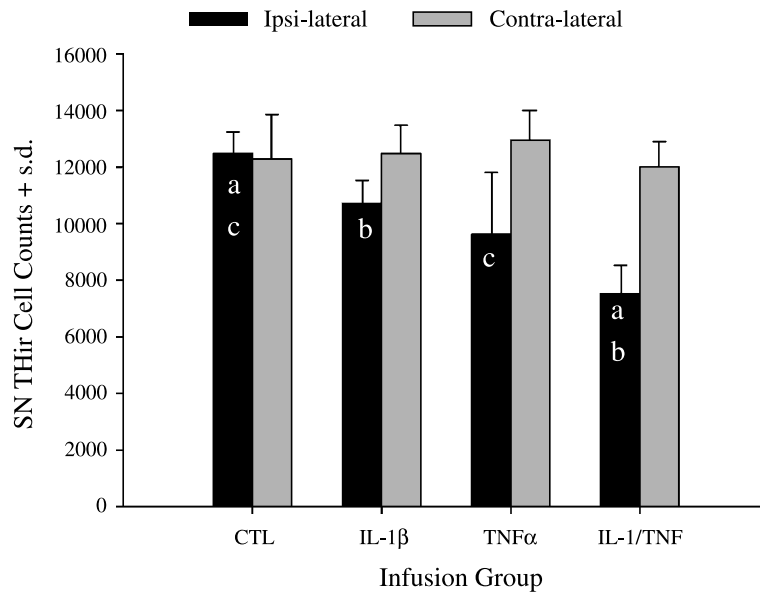


Fig. 2. The effects of IL-1 β (10 ng) and TNF α (200 ng) injected into the medial forebrain bundle (MFB) alone and together on SN THir cell counts. Animals were sacrificed 14 days following injection. Bars sharing a common letter are statistically different from one another at $p < 0.05$

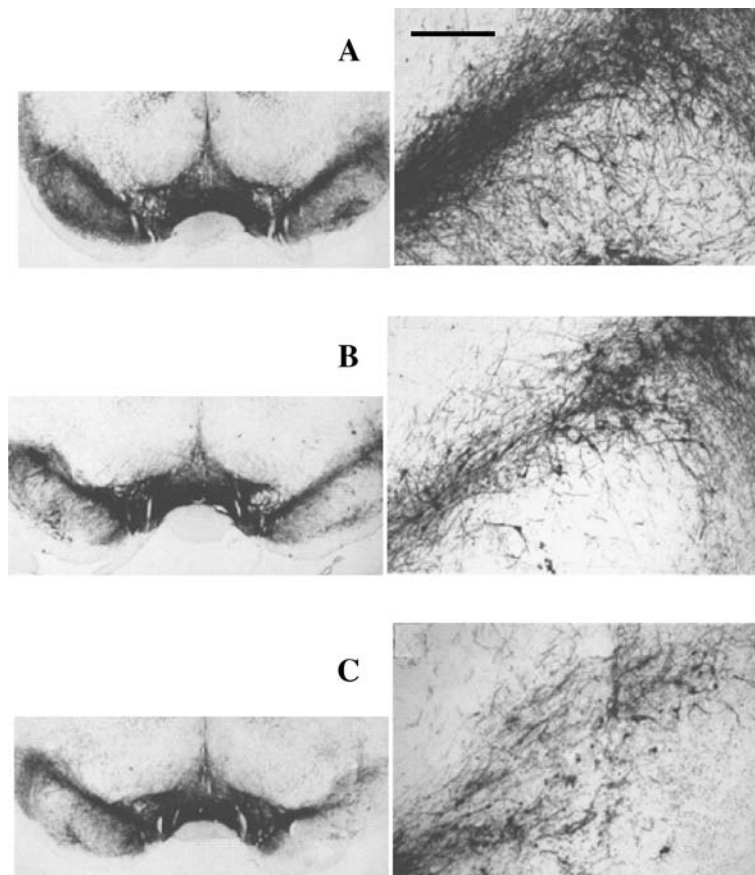


Fig. 3. Representative photomicrographs of the TH immunostaining of the mesencephalon injected with vehicle (**A**), $\text{TNF}\alpha$ (200 ng) (**B**), and $\text{TNF}\alpha$ (200 ng) plus $\text{IL-1}\beta$ (10 ng) (**C**). Note that the pattern of cell loss is most pronounced in the lateral regions of the SN ipsilateral to injection and its ventral tier while sparing the VTA (right side in the left column). Within the areas of cell loss, the density of the immunoreactivity is reduced as seen in the associated higher power photomicrographs of the same sections (right column). Bar = 0.50 mm

Thus, injection of $\text{IL-1}\beta$ (10 ng) produced a 12.2% decrease in THir cell counts while $\text{TNF}\alpha$ (200 ng) produced a 21.1% decrease. Both injections combined produced a 36.7% decrease in THir cell counts. Examination of the THir histology in the animals suggested that injection of either cytokine or combination produced greater cell loss in the lateral regions of the SN and its ventral tier (Fig. 3), but did not alter cell counts in the ventral tegmental area (VTA). The SN THir cell counts were positively correlated with the levels of DA in the striatum ($r = 0.608$, $P < 0.001$).

Effect of recovery period after injection

In one study, the animals were sacrificed 7 days following acute injection, while a second group was sacrificed after 14 days. Interestingly, neither $\text{IL-1}\beta$ nor $\text{TNF}\alpha$ altered DA biochemistry or THir cell counts in the animals sacrificed 7

days after injection (Table 1). In contrast, both striatal DA and THir cell counts were decreased in animals sacrificed 14 days following injection suggesting that these losses were affected by the duration of recovery.

Discussion

The results from the present study revealed that IL-1 β and, in particular, TNF α were both able to induce THir neuron loss, reduce striatal DA and increase DA activity in a dose- and time-to sacrifice-dependent fashion. Both pro-inflammatory cytokines had this effect and when both cytokines were combined, the effects seen were more pronounced, although best characterized as additive. Indeed, the combined effects of both agents often produced less than additive effects. In addition, the relative ability to produce a loss of THir cells was dependent upon how long after injection the animals were examined. Thus, at an intermediate dose (200 pg IL-1 β or 50 ng TNF α), significant alterations were not seen after 7 days, but by 14 days, both THir cell counts and striatal DA were decreased. Taken together, these results extend previous studies and suggest that IL-1 β and/or TNF α can induce DA neuron loss independent of other actions resulting from LPS exposure.

A previous study by Castano and colleagues (2002) injected TNF α and/or IL-1 β into the SN and analyzed the brains one week after injection. They injected only one dose of each cytokine that was 10 times lower than our highest dose of TNF α (1,000 U = \sim 20 ng), but 10 times lower than our highest dose of IL-1 β (1,000 U = \sim 100 ng). In their study, they failed to demonstrate any significant changes in striatal biochemistry or DA cell counts in the SN seven days after injection, despite seeing reductions in these parameters following intranigral LPS injection. They argued that mechanisms other than IL-1 β and TNF α must be responsible for the cell loss seen. The apparent differences between their results and the current findings are likely a consequence of several differences in experimental procedure. First, we also failed to demonstrate reductions in the DA indices one week after the injection and also observed that the effects were dose-dependent. Had they used different dosages or waited longer until sacrifice, they may also have seen statistically significant effects. Second, they injected the cytokines directly into the SN. This produces only focal distribution of the injectate. In contrast, we injected the cytokines into the medial forebrain bundle just rostral to the SN. Injections at this location are distributed more evenly throughout the SN by coursing back to the cell bodies along the low resistance fiber bundles coming out of the nigra (Carvey et al., 1994). Indeed, examination of photomicrographs of the SN in their manuscript revealed THir cell loss only around the needle site in contrast to the cell loss seen in our study which was more widely distributed. Finally, just because LPS was able to produce DA cell loss in their study while the cytokines did not, does not rule IL-1 β and TNF α out as the factors responsible for DA cell loss. There are issues of the dose of LPS used and the resulting increases in the pro-inflammatory cytokines that must be considered. It also, however, does not rule out the possibility that indeed factors in addition to IL-1 β and/or TNF α are involved in the toxicity as originally suggested in their study. Regardless, it

is clear from the present results that IL-1 β and TNF α can indeed produce DA neuron loss by themselves.

The fact that IL-1 β and/or TNF α produced DA cell loss after a single acute injection is remarkable, especially given the fact that significant losses required two weeks to develop. This might suggest that these pro-inflammatory cytokines either induced a cascade of events that required a prolonged period of time to kill the DA neuron, or directly killed the DA neurons, but did so slowly. A previous study demonstrated that TNF α kills DA neurons via apoptosis (McGuire et al., 2001), but this is generally a rapid process taking only 24 hours. However, even if a necrotic mechanism were involved, it is unlikely that the cell death would require more than a week. IL-1 β and TNF α are known to participate in a positive, feed-forward fashion to increase the effect of one another. Thus, IL-1 β increases the release of TNF α (Chao et al., 1995) while TNF α increase IL-1 β (Cai et al., 2003). Anti-inflammatory cytokines are likely involved in limiting this response. However, these reciprocal feed-forward mechanisms, similarly develop rapidly (Cai et al., 2003). It is also important to appreciate that loss of DA neurons leads to increases in DA metabolism, as seen in the current study where DA activity was significantly increased. This is associated with increased production of reactive oxygen species (ROS) which, by themselves, also increase production of pro-inflammatory cytokines (Jenner, 2003). However, all of these processes would develop quickly.

It is also possible that the injected cytokines recruited the activity of another cell type. Indeed, Gao et al. (2002), demonstrated that a slow infusion of LPS into brain led to loss of DA neurons that was delayed and associated with the localized activation of microglia. Despite the infusion of LPS and the presumed increased production of pro-inflammatory cytokines such as TNF α and IL-1 β produced by LPS, DA neurodegeneration was not seen in the animals for at least 4 weeks and continued even after discontinuation of the LPS infusion. Thus, the results from Gao and colleagues are not unlike those reported here. This may be significant since activated microglia are present in the PD brain where they are often seen in proximity to degenerating DA neurons (McGeer et al., 1988). Activated microglia are also often associated with degenerating DA neurons in animals treated with the DA neurotoxin 1-methyl-4-phenyl-1,2,3,6-tetrahydropyridine (MPTP; McGeer et al., 2003). It is thus possible in the present study that the injected cytokines initiated a low level inflammatory response that produced a small amount of cell loss and recruited microglia into the vicinity. This led to further inflammatory events (e.g., ROS resulting from increased DA activity) that recruited additional microglia that participated in a feed-forward process that was eventually able to produce significant cell loss. Although the exact mechanism(s) responsible for the cell loss in the current study is unknown, it is important that it (they) be determined so as to provide potential clues for the delayed and prolonged cell loss seen in patients with PD.

The pattern of DA cell loss in these animals was similar to that seen in animals exposed to other DA neuron toxins including 6-hydroxydopamine (Rodriguez et al., 2001), MPTP (Varastet et al., 1994), and prenatal LPS (Ling et al., 2004). The pattern seen in the present study is also similar to that seen in patients with PD (Hornykiewicz and Kish, 1987; Javoy-Agid et al., 1981).

Thus, cells in the lateral regions of the SN as well its ventral tier were more affected than cells in the ventral tegmental area (VTA) or more medial regions of the SN. The fact that four different toxins produce the same pattern of cell loss would suggest a common mechanism is involved or, that there is a selective vulnerability at work as originally hypothesized (Mouatt-Prigent et al., 1994).

It is likely that PD is a consequence of multiple etiological agents that are a consequence of several risk factors that involve both genetic predispositions and environmental insults. Regardless of cause, it appears that inflammatory events are involved. A central question has been, and remains; “is inflammation a consequence of the degenerative process or the cause of the DA cell loss?” The results from the present study clearly suggest that inflammation by itself can produce DA cell loss. Although it seems intuitively obvious, it demonstrates the possibility that DA cell loss does not necessarily need to be involved with the initial stages of PD pathogenesis. Thus, an initiating agent does not have to be a DA neurotoxin. Rather, it could be a non-specific toxin that produces inflammation that then happens to kill DA neurons. If true, the list of possible environmental causes and genetic risk factors would be significantly broadened.

Acknowledgements

This work was supported by a grant from the Department of Defense (17-01-1-0771), NIEHS (ES10776) and NINDS (NS0453161).

References

- Boka G, Anglade P, Wallach D, Javoy-Agid F, Agid Y, Hirsch EC (1994) Immunocytochemical analysis of tumor necrosis factor and its receptors in Parkinson's disease. *Neurosci Lett* 172: 151–154
- Bronstein DM, Perez-Otano I, Sun V, Mullis SS, Chan J, Wu GC, Hudson PM, Kong LY, Hong JS, McMillian MK (1995) Glia-dependent neurotoxicity and neuroprotection in mesencephalic cultures. *Brain Res* 704: 112–116
- Cai Z, Pang Y, Lin S, Rhodes PG (2003) Differential roles of tumor necrosis factor- α and interleukin-1 β in lipopolysaccharide-induced brain injury in the neonatal rat. *Brain Res* 975: 37–47
- Carvey PM, Maag TJ, Lin DH (1994) Injection of biologically active substances into the brain. In: Flanagan RT et al. (eds) *Providing pharmacological access to the brain*. Academic Press, New York, pp 214–234
- Carvey PM, Chang Q, Tong CW, Landers TM, Ling ZD (2002) Prenatal lipopolysaccharide (LPS) produces permanent and specific dopamine (DA) cell loss in the substantia nigra of the rat associated with Lewy-like bodies. *SFN, 32nd Annual meeting*, 3868
- Castano A, Herrera AJ, Cano J, Machado A (1998) Lipopolysaccharide intranigral injection induces inflammatory reaction and damage in nigrostriatal dopaminergic system. *J Neurochem* 70: 1584–1592
- Castano A, Herrera AJ, Cano J, Machado A (2002) The degenerative effect of a single intranigral injection of LPS on the dopaminergic system is prevented by dexamethasone, and not mimicked by rh-TNF- α , IL-1 β and IFN- γ . *J Neurochem* 81: 150–157
- Chao CC, Hu S, Sheng WS, Peterson PK (1995) Tumor necrosis factor- α production by human fetal microglial cells: regulation by other cytokines. *Dev Neurosci* 17: 97–105
- Ferger B, Leng A, Mura A, Hengerer B, Feldon J (2004) Genetic ablation of tumor necrosis factor- α (TNF- α) and pharmacological inhibition of TNF-synthesis attenuates MPTP toxicity in mouse striatum. *J Neurochem* 89: 822–833

- Floor E, Wetzel MG (1998) Increased protein oxidation in human substantia nigra pars compacta in comparison with basal ganglia and prefrontal cortex measured with an improved dinitrophenylhydrazine assay. *J Neurochem* 70: 268–275
- Gao HM, Jiang J, Wilson B, Zhang W, Hong JS, Liu B (2002) Microglial activation-mediated delayed and progressive degeneration of rat nigral dopaminergic neurons: relevance to Parkinson's disease. *J Neurochem* 81: 1285–1297
- Gayle DA, Ling Z, Tong C, Landers T, Lipton JW, Carvey PM (2002) Lipopolysaccharide (LPS)-induced dopamine cell loss in culture: roles of tumor necrosis factor- α , interleukin-1 β , and nitric oxide. *Brain Res Dev Brain Res* 133: 27–35
- Herrera AJ, Castano A, Venero JL, Cano J, Machado A (2000) The single intranigral injection of LPS as a new model for studying the selective effects of inflammatory reactions on dopaminergic system. *Neurobiol Dis* 7: 429–447
- Hornykiewicz O, Kish SJ (1987) Biochemical pathophysiology of Parkinson's disease. *Adv Neurol* 45: 19–34
- Hunot S, Hirsch EC (2003) Neuroinflammatory processes in Parkinson's disease. *Ann Neurol* 53 [Suppl 3]: S49–S58
- Jarskog LF, Xiao H, Wilkie MB, Lauder JM, Gilmore JH (1997) Cytokine regulation of embryonic rat dopamine and serotonin neuronal survival in vitro. *Int J Dev Neurosci* 15: 711–716
- Javoy-Agid F, Taquet H, Ploska A, Cherif-Zahar C, Ruberg M, Agid Y (1981) Distribution of catecholamines in the ventral mesencephalon of human brain, with special reference to Parkinson's disease. *J Neurochem* 36: 2101–2105
- Jenner P (2003) Oxidative stress in Parkinson's disease. *Ann Neurol* 53 [Suppl 3]: S26–S36
- Kabiersch A, Furukawa H, del Rey A, Besedovsky HO (1998) Administration of interleukin-1 at birth affects dopaminergic neurons in adult mice. *Ann NY Acad Sci* 840: 123–127
- Kim CH, Song YH, Park K, Oh Y, Lee TH (1995) Induction of cell death by myristylated death domain of p55 TNF receptor is not abolished by Iprcg-like point mutation in death domain. *J Inflamm* 45: 312–322
- Kim WG, Mohny RP, Wilson B, Jeohn GH, Liu B, Hong JS (2000) Regional difference in susceptibility to lipopolysaccharide-induced neurotoxicity in the rat brain: role of microglia. *J Neurosci* 20: 6309–6316
- Knott C, Stern G, Wilkin GP (2000) Inflammatory regulators in Parkinson's disease: iNOS, lipocortin-1, and cyclooxygenases-1 and -2. *Mol Cell Neurosci* 16: 724–739
- Ling Z, Gayle DA, Ma SY, Lipton JW, Tong CW, Hong JS, Carvey PM (2002) In utero bacterial endotoxin exposure causes loss of tyrosine hydroxylase neurons in the postnatal rat midbrain. *Mov Disord* 17: 116–124
- Ling ZD, Chang Q, Lipton JW, Tong CW, Landers TM, Carvey PM (2004) Combined toxicity of prenatal bacterial endotoxin exposure and postnatal 6-hydroxydopamine in the adult rat midbrain. *Neuroscience* 124: 619–628
- McGeer PL, Itagaki S, Boyes BE, McGeer EG (1988) Reactive microglia are positive for HLA-DR in the substantia nigra of Parkinson's and Alzheimer's disease brains. *Neurology* 38: 1285–1291
- McGeer PL, McGeer EG (1998) Glial cell reactions in neurodegenerative diseases: pathophysiology and therapeutic interventions. *Alzheimer Dis Assoc Disord* 12 [Suppl 2]: S1–S6
- McGeer PL, Schwab C, Parent A, Doudet D (2003) Presence of reactive microglia in monkey substantia nigra years after 1-methyl-4-phenyl-1,2,3,6-tetrahydropyridine administration. *Ann Neurol* 54: 599–604
- McGuire SO, Carvey PM, Ling ZD (2001) Tumor necrosis factor is toxic to mesencephalic dopamine neurons. *Exp Neurol* 169: 219–230
- Mouatt-Prigent A, Agid Y, Hirsch EC (1994) Does the calcium binding protein calretinin protect dopaminergic neurons against degeneration in Parkinson's disease? *Brain Res* 668: 62–70
- Nagatsu T, Mogi M, Ichinose H, Togari A (2000) Changes in cytokines and neurotrophins in Parkinson's disease. *J Neural Transm [Suppl]*: 277–290

- Paludan SR (2000) Synergistic action of pro-inflammatory agents: cellular and molecular aspects. *J Leukoc Biol* 67: 18–25
- Qureshi GA, Baig S, Bednar I, Sodersten P, Forsberg G, Siden A (1995) Increased cerebrospinal fluid concentration of nitrite in Parkinson's disease. *Neuroreport* 6: 1642–1644
- Rodriguez M, Barroso-Chinea P, Abdala P, Obeso J, Gonzalez-Hernandez T (2001) Dopamine cell degeneration induced by intraventricular administration of 6-hydroxydopamine in the rat: similarities with cell loss in Parkinson's disease. *Exp Neurol* 169: 163–181
- Rousselet E, Callebert J, Parain K, Joubert C, Hunot S, Hartmann A, Jacque C, Perez-Diaz F, Cohen-Salmon C, Launay JM, Hirsch EC (2002) Role of TNF-alpha receptors in mice intoxicated with the Parkinsonian toxin MPTP. *Exp Neurol* 177: 183–192
- Schapira AH, Cooper JM, Dexter D, Clark JB, Jenner P, Marsden CD (1990) Mitochondrial complex I deficiency in Parkinson's disease. *J Neurochem* 54: 823–827
- Sofic E, Lange KW, Jellinger K, Riederer P (1992) Reduced and oxidized glutathione in the substantia nigra of patients with Parkinson's disease. *Neurosci Lett* 142: 128–130
- Sriram K, Matheson JM, Benkovic SA, Miller DB, Luster MI, O'Callaghan JP (2002) Mice deficient in TNF receptors are protected against dopaminergic neurotoxicity: implications for Parkinson's disease. *FASEB J* 16: 1474–1476
- Varastet M, Riche D, Maziere M, Hantraye P (1994) Chronic MPTP treatment reproduces in baboons the differential vulnerability of mesencephalic dopaminergic neurons observed in Parkinson's disease. *Neuroscience* 63: 47–56
- Vu TQ, Ling ZD, Ma SY, Robie HC, Tong CW, Chen EY, Lipton JW, Carvey PM (2000) Pramipexole attenuates the dopaminergic cell loss induced by intraventricular 6-hydroxydopamine. *J Neural Transm* 107: 159–176
- Yoritaka A, Hattori N, Uchida K, Tanaka M, Stadtman ER, Mizuno Y (1996) Immunohistochemical detection of 4-hydroxynonenal protein adducts in Parkinson's disease. *Proc Natl Acad Sci USA* 93: 2696–2701
- Zhang J, Perry G, Smith MA, Robertson D, Olson SJ, Graham DG, Montine TJ (1999) Parkinson's disease is associated with oxidative damage to cytoplasmic DNA and RNA in substantia nigra neurons. *Am J Pathol* 154: 1423–1429

Authors' address: P. M. Carvey, PhD, Department of Pharmacology, 1735 West Harrison St (Cohn 406), Chicago, IL 60612, USA, e-mail: pcarvey@rush.edu

Striatal trophic factor activity in aging monkeys with unilateral MPTP-induced parkinsonism

Timothy J. Collier^{a,*}, Zao Dung Ling^b, Paul M. Carvey^b, Anita Fletcher-Turner^c,
David M. Yurek^c, John R. Sladek Jr.^d, Jeffrey H. Kordower^a

^aDepartment of Neurological Sciences, Rush University Medical Center, Chicago, IL 60612, USA

^bDepartment of Pharmacology, Rush University Medical Center, Chicago, IL 60612, USA

^cDepartment of Neurosurgery, University of Kentucky School of Medicine, Lexington, KY 40536, USA

^dDepartment of Psychiatry, University of Colorado Health Sciences Center, Denver, CO 80262, USA

Received 12 April 2004

Available online 14 October 2004

Abstract

Striatal trophic activity was assessed in female rhesus monkeys of advancing age rendered hemiparkinsonian by unilateral intracarotid administration of MPTP. Three age groups were analyzed: young adults (8–9.5 years) $n = 4$, middle-aged adults (15–17 years) $n = 4$, and aged adults (21–31 years) $n = 7$. Fresh frozen tissue punches of caudate nucleus and putamen were collected 3 months after MPTP treatment and assayed for combined soluble striatal trophic activity, brain-derived neurotrophic factor (BDNF) and glial cell line-derived neurotrophic factor (GDNF). This time point was chosen in an effort to assess a relatively stable phase of the dopamine (DA)-depleted state that may model the condition of Parkinson's disease (PD) patients at the time of therapeutic intervention. Analyses were conducted on striatal tissue both contralateral (aging effects) and ipsilateral to the DA-depleting lesion (lesion \times aging effects). We found that combined striatal trophic activity in the contralateral hemisphere increased significantly with aging. Activity from both middle-aged and aged animals was significantly elevated as compared to young adults. Following DA depletion, young animals significantly increased combined striatal trophic activity, but middle-aged and aged animals did not exhibit further increases in activity over their elevated baselines. BDNF levels in the contralateral hemisphere were significantly reduced in aged animals as compared to young and middle-aged subjects. With DA depletion, BDNF levels declined in young and middle-aged animals but did not change from the decreased baseline level in old animals. GDNF levels were unchanged with aging and at 3 months after DA depletion. The results are consistent with several conclusions. First, by middle age combined striatal trophic activity is elevated, potentially reflecting a compensatory reaction to ongoing degenerative changes in substantia nigra DA neurons. Second, in response to DA depletion, young animals were capable of generating a significant increase in trophic activity that was sustained for at least 3 months. This capacity was either saturated or was not sustained in middle-aged and aged animals. Third, the aging-related chronic increase in combined striatal trophic activity was not attributable to BDNF or GDNF as these molecules either decreased or did not change with aging.

© 2004 Elsevier Inc. All rights reserved.

Keywords: Neurotrophic; Monkey; Nonhuman primate; GDNF; BDNF; Substantia nigra; Striatum; Dopamine; MPTP; Parkinsonism

Introduction

Animal models are essential tools for understanding neural mechanisms associated with neurodegenerative

diseases and for the design of effective experimental therapeutic interventions. One primary risk factor for neurodegenerative disease is advancing age (Baldereschi et al., 2003; Lindsay et al., 2002; Wakisaka et al., 2003). While there are several animal models of Parkinson's disease (PD) (Cenci et al., 2002; Collier et al., 2003a,b; Orth and Tabrizi, 2003; Shimohama et al., 2003), the impact of aging on the brain's response to dopamine (DA)

* Corresponding author. Department of Neurological Sciences, Rush University Medical Center, Cohn Building, Suite 300, 1735 West Harrison Street, Chicago, IL 60612. Fax: +1 312 563 3571.

E-mail address: tcollier@rush.edu (T.J. Collier).

depletion in these models has not received much attention until recently. Indeed, the common use of young adult animals depleted of striatal DA as a test system for novel therapies for PD may yield overly optimistic views of efficacy. It is unlikely that compensatory mechanisms expressed in the injured young adult brain remain fully functional in the aged brain, when individuals most often manifest neurodegenerative disease. In this regard, we have demonstrated that embryonic DA neurons grafted into aged hosts survive more poorly and exert a less potent therapeutic benefit than identical grafts placed in young hosts in a rat model of PD (Collier et al., 1999; Sortwell et al., 2001). These studies were predictive of data collected in a double-blind human clinical transplant trial in which superior benefit was observed in younger patients than in older patients (Freed et al., 2001). We have identified one potential contributing factor to the poorer graft outcome in aged rats: an aging-related reduction in striatal DA neurotrophic activity (Kaselow et al., 1996; Ling et al., 2000). Indeed, supplementation of trophic support in the environment of grafted DA neurons dramatically enhances graft survival in aged rat hosts (Collier et al., 1999).

The present study sought to determine whether the development of an impoverished striatal neurotrophic environment resulting from advancing age presents a challenge for experimental therapeutics in a species more closely related to humans. We compared measures of striatal trophic factors for DA neurons in the intact and DA-depleted hemispheres of female rhesus monkeys of advancing age treated with unilateral intracarotid administration of MPTP. The striatum contralateral to MPTP lesion permits assessment of trophic factors as affected primarily by aging processes. The striatum ipsilateral to MPTP lesion allows for the assessment of these molecules in the context of the interaction between aging and severe DA depletion. Samples from the DA-depleted hemisphere were collected at 3 months after MPTP treatment. This time point was chosen in an effort to assess a relatively stable phase of the DA-depleted state that may model the condition of PD patients embarking upon a therapeutic intervention. Three assays were conducted. First, we assessed the ability of aggregate soluble trophic activity in extracts of the striatum to support DA neurons in culture. Trophic activity measured in this fashion is inversely related to DA tone in preclinical studies (Carvey et al., 1989, 1991, 1993a,b, 1996; Nijima et al., 1990; Tomozawa and Appel, 1986) and is increased in PD (Carvey et al., 1993b; Yu et al., 1994). Second, brain-derived neurotrophic factor (BDNF) levels were assayed by enzyme-linked immunosorbent assay (ELISA). Converging lines of evidence support the concept that BDNF is a potent trophic factor for DA neurons in vitro and in vivo (Collier and Sortwell, 1999). BDNF is present in substantia nigra DA neurons (Seroogy and Gall, 1993; Seroogy et al., 1994) and in the striatum (Conner et al., 1997; Kawamoto et al., 1996) is regulated during nigral development (Friedman et al.,

1991), increases in response to DA depletion (Funa et al., 1996; Yurek and Fletcher-Turner, 2000, 2001; Zhao et al., 1996), and the response to DA depletion is lost with aging in rats (Yurek and Fletcher-Turner, 2000, 2001). Substantia nigra BDNF is decreased in PD (Howells et al., 2000; Mogi et al., 1999; Parain et al., 1999). Third, glial cell line-derived neurotrophic factor (GDNF) was assayed by ELISA. GDNF also is a potent trophic factor for DA neurons in vitro and in vivo (Collier and Sortwell, 1999). GDNF is retrogradely transported from the striatum to the substantia nigra (Ai et al., 2003; Kordower et al., 2000; Wang et al., 2002). Within the nigra, GDNF is found in astrocytes (Choi-Lundberg and Bohn, 1995; Schaar et al., 1993), is regulated during development (Choi-Lundberg and Bohn, 1995; Stromberg et al., 1993), and declines with aging in rats (Yurek and Fletcher-Turner, 2001). Immunohistochemical studies have reported decreases in nigral GDNF in PD (Chauhan et al., 2001).

Our findings indicate that total trophic activity is significantly increased in the intact striatum by middle age and remains elevated in old age. In response to DA depletion, this combined activity is significantly increased in young adult monkeys but is not elevated above the already increased basal levels in middle-aged and aged monkeys. Striatal BDNF levels decrease significantly in the intact striatum in the oldest age group only and following DA depletion in young and middle-aged animals declines to the same extent seen in aged monkey. No significant changes were detected in striatal GDNF levels with aging or in response to DA depletion at 3 months post-MPTP.

Materials and methods

Animals

Subjects were female rhesus monkeys (*Macaca mulatta*) weighing 6–9 kg. Three age groups were studied: young adult (8–9.5 years) $n = 4$, middle-aged (15–17 years) $n = 4$, and aged (21–31 years) $n = 7$. Rhesus monkeys age at a rate of 3:1 as compared to humans (Andersen et al., 1999). Thus, our groups model the equivalent of 24 years, 45–51 years, and 63–93 years of human life. Animals were housed in individual primate cages and cared for in the AALAC approved Biological Resources Laboratory at the University of Illinois-Chicago. All monkeys were treated with unilateral intracarotid administration of 1-methyl-4-phenyl-1,2,3,6-tetrahydropyridine (MPTP) (3–4 mg) as previously described (Emborg et al., 2001). Treatment resulted in equivalent behavioral signs in all subjects, principally characterized by complete disuse of the forelimb contralateral to infusion. Care and use of these animals was in compliance with all applicable laws and regulations as well as principles expressed in the National Institutes of Health, United States Public Health Service Guide for the

Care and Use of Laboratory Animals. This study was approved by the Animal Care and Use Committees of the University of Illinois-Chicago and Rush University Medical Center.

Tissue

Three months following induction of behavioral symptoms, animals were killed by pentobarbital overdose (50 mg/kg with effect confirmed by absence of corneal reflex) and perfused with physiological saline. Brains were removed, and each forebrain was divided into coronal slabs of 4 mm thickness on ice. Tissue punches, 1.3 mm in diameter, were taken from standard locations (Sladek et al., 1995) in the ventral-medial caudate nucleus and putamen at precommissural and commissural levels of the striatum. Punches were frozen on dry ice and stored at -70°C until processing. Caudate and putamen punches from the precommissural striatum were devoted to the assay of combined soluble trophic activity, and punches from the commissural striatum were devoted to ELISAs for BDNF and GDNF. Samples from all animals were not available for all assays. For all assays, measures derived from caudate nucleus and putamen were not statistically different and were combined for presentation as “striatal” trophic factor activity or levels.

Trophic activity and tissue culture

Striatal tissue was homogenized in ice-cold Hank's balanced salt solution (HBSS), centrifuged at $18,000 \times g$ for 15 min, and the protein concentration of the supernatant extracts was assessed for total protein using the Bio-Rad kit. The extract was adjusted to 200 μg protein/ml and assessed for trophic activity as described previously (Ling et al., 2000). Briefly, ventral mesencephalon from embryonic day 14.5 rats was dissected and dissociated into a cell suspension. Cells were plated at 125,000 cells/cm² in 96-well plates and incubated in 75% serum-free-defined media (DM) + 25% striatal tissue extract. On every plate, controls were used to assess baseline growth. These control cultures were incubated in 75% DM + 25% HBSS instead of striatal extract. Each plate also had 2 wells in which cells were incubated in 90% DM + 10% fetal calf serum. These positive controls were used to establish that cultures were growth responsive. Plates in which the tyrosine hydroxylase immunoreactive (THir) cell counts in the positive controls were not at least $2\times$ that seen in plate controls were discarded. After incubation for 72 h, cultures were fixed, stained, and counts of THir neurons were performed. Cells were counted in a cross pattern covering 44% of the well surface. The THir cell counts in each well were divided by the average THir cell count in the plate controls and used as a survival index. Each extract was tested in at least two independent culture runs.

Enzyme-linked immunosorbent assay (ELISA) for BDNF and GDNF

ELISAs for BDNF and GDNF followed previously published protocols (Yurek and Fletcher-Turner, 2000, 2001). Each tissue sample was weighed prior to freezing at -80°C . Subsequently, tissue samples were homogenized in 25 volumes of buffer [400 mM NaCl, 0.1% Triton-X, 2.0 mM EDTA, 0.1 mM benzethonium chloride, 2.0 mM benzamidine, 0.1 mM PMSF, Aprotinin (9.7 TIU/ml), 0.5% BSA, 0.1 M phosphate buffer, pH 7.4]. The homogenate was centrifuged for 10 min at $10,000 \times g$ at 4°C . The neurotrophic factor content was determined in 100 μl aliquots of supernatant with an antibody sandwich format: extracted neurotrophic factor from each sample was captured with a neurotrophic factor-specific monoclonal antibody (mAb), the captured neurotrophic factor was then bound to the second, neurotrophic factor-specific polyclonal antibody (pAb). After washing, the amount of specifically bound pAb was detected using a species-specific anti-IgY antibody conjugated to horseradish peroxidase (HRP) as a tertiary reactant. Unbound conjugate was removed by washing, and following an incubation period with a chromogenic substrate the color change was measured. The amount of BDNF or GDNF is proportional to the color change generated in an oxidation-reduction reaction (Promega E_{max}TM Immuno-Assay System) and detected in a microplate reader set at 450 nm.

Statistics

Comparisons of counts of THir neurons in culture and trophic factor levels were analyzed with analysis of variance (ANOVA) followed by Fisher's protected least significant differences (PLSD) test.

Results

Combined striatal trophic activity

There was an aging-related increase in the combination of soluble trophic factors derived from the caudate nucleus and putamen contralateral to MPTP exposure. This was demonstrated by the significant increase in the capacity for this trophic activity to support survival and growth of cultured rat DA neurons [$F(5,49) = 3.857$, $P = 0.005$]. The approximate 50% increase in survival of THir neurons in culture was evident by middle age and sustained in old age (Figs. 1 and 2). For young adult monkeys, extracts derived from the DA-depleted hemisphere produced a significant 50% increase in survival of cultured DA neurons, matching the elevated baseline levels of older monkeys. In contrast, samples from the DA-depleted hemisphere of middle-aged and aged subjects maintained

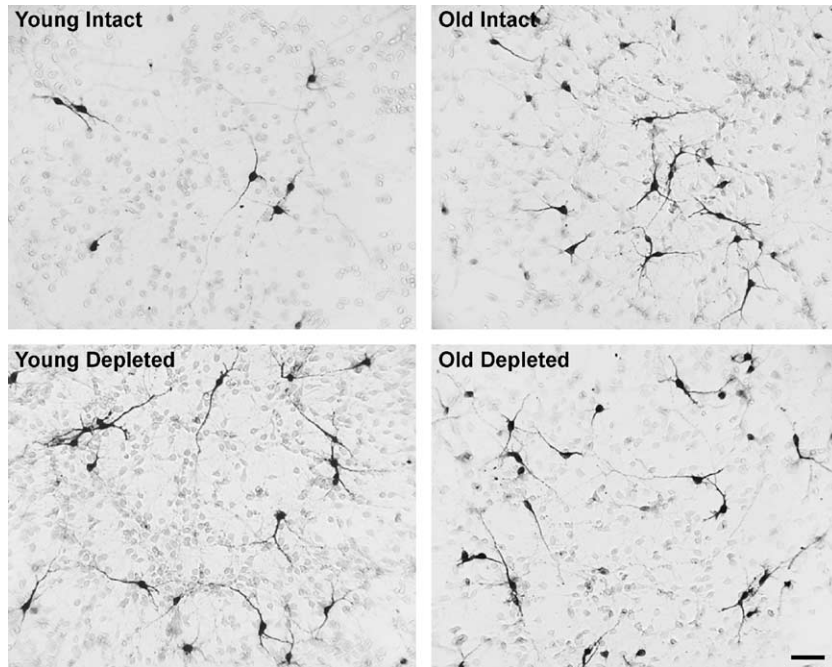


Fig. 1. Striatal-derived trophic activity for cultured rat dopamine (DA) neurons is increased with aging and in response to DA depletion in young adult, but not aged, monkeys. Micrographs illustrate representative fields of cultured embryonic day 14.5 rat ventral mesencephalon immunostained for tyrosine hydroxylase (TH) to visualize DA neurons. Cultures were exposed to striatal extracts from monkeys of varying ages for 72 h and quantified for TH-positive cell numbers relative to control cultures not exposed to extracts. As shown, extracts from the intact striatum exhibit an aging-related increase in trophic support for DA neurons. Comparison of effects of extracts from the intact and DA depleted hemispheres of young and old monkeys indicates that striatal DA depletion triggers increased trophic activity in young adult monkeys, but that aged monkeys do not exhibit any further increase in trophic activity over their already elevated baseline levels. Scale bar = 50 μ m.

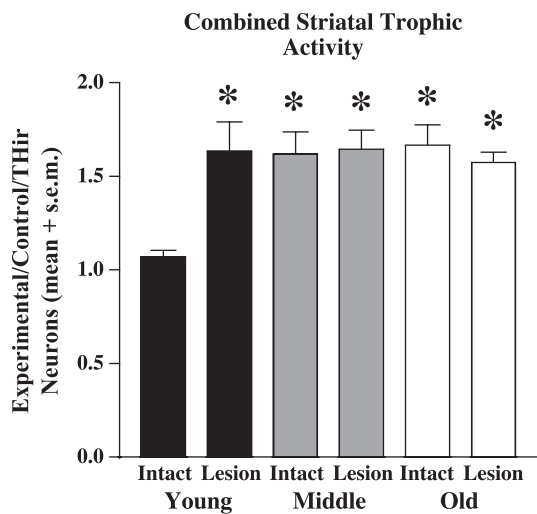


Fig. 2. Combined nonhuman primate striatal trophic activity for cultured dopamine (DA) neurons. Counts of tyrosine hydroxylase (TH)-positive neurons in cultures exposed to striatal extracts are presented as compared to control cultures not exposed to extracts. For extracts derived from the intact striatum, an approximately 50% increase in trophic activity is detectable by middle age and sustained in old age. In response to striatal DA depletion, young adult monkeys generate a similar 50% increase in trophic activity, but further increases beyond elevated baseline levels are not produced in middle-aged and aged monkeys. ANOVA: $F(5,49) = 3.857$, $P = 0.005$. Fisher's PLSD: * $P < 0.002$ for young intact as compared to all other groups.

increased trophic support but were not elevated above the already increased levels of the contralateral hemisphere attributable to aging.

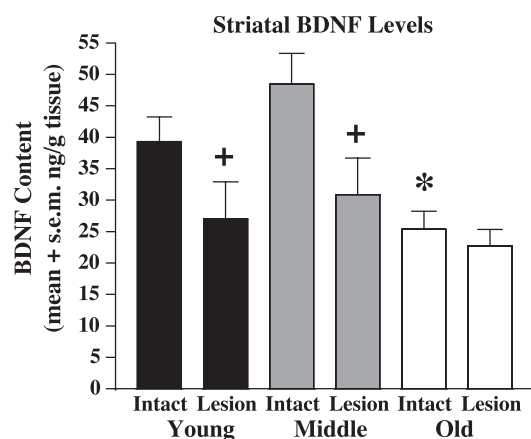


Fig. 3. Striatal BDNF levels as measured with ELISA. BDNF levels are presented as nanograms of BDNF per gram tissue. For the intact striatum, BDNF levels were found to be maintained from young adulthood into middle age but decreased significantly in old age. Following dopamine depletion, young adult and middle-aged monkeys exhibited significant decreases in striatal BDNF. Aged monkeys showed no further decline in BDNF beyond their depleted baseline levels. ANOVA: $F(5,42) = 4.508$, $P = 0.002$. Fisher's PLSD: + $P < 0.05$ as compared to intact hemisphere; * $P < 0.02$ as compared to intact hemisphere of young and middle-aged monkeys.

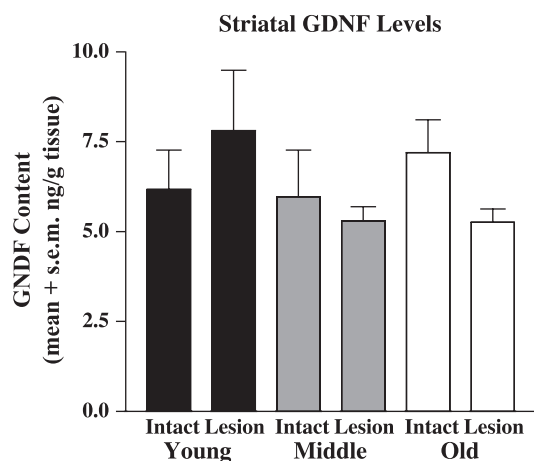


Fig. 4. Striatal GDNF levels as measured with ELISA. GDNF levels are presented as nanograms of GDNF per gram tissue. No differences were found in striatal levels of GDNF with aging or at 3 months after dopamine depletion. ANOVA: $F(5,38) = 0.729$, $P = 0.606$.

Striatal BDNF levels

BDNF levels measured in striatal samples from the hemisphere contralateral to MPTP exposure exhibited a significant aging-related decline of approximately 40% that was detectable only in the oldest age group [$F(5,42) = 4.508$, $P = 0.002$] (Fig. 3). In response to DA depletion, striatal BDNF decreased significantly in young adult and middle-aged subjects but did not decrease further in the already BDNF-depleted-aged subjects.

Striatal GDNF levels

GDNF levels assayed from the striatum of the hemisphere contralateral to MPTP exposure showed no changes associated with advancing age [$F(5,38) = 0.729$, $P = 0.606$] (Fig. 4). Similarly, at 3 months after MPTP-induced DA depletion, striatal GDNF levels were not significantly different from levels in the contralateral hemisphere.

Discussion

The expression of neurotrophic factors is a dynamic process and a defining event associated with nervous system development, aging, and the response to damage and disease. For the nigrostriatal system, BDNF and GDNF perhaps are the most studied of the more than 20 molecules with known neurotrophic effects for DA neurons (Collier and Sortwell, 1999). Abundant information exists in the literature on the regulation of neurotrophic factors during early development of the nervous system, and these data serve in part as the rationale for their potential therapeutic efficacy. Our understanding of how aging influences neurotrophic function is in its relatively early stages. Most studies examining aging effects of trophic factors upon the nigrostriatal DA system have been conducted on aged rats.

Virtually no such studies have been performed in aging nonhuman primates, and the data collected in our study present several differences from what has been found in rodents.

Similar to the present study, the majority of evidence on striatal trophic factor levels obtained from aging rats used a unilateral DA depletion model. The hemisphere contralateral to unilateral infusion of 6-hydroxydopamine (6-OHDA) has been assayed for changes in trophic factors as a function of chronological age and the hemisphere ipsilateral to 6-OHDA was assayed for the reaction of the aging striatum to severe DA depletion. It should be noted that the use of the hemisphere contralateral to unilateral DA depletion might not be a perfect representation of a truly "intact" striatum from untreated animals. Unilateral lesions will remove the very small percentage of nigrostriatal DA fibers that cross to the contralateral striatum (Hedreen and DeLong, 1991), and in the case of intracarotid administration of MPTP there can be evidence of exposure contralaterally (Eberling et al., 2002). The presence or absence of crossover effects appears to be dose related, occurring with increased frequency at relatively higher doses (Guttman et al., 1990). For the present study, parallel analysis of substantia nigra cell numbers in the same monkeys using unbiased stereology has found no difference between counts in the hemisphere contralateral to MPTP exposure and counts derived from untreated monkeys. Thus, for the cases presented here, we have no evidence of significant MPTP exposure to the contralateral hemisphere. With this potential caveat in mind, we will refer to the hemisphere contralateral to unilateral DA depletion as "intact," for convenience, in the remainder of the discussion.

Studies in aging rats have been conducted using the same assays reported here. For effects on combined striatal trophic activity attributable to aging, parallel analysis of the striatum of untreated rats and the striatum contralateral to a unilateral 6-OHDA lesion detected identical results. This supports the view that the hemisphere contralateral to unilateral DA depletion can be appropriate for study as an intact control. For aging rats, combined striatal trophic activity for cultured DA neurons derived from intact striatum was relatively preserved through middle age (4, 12, and 18 months old) but declined significantly in advanced age (23 months old) (Ling et al., 2000). Striatal levels of GDNF, but not BDNF, decreased significantly in aged rats (4–5 months old as compared to 31–34 months old) (Yurek and Fletcher-Turner, 2000, 2001).

Our evidence from the intact hemisphere of aging monkeys is considerably different from the pattern detected in rats. We found that combined striatal trophic activity for cultured DA neurons is significantly increased by middle age and remains elevated in old age. No change in striatal GDNF levels was detected with advancing age. Striatal levels of BDNF were stable from young adulthood through middle age but declined significantly in the oldest monkeys. These same monkey subjects have been assessed for

biochemical and morphological markers of the nigrostriatal DA system, providing a context not available in the rat studies. Our studies show that striatal DA levels are significantly decreased by middle age in the intact striatum, and that THir neurons in substantia nigra exhibit no overt cell loss but do show decreasing soma size and intensity of TH immunoreactivity that is progressive from young adulthood through middle age into old age (Collier et al., 2003a,b). Thus, the increase in combined striatal trophic activity detected parallels the timing of degenerative changes in DA neurons and is likely to be a compensatory response triggered during the aging process in this system. Furthermore, our evidence suggests that chronic increases in striatal trophic activity generated during aging cannot be attributed to increases in GDNF or BDNF as these neurotrophic factors either do not change or decline. Finally, the trophic compensation generated at best appears to maintain a reduced level of striatal DA from middle age into old age and does not forestall progressive signs of morphological deterioration at the level of substantia nigra DA cell bodies.

The findings from the DA-depleted striatum of aging rats and monkeys must necessarily be interpreted in the context of the timing of sample collection following lesion. Both rat studies and our monkey study endeavored to examine trophic factor levels at a time believed to represent the characteristics of stable DA depletion and were meant to model the state of the striatum when therapeutic intervention might be instituted for a PD patient. Still, the scope of such analyses is limited by the required focus on selected time points. In rats, combined striatal trophic activity ipsilateral to DA depletion is significantly increased in younger animals (4 and 12 months old) and this response is entirely absent in older animals (18 and 23 months old) (Ling et al., 2000). This assay was performed at 8 weeks after unilateral 6-OHDA lesion. Striatal levels of BDNF and GDNF have been demonstrated to increase significantly at 2–4 weeks ipsilateral to unilateral DA depletion in young adult rats (4–5 months old), but no increase is detected in aged rats (31–34 months old) (Yurek and Fletcher-Turner, 2000, 2001). There is evidence that this 2- to 4-week timeframe may represent a period of maximal response for these factors, as BDNF levels while elevated in young adult rats at 2 weeks after DA depletion decline to baseline by 7 weeks after lesion (Zhao et al., 1996). Taken together, the evidence from aging rats supports the view that DA depletion triggers increased striatal trophic activity in young rats, but that this response is compromised in aged rats.

Consistent with findings in rats, young adult monkeys increased striatal trophic activity in response to severe DA depletion, while middle-aged and aged adults did not. This increase in young monkeys was sustained at 3 months after unilateral MPTP administration. The failure to detect an increase in trophic activity in older monkeys was potentially the result of the aged animals' inability to generate further increases beyond the already elevated baseline levels. Thus, the compensatory response in older monkeys may be

saturated by the response to aging per se. Alternatively, we cannot rule out the possibility that older animals generate further increases in trophic activity over a transient time course. However, it is interesting that the combined striatal trophic response generated in young monkeys following sudden severe DA depletion is of the same magnitude as the response triggered by gradual aging-related deterioration of the DA system. This might favor the interpretation that the increase observed represents a biological maximum for this compensatory response.

Changes in BDNF and GDNF predicted by rat studies also did not hold true for monkeys. While young adult rats increased striatal BDNF levels at 2–4 weeks following DA depletion, young and middle-aged monkeys exhibited significant decreases in BDNF levels following DA depletion. Like aged rats, aged monkeys did not exhibit any change in BDNF following DA depletion. The equivalent levels of striatal BDNF displayed by DA-depleted young and middle-aged monkeys and the intact hemisphere of old monkeys is consistent with exhaustion of the pool of BDNF that resides within nigrostriatal DA neurons. The compensatory increase of BDNF seen in young rats following DA depletion is hypothesized to be a consequence of increased BDNF derived from non-DA neuron sources in the striatum (Yurek and Fletcher-Turner, 2000, 2001). The most likely source is provided by anterograde transport from cortex (Altar and DiStefano, 1998; Altar et al., 1997; Mufson et al., 1999). To the extent that this is accurate, our findings indicate that BDNF compensation from other sources either does not occur in nonhuman primates or occurs over a shorter time course and is not maintained. Our cases showed no significant change in striatal GDNF levels following DA depletion. While this indicates that any change in GDNF is not maintained over time, it does not rule out the possibility that a more transient response is generated as suggested by rat studies. Furthermore, these data indicate that any enhancement of endogenous GDNF that might be provoked by DA depletion is unlikely to be active at the time of therapeutic intervention in PD patients.

The disconnect between changes in striatal trophic activity during aging and in response to DA depletion in rats and monkeys was unanticipated but supports the importance of the nonhuman primate model for the final evaluation of experimental therapeutics for humans. The presence of elevated combined striatal trophic activity that is sustained in aging, and in response to MPTP-induced DA depletion, argues against the view that aging produces a generalized impoverished trophic environment that may adversely affect therapeutic strategies dependent upon this activity. However, we demonstrate that this increased trophic response is unable to forestall degenerative changes in the DA system, as these same monkeys display aging-related decreases in striatal DA and morphological signs of deterioration in nigral cell bodies. The combination of trophic molecules constituting this striatal response remains

to be determined, but the failure of trophic signaling to completely preserve DA neuron integrity appears not to be a product of decreased levels of all molecules that can generate DA neurotrophic effects. Our findings suggest that chronic increases in striatal trophic activity expressed during aging and the compensatory response generated by DA depletion in young adult monkeys are not attributable to increased levels of BDNF or GDNF as these molecules either decreased or remained stable. This may suggest that declines in BDNF in conjunction with low adult levels of GDNF are specifically associated with aging-related deterioration of the DA system.

Acknowledgments

This work was supported by AG17092 (TJC), DAMD17-01-1-0766 (DMY), NS045316 (ZDL), 5R21 ES012307, USARMRA W81XWH0410365, and the Michael J. Fox Foundation (PMC). The authors are grateful for the excellent technical assistance of Mr. Brian Daley and Ms. Michelle Gartland.

References

- Ai, Y., Markesbery, W., Zhang, Z., Grondin, R., Elseberry, D., Gerhardt, G.A., Gash, D.M., 2003. Intraputamenal infusion of GDNF in aged rhesus monkeys: distribution and dopaminergic effects. *J. Comp. Neurol.* 461, 250–261.
- Altar, C.A., DiStefano, P.S., 1998. Neurotrophin trafficking by anterograde transport. *Trends Neurosci.* 21, 433–437.
- Altar, C.A., Cai, N., Bliven, T., Juhasz, M., Conner, J.M., Acheson, A.L., Lindsay, R.M., Wiegand, S.J., 1997. Anterograde transport of brain-derived neurotrophic factor and its role in the brain. *Nature* 389, 856–860.
- Andersen, A.H., Zhang, Z., Zhang, M., Gash, D.M., Avison, M.J., 1999. Age-associated changes in rhesus CNS composition identified by MRI. *Brain Res.* 829, 90–98.
- Baldereschi, M., Di Carlo, A., Vanni, P., Ghetti, A., Carbonin, P., Amaducci, L., Inzitari, D., 2003. Lifestyle-related risk factors for Parkinson's disease: a population-based study. *Acta Neurol. Scand.* 108, 239–244.
- Carvey, P.M., Ptak, L.R., Kao, L.-C., Klawans, H.L., 1989. Striatal homogenates from animals chronically treated with haloperidol stimulate dopamine and GABA uptake in cultures of rostral mesencephalic tegmentum. *Clin. Neuropharmacol.* 12, 425–434.
- Carvey, P.M., Ptak, L.R., Lo, E.S., Lin, D., Buhrfiend, C.M., Goetz, C.G., Klawans, H.L., 1991. Levodopa reduces the growth promoting effects of striatal extracts on rostral mesencephalic tegmentum cultures. *Exp. Neurol.* 114, 28–34.
- Carvey, P.M., Ptak, L.R., Lin, D., Lo, E.S., Buhrfiend, C.M., Drucker, G.E., Fields, J.Z., 1993a. Alterations in striatal neurotrophic activity induced by dopaminergic drugs. *Pharmacol. Biochem. Behav.* 46, 195–204.
- Carvey, P.M., Ptak, L.R., Nath, S.T., Sierens, D.K., Mufson, E.J., Goetz, C.G., Klawans, H.L., 1993b. Striatal extracts from patients with Parkinson's disease promote dopamine neuron growth in mesencephalic cultures. *Exp. Neurol.* 120, 149–152.
- Carvey, P.M., Lin, D.H., Faselis, C.J., Notermann, J.K., Ling, Z.D., 1996. Loss of striatal DA innervation increases striatal trophic activity directed at DA neurons in culture. *Exp. Neurol.* 140, 184–197.
- Cenci, M.A., Whishaw, I.Q., Schallert, T., 2002. Animal models of neurological deficits: how relevant is the rat? *Nat. Rev., Neurosci.* 3, 574–579.
- Chauhan, N.B., Siegel, G.J., Lee, J.M., 2001. Depletion of glial cell line-derived neurotrophic factor in substantia nigra neurons of Parkinson's disease brain. *J. Chem. Neuroanat.* 21, 277–288.
- Choi-Lundberg, D.L., Bohn, M.C., 1995. Ontogeny and distribution of glial cell line-derived neurotrophic factor (GDNF) mRNA in rat. *Dev. Brain Res.* 85, 80–88.
- Collier, T.J., Sortwell, C.E., 1999. Therapeutic potential for nerve growth factors in Parkinson's disease. *Drugs Aging* 14, 261–287.
- Collier, T.J., Sortwell, C.E., Daley, B.F., 1999. Diminished viability, growth, and behavioral efficacy of fetal dopamine neuron grafts in aging rats with long-term dopamine depletion: an argument for neurotrophic supplementation. *J. Neurosci.* 19, 5563–5573.
- Collier, T.J., Steece-Collier, K., Kordower, J.H., 2003a. Primate models of Parkinson's disease. *Exp. Neurol.* 183, 258–262.
- Collier, T.J., Daley, B.F., Lipton, J.W., Chu, Y., Ling, Z.D., Sortwell, C.E., Fletcher-Turner, A., Yurek, D.M., Emborg, M.E., Blanchard, B.C., 2003b. Abstract 878.4, Society for Neuroscience.
- Conner, J.M., Lauterborn, J.C., Yan, Q., Gall, C.M., Varon, S., 1997. Distribution of brain derived neurotrophic factor (BDNF) protein and mRNA in the normal adult rat CNS: evidence for anterograde axonal transport. *J. Neurosci.* 17, 2295–2313.
- Eberling, J.L., Pivrotto, P., Bringas, J., Steiner, J.P., Kordower, J.H., Chu, Y., Emborg, M.E., Bankiewicz, K.S., 2002. The immunophilin ligand GPI-1046 does not have neuroregenerative effects in MPTP-treated monkeys. *Exp. Neurol.* 178, 236–242.
- Emborg, M.E., Shin, P., Roitberg, B., Sramek, J.G., Chu, Y., Stebbins, G.T., Hamilton, J.S., Suzdak, P.D., Steiner, J.P., Kordower, J.H., 2001. Systemic administration of the immunophilin ligand GPI 1046 in MPTP-treated monkeys. *Exp. Neurol.* 168, 171–182.
- Freed, C.R., Green, P.E., Breeze, R.E., Tsai, W.Y., DuMouchel, W., Kao, R., Dillon, S., Winfield, H., Culver, S., Trojanowski, J.Q., Eidelberg, D., Fahn, S., 2001. Transplantation of embryonic dopamine neurons for severe Parkinson's disease. *N. Engl. J. Med.* 344, 710–719.
- Friedman, W.J., Olson, L., Persson, H., 1991. Cells that express brain-derived neurotrophic factor mRNA in the developing postnatal rat brain. *Eur. J. Neurosci.* 3, 688–697.
- Funahashi, K., Yamada, N., Brodin, G., Pietz, K., Ahgren, A., Victorin, K., Lindvall, O., Odin, P., 1996. Enhanced synthesis of platelet-derived growth factor following injury induced by 6-hydroxydopamine in rat brain. *Neuroscience* 74, 825–833.
- Guttman, M., Fibiger, H.C., Jakubovic, A., Calne, D.B., 1990. Intracarotid 1-methyl-4-phenyl-1,2,3,6-tetrahydropyridine administration: biochemical and behavioral observations in a primate model of hemiparkinsonism. *J. Neurochem.* 54, 1329–1334.
- Hedreen, J.C., DeLong, M.R., 1991. Organization of striatopallidal, striatonigral, and nigrostriatal projections in the macaque. *J. Comp. Neurol.* 304, 569–595.
- Howells, D.W., Porritt, M.J., Wong, J.Y., Batchelor, P.E., Kalnins, R., Hughes, A.J., Donnan, G.A., 2000. Reduced BDNF mRNA expression in the Parkinson's disease substantia nigra. *Exp. Neurol.* 166, 127–135.
- Kaselow, P.A., Lis, A., Asads, H., Barone, T.A., Plunkett, R.J., 1996. In vitro assessment of neurotrophic activity from the striatum of aging rats. *Neurosci. Lett.* 218, 157–160.
- Kawamoto, Y., Nakamura, S., Nakano, S., Oka, N., Akiguchi, I., Kimura, J., 1996. Immunohistochemical localization of brain-derived neurotrophic factor in adult rat brain. *Neurosci.* 74, 1209–1226.
- Kordower, J.H., Emborg, M.E., Bloch, J., Ma, S.Y., Chu, Y., Leventhal, L., McBride, J., Chen, E.Y., Palfi, S., Roitberg, B.Z., Brown, W.D., Holden, J.E., Pyzalski, R., Taylor, M.D., Carvey, P., Ling, Z., Trono, D., Hantraye, P., Geglion, N., Aebischer, P., 2000. Neurodegeneration prevented by lentiviral vector delivery of GDNF in primate models of Parkinson's disease. *Science* 290, 767–773.
- Lindsay, J., Laurin, D., Verreault, R., Hebert, R., Helliwell, B., Hill, G.B.,

- Carvey, P.M., 2002. Risk factors for Alzheimer's disease: a prospective analysis from the Canadian Study of Health and Aging. *Am. J. Epidemiol.* 156, 445–453.
- Ling, Z.D., Collier, T.J., Sortwell, C.E., Lipton, J.W., Vu, T.Q., Robie, H.C., Carvey, P.M., 2000. Striatal trophic activity is reduced in the aged rat brain. *Brain Res.* 856, 301–309.
- Mogi, M., Togari, A., Kondo, T., Mizuno, Y., Komure, O., Kuno, S., Ichinose, H., Nagatsu, T., 1999. Brain-derived growth factor and nerve growth factor concentrations are decreased in substantia nigra in Parkinson's disease. *Neurosci. Lett.* 270, 45–48.
- Mufson, E.J., Kroin, J.S., Sendera, T.J., Sobreviela, T., 1999. Distribution and retrograde transport of trophic factors in the central nervous system: functional implications for the treatment of neurodegenerative diseases. *Prog. Neurobiol.* 57, 451–484.
- Nijima, K., Araki, M., Ogawa, M., Nagatsu, I., Sato, F., Kimura, H., Yoshida, M., 1990. Enhanced survival of cultured dopamine neurons by treatment with soluble extracts from chemically deafferented striatum of adult rat brain. *Brain Res.* 528, 151–154.
- Orth, M., Tabrizi, S.J., 2003. Models of Parkinson's disease. *Mov. Disord.* 18, 729–737.
- Parain, K., Murer, M.G., Yan, Q., Faucheux, B., Agid, Y., Hirsch, E., Raisman-Vozari, R., 1999. Reduced expression of brain-derived neurotrophic factor protein in Parkinson's disease substantia nigra. *Neuro-Report* 10, 557–561.
- Schaar, D.G., Sieber, B.A., Dreyfus, C.F., Black, I.B., 1993. Regional and cell-specific expression of GDNF in rat brain. *Exp. Neurol.* 124, 368–371.
- Seroogy, K.B., Gall, C.M., 1993. Expression of neurotrophins by midbrain dopaminergic neurons. *Exp. Neurol.* 124, 119–128.
- Seroogy, K.B., Lundgren, K.H., Tran, T.M., Guthrie, K.M., Isackson, P.J., Gall, C.M., 1994. Dopaminergic neurons in rat ventral midbrain express brain derived neurotrophic factor and neurotrophin-3 mRNAs. *J. Comp. Neurol.* 342, 321–334.
- Shimohama, S., Sawada, H., Kitamura, Y., Taniguchi, T., 2003. Disease model: Parkinson's disease. *Trends Mol. Med.* 9, 360–365.
- Sladek Jr., J.R., Elsworth, J., Taylor, J.R., Roth, R.H., Redmond Jr., D.E., 1995. Techniques for neural transplantation in non-human primates. *Methods in Cell Transplantation*. R.G. Landes, Austin, TX, pp. 391–408.
- Sortwell, C.E., Camargo, M.D., Pitzer, M.R., Gyawali, S., Collier, T.J., 2001. Diminished survival of mesencephalic dopamine neurons grafted into aged hosts occurs during the immediate postgrafting interval. *Exp. Neurol.* 169, 23–29.
- Stromberg, I., Bjorklund, L., Johansson, M., Tomac, A., Collins, F., Olson, L., Hoffer, B., Humpel, C., 1993. Glial cell line-derived neurotrophic factor is expressed in the developing but not adult striatum and stimulates developing dopamine neurons in vivo. *Exp. Neurol.* 124, 401–412.
- Tomozawa, Y., Appel, S.H., 1986. Soluble striatal extracts enhance development of mesencephalic dopaminergic neurons in vitro. *Brain Res.* 399, 111–124.
- Wakisaka, Y., Furuta, A., Tanizaki, Y., Kiyohara, Y., Iida, M., Iwaki, T., 2003. Age-associated prevalence and risk factors of Lewy body pathology in a general population: the Hisayama study. *Acta Neuropathol. (Berl.)* 106, 374–382.
- Wang, L., Muramatsu, S., Lu, Y., Ikeguchi, K., Fujimoto, K., Okada, T., Mizukami, H., Hanazono, Y., Kume, A., Urano, F., Ichinose, H., Nagatsu, H., Nakano, I., Ozawa, K., 2002. Delayed delivery of AAV-GDNF prevents nigral neurodegeneration and promotes functional recovery in a rat model of Parkinson's disease. *Gene Ther.* 9, 381–389.
- Yu, S.J., Lo, E.S., Cochran, E.J., Lin, D.H., Faselis, C.J., Klawans, H.L., Carvey, P.M., 1994. Cerebrospinal fluid from patients with Parkinson's disease alters the survival of dopamine neurons in mesencephalic culture. *Exp. Neurol.* 125, 15–24.
- Yurek, D.M., Fletcher-Turner, A., 2000. Lesion-induced increase of BDNF is greater in the striatum of young versus old rat brain. *Exp. Neurol.* 161, 392–396.
- Yurek, D.M., Fletcher-Turner, A., 2001. Differential expression of GDNF, BDNF, and NT-3 in the aging nigrostriatal system following neurotoxic lesion. *Brain Res.* 891, 228–235.
- Zhao, J., Pliego-Rivero, B., Bradford, H.F., Stern, G.M., 1996. The BDNF content of postnatal and adult rat brain: the effects of 6-hydroxydopamine lesions in adult brain. *Dev. Brain Res.* 97, 297–303.

6-Hydroxydopamine-induced alterations in blood–brain barrier permeability

P. M. Carvey, C. H. Zhao, B. Hendey, H. Lum, J. Trachtenberg, B. S. Desai, J. Snyder, Y. G. Zhu and Z. D. Ling
Rush University Medical Center, Department of Pharmacology, 1735 West Harrison Street, Cohn 406, Chicago, IL 60612, USA

Keywords: inflammation, microglia, neurodegeneration, Parkinson

Abstract

Vascular inflammation is well known for its ability to compromise the function of the blood–brain barrier (BBB). Whether inflammation on the parenchymal side of the barrier, such as that associated with Parkinson's-like dopamine (DA) neuron lesions, similarly disrupts BBB function, is unknown. We assessed BBB integrity by examining the leakage of FITC-labeled albumin or horseradish peroxidase from the vasculature into parenchyma in animals exposed to the DA neurotoxin 6-hydroxydopamine (6OHDA). Unilateral injections of 6OHDA into the striatum or the medial forebrain bundle produced increased leakage in the ipsilateral substantia nigra and striatum 10 and 34 days following 6OHDA. Microglia were markedly activated and DA neurons were reduced by the lesions. The areas of BBB leakage were associated with increased expression of P-glycoprotein and β 3-integrin expression suggesting, respectively, a compensatory response to inflammation and possible angiogenesis. Behavioural studies revealed that domperidone, a DA antagonist that normally does not cross the BBB, attenuated apomorphine-induced stereotypic behaviour in animals with 6OHDA lesions. This suggests that drugs which normally have no effect in brain can enter following Parkinson-like lesions. These data suggest that the events associated with DA neuron loss compromise BBB function.

Introduction

Parkinson's disease (PD) is a progressive neurodegenerative disorder characterized by bradykinesia, tremor, and rigidity secondary to the loss of dopamine (DA) neurons in the substantia nigra (SN). A genetic cause has been implicated in some cases (Hedrich *et al.*, 2004), but the majority of cases are considered idiopathic and probably a consequence of an environmental toxin (Di Monte, 2003). Regardless of cause, it is clear that inflammatory events are associated with the DA neuron loss (Hirsch *et al.*, 2003; Jenner, 2003). Thus, microgliosis and astrogliosis are prevalent in the SN of PD patients (McGeer & McGeer, 2004b), the inducible form of nitric oxide synthase (iNOS) and cyclooxygenase 1- and 2-containing microglia are elevated (Knott *et al.*, 2000), while the reduced form of glutathione is decreased, all suggesting oxidative stress (Pearce *et al.*, 1997). Moreover, elevations in tumour necrosis factor alpha (TNF α) and other proinflammatory cytokines are observed (Boka *et al.*, 1994; Mogi *et al.*, 1994). Whether or not this inflammation is a cause of PD, a consequence of the degenerative process or a contributing factor to disease progression is unknown at this time (McGeer & McGeer, 2004a).

Inflammation is known to disrupt the function of the blood–brain barrier (BBB) as is true in meningitis and sepsis, and as shown more recently in trauma, stroke, multiple sclerosis and epilepsy (Huber *et al.*, 2001a). Whether or not the inflammatory events that accompany a neurodegenerative disorder such as PD alter the BBB have not been carefully studied, however. One study by Haussermann *et al.* (2001) revealed no changes in blood–cerebrospinal fluid (CSF) barrier function by examining CSF : serum ratios and oligoclonal bands in PD

patients. In contrast, Faucheux *et al.* (1999) showed an increase in vascular density in the SN suggesting vascular remodeling potentially resulting from vascular inflammation. Barcia *et al.* (2004) described microangiogenesis in the PD brain which is often associated with barrier dysfunction, while Farkas *et al.* (2000) reported pathological changes in capillary microanatomy in patients with PD and Alzheimer's disease. Dysfunction of the BBB has also been suggested more recently by Barcia *et al.* (2005) who demonstrated increased levels of vascular endothelial growth factor and increased numbers of vessels in the SNs of PD patients, and by Kortekaas *et al.* (2005) who reported reduced amounts of P-glycoprotein (P-gp) in the SN. Despite these studies which suggest abnormality of function in the BBB of PD patients, the relationships among DA neuron loss and actual barrier leakage has never been formally tested.

Neuroinflammation is associated with microglial activation which, interestingly, has been shown to occur prior to BBB disruption in other neuroinflammatory models (Lynch *et al.*, 2004). A primary product of microglial activation is TNF α , which is also known to increase BBB permeability (Tsao *et al.*, 2001; Didier *et al.*, 2003). Because our group (Ling *et al.*, 2002a; Ling *et al.*, 2002b; Carvey *et al.*, 2003; Ling *et al.*, 2004a) and several others (Gao *et al.*, 2002; Sriram *et al.*, 2002; Ferger *et al.*, 2004; Mladenovic *et al.*, 2004) have shown that neurotoxins which kill DA neurons are associated with neuro-inflammation, microgliosis and increases in TNF α , we wondered whether this type of lesion would disrupt the BBB. We therefore studied the leakage of large molecules [fluorescein isothiocyanate (FITC)-labeled albumin and horseradish peroxidase (HRP)] from vasculature into brain following 6OHDA lesions of the striatum and medial forebrain bundle (MFB) to determine whether a Parkinson-like lesion leads to leakage of these large molecules into brain.

Correspondence: Dr Paul M. Carvey, as above.
E-mail: pcarvey@rush.edu

Received 10 November 2005, revised 20 April 2005, accepted 29 April 2005

Materials and methods

Experimental animals

Seventy-two young adult male Sprague-Dawley rats (225–250 g) were used in this study. The animals were housed in pairs in environmentally regulated quarters (lights on 06.00–18.00 h) with free access to food and water for the duration of the study. This study was conducted in accordance with the Policies on the Use of Animals and Humans in Neuroscience Research, and was approved by Rush University's Institutional Animal Care and Utilization Committee.

Animal surgery

We first studied an intrastriatal 6OHDA lesion so that puncture wounds, which are known to disrupt the BBB (Borlongan *et al.*, 2004), would not compromise the study of barrier function in the SN. Twelve rats were injected under pentobarbital anesthesia (40 mg/kg) with 6OHDA unilaterally into three sites within the striatum, according to a modified method of Sauer (Sauer & Oertel, 1994). The coordinates of three sites were: bregma –0.4, lateral –3.0 and ventral –4.5 mm; bregma –0.4, lateral –4.0 and ventral –6.0 mm; and bregma –0.4, lateral –4.0 and ventral –7.5 mm. Another group of 18 rats was injected with 6OHDA unilaterally into the MFB (coordinates: bregma –3.6, lateral –2.0 and ventral –7.5 mm). 6OHDA was infused at a dose of 8 µg in 2 µL in 0.2% ascorbic acid in each location. Two groups of control animals ($n = 6$ each) were injected with 2 µL 0.2% ascorbate vehicle in the same locations as their respective experimental groups.

FITC-labeled albumin leakage

Ten days following 6OHDA injection (a time of anticipated significant inflammation in the SN secondary to degeneration from 6OHDA in the striatum or MFB), the animals were anaesthetized (60 mg/kg pentobarbital) and killed. A second group of animals were killed 34 days following 6OHDA injection into the MFB.

Heparin [100 units/kg in 0.2 mL Hanks' balanced salt solution (HBSS)] was injected into the common carotid artery following cardiac puncture in all animals. Immediately after heparin injection, 10 mL FITC-labeled albumin (5 mg/mL) was similarly infused according to the method of Cavaglia *et al.* (2001). The right atrium was opened and the descending circulation was clamped off during infusion. Within 2 min, the brains were removed and immediately immersed into 10 mL Zamboni's fixative (7.5% saturated picric acid, 12 mM NaH₂PO₄, 88 mM Na₂HPO₄ and 4% paraformaldehyde). Three days later, the fixative was replaced with 30% sucrose as described previously (Ling *et al.*, 2004a,b). In a variation on this procedure, we perfused Zamboni's fixative into the ascending carotid artery immediately following the 2-min FITC-labeled albumin infusion (four 6OHDA-lesioned animals and four ascorbate-injected animals).

HRP leakage

In a parallel experimental series, three rats were injected with 6OHDA and three with ascorbate into MFB as described above and perfused 10 days later under pentobarbital anesthesia with 10 mL HRP (500 µg/mL; Sigma) over 2 min. After 2 min the brains were removed and immediately immersed in Zamboni's fixative and processed as described above.

Visualizing and quantifying the FITC-labeled albumin leakage

The brains from the animals were sectioned (40 µm) and mounted on slides for visualization using confocal microscopy (Olympus, Japan). Series of sections (six sections/series) were taken through the striatum, hypothalamus, parietal cortex, SN and the area postrema. For studies involving leakage quantification, the animals were perfused with FITC-labeled albumin and subsequently perfusion-fixed with Zamboni's fixative. The confocal microscope was set using brain sections from a normal animal to determine the photomultiplier tube, gain and offset settings in the window. This step was performed to eliminate auto-fluorescence in the brain tissue. Once these were determined, all the tissue sections were recorded using the same settings. The SN was outlined anatomically and the relative fluorescence units read automatically using FluoView software.

Immunohistochemistry

All brains were processed for the number of tyrosine hydroxylase (TH)-immunoreactive (-ir) cells; this number was used as an index of dopaminergic neuron survival. The brains were sectioned at 40 µm using a sliding microtome and divided into six consecutive series. For TH-ir cell counts, the sections from one series were stained overnight with primary antibody [mouse vs. rat TH (1 : 10 000; Immunostar, Hudson, WI) followed by biotinylated secondary antibody (horse vs. mouse IgG; Vector Laboratories)]. The TH was visualized using either a peroxidase-conjugated avidin–biotin complex and 3,3'-diaminobenzidine (DAB) with nickel enhancement as described previously (Ling *et al.*, 2002b) for stereological assessment, or with cyanine 5 (Cy5) (FluoroLink Cy5-labeled streptavidin; Amersham) for fluorescence visualization.

Selected sections were also processed for Ox-6 as a marker for activated microglia, β3-integrin as a marker for neovascularization, or P-gp. Ox-6 (mouse vs. rat Major Histocompatibility Complex (MHC) class II, 1 : 10 000; Novus Biological, Littleton, CO) was incubated with the sections overnight and then processed using DAB and nickel as described above. Primary antibody to β3-integrin (mouse vs. human β3-integrin, 1 : 10 000; SZ21, Immunotech) or P-gp (mouse vs. human, 1 : 5000; Becton Dickinson) was incubated overnight with sections and processed using biotinylated horse vs. mouse IgG secondary antibody followed by Cy5-conjugated streptavidin (FluoroLink Cy5-labeled streptavidin; Amersham) for confocal analysis.

Stereological assessment of TH-ir cell counts

The estimation of the total number of TH-ir neurons in the SN was determined using the computerized optical dissector method using MicroBrightField software as described previously (Gundersen *et al.*, 1988; Vu *et al.*, 2000). Briefly, the antibody penetration throughout the whole tissue section was assessed by dissectors using an imaging capture technique. The total number (N) of SN cells was calculated using the formula $N = NV \times V_{SN}$, where NV is the numerical density and V_{SN} is the volume of the SN, as determined by Cavalieri's principle (Cavalieri, 1966).

Behavioural testing

Twenty-four additional rats were separated into four groups for behavioural testing following MFB lesioning. For lesioning, 12 animals were injected with 6OHDA and 12 were injected with the ascorbate vehicle. After 17 days, half of each of these groups received

a single i.v. injection of domperidone [10 mg/kg in dimethyl sulfoxide (DMSO) at 1 mL/kg] or the DMSO vehicle (1 mL/kg). The animals were placed into a restraining tube and the tail was immersed in warm water ($\approx 37^\circ\text{C}$) to allow for easy visualization of the tail vein. The drug or vehicle was then administered i.v. at the base of the tail. Sixty minutes later, each animal received a s.c. injection of apomorphine HCl (0.75 mg/kg). Stereotypic behaviour (SB) was assessed as described previously (Carvey *et al.*, 1990) by an investigator blinded to treatment history. Briefly, the SB response was assessed using a 5-point rating scale (from 0+ as quietly resting to 5+ as compulsive gnawing on the cage). These interval scores were recorded every 5 min through the completion of the response, defined as two consecutive intervals of 0+ behaviour (≈ 60 min). The sum of these interval scores was used to generate an Animal Score which was used as an index of the overall response of the animal. In addition to SB, the animals were also observed for other behaviours (e.g. rotation).

Statistical analyses

Ipsilateral–contralateral and treatment differences (6OHDA vs. ascorbate) for the TH-ir cell counts and the optical density of fluorescence leakage were assessed using two-way ANOVA. Individual interval SB assessments were summed for a given animal to yield an Animal Score for each animal within the four treatment groups (domperidone vs. DMSO and 6OHDA vs. ascorbate). The Animal Scores were assessed using two-way ANOVA. If statistical differences were detected, *post hoc* group differences were determined using Tukey's test ($P < 0.05$).

Results

6OHDA increased FITC-labeled albumin leakage

We injected 6OHDA into the striatum and assessed FITC-labeled albumin leakage into the SN and striatum 10 days later. This strategy was used to produce a retrograde neurodegeneration response in the SN at a site remote from the puncture wound. In animals injected with ascorbate, the blood vessels in the SN, both ipsi- and contralateral to the injection, were well defined with no apparent leakage of the fluorescent dye (Fig. 1a and b). Similar results were seen in the contralateral SN of the animals treated with 6OHDA (Fig. 1c). Although vessels could be clearly identified in the SN ipsilateral to the 6OHDA lesion, there were also patchy areas of significant leakage ('hot spots') where individual vessels could not be detected because of the apparent leakage of the FITC-labeled albumin into the surrounding parenchyma (Fig. 1d). Ten days after stereotaxic surgery, little apparent FITC-labeled albumin leakage was seen around the needle tracks of the ascorbate injection site in the striatum (Fig. 1e) whereas there was intense leakage around the 6OHDA injection site (Fig. 1f). As previously suggested by Cavaglia *et al.* (2001) the number of FITC-labeled albumin-filled vessels differed by region and, based on gross inspection of the sections, it appeared that the striatum had fewer FITC-labeled albumin vessels than did the SN. However, we also observed areas of incomplete FITC-labeled albumin perfusion in some animals, potentially due to inadequate perfusion pressure.

A second study was performed in animals killed 10 and 34 days after unilateral MFB injections of 6OHDA. This strategy was used to determine whether a second type of lesion (between the SN and the striatum) produced a similar pattern of leakage, and also to determine whether the leakage was long-lived. In addition, this strategy also allowed us to determine whether DA neuron loss in the SN and the axon degeneration response in the striatum would similarly produce BBB damage. As was true following intrastriatal injection, the

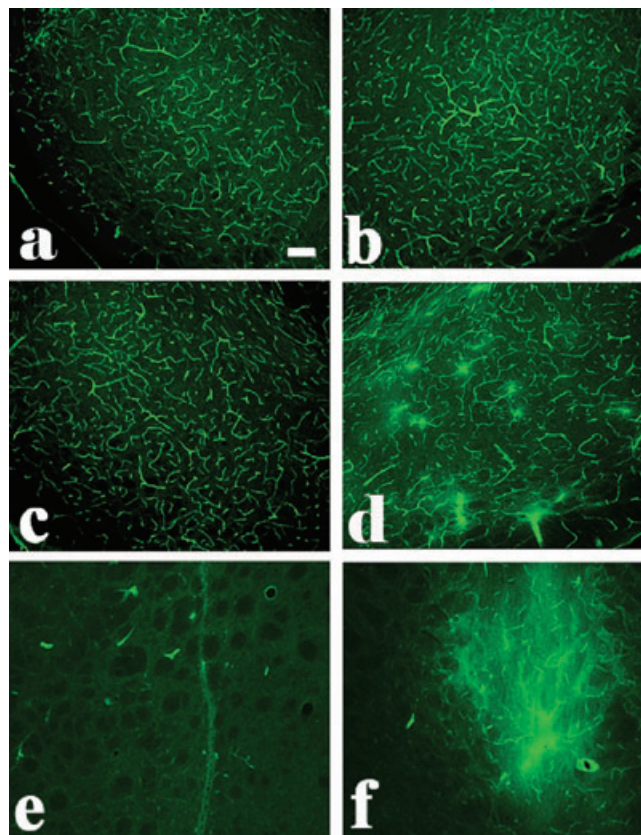


FIG. 1. FITC-labeled albumin leakage 10 days after 6OHDA injection. FITC-labeled albumin leakage in the ipsilateral (d) SN and (f) striatum 10 days following unilateral intrastriatal injection of 6OHDA. No leakage was seen in (a) the contra- and (b) ipsilateral SN of a vehicle-injected animal or in (c) the contralateral SN of a 6OHDA-injected animal. Note that there is a generalised diffuse background fluorescence in the majority of the SN in d as well as areas of intense fluorescence ('hot spots'). Also note (e) the clearly defined needle track in the ascorbate-injected striatum compared with (f) significant FITC-labeled albumin leakage in a 6OHDA-injected animal. Scale bar, 0.1 mm.

vasculature was well defined in both the striatum and the SN of animals injected with ascorbate and killed at both 10 (Fig. 2a and b) and 34 days (Fig. 2e and f). In contrast, MFB injections of 6OHDA produced significant FITC-labeled albumin leakage in both the striatum and SN ipsilateral to the injection site in animals killed 10 days following lesion (Fig. 2c and d) that was still obvious 34 days following lesion (Fig. 2g and h). No leakage was seen in the contralateral hemispheres of either group of animals (data not shown).

It is possible that the leakage seen was a consequence of the FITC-labeled albumin slowly leaking from vessels into brain while the brains were stored in the freezer. In order to exclude this possibility, another group of animals was perfused with FITC-labeled albumin and then immediately perfused with Zamboni's fixative. The assumption was that the vascular FITC label would be washed out of the vessels by the perfusion fixation step but, if it had leaked into the parenchyma during the FITC perfusion, it would remain in the parenchyma following the Zamboni's fixative perfusion. This appeared to be the case (Fig. 3). Thus, following perfusion fixation, neither the ipsi- nor contralateral SN of the controls, nor the contralateral SN of the 6OHDA-lesioned animals, exhibited much FITC-labeled albumin leakage (Fig. 3a–c). In contrast, patchy areas of FITC-labeled albumin leakage were again present in the SN ipsilateral to 6OHDA lesions (Fig. 3d), suggesting it was in brain parenchyma. In addition, this

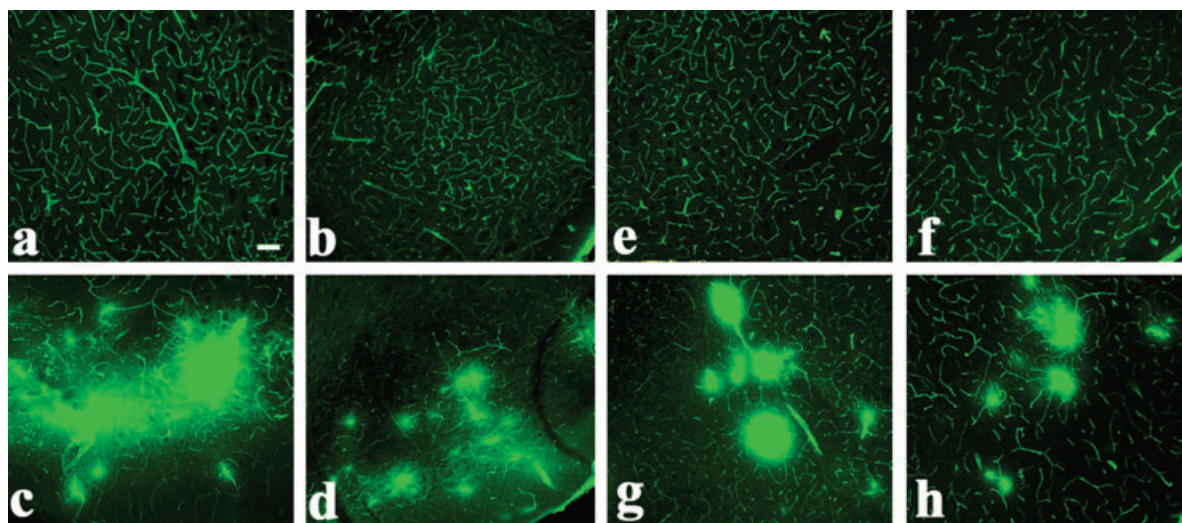


FIG. 2. FITC-labeled albumin leakage 10 and 34 days after MFB 6OHDA injection. FITC-labeled albumin leakage was obvious in the ipsilateral striata (c) 10 and (g) 34 days after an MFB 6OHDA injection. Significant leakage was also seen in the SN (d) 10 days and (h) 34 days after MFB 6OHDA injection. No leakage was noted in (a and e) ipsilateral striata or (b and f) SNs, (a and b) 10 and (e and f) 34 days after MFB ascorbate injections (upper row). Scale bar, 0.1 mm.

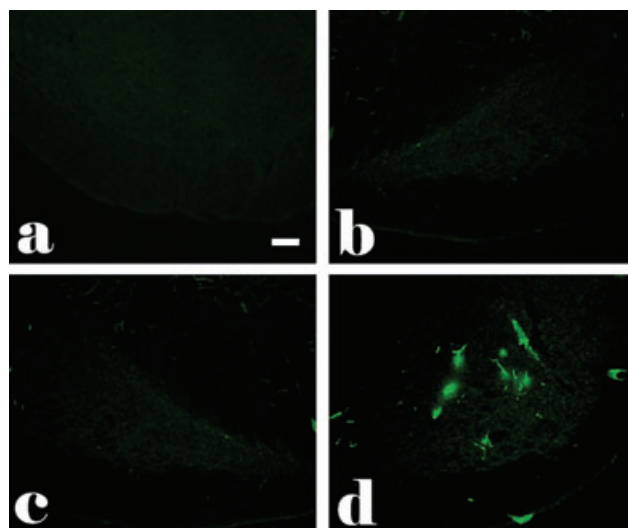


FIG. 3. FITC-labeled albumin leakage remained after perfusion. This was a parallel assay to the one shown in Fig. 1, except that the brains were perfused with Zamboni's fixative to wash out FITC-labeled albumin in the blood vessels immediately after FITC-labeled albumin injection. The remaining bright spots in (d) indicate that FITC-labeled albumin leaked into parenchyma of the SN ipsilateral to the 6OHDA lesion. No leakage was observed in (a) the contra- or (b) ipsilateral SN 10 days after ascorbate injections or (c) the contralateral SN 10 days after 6OHDA injection. Scale bar, 0.1 mm.

procedure allowed us to assess the amount of FITC-labeled albumin that had leaked into the parenchyma to quantify the amount present in brain tissue. Comparison of fluorescence units in the ipsi- and contralateral SNs of ascorbate and 6OHDA-lesioned animals using FluoView Software revealed a 10-fold statistically significant ($F_{1,7} = 249.977$, $P < 0.001$) increase in leakage into the ipsilateral SN relative to contralateral SN of the lesioned animals (Table 1).

6OHDA increased HRP leakage

Leakage was assessed using HRP, a more widely used tracer than albumin to assess BBB integrity. 6OHDA or ascorbate was injected

TABLE 1. Fluorescence intensity in the SNs of perfusion-fixed animals following FITC-labeled albumin infusion

	6OHDA	Ascorbate
Ipsilateral	1056.15 \pm 161.85*	96.97 \pm 12.6
Contralateral	101.30 \pm 25.61	77.56 \pm 8.65

Animals were injected intrastrially with 6OHDA or ascorbate vehicle and intracardially injected with FITC-labeled albumin 10 days later. Immediately after FITC-labeled albumin injection, animals were perfused with Zamboni's fixative to wash out intravascular FITC-labeled albumin. The relative fluorescence units represent the leakage of FITC-labeled albumin into the brain parenchyma ipsilateral or contralateral to the 6OHDA or ascorbate injection.

* $P < 0.001$ vs. vehicle-injected ipsilateral side.

unilaterally into MFB of the rats and, 10 days later, HRP was infused into the vasculature within minutes following a heparin injection. As was true for FITC-labeled albumin, HRP also appeared to leak into surrounding ipsilateral parenchyma in both the striatum and the SN of animals injected with 6OHDA. The parenchyma of the ascorbate-injected animals did not reveal significant leakage of HRP in either the striatum or the SN (data not shown). However, in the striata of the 6OHDA-injected animals, there was clear evidence of diffuse leakage into surrounding parenchyma in the ipsilateral striatum that was not apparent in the contralateral striatum (Fig. 4a). The HRP leakage was confined to the striatum and was not seen in other regions of the brain such as the cortex or thalamus. A pattern of HRP leakage similar to that of the FITC-labeled albumin leakage was also seen in the SN. Thus, there appeared to be diffuse leakage into brain parenchyma as well as areas of significant leakage ('hot-spots'), as was seen using the FITC technique (Fig. 4c). In contrast, in the contralateral SN the HRP was confined to the vasculature (Fig. 4b).

6OHDA lesion-induced FITC-labeled albumin leakage was specific

In order to assess the specificity of the FITC-labeled albumin leakage, we looked at other areas of the brain. In animals injected intrastrially with 6OHDA, there was no apparent leakage of FITC-labeled albumin

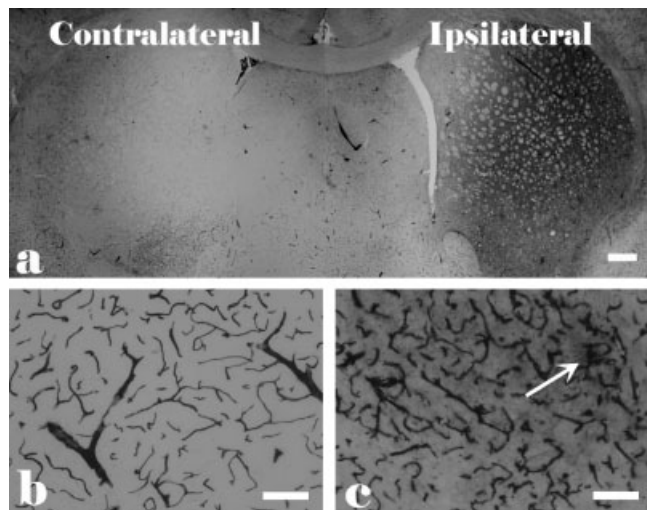


FIG. 4. HRP leakage 10 days following MFB 6OHDA injection. BBB damage was assessed by examining HRP leakage assay. (a, right side) The ipsilateral striatum was darker than the contralateral side, indicating leakage into the striatum. (b) No HRP leakage was seen in the ipsilateral SN of an animal injected with ascorbate, whereas clear leakage was detected in the SN ipsilateral to an MFB 6OHDA injection made 10 days earlier. As was true using FITC-labeled albumin, there was a diffuse background leakage of HRP as well as areas of significant leakage (c, arrow indicates a 'hot spot'). Scale bars, 0.5 mm (a), 0.05 mm (b and c).

into the ipsilateral parietal cortex (Fig. 5a) or hippocampus (Fig. 5b), or into contralateral structures (data not shown). However, when we examined areas of the brain that are not normally protected by the BBB, there was apparent leakage into the hypothalamus around the third ventricle (Fig. 5c, ventromedial hypothalamus) as well as in the area postrema along the floor of the fourth ventricle (Fig. 5d).

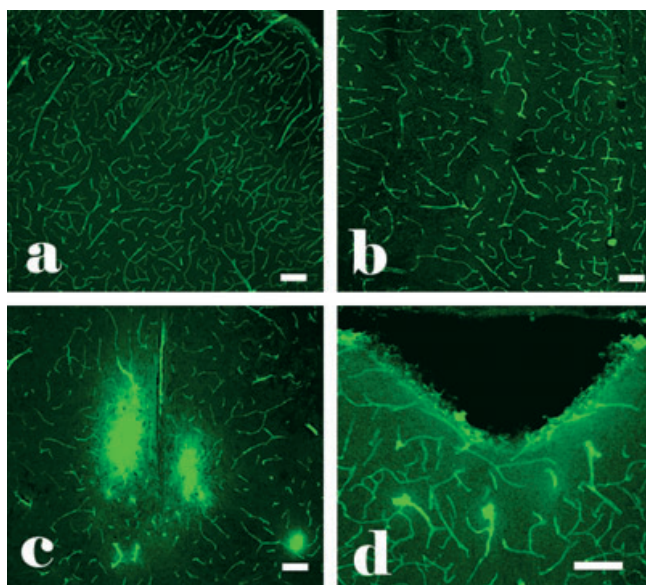


FIG. 5. Negative and positive controls of BBB leakage. The ipsilateral (a) parietal cortex and (b) hippocampus of an animal injected 10 days earlier with 6OHDA did not exhibit any observable leakage of FITC-labeled albumin. However, obvious leakage of FITC-labeled albumin was seen in areas not normally protected by the BBB including (c) the hypothalamus and (d) the area postrema. Scale bar, 0.1 mm.

Leakage was observed in these areas in all animals regardless of prior treatment. Interestingly, although there were occasional areas of leakage that were similar to the 'hot spots' observed in the SN and striatum of the 6OHDA animals, the pattern of leakage was best characterized as diffuse and evenly distributed. The leakage in these areas was also used as a criterion for the efficiency of FITC-labeled albumin perfusion. Thus, failure to see FITC-labeled albumin leakage into the hypothalamus or area postrema would indicate incomplete perfusion, necessitating removal of that animal from subsequent analysis.

FITC-labeled albumin leakage was associated with DA neuron loss

The SNs of the ascorbate and 6OHDA intrastrially-injected animals killed 10 days later were assessed for TH-ir cell loss using fluorescence and DAB immunocytochemistry. Confocal fluorescence of FITC-labeled albumin (green) and TH-ir cells (red) revealed normal vasculature, and TH-ir cells in both the compacta and reticulata regions of animals in the ascorbate-injected group (Fig. 6a–c). In contrast, TH immunoreactivity was less intense in both the ipsilateral SN compacta and reticulata of the 6OHDA-injected animals (Fig. 6e). In these animals, both the SN compacta and reticulata revealed numerous areas of FITC-labeled albumin leakage (hot-spots; Fig. 6d) that were generally associated with an area of TH immunoreactivity (Fig. 6f). Interestingly, the hot-spots were often concordant with the red fluorescence, suggesting that FITC-labeled albumin leakage was more often seen in areas where TH immunoreactivity was present (yellow in Fig. 6f). Adjacent sections were processed for TH immunocytochemistry using DAB, submitted to quantitative stereology. Intrastriatal 6OHDA produced a statistically significant ($F_{3,19} = 18.83$; $P < 0.001$) 38.46% decrease in TH-ir cells in the SN relative to the ipsilateral side of the ascorbate-injected controls, in good agreement with the 40% TH-ir cell loss seen by Sauer & Oertel (1994) at 14 days following intrastriatal lesions. There were no other statistically significant pair-wise comparisons among the treatment groups.

$\beta 3$ -Integrin was increased in areas of increased FITC-labeled albumin leakage

Additional sections from animals injected intrastrially with 6OHDA or ascorbate were processed for FITC-labeled albumin leakage and $\beta 3$ -integrin. FITC-labeled albumin leaked into surrounding parenchyma in the SNs of the 6OHDA animals (Fig. 7d), but not the controls. Although $\beta 3$ -integrin reactivity was diffusely seen in control SN (Fig. 7b), it was dramatically increased in animals injected with 6OHDA (Fig. 7e). Indeed, the apparent hot-spots for FITC leakage were highly concordant with areas of intense $\beta 3$ -integrin signal in the 6OHDA animals (Fig. 7f), whereas little concordance was seen in the ascorbate controls (Fig. 7c). It is important to note that $\beta 3$ -integrin is also expressed on platelets (Akiyama *et al.*, 1991), which could have contributed to the apparent increases seen. However, if this were the case, then the increase would also be seen in the contralateral SNs of animals injected with 6OHDA or in animals injected with ascorbate.

TH-ir cell loss was associated with increased microglial activation

Additional SN sections from the animals injected intrastrially with ascorbate or 6OHDA and killed 10 days later were processed for Ox-6

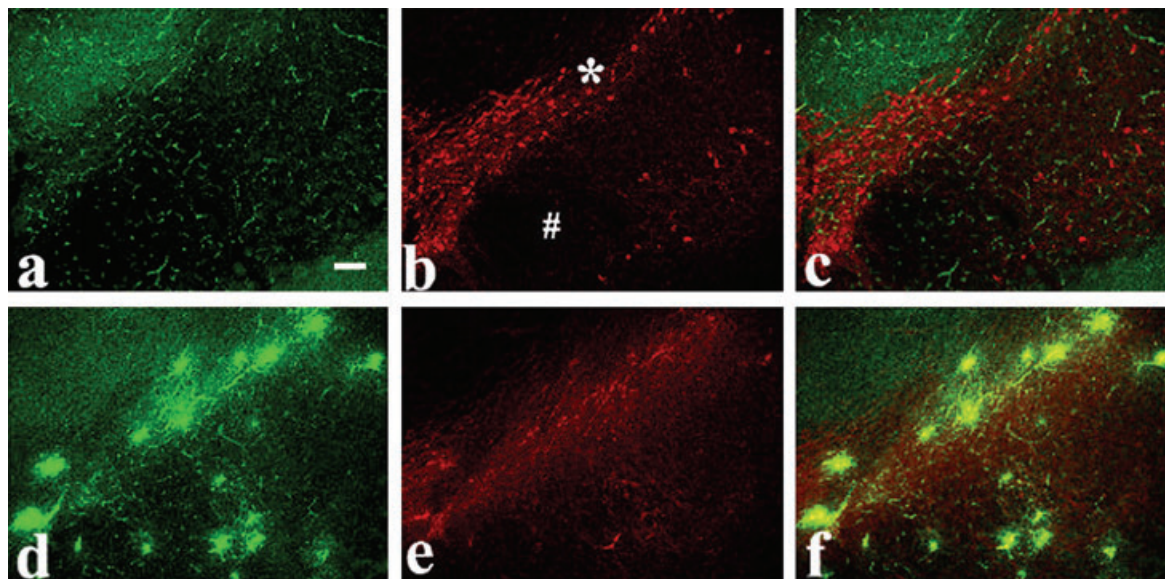


FIG. 6. Association of FITC-labeled albumin leakage and TH-ir cell loss. FITC-labeled albumin (green) and TH-ir cells (red) in the ipsilateral SN of an animal injected intrastratially with (a–c) ascorbate or (d–f) 6OHDA and killed 10 days later. (a) Ascorbate injection was associated with well-defined vascular FITC-labeled albumin filling in these animals. (b) The density of the TH-ir cells was greater in the SN compacta (*) than in the SN reticulata (#), a TH-ir cell pattern typical of a normal mesencephalon. (d) In contrast, diffuse FITC-labeled albumin leakage, as well as areas of intense signal, was seen in the compacta and reticulata region of the ipsilateral SN of an animal injected with 6OHDA. (e) TH-ir fluorescence was less intense in the SN of the 6OHDA-injected animal, indicating DA neuron loss. Interestingly, the areas of significant FITC-labeled albumin leakage were often associated with areas of TH-ir cells (yellow in f) which was not the case in (c) the SN of the control animal. Scale bar, 0.1 mm.

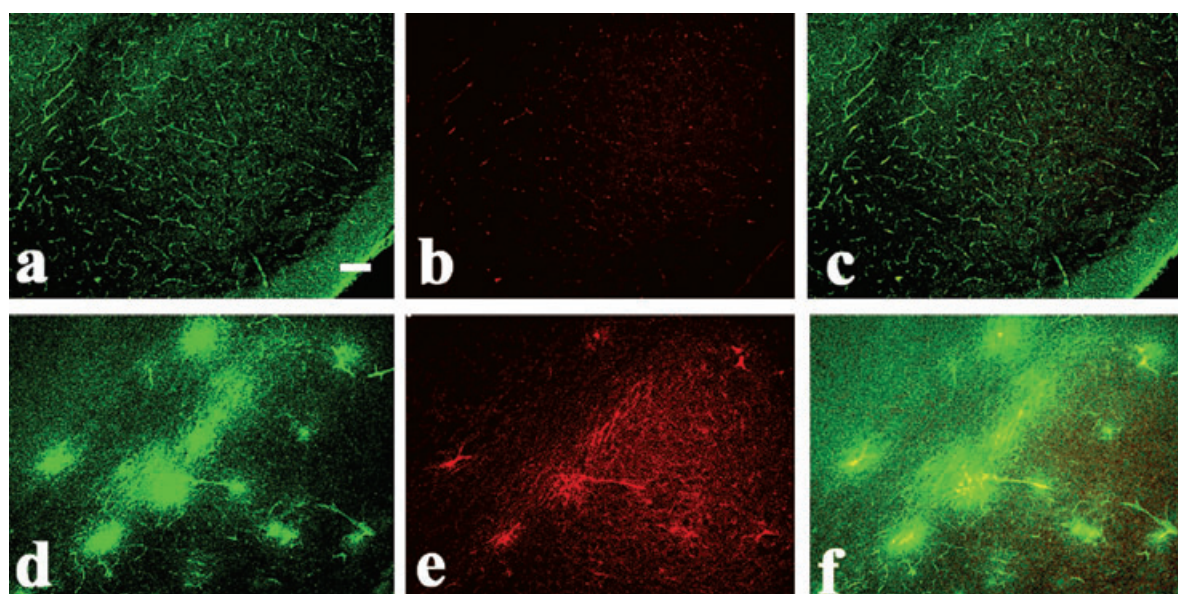


FIG. 7. Elevation of $\beta 3$ -integrin protein levels in the SN following 6OHDA injections. FITC-labeled albumin (green) and $\beta 3$ -integrin (red) in the SN of an animal injected intrastratially with (a–c) ascorbate or (d–f) 6OHDA and killed 10 days later. Ascorbate injection produced (a) well-defined vascular filling in the SN, but (b) only a very light and diffuse $\beta 3$ signal was seen, suggesting a low level of $\beta 3$ -integrin immunoreactivity. (c) There was little concordance between the two markers. (e) In contrast, the $\beta 3$ -integrin signal was dramatically increased in animals injected with 6OHDA and (f) was highly concordant with areas of intense FITC signal (yellow colour) as seen in the merged image. Scale bar, 0.1 mm.

immunoreactivity to visualize activated microglia. In most sections from the control animals, Ox-6-ir cells could not be seen. One control animal had a few Ox-6-ir cells (Fig. 8a) ipsilateral to the ascorbate injection. In contrast, Ox-6-ir cells were highly abundant in the ipsilateral SNs of all animals injected with 6OHDA (Fig. 8b), in agreement with previous studies (Depino *et al.*, 2003).

Domperidone attenuated SB in 6OHDA-injected animals

A separate set of animals was assessed for their SB response to apomorphine 17 days following unilateral MFB injection of 6OHDA or ascorbate and 1 h following injection of domperidone or vehicle (DMSO). Animals injected with 6OHDA and then pretreated with

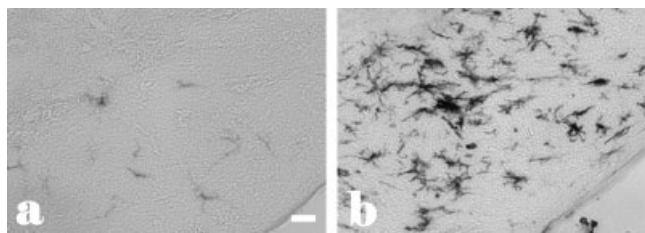


FIG. 8. Microglial activation after 6OHDA lesions. DAB, nickel-enhanced Ox-6 immunoreactivity in the ipsilateral SN of an animal injected intrastratially with (a) ascorbate or (b) 6OHDA and killed 10 days later. Note the dramatic increase in activated microglia in the animal injected with 6OHDA. Scale bar, 0.05 mm.

domperidone showed a 17% reduction in their overall behavioural response to apomorphine (mean Animal Scores) relative to ascorbate-injected animals pretreated with domperidone, and a 22% reduction relative to 6OHDA–DMSO controls ($F_{3,24} = 13.07$, $P < 0.001$; Fig. 9a). Examination of the Interval Scores revealed an attenuated and delayed peak behavioural response and a more rapid return to behavioural baseline typical of animals on a direct-acting DA agonist pretreated with a low dose of DA antagonist (Fig. 9b). Three animals in the unilateral 6OHDA–DMSO group exhibited slow contralateral rotations following apomorphine injection, indicative of partially lesioned animals. No rotations were seen in the 6OHDA–domperidone group or either of the ascorbate-injected groups.

P-gp immunoreactivity was increased by 6OHDA

Drug pumps including P-gp contribute to barrier function and return drugs such as domperidone to the lumen of vasculature if they enter the endothelial cells. Examination of P-gp immunoreactivity in ascorbate-injected animals 34 days following intrastratial injection showed that much of the immunoreactivity was colocalized with FITC-filled vessels in the SN (Fig. 10b). Some of the immunoreactivity was not associated with FITC-labeled albumin-filled vessels, however, suggesting that some vessels were incompletely filled with FITC-labeled albumin or that vessels were out of the plane of focus in

these 40- μ m sections (Fig. 10a). No overt leakage of FITC-labeled albumin into parenchyma was seen. In contrast, P-gp immunoreactivity was markedly elevated in animals injected with 6OHDA (Fig. 10e) and that also exhibited FITC-labeled albumin leakage (Fig. 10d). There was clear concordance between P-gp and FITC-labeled albumin in many vessels (yellow in Fig. 10e), but there was also a considerable amount of P-gp immunoreactivity in areas not associated with vessels. Although some of this vessel-unrelated immunoreactivity may be due to incomplete vascular filling and vessels out of focus, it is also likely that some of the P-gp immunoreactivity is in other tissue (Fig. 10f). This is consistent with the recent findings by Volk *et al.* (2005) who concluded that P-gp was up-regulated in neurons and astrocytes following kainate-induced seizures. Therefore, unlike the increase in β integrin, the apparent increase in P-gp was more generalized and present in areas of increased FITC-labeled albumin leakage as well as in areas with no significant leakage.

Discussion

This study represents the first evaluation of BBB leakage following a Parkinson-like lesion in animals. The results showed that 6OHDA injected into either the striatum or the MFB produced leakage of FITC-labeled albumin into both the striatum and SN. These findings were confirmed using a second tracer, HRP. The leakage seen was long-lived because it was still present 34 days following 6OHDA injection and was associated with verified DA neuron loss and increased numbers of activated microglia. The leakage was clearly associated with neovascularization because the areas of leakage were highly concordant with increases in $\beta 3$ -integrin immunoreactivity. The 6OHDA lesions also increased the entry of small molecules into brain, because domperidone was able to attenuate the behavioural response to apomorphine despite an apparent increase of P-gp immunoreactivity. Taken together, these data suggest that 6OHDA-induced DA neuron loss or axon degeneration was associated with dysfunction of the BBB.

It is possible that the stereotaxic surgery produced the leakages seen, but this seems unlikely for several reasons. First, ascorbate control animals did not exhibit any FITC-labeled albumin or HRP leakage into the SN or striatum 10 days after surgery. Although

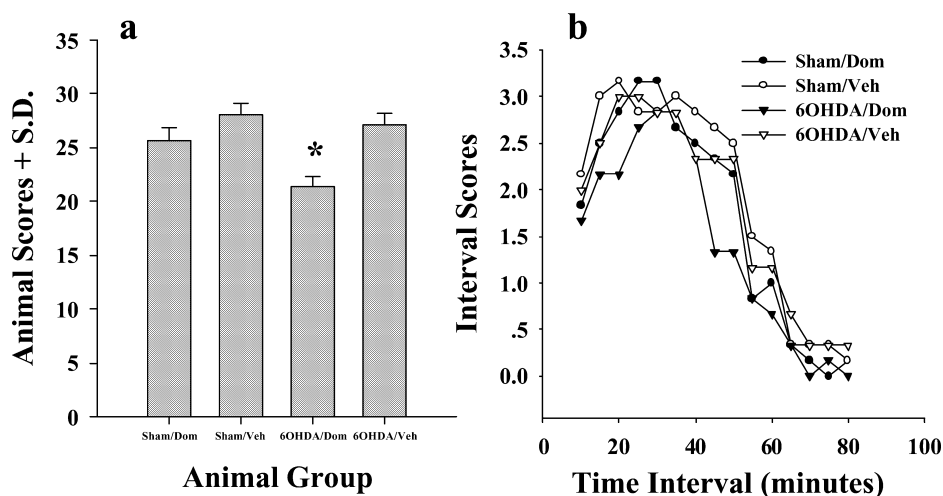


FIG. 9. Domperidone attenuated apomorphine-induced SB. SB response (a, Animal Scores; b, Interval Scores) to apomorphine 17 days following stereotaxic injection of ascorbate vehicle (Sham) or 6OHDA unilaterally into the MFB. Half of the animals in each group were pretreated with domperidone (Dom) and the other half with DMSO (Veh) 1 h prior to apomorphine injection. Domperidone pretreatment (a) attenuated apomorphine-induced SB and (b) attenuated and reduced the peak behavioural response in the animals injected with 6OHDA. (* $P < 0.05$ relative to all other treatment groups).

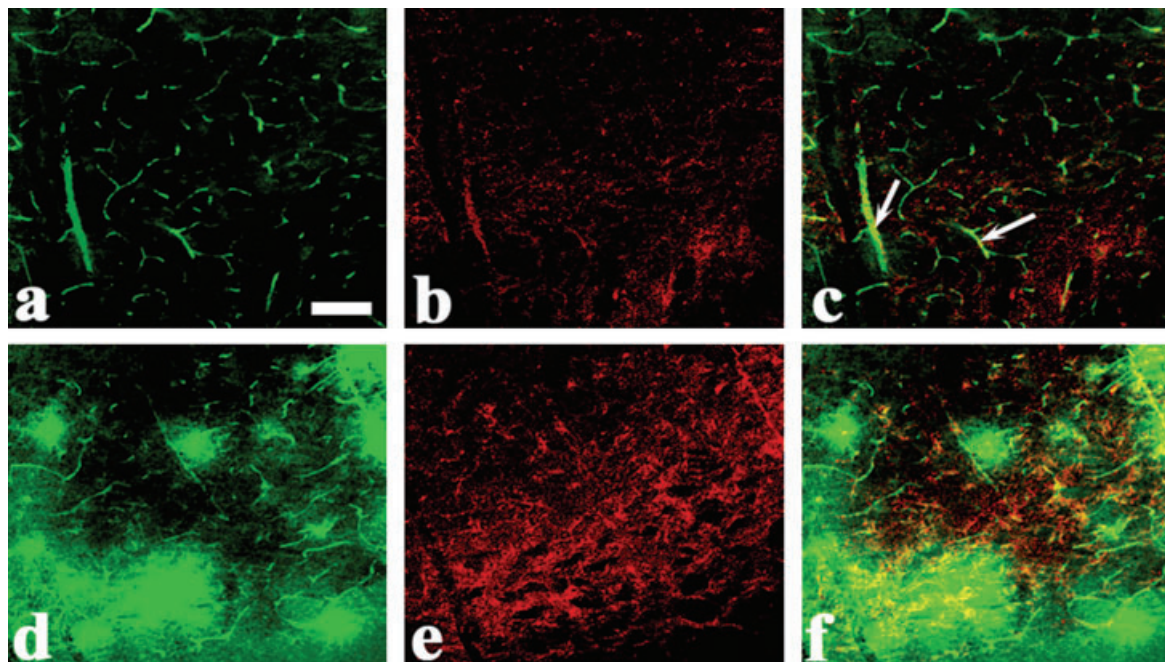


FIG. 10. Elevation of P-gp in the SN following 6OHDA injection. FITC-labeled albumin (green) and P-gp (red) in the SN of animals injected intrastratially with (a–c) ascorbate or (d–f) 6OHDA and killed 34 days later. Much of the P-gp immunoreactivity was colocalized with vessels in the control SN (c, shown by arrows). (e) P-gp was markedly increased by 6OHDA lesions in the SN and there was clear concordance between P-gp and FITC-labeled albumin in many vessels, which (f) showed yellow in the overlay. Scale bar, 0.1 mm.

detailed time course studies on re-establishing barrier function following 6OHDA injury need to be performed, the 10-day time point studied here was similar to the 10 days needed to fully re-establish normal barrier function following a transection injury (Reynolds & Morton, 1998) or a contusion (Duvdevani *et al.*, 1995). Thus, most studies suggest that barrier function returns to normal within 10–14 days even following the severest injuries (Geist *et al.*, 1991; Schnell *et al.*, 1999; Borlongan *et al.*, 2004). Second, leakage was still seen in animals 34 days following injection; this is well past any of the recovery periods studied by others. Third, both intrastratial and MFB injections of 6OHDA produced FITC-labeled albumin leakage at sites remote from the injection. It therefore appears that factors other than mechanical injury were responsible for the barrier dysfunction.

The FITC-labeled albumin and HRP leakage seen in the lesioned animals was confined to areas normally affected by 6OHDA lesions or areas not protected by the BBB. Thus, leakage was seen in the SN and the striatum ipsilateral to the lesion. Other areas of the brain such as the parietal cortex and hippocampus, or the SN or striatum on the contralateral sides of the brains, were unaffected. Although leakage was also detected in the hypothalamus and area postrema, this was expected because these areas are not protected by the BBB. It therefore appears that the leakage was associated with the neurotoxic process taking place in the nigro-striatal pathway brought about by injecting 6OHDA into either the striatum or the MFB. These neurotoxic effects were confirmed using fluorescence labelling and stereological cell counting techniques, both of which demonstrated significant TH-ir cell loss in the SN.

The leakage seen in the SN and striatum was always patchy in appearance whereas that seen in the area postrema and the ventromedial hypothalamus was diffuse and homogeneous. This suggests that the 6OHDA injections led to multiple focal breakdowns in the BBB function. These 'hot spots' were highly concordant with increased

β 3-integrin immunoreactivity. This cell-surface marker is present on angiogenic endothelial cells and virtually absent on intact vessels (Brooks *et al.*, 1995). Members of this family of integrins (β 3-integrin is a member of the α v- β 3 family of integrins) are thought to stabilize the endothelium in the brain during neovascularization (Milner & Campbell, 2002). Because angiogenesis occurs following damage to endothelial cells and the up-regulation of β 3-integrin was highly concordant with FITC-labeled albumin leakage, it can be argued that the vasculature in these animals was undergoing focal reorganisation and repair following 6OHDA. This is consistent with the studies discussed by Barcia *et al.* (2004), who demonstrated angiogenesis in the SN of patients with PD. Our results are also consistent with those of a more recent study in which increased expression of vascular endothelial growth factor was observed in the SNs of patients with PD (Barcia *et al.*, 2005). Moreover, the present results also extend the findings of these prior studies by suggesting that the BBB dysfunction described in patients is not likely to reflect total disruption of BBB function within the SN or striatum, but rather numerous small, focal areas of dysfunction that, none the less, could have significant implications for function within the nigro-striatal pathway.

The fact that we did not observe diffuse areas of FITC-labeled albumin leakage in the SN or striatum suggests that the BBB is not broken down throughout the breadth of these structures. If it were, the resulting oedema would totally compromise function. However, even patchy dysfunction appeared to have functional consequences because domperidone was able to statistically attenuate apomorphine-induced SB. Domperidone is a DA antagonist most frequently used clinically to treat peripheral DA side-effects during antiparkinsonian therapy (Schubring *et al.*, 1999). It normally does not enter the brain due its high affinity for P-gp located on endothelial cells (El Ela *et al.*, 2004). Indeed, drugs such as cyclosporin, which block the actions of P-gp, allow domperidone to enter brain (Tsujikawa *et al.*, 2003). As a substrate for P-gp, it was therefore surprising that

the domperidone-induced attenuation of apomorphine-induced SB was seen despite an apparent up-regulation of P-gp. This might suggest that the domperidone entered the brain via a paracellular route following disruption of the tight junctions, and that the magnitude of the attenuation might have been larger if an increase in P-gp had not occurred. However, a recent clinical study argued that PD was associated with reduced function of P-gp (Kortekaas *et al.*, 2005). Patients exhibited an 18% increase in the uptake of [^{11}C]-verapamil relative to controls. Because verapamil is also a substrate for P-gp, the authors argued that reduced extrusion by P-gp was associated with PD and might contribute to increased entry of toxic substances in these patients. It is possible that the reduced extrusion seen in this study was a consequence of increased leakage although it is difficult to compare these two studies. Regardless, the results from both studies point to abnormalities in BBB and P-gp function following damage to the SN.

The apparent dysfunction seen in the BBB could result from a number of different mechanisms. These include interruption of blood flow due to occlusion, formation of new vessels (neovascularization), which often leak during formation (Wang *et al.*, 2005), functional abnormalities in astrocytes that are responsible for maintaining the tight junctions in the BBB (Ballabh *et al.*, 2004), and increased transcytosis (Predescu *et al.*, 2004). In addition, numerous studies have shown that inflammation is able to disrupt barrier function (Huber *et al.*, 2001b; Lenzlinger *et al.*, 2001; Nimmo *et al.*, 2004). Initially, it was thought that only vascular inflammogens were involved. However, more recently it has become apparent that inflammation on the parenchymal side of the barrier (abluminal side) is also able to disrupt the BBB as demonstrated in multiple sclerosis (Minagar & Alexander, 2003) and epilepsy (Janigro, 1999). In addition, several factors thought to be involved with the neuroinflammation underlying Alzheimer's disease may also affect BBB function. Injection of β -amyloid was shown to affect barrier function (Fiala *et al.*, 1998; Berzin *et al.*, 2000; Giri *et al.*, 2000; Farkas *et al.*, 2003) and Claudio (1996) reported ultrastructural changes and collagen deposition in areas of cell loss from patients with Alzheimer's disease that are also seen in animals with compromised barrier function. Thus, it appears that neuroinflammation, as well as vascular inflammogens, can disrupt barrier function. Because injection of 6OHDA produces neuroinflammation (Cicchetti *et al.*, 2002; Depino *et al.*, 2003; Ling *et al.*, 2004b) and degeneration of DA neurons is associated with inflammatory events, regardless of the toxin involved (Castano *et al.*, 2002; Hebert *et al.*, 2003), it is possible that 6OHDA-induced parenchymal inflammation disrupted barrier function in the present study.

Although more detailed studies need to be performed to assess the linkage between neuroinflammation and BBB dysfunction, the results from the present study partially support this hypothesis. In particular, the 6OHDA-induced reduction in TH-ir cell counts was associated with increased numbers of Ox-6-ir cells in the SN, suggesting activation of microglia. Interestingly, Lynch *et al.* (2004) showed that microglia were activated prior to breakdown of BBB. Activation of microglia can result in the release of TNF α (Stoll *et al.*, 2002), and this pro-inflammatory cytokine is well known for its ability to disrupt barrier function, both *in vitro* and *in vivo* (Mark & Miller, 1999; Tsao *et al.*, 2001; Didier *et al.*, 2003; Lynch *et al.*, 2004). It is therefore possible that 6OHDA, or the degeneration of DA neurons, led to activation of microglia which in turn released TNF α , leading to the breakdown of the BBB. In addition, intrastratial 6OHDA lesions have been shown to produce microglial activation that is still present 4 weeks following injection (Cicchetti *et al.*, 2002). However, it is also important to note that Depino *et al.* (2003) failed to detect

increases in TNF α protein following intrastratial lesions despite observing increases in microglial activation, and microglial activation has been demonstrated without pro-inflammatory cytokine production (Perry *et al.*, 2002). Thus, any potential link between neuroinflammation and BBB dysfunction will require further study.

The results from the present study raise several questions regarding our understanding of PD and its treatment.

Firstly, they suggest that drugs normally excluded from the brain may potentially have the ability to enter. The fact that carbidopa, a widely used adjunctive drug with levodopa therapy, does not appear to compromise levodopa therapy, probably contributes to the belief that the BBB is intact in PD. Indeed, carbidopa was developed based on its inability to cross the BBB while blocking peripheral decarboxylase (Celesia & Wanamaker, 1976). Obviously there is no radical disruption of barrier function in PD patients because the PD brain is not characterized by oedema. However, it is possible that a small amount of carbidopa might leak into brain in the SN and striatum and reduce the potency of levodopa; this potency would otherwise be greater if barrier function were intact. Another potential consequence of patchy leakage might be dyskinesias that plague levodopa therapy. Thus, intermittent or nonhomogeneous levodopa entry into the striatum due to sporadic barrier disruption would produce nonhomogeneous areas of DA stimulation which could lead to dyskinesias (Chase, 1998).

Secondly, if DA neuron degeneration led to long-term disruption of barrier function, then those regions of the brain would be exposed to higher quantities of peripheral neurotoxins which could contribute to further disease progression.

Thirdly, if the BBB is disrupted it is also possible that peripheral inflammogens and immune mediators play a role in PD pathogenesis, as previously suggested (McRae-Degueurce *et al.*, 1988; Appel *et al.*, 1992).

Finally, repairing BBB breakdown would offer a new therapeutic strategy in the treatment of PD.

Clearly these results need to be extended further in animal models and verified in patients. However, they imply a heretofore under-recognised characteristic of DA degeneration that provides new insight into PD.

Acknowledgements

The Authors wish to thank Ms Chong Wai Tong for her help in processing the tissue sections. This work was supported by NINDS NS045316, NIEHS 012307, W81XWH-04-01-0365 and the Michael J. Fox Foundation.

Abbreviations

6OHDA, 6-hydroxydopamine; BBB, blood-brain barrier; CSF, cerebrospinal fluid; DA, dopamine; DAB, 3,3'-diaminobenzidine; DMSO, dimethyl sulfoxide; FITC, fluorescein isothiocyanate; HBSS, Hanks' balanced salt solution; HRP, horseradish peroxidase; iNOS, inducible form of nitric oxide synthase; -ir, -immunoreactive; MFB, medial forebrain bundle; PD, Parkinson's disease; P-gp, P-glycoprotein; SB, stereotypic behaviour; SN, substantia nigra; TH, tyrosine hydroxylase; TNF α , tumour necrosis factor alpha.

References

- Akiyama, H., Kawamata, T., Dedhar, S. & McGeer, P.L. (1991) Immunohistochemical localization of vitronectin, its receptor and beta-3 integrin in Alzheimer brain tissue. *J. Neuroimmunol.*, **32**, 19–28.
- Appel, S.H., Le, W.D., Tajti, J., Haverkamp, L.J. & Engelhardt, J.I. (1992) Nigral damage and dopaminergic hypofunction in mesencephalon-immunized guinea pigs. *Ann. Neurol.*, **32**, 494–501.

- Ballabh, P., Braun, A. & Nedergaard, M. (2004) The blood–brain barrier: an overview: structure, regulation, and clinical implications. *Neurobiol. Dis.*, **16**, 1–13.
- Barcia, C., Bautista, V., Sanchez-Bahillo, A., Fernandez-Villalba, E., Faucheux, B., Poza, Y.P., Fernandez, B.A., Hirsch, E.C. & Herrero, M.T. (2005) Changes in vascularization in substantia nigra pars compacta of monkeys rendered parkinsonian. *J. Neural Transm.*, in press.
- Barcia, C., Emborg, M.E., Hirsch, E.C. & Herrero, M.T. (2004) Blood vessels and parkinsonism. *Front. Biosci.*, **9**, 277–282.
- Berzin, T.M., Zipser, B.D., Rafii, M.S., Kuo-Leblanc, V., Yancopoulos, G.D., Glass, D.J., Fallon, J.R. & Stopa, E.G. (2000) Agrin and microvascular damage in Alzheimer's disease. *Neurobiol. Aging*, **21**, 349–355.
- Boka, G., Anglade, P., Wallach, D., Javoy-Agid, F., Agid, Y. & Hirsch, E.C. (1994) Immunocytochemical analysis of tumor necrosis factor and its receptors in Parkinson's disease. *Neurosci. Lett.*, **172**, 151–154.
- Borlongan, C.V., Lind, J.G., Dillon-Carter, O.Yu.G., Hadman, M., Cheng, C., Carroll, J. & Hess, D.C. (2004) Bone marrow grafts restore cerebral blood flow and blood brain barrier in stroke rats. *Brain Res.*, **1010**, 108–116.
- Brooks, P.C., Montgomery, A.M., Rosenfeld, M., Reisfeld, R.A., Hu, T.G.K. & Chersesh, D.A. (1995) Integrin alpha v beta 3 antagonists promote tumor regression by inducing apoptosis of angiogenic blood vessels. *Cell*, **79**, 1157–1164.
- Carvey, P.M., Chang, Q., Lipton, J.W. & Ling, Z. (2003) Prenatal exposure to the bacteriotoxin lipopolysaccharide leads to long-term losses of dopamine neurons in offspring: a potential, new model of Parkinson's disease. *Front. Biosci.*, **8**, s826–s837.
- Carvey, P.M., Kao, L.C., Zhang, T.J., Amdur, R.L., Lin, D.H., Singh, R. & Klawans, H.L. (1990) Dopaminergic alterations in cotreatments attenuating haloperidol-induced hypersensitivity. *Pharmacol. Biochem. Behav.*, **35**, 291–300.
- Castano, A., Herrera, A.J., Cano, J. & Machado, A. (2002) The degenerative effect of a single intranigral injection of LPS on the dopaminergic system is prevented by dexamethasone, and not mimicked by rh-TNF-alpha, IL-1beta and IFN-gamma. *J. Neurochem.*, **81**, 150–157.
- Cavaglia, M., Dombrowski, S.M., Drazba, J., Vasanji, A., Bokesch, P.M. & Janigro, D. (2001) Regional variation in brain capillary density and vascular response to ischemia. *Brain Res.*, **910**, 81–93.
- Cavalieri, B. (1966) *Geometria degli Indivisibili*. Unione Tipografica Editrice, Torino.
- Celesia, G.G. & Wanamaker, W.M. (1976) 1-dopa-carbidopa: combined therapy for the treatment of Parkinson's disease. *Dis. Nerv. Syst.*, **37**, 123–125.
- Chase, T.N. (1998) The significance of continuous dopaminergic stimulation in the treatment of Parkinson's disease. *Drugs*, **55** (Suppl. 1), 1–9.
- Cicchetti, F., Brownell, A.L., Williams, K., Chen, Y.I., Livni, E. & Isacson, O. (2002) Neuroinflammation of the nigrostriatal pathway during progressive 6-OHDA dopamine degeneration in rats monitored by immunohistochemistry and PET imaging. *Eur. J. Neurosci.*, **15**, 991–998.
- Claudio, L. (1996) Ultrastructural features of the blood–brain barrier in biopsy tissue from Alzheimer's disease patients. *Acta Neuropathol. (Berl.)*, **91**, 6–14.
- Depino, A.M., Earl, C., Kaczmarczyk, E., Ferrari, C., Besedovsky, H., del Rey, A., Pitossi, F.J. & Oertel, W.H. (2003) Microglial activation with atypical proinflammatory cytokine expression in a rat model of Parkinson's disease. *Eur. J. Neurosci.*, **18**, 2731–2742.
- Di Monte, D.A. (2003) The environment and Parkinson's disease: is the nigrostriatal system preferentially targeted by neurotoxins? *Lancet Neurol.*, **2**, 531–538.
- Didier, N., Romero, I.A., Creminon, C., Wijkhuisen, A., Grassi, J. & Mabondzo, A. (2003) Secretion of interleukin-1beta by astrocytes mediates endothelin-1 and tumour necrosis factor-alpha effects on human brain microvascular endothelial cell permeability. *J. Neurochem.*, **86**, 246–254.
- Duvdevani, R., Roof, R.L., Fulop, Z., Hoffman, S.W. & Stein, D.G. (1995) Blood–brain barrier breakdown and edema formation following frontal cortical contusion: does hormonal status play a role? *J. Neurotrauma*, **12**, 65–75.
- El Ela, A.A., Hartter, S., Schmitt, U., Hiemke, C., Spahn-Langguth, H. & Langguth, P. (2004) Identification of P-glycoprotein substrates and inhibitors among psychoactive compounds – implications for pharmacokinetics of selected substrates. *J. Pharm. Pharmacol.*, **56**, 967–975.
- Farkas, I.G., Czigner, A., Farkas, E., Dobo, E., Soos, K., Penke, B., Endresz, V. & Mihaly, A. (2003) Beta-amyloid peptide-induced blood–brain barrier disruption facilitates T-cell entry into the rat brain. *Acta Histochem.*, **105**, 115–125.
- Farkas, E., De Jong, G.I., de Vos, R.A., Jansen Steur, E.N. & Luiten, P.G. (2000) Pathological features of cerebral cortical capillaries are doubled in Alzheimer's disease and Parkinson's disease. *Acta Neuropathol. (Berl.)*, **100**, 395–402.
- Faucheux, B.A., Bonnet, A.M., Agid, Y. & Hirsch, E.C. (1999) Blood vessels change in the mesencephalon of patients with Parkinson's disease. *Lancet*, **353**, 981–982.
- Ferger, B., Leng, A., Mura, A., Hengerer, B. & Feldon, J. (2004) Genetic ablation of tumor necrosis factor-alpha (TNF-alpha) and pharmacological inhibition of TNF-synthesis attenuates MPTP toxicity in mouse striatum. *J. Neurochem.*, **89**, 822–833.
- Fiala, M., Zhang, L., Gan, X., Sherry, B., Taub, D., Graves, M.C., Hama, S., Way, D., Weinand, M., Witte, M., Lorton, D., Kuo, Y.M. & Rohrer, A.E. (1998) Amyloid-beta induces chemokine secretion and monocyte migration across a human blood–brain barrier model. *Mol. Med.*, **4**, 480–489.
- Gao, B., Saba, T.M. & Tsan, M.F. (2002) Role of alpha (v) beta (3)-integrin in TNF-alpha-induced endothelial cell migration. *Am. J. Physiol. Cell Physiol.*, **283**, 1196–1205.
- Geist, M.J., Maris, D.O. & Grady, M.S. (1991) Blood–brain barrier permeability is not altered by allograft or xenograft fetal neural cell suspension grafts. *Exp. Neurol.*, **111**, 166–174.
- Giri, R., Shen, Y., Du Stins, M.Y.S., Schmidt, A.M., Stern, D., Kim, K.S., Zlokovic, B. & Kalra, V.K. (2000) Beta-amyloid-induced migration of monocytes across human brain endothelial cells involves RAGE and PECAM-1. *Am. J. Physiol. Cell Physiol.*, **279**, C1772–C1781.
- Gunderson, H.J.G., Bagger, P., Bendtsen, T.F., Evans, S.M., Korbo, L., Marcussen, M., Fflier, A., Nielsen, K., Nyengaard, J.R., Pakkenberg, B., Sørensen, F.B., Vesterby, A. & West, M.J. (1988) The new stereological tools: disector, fractionator, nucleator and point sampled intercepts and their use in pathological research and diagnosis. *APMIS*, **96**, 857–881.
- Haussermann, P., Kuhn, W., Przuntek, H. & Müller, T. (2001) Integrity of the blood–cerebrospinal fluid barrier in early Parkinson's disease. *Neurosci. Lett.*, **300**, 182–184.
- Hebert, G., Arsaut, J., Dantzer, R. & Demotes-Mainard, J. (2003) Time-course of the expression of inflammatory cytokines and matrix metalloproteinases in the striatum and mesencephalon of mice injected with 1-methyl-4-phenyl-1,2,3,6-tetrahydropyridine, a dopaminergic neurotoxin. *Neurosci. Lett.*, **349**, 191–195.
- Hedrich, K., Djarmati, A., Schafer, N., Hering, R., Wellenbrock, C., Weiss, P.H., Hilker, R., Viergege, P., Ozelius, L.J., Heutink, P., Bonifati, V., Schwinger, E., Lang, A.E., Noth, J., Bressman, S.B., Pramstaller, P.P., Riess, O. & Klein, C. (2004) DJ-1 (PARK7) mutations are less frequent than Parkin (PARK2) mutations in early-onset Parkinson disease. *Neurology*, **62**, 389–394.
- Hirsch, E.C., Breidert, T., Rousselet, E., Hunot, S., Hartmann, A. & Michel, P.P. (2003) The role of glial reaction and inflammation in Parkinson's disease. *Ann. NY Acad. Sci.*, **991**, 214–228.
- Huber, J.D., Egleton, R.D. & Davis, T.P. (2001a) Molecular physiology and pathophysiology of tight junctions in the blood–brain barrier. *Trends Neurosci.*, **24**, 719–725.
- Huber, J.D., Witt, K.A., Hom, S., Egleton, R.D., Mark, K.S. & Davis, T.P. (2001b) Inflammatory pain alters blood–brain barrier permeability and tight junctional protein expression. *Am. J. Physiol. Heart Circ. Physiol.*, **280**, H1241–H1248.
- Janigro, D. (1999) Blood–brain barrier, ion homeostasis and epilepsy: possible implications towards the understanding of ketogenic diet mechanisms. *Epilepsy Res.*, **37**, 223–232.
- Jenner, P. (2003) Oxidative stress in Parkinson's disease. *Ann. Neurol.*, **53** (Suppl. 3), S26–S36.
- Knott, C., Stern, G. & Wilkin, G.P. (2000) Inflammatory regulators in Parkinson's disease: iNOS, lipocortin-1, and cyclooxygenases-1 and -2. *Mol. Cell Neurosci.*, **16**, 724–739.
- Kortekaas, R., Leenders, K.L., van Oostrom, J.C., Vaalburg, W., Bart, J., Willemsen, A.T. & Hendrikse, N.H. (2005) Blood–brain barrier dysfunction in parkinsonian midbrain in vivo. *Ann. Neurol.*, **57**, 176–179.
- Lenzinger, P.M., Morganti-Kossmann, M.C., Laurer, H.L. & McIntosh, T.K. (2001) The duality of the inflammatory response to traumatic brain injury. *Mol. Neurobiol.*, **24**, 169–181.
- Ling, Z.D., Chang, Q., Lipton, J.W., Tong, C.W., Landers, T.M. & Carvey, P.M. (2004a) Combined toxicity of prenatal bacterial endotoxin exposure and postnatal 6-hydroxydopamine in the adult rat midbrain. *Neuroscience*, **124**, 619–628.
- Ling, Z.D., Q.A.Chang, C.W. Tong, S.E. Leurgans, J.W. Lipton & P.M.Carvey. (2004b) Rotenone potentiates dopamine neuron loss in animals exposed to lipopolysaccharide prenatally. *Exp. Neurol.*, **190**, 373–383.
- Ling, Z.D., Gayle, D.A., Lipton, J.W. & Carvey, P.M. (2002b) Prenatal lipopolysaccharide alters postnatal dopamine in the laboratory rat. In

- Nagatsu, T., Nabeshima, T., McCarty, R. & Goldstein, D. (eds), *Catecholamine Research: from Molecular Insights to Clinical Medicine*. Kluwer Academic/Plenum Publishers, New York, pp. 209–212.
- Ling, Z., Gayle, D.A., Ma, S.Y., Lipton, J.W., Tong, C.W., Hong, J.S. & Carvey, P.M. (2002a) In utero bacterial endotoxin exposure causes loss of tyrosine hydroxylase neurons in the postnatal rat midbrain. *Mov. Disord.*, **17**, 116–124.
- Lynch, N.J., Willis, C.L., Nolan, C.C., Roscher, S., Fowler, M.J., Weihe, E., Ray, D.E. & Schwab, W.J. (2004) Microglial activation and increased synthesis of complement component C1q precedes blood–brain barrier dysfunction in rats. *Mol. Immunol.*, **40**, 709–716.
- Mark, K.S. & Miller, D.W. (1999) Increased permeability of primary cultured brain microvessel endothelial cell monolayers following TNF- α exposure. *Life Sci.*, **64**, 1941–1953.
- McGeer, P.L. & McGeer, E.G. (2004a) Inflammation and neurodegeneration in Parkinson's disease. *Parkinsonism Relat. Disord.*, **10** (Suppl. 1), S3–S7.
- McGeer, P.L. & McGeer, E.G. (2004b) Inflammation and neurodegeneration in Parkinson's disease. *Parkinsonism Relat. Disord.*, **10** (Suppl. 1), S3–S7.
- McRae-Deguerce, A., Klawans, H.L., Penn, R.D., Dahlstrom, A., Tanner, C.M., Goetz, C.G. & Carvey, P.M. (1988) An antibody in the CSF of Parkinson's disease patients disappears following adrenal medulla transplantation. *Neurosci. Lett.*, **94**, 192–197.
- Milner, R. & Campbell, I.L. (2002) Developmental regulation of betal integrins during angiogenesis in the central nervous system. *Mol. Cell Neurosci.*, **20**, 616–626.
- Minagar, A. & Alexander, J.S. (2003) Blood–brain barrier disruption in multiple sclerosis. *Mult. Scler.*, **9**, 540–549.
- Mladenovic, A., Perovic, M., Raicevic, N., Kanazir, S., Rakic, L. & Ruzdijic, S. (2004) 6-Hydroxydopamine increases the level of TNF α and bax mRNA in the striatum and induces apoptosis of dopaminergic neurons in hemiparkinsonian rats. *Brain Res.*, **996**, 237–245.
- Mogi, M., Harada, M., Kondo, T., Riederer, P., Inagaki, H., Minami, M. & Nagatsu, T. (1994) Interleukin-1 beta, interleukin-6, epidermal growth factor and transforming growth factor- α are elevated in the brain from parkinsonian patients. *Neurosci. Lett.*, **180**, 147–150.
- Nimmo, A.J., Cernak, I., Heath, D.L., Hu, X., Bennett, C.J. & Vink, R. (2004) Neurogenic inflammation is associated with development of edema and functional deficits following traumatic brain injury in rats. *Neuropeptides*, **38**, 40–47.
- Pearce, R.K., Owen, A., Daniel, S., Jenner, P. & Marsden, C.D. (1997) Alterations in the distribution of glutathione in the substantia nigra in Parkinson's disease. *J. Neural Transm.*, **104**, 661–677.
- Perry, V.H., Cunningham, C. & Boche, D. (2002) Atypical inflammation in the central nervous system in prion disease. *Curr. Opin. Neurol.*, **15**, 349–354.
- Predescu, D., Vogel, S.M. & Malik, A.B. (2004) Functional and morphological studies of protein transcytosis in continuous endothelia. *Am. J. Physiol. Lung Cell Mol. Physiol.*, **287**, L895–L901.
- Reynolds, D.S. & Morton, A.J. (1998) Changes in blood–brain barrier permeability following neurotoxic lesions of rat brain can be visualised with trypan blue. *J. Neurosci. Meth.*, **79**, 115–121.
- Sauer, H. & Oertel, W.H. (1994) Progressive degeneration of nigrostriatal dopamine neurons following intrastriatal terminal lesions with 6-hydroxydopamine: a combined retrograde tracing and immunocytochemical study in the rat. *Neuroscience*, **59**, 401–415.
- Schnell, L., Fearn, S., Klassen, H., Schwab, M.E. & Perry, V.H. (1999) Acute inflammatory responses to mechanical lesions in the CNS: differences between brain and spinal cord. *Eur. J. Neurosci.*, **11**, 3648–3658.
- Schubring, C., Prohaska, F., Prohaska, A., Englaro, P., Blum, W., Siebler, T., Kratzsch, J. & Kiess, W. (1999) Leptin concentrations in maternal serum and amniotic fluid during the second trimester: differential relation to fetal gender and maternal morphometry. *Eur. J. Obstet. Gynecol. Reprod. Biol.*, **86**, 151–157.
- Sriram, K., Matheson, J.M., Benkovic, S.A., Miller, D.B., Luster, M.I. & O'Callaghan, J.P. (2002) Mice deficient in TNF receptors are protected against dopaminergic neurotoxicity: implications for Parkinson's disease. *FASEB J.*, **16**, 1474–1476.
- Stoll, G., Jander, S. & Schroeter, M. (2002) Detrimental and beneficial effects of injury-induced inflammation and cytokine expression in the nervous system. *Adv. Exp. Med. Biol.*, **513**, 87–113.
- Tsao, N., Hsu, H.P., Wu, C.M., Liu, C.C. & Lei, H.Y. (2001) Tumour necrosis factor- α causes an increase in blood–brain barrier permeability during sepsis. *J. Med. Microbiol.*, **50**, 812–821.
- Tsujikawa, K., Dan, Y., Nogawa, K., Sato, H., Yamada, Y., Murakami, H., Ohtani, H., Sawada, Y. & Iga, T. (2003) Potentiation of domperidone-induced catalepsy by a P-glycoprotein inhibitor, cyclosporin A. *Biopharm. Drug Dispos.*, **24**, 105–114.
- Volk, H., Potschka, H. & Loscher, W. (2005) Immunohistochemical localization of P-glycoprotein in rat brain and detection of its increased expression by seizures are sensitive to fixation and staining variables. *J. Histochem. Cytochem.*, **53**, 517–531.
- Vu, T.Q., Ling, Z.D., Ma, S.Y., Robie, H.C., Tong, C.W., Chen, E.Y., Lipton, J.W. & Carvey, P.M. (2000) Pramipexole attenuates the dopaminergic cell loss induced by intraventricular 6-hydroxydopamine. *J. Neural Transm.*, **107**, 159–176.
- Wang, Y., Kilic, E., Kilic, U., Weber, B., Bassetti, C.L., Marti, H.H. & Hermann, D.M. (2005) VEGF overexpression induces post-ischaemic neuroprotection, but facilitates haemodynamic steal phenomena. *Brain*, **128**, 52–63.

Age-dependent Motor Deficits and Dopaminergic Dysfunction in DJ-1 Null Mice*

Received for publication, December 13, 2004, and in revised form, March 8, 2005
Published, JBC Papers in Press, March 30, 2005, DOI 10.1074/jbc.M413955200

Linan Chen[‡], Barbara Cagniard[‡], Tiffany Mathews[§], Sara Jones[§], Hyun Chul Koh[¶],
Yunmin Ding[¶], Paul M. Carvey[¶], Zaidong Ling[¶], Un Jung Kang[¶], and Xiaoxi Zhuang^{‡**}

From the [‡]Department of Neurobiology, Pharmacology and Physiology, The University of Chicago, Chicago, Illinois 60637, the [§]Department of Physiology and Pharmacology, Wake Forest University School of Medicine, Winston-Salem, North Carolina 27157, the [¶]Department of Neurology, The University of Chicago, Chicago, Illinois 60637, and the [¶]Department of Pharmacology, Rush University Medical Center, Chicago, Illinois 60612

Mutations in the DJ-1 gene were recently identified in an autosomal recessive form of early-onset familial Parkinson disease. Structural biology, biochemistry, and cell biology studies have suggested potential functions of DJ-1 in oxidative stress, protein folding, and degradation pathways. However, animal models are needed to determine whether and how loss of DJ-1 function leads to Parkinson disease. We have generated DJ-1 null mice with a mutation that resembles the large deletion mutation reported in patients. Our behavioral analyses indicated that DJ-1 deficiency led to age-dependent and task-dependent motoric behavioral deficits that are detectable by 5 months of age. Unbiased stereological studies did not find obvious dopamine neuron loss in 6-month- and 11-month-old mice. Neurochemical examination revealed significant changes in striatal dopaminergic function consisting of increased dopamine reuptake rates and elevated tissue dopamine content. These data represent the *in vivo* evidence that loss of DJ-1 function alters nigrostriatal dopaminergic function and produces motor deficits.

Mutations in DJ-1 were recently identified in an autosomal recessive form of early-onset familial Parkinson disease (PD)¹ (1). The first reported mutation involves one large deletion of the first 5 exons and part of the promoter and another mutation was a missense mutation (L166P) that might cause instability of the DJ-1 protein by preventing it from folding properly and forming homodimers (2–5). Since this first report, a number of other mutations of DJ-1 including deletion mutations, point mutations, and a frameshift mutation have been found to cause PD (6–10). These studies suggest that the loss of the normal function of DJ-1 leads to PD.

However, the nature of the normal function of DJ-1 and the mechanism by which DJ-1 deficiency leads to PD are not well

established. Studies prior to the report of its association with PD suggested that DJ-1 might play a role in oncogenesis (11), male fertility (12, 13), control of protein-RNA interaction (14), and in modulating androgen receptor transcription activity (15, 16). In addition, the DJ-1 protein was shown to be responsive to oxidation (17, 18), suggesting a potential role in oxidative stress, a process often implicated in PD. Studies on PD-linked DJ-1 mutations indicate that wild-type, but not mutant, DJ-1 protects cells from oxidative stress (19–21). Canet-Aviles *et al.* (22) reported that oxidation of the Cys¹⁰⁶ residue in DJ-1 could lead to its relocalization in mitochondria and protect cells from mitochondrial damage. Structurally, DJ-1 closely resembles the members of the ThiJ/PfpI family that have protease and chaperone activities (23–27). Recent biochemical studies suggested that DJ-1 might have protease (5) and redox-dependent chaperone activities (28). Therefore, putative functions of DJ-1 seem to converge on the common pathogenesis of PD implicated in other genetic and sporadic forms of PD.

Despite those new insights into the biochemical and cellular functions of DJ-1, the *in vivo* evidence of how the loss of DJ-1 function leads to PD has not been presented. Specifically, it will be important to find out whether animal models that harbor similar mutations to those found in PD patients will develop dopamine neuron degeneration and/or parkinsonian motor symptoms. Since human genetic studies suggest that a loss-of-function of DJ-1 is responsible for the pathogenesis of this genetic form of PD, we have generated DJ-1 null mice with a mutation that resembles the large deletion mutation reported in patients. Our behavioral analyses indicate that DJ-1 deficiency leads to age-dependent motoric behavioral deficits. Even though no obvious dopamine neuron loss was found in 6-month- and 11-month-old mice, neurochemical examination of dopaminergic function revealed significant alterations in tissue dopamine content and reuptake in DJ-1 null mice.

MATERIALS AND METHODS

Generation of DJ-1 Null Mice—We generated DJ-1 null mice by deleting 9.3-kb genomic DNA including the first 5 exons and part of the promoter region of DJ-1 gene to mimic the deletion mutation in humans (1) (Fig. 1A). Both the 5.4- and 3.3-kb fragments of the targeting construct were amplified by PCR using genomic DNA isolated from E14Tg2A.4 embryonic stem cells (BayGenomics) as a template. The selection marker PGK-neo-poly(A) was flanked by FRT sequences. E14Tg2A.4 embryonic stem cells were electroporated (800 V and 3 microfarads) with 30 μ g of linearized targeting construct. G418-resistant clones were screened by Southern blot for homologous recombination with a 5'-external probe. Positive cells were injected into C57BL/6J blastocysts to generate chimeras, which were then mated with C57BL/6J wild-type mice to generate heterozygotes. Heterozygous mutant mice on a 129 \times C57B/6 mixed background were bred to generate DJ-1 null mice and their wild-type littermate controls for experiments.

* This work was supported in part by the M. J. Fox Foundation (to X. Z.) and National Institutes of Health Grants NS43286 and NS32080 (to U. J. K.) and AA014091 (to S. J.). The costs of publication of this article were defrayed in part by the payment of page charges. This article must therefore be hereby marked "advertisement" in accordance with 18 U.S.C. Section 1734 solely to indicate this fact.

** To whom correspondence should be addressed: Dept. of Neurobiology, Pharmacology and Physiology, The University of Chicago, 924 East 57th St., Chicago, IL 60637. Tel.: 773-834-9063; Fax: 773-834-3808; E-mail: xzhuang@bsd.uchicago.edu.

¹ The abbreviations used are: PD, Parkinson disease; TH, tyrosine hydroxylase; SNc, substantia nigra pars compacta; THir, TH-immunoreactive; DAT, dopamine transporter; VMAT2, vesicular monoamine transporter-2; GAPDH, glyceraldehyde-3-phosphate dehydrogenase; HPLC, high performance liquid chromatography.

Mice were genotyped by multiplex PCR on genomic DNA extracted from tail snips (Fig. 1B): first primer pair amplifies part of intron 6 of DJ-1 (present in all mice); second primer pair amplifies part of *neo*^r (absent in wild-type mice); third primer pair amplifies part of intron 3 (absent in homozygous mutants). The genotypes of some mice were confirmed by Southern blot analysis (Fig. 1C). The absence of DJ-1 expression was confirmed by *in situ* hybridization. A full-length mouse DJ-1 cDNA was amplified by reverse transcription-PCR and used as an *in situ* hybridization probe. All animal procedures were approved by the Institutional Animal Care and Usage Committee of The University of Chicago.

Behavioral Studies—All mice were kept on a 06:00–18:00 light cycle with *ad libitum* food and water. Behavioral tests were performed during the light period.

Open Field Test—Each mouse was placed in an open field chamber (40 cm long × 40 cm wide × 37 cm high, Med Associates). Illumination of open field was set to 20 lux. No background noise was provided. They were monitored by infrared beams that record the location and path of the animal (locomotor activity) as well as the number of rearing movements (vertical activity). Data were collected in 5-min trials for six trials, and the average was reported.

Rotarod Test—Mice were first trained to stay on the rod of the rotarod (Columbus Instrument) at a constant speed of 5 rpm for at least 1 min. Following training, mice were tested for a total of three trials with an accelerating speed of 0.2 rpm/s, starting at 5 rpm. The latency to fall was recorded for each trial, and the average of three trials was reported.

Adhesive Tape Removal Task—Adhesive tapes (Avery labels) of five sizes (0.625, 0.5, 0.375, 0.25, 0.125 in²) were placed on the forehead in the above order. To remove the tape, mice typically raised both forepaws and swiped off the tape. Each trial was given a score equal to the size of the largest tape the mouse was unable to remove within 60 s (5 to 1, a higher score indicates worse performance). Results were obtained from the average over two trials.

Tyrosine Hydroxylase (TH) Immunohistochemistry and Stereology—TH catalyzes the rate-limiting step of dopamine synthesis and was used as a marker for dopamine neurons in the substantia nigra pars compacta (SNc). The number of TH-immunoreactive (THir) cells was assessed using an unbiased stereological procedure (29). Briefly, mice were perfused by 4% paraformaldehyde, post-fixed in 4% paraformaldehyde, and cryoprotected in 30% sucrose. The entire brain was sliced on a sliding microtome into consecutive 40-μm sections. Every third section was immunohistochemically processed for TH and NeuN. For TH staining, rabbit anti-mouse TH antibody (1:1000, Pel-Freez), biotinylated horse anti-rabbit IgG (1:500; Vector Laboratories), and peroxidase-conjugated avidin-biotin complex (VECTASTAIN Elite ABC kit, Vector Laboratories) were used. The reaction was visualized by using Sigmafast diaminobenzidine tablets (Sigma) with the addition of nickel sulfate. For NeuN staining, mouse anti-mouse NeuN antibody (1:1000, Chemicon), biotinylated goat anti-mouse IgG (1:500; Vector Laboratories) and diaminobenzidine without nickel sulfate were used. The estimation of the total number of THir neurons in the SNc was determined using the computerized optical fractionator probe (Stereo Investigator 6 from MicroBrightField), which allowed for the stereological estimation of THir cells in the entire structure independent of size, shape, orientation, tissue shrinkage, or anatomical level. The 100 × 100-μm grid and 40 × 40-μm counting frame were used. Sections were counted in rostral-caudal order. The most rostral section containing THir neurons was designated as the first section. The absolute THir neuron number was directly calculated without estimating reference volume. The Gundersen's coefficient of error was 0.06 (*m* = 1) in this study.

Immunofluorescence Double Labeling—Rabbit anti-mouse TH (1:500, Pel-Freez) and mouse anti-mouse α-synuclein (1:500, BD Transduction Laboratories) antibodies were used to detect α-synuclein expression in dopamine neurons. Mouse anti-mouse TH (1:500, BD Transduction Laboratories) and rabbit anti-ubiquitin antibodies (1:500, Dako) were used to detect protein ubiquitination in dopamine neurons. All fluorescence secondary antibodies were purchased from Jackson ImmunoResearch Laboratories and used according to the manufacturer's instructions. Sections were analyzed under a Zeiss Confocal LSM510 Microscope.

HPLC Assessment of Brain Tissue Content of Dopamine and Metabolites—Mice were killed by cervical dislocation. Dissected striata of adult mice were homogenized in 0.1 M perchloric acid containing 1 × 10⁻⁶ M methyl dopa as an internal standard. Homogenates were centrifuged for 10 min at 1500 × *g*. Supernatants were filtered through an YM-10 Microcon centrifugal filter unit (Millipore) and analyzed for dopamine and metabolites using high performance liquid chromatogra-

phy with electrochemical detection. Dopamine and metabolites were separated on a reverse-phase column (Velosep RP-18, 3 μm, 100 × 3.2 mm, PerkinElmer Life Sciences) with a mobile phase consisting of 0.1 M phosphate buffer with 0.6 mM octyl sodium sulfate, 0.1 mM EDTA, and 3% methanol (pH 2.6) at a flow rate of 0.8 ml/min. Samples (25 μl) were injected with a Rheodyne injector, and the compounds were analyzed using a coulometric detector with analytical cell (model 5014, ESA). The potential for the first and second cell was set at -100 and +310 mV, respectively. A guard cell (model 5020, ESA, potential +330 mV) was placed before the injector. Levels of dopamine and metabolites detected in the supernatants were calculated using internal standards. Final concentrations of dopamine and metabolites were expressed per protein amount. Protein levels were measured by BCA protein assay kit (Pierce).

Western Blot—Mice were killed by cervical dislocation. Brains were dissected and frozen immediately on powdered dry ice and stored in -80 °C until use. Frozen brains were lysed in NTE buffer (150 mM NaCl, 50 mM Tris pH 8.0, 5 mM EDTA, 0.25 mM phenylmethylsulfonyl fluoride, 1% protease inhibitor mixture (Sigma), 2% β-mercaptoethanol, 2% SDS), and 50 μg of protein was subjected to SDS-polyacrylamide gel electrophoresis. Proteins were electrophoretically transferred to PVDF membrane and nonspecific sites blocked in 5% nonfat dry milk in TBS (135 mM NaCl, 2.5 mM KCl, 50 mM Tris, 0.1% Tween 20 (pH 7.4)). Membranes were then incubated with various primary antibodies in TBS with 2% nonfat dry milk: rat anti-mouse dopamine transporter (DAT) antibody (1:4000, Chemicon), rabbit anti-mouse TH antibody (1:2000, Pel-Freez), goat anti-mouse vesicular monoamine transporter-2 (VMAT2) antibody (1:500, Santa Cruz Biotechnology), mouse anti-mouse α-synuclein antibody (1:2000, BD Transduction Laboratories), rabbit anti-mouse androgen receptor antibody (1:1000, Abcam), mouse anti-mouse glyceraldehyde-3-phosphate dehydrogenase (GAPDH) antibody (1:200,000, Abcam). Signals were then detected by horseradish peroxidase-conjugated secondary antibodies (ICN) and enhanced chemiluminescence (Pierce). Membranes were then stripped and reprobed with the monoclonal mouse antibodies against mouse β-actin (1:200,000, Abcam) to confirm equal loading of samples.

Protein Carbonyl Analysis—The commonly used indicator of protein oxidation is protein carbonyl content (30). The OxyBlot protein oxidation detection kit from Chemicon was used following the manufacturer's instructions.

Cyclic Voltammetry in Brain Slices—Mice were killed by decapitation, and the brain was rapidly removed and placed in ice-cold, preoxygenated (95% O₂/5% CO₂) modified Krebs's buffer. The tissue was then sectioned into 400-μm-thick coronal slices containing the caudate-putamen and nucleus accumbens with a vibrating tissue slicer (Leica VT100S, Leica Instruments). Slices were kept in a reservoir of oxygenated Krebs buffer at room temperature until required. Thirty minutes before each experiment, a brain slice was transferred to a submersion recording chamber. The slices were perfused at 1 ml/min with room temperature (20 °C) oxygenated Krebs and allowed to equilibrate. The Krebs's buffer contained (in mM): NaCl, 126; KCl, 2.5; NaH₂PO₄, 1.2; CaCl₂, 2.4; MgCl₂, 1.2; NaHCO₃, 25; glucose, 11; HEPES, 20; and L-ascorbic acid, 0.4 (pH 7.4). Dopamine release was evoked by a single, rectangular, electrical pulse (300 μA, 2 ms per phase, biphasic) applied every 5 min. Dopamine was detected by using fast-scan cyclic voltammetry as described earlier (31, 32). Electrodes were placed in the dorsal and ventral portion of the caudate-putamen and in the core and shell of the nucleus accumbens.

Data Analysis—Data were analyzed using StatView 5.0.1. Unpaired two-tailed Student's *t* test was used when genotype was the only grouping variable. Analysis of variance was used when genotype was not the only grouping variable and when data were collected in a single trial. Repeated measure analysis of variance was used when data were collected in multiple trials.

RESULTS

Generation of DJ-1 Null Mice—DJ-1 null mice were generated by deleting the first 5 exons and part of the promoter to mimic the deletion mutation reported in human PD patients (1) (Fig. 1A). The lack of DJ-1 transcript expression in homozygous mutants was confirmed both by reverse transcription-PCR in cultured adult skin fibroblasts (Fig. 1D) and by *in situ* hybridization on brain sections (Fig. 1E). DJ-1 mRNA signal was detected throughout the wild-type mouse brain by *in situ* hybridization. The high expression level of DJ-mRNA was found in the SNc, cerebellum, cerebral cortex (Fig. 1E), hippocampus,

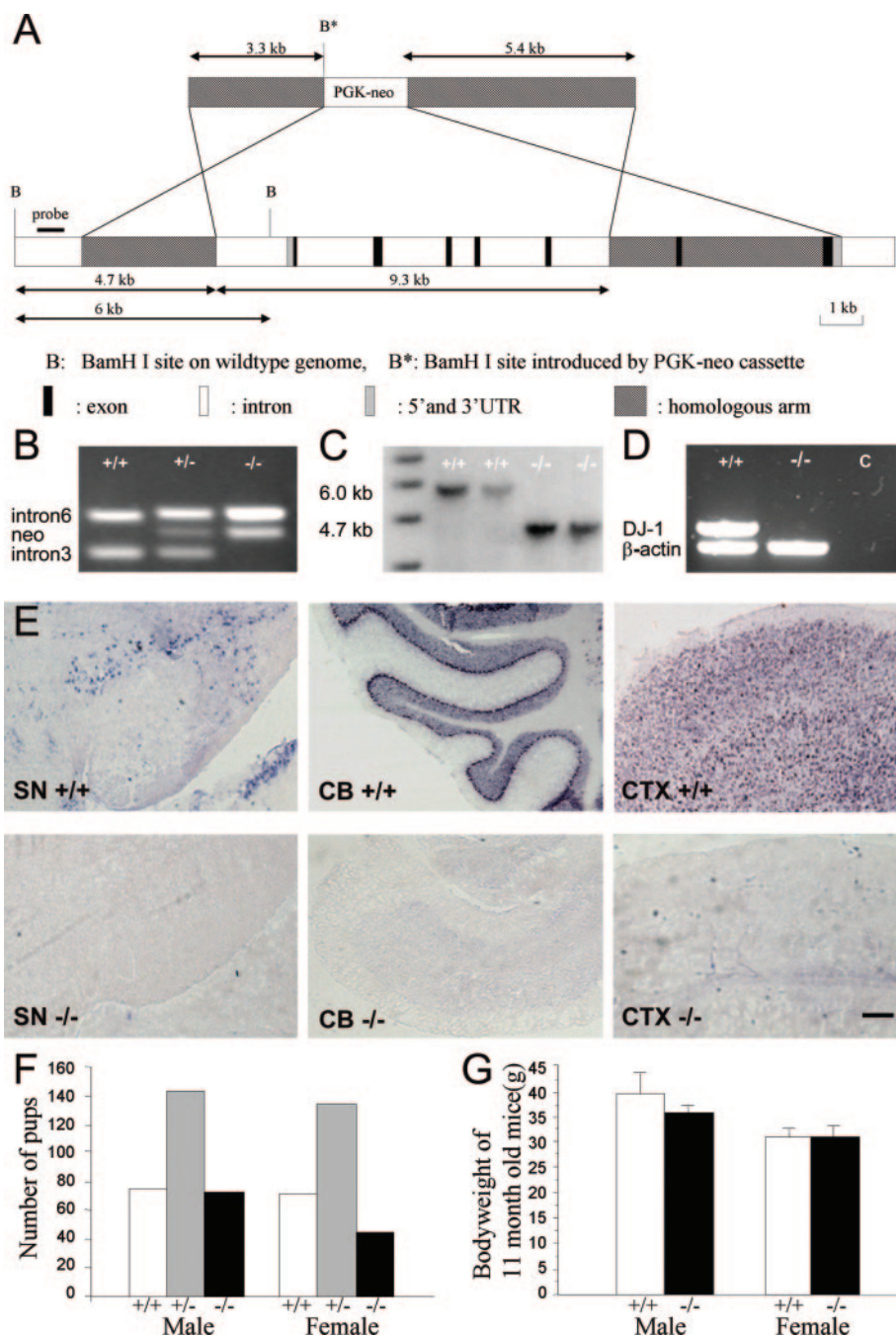


FIG. 1. Generation of DJ-1 null mice. DJ-1 null mice were generated by gene targeting that resulted in 9.3-kb deletion that included the first 5 exons and part of the promoter. **A**, design of the targeting construct. The FRT sequence-flanked selection cassette (FRT-PGK-neo^r-poly(A)-FRT) was inserted in between two homologous arms. BamHI digestion will give a 6-kb band for the wild-type allele and a 4.7-kb band for the mutant allele in Southern blot. **B** and **C**, PCR (**B**) and Southern blot (**C**) analyses of genomic DNA from tail snips confirm transmission of the mutation. **D**, reverse transcription-PCR analysis of mRNA from cultured skin fibroblast confirms the loss of DJ-1 transcript. **E**, *in situ* hybridization demonstrates the loss of DJ-1 transcript in brains of mutant mice. **F**, genotype distribution conforms to Mendelian ratio. The χ^2 test did not reveal significant deviation from Mendelian law ($p = 0.09$). **G**, no significant body weight difference was found among different genotypes in 11-month-old mice ($p = 0.41$; $n = 12$ for each genotype). Scale bar is 100 μ m. SN, substantia nigra; CB, cerebellum; CTX, cerebral cortex; UTR, untranslated region.

striatum, and olfactory bulb (data not shown). Most of the expression was in cells exhibiting neuronal morphology. However, strong expression was also present in the choroid plexus (data not shown). These data are similar to the expression patterns reported by others (33, 34). The ratios of wild-type: heterozygotes:homozygotes of both sexes were consistent with Mendelian inheritance (Fig. 1F, $p = 0.09$ by χ^2 test). DJ-1 null mice were viable and appeared indistinguishable from the wild-type or heterozygotes littermates in gross inspection. No significant body weight difference was found between genotypes ($p = 0.41$; Fig. 1G).

Age-dependent Motor Deficits in DJ-1 Null Mice—Three independent age groups of DJ-1 null mice (5, 9, and 11 months) and their wild-type littermate controls were subjected to systematic behavioral assessment of various motor functions. In the open field test, DJ-1 null mice displayed decreased locomotor ($p = 0.001$) and rearing ($p = 0.005$) activities (Fig. 2). Such a deficit

seemed to be age-dependent (genotype \times age interaction: $p = 0.032$ for rearing and $p = 0.068$ for locomotion). *Post hoc* test revealed that only 11-month-old DJ-1 null mice showed significantly impaired locomotion and rearing compared with their wild-type controls ($p = 0.002$ for locomotion and $p = 0.037$ for rearing). There was no significant genotype \times sex interaction.

To determine whether more sensitive measures of nigrostriatal dysfunction could differentiate DJ-1 null mice from their wild-type controls at an earlier age, an adhesive tape removal test that has been shown to be a good discriminator in mouse models of PD was employed (35, 36). Behavioral deficits in the adhesive tape removal test could be seen as early as 5 months of age in DJ-1 null mice compared with their wild-type controls (Fig. 3). The behavioral deficit in DJ-1 null mice was more pronounced at 11 months of age than at 5 months ($p = 0.0001$ for overall genotype effect, $p = 0.013$ for 5-month group, and $p = 0.007$ for 11-month group), although there was no statis-

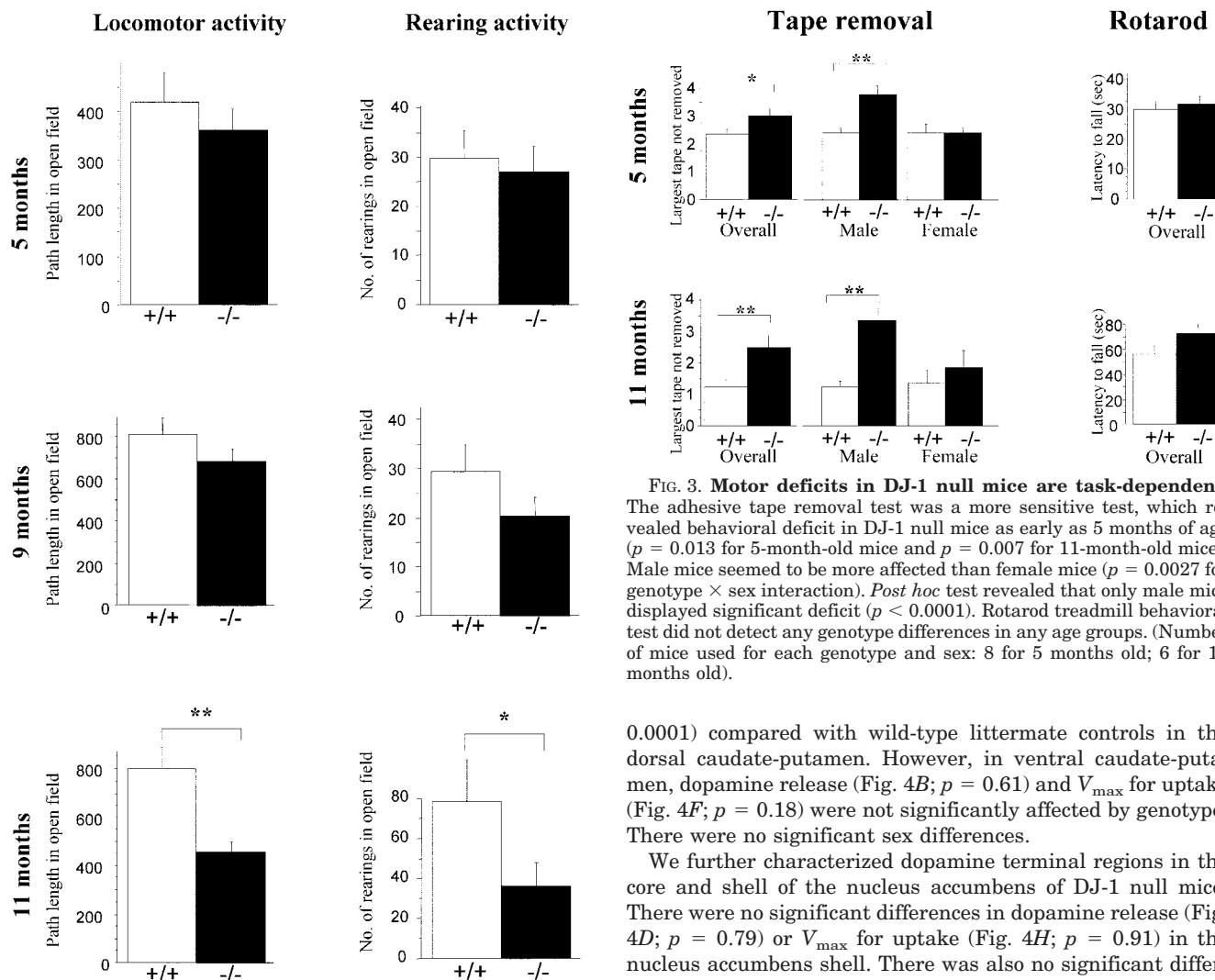


FIG. 2. Age-dependent motor deficits in DJ-1 null mice. DJ-1 null mice displayed decreased locomotor ($p = 0.001$) and rearing ($p = 0.005$) activities in the open field. Such a deficit seemed to be age-dependent (genotype \times age interaction: $p = 0.032$ for rearing and $p = 0.068$ for locomotion). *Post hoc* test revealed that only 11-month-old DJ-1 null mice were significantly impaired in their locomotor ($p = 0.002$) and rearing ($p = 0.037$). (Number of mice used for each genotype: 16 for 5 months old; 15 for 9 months old; 12 for 11 months old).

tically significant genotype \times age interaction ($p = 0.19$). Interestingly, male mice seemed to be more affected than female mice on this task ($p = 0.0027$ for genotype \times sex interaction). *Post hoc* tests revealed that only male mice displayed significant deficits ($p < 0.0001$ for males and $p = 0.50$ for females). The rotarod treadmill behavioral test is also widely used as a measure of various neurological dysfunctions. However, the rotarod treadmill test did not detect any genotype differences in any age groups including 11 months of age (Fig. 3).

Functional Alterations in Dopaminergic Neurotransmission in DJ-1 Null Mice—Since functional alterations in dopaminergic neurotransmission may precede obvious dopaminergic neuronal loss or pathological abnormalities, we examined dopamine release, uptake kinetics, and total striatal tissue content of dopamine in DJ-1 null mice and their wild-type controls.

Fast-scan cyclic voltammetry was employed to evaluate electrically stimulated dopamine release and uptake kinetics of the dopamine transporter. The caudate-putamen was divided into dorsal and ventral halves for data analysis. At 4 months of age, DJ-1 null mice had increased stimulated dopamine release (Fig. 4A; $p = 0.0002$) and faster uptake (V_{\max}) (Fig. 4E; $p =$

FIG. 3. Motor deficits in DJ-1 null mice are task-dependent. The adhesive tape removal test was a more sensitive test, which revealed behavioral deficit in DJ-1 null mice as early as 5 months of age ($p = 0.013$ for 5-month-old mice and $p = 0.007$ for 11-month-old mice). Male mice seemed to be more affected than female mice ($p = 0.0027$ for genotype \times sex interaction). *Post hoc* test revealed that only male mice displayed significant deficit ($p < 0.0001$). Rotarod treadmill behavioral test did not detect any genotype differences in any age groups. (Number of mice used for each genotype and sex: 8 for 5 months old; 6 for 11 months old).

0.0001) compared with wild-type littermate controls in the dorsal caudate-putamen. However, in ventral caudate-putamen, dopamine release (Fig. 4B; $p = 0.61$) and V_{\max} for uptake (Fig. 4F; $p = 0.18$) were not significantly affected by genotype. There were no significant sex differences.

We further characterized dopamine terminal regions in the core and shell of the nucleus accumbens of DJ-1 null mice. There were no significant differences in dopamine release (Fig. 4D; $p = 0.79$) or V_{\max} for uptake (Fig. 4H; $p = 0.91$) in the nucleus accumbens shell. There was also no significant difference in dopamine release (Fig. 4C; $p = 0.47$) in the nucleus accumbens core. However, in the core, there was a trend toward an increased V_{\max} value for dopamine uptake (Fig. 4G; $p = 0.084$).

To investigate whether the increases in uptake and release reflect changes in dopamine tissue content, the caudate-putamens of 6-month- and 11-month-old mice were dissected out and subjected to HPLC analysis for dopamine and metabolite content. Dopamine levels in DJ-1 null mice were higher than those in wild-type control mice in both age groups ($p = 0.0014$ for genotype effect; $p < 0.0001$ for age effect Fig. 4I). There was no significant age \times genotype interaction or sex differences. There was an insignificant trend for elevation of 3,4-dihydroxyphenylacetic acid ($p = 0.11$) and homovanillic acid ($p = 0.14$) in DJ-1 null mice compared with wild-type control mice.

We investigated whether the increases in tissue dopamine content, release, and uptake are due to changes in expression levels of dopamine synthesis enzymes or transporters. However, no significant differences between genotypes were seen in TH, DAT, or VMAT2 protein levels in 5-month- (not shown) and 11-month-old (Fig. 4J) mouse brains measured by Western blot analysis.

DJ-1 Null Mice Did Not Show Loss of SN Dopamine Neurons or Obvious Neuropathology—To determine whether the behavioral deficits resulted from the loss of dopaminergic neurons, stereological analysis of THir neurons in the SNc was performed in 6-month- and 11-month-old mice. However, comparable numbers of dopaminergic neurons were present in DJ-1 null mice and their wild-type controls (Fig. 5).

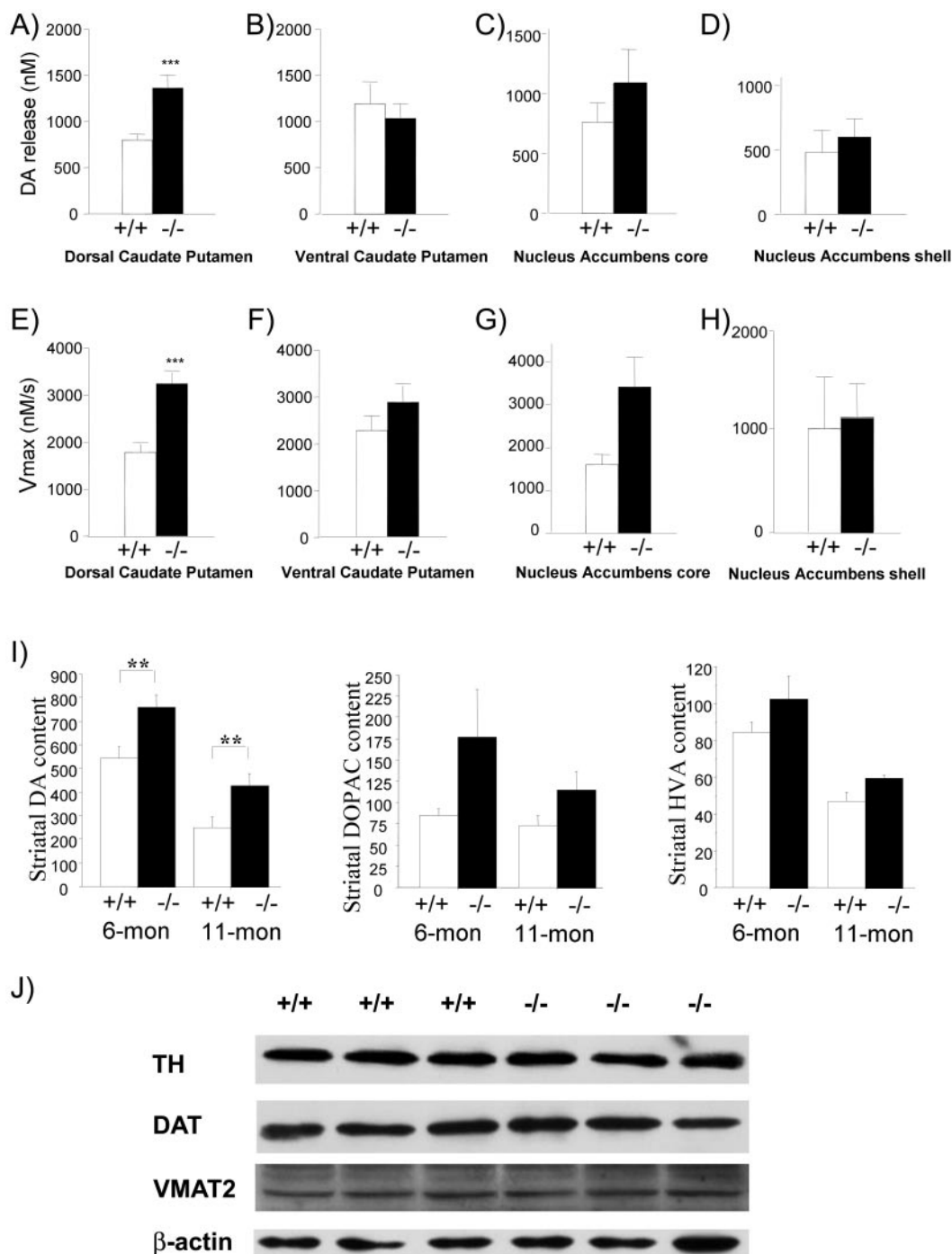


FIG. 4. Impaired nigrostriatal dopaminergic function in DJ-1 null mice. A–H, cyclic voltammetry examination of dopamine (DA) release in response to a single stimulus pulse and maximal uptake rate (V_{max}) in brain slices from 4-month-old mice ($n = 8$ for each genotype). DJ-1 null mice released more dopamine in the dorsal (A; $p = 0.0002$) but not in the ventral caudate-putamen (B; $p = 0.61$), the nucleus accumbens shell (D; $p = 0.91$), or core (C; $p = 0.47$). In addition, DJ-1 null mice displayed higher maximal dopamine uptake rate in the dorsal (E; $p = 0.0001$) but not in the ventral caudate-putamen (F; $p = 0.18$) or the nucleus accumbens core (G; $p = 0.084$). I, DJ-1 null mice had elevated dopamine (DA) (ng/mg of protein) levels in the striatum than wild type mice ($p = 0.0014$; $n = 13$ for each genotype of 6-month-old and $n = 7$ for each genotype of 11-month-old group). There was a trend for higher 3,4-dihydroxyphenylacetic acid (DOPAC) and homovanillic acid (HVA) levels in DJ-1 null mice than in wild type mice. J, Western blot analysis of TH, DAT, and VMAT2 levels in 11-month-old brains did not reveal any genotype differences.

DJ-1 has been implicated in oxidative stress and protein folding and degradation. The pathological inclusions are commonly found in neurodegenerative diseases in susceptible population of remaining neurons and the presence of such inclusions could indicate dysfunctional cells. Intracytoplasmic Lewy body inclusion is characteristic of PD and the Lewy bodies contain α -synuclein and ubiquitin (37–41). Therefore, we

stained midbrain sections from 6-month- (not shown) and 11-month-old (Fig. 6, A and B) mice with α -synuclein and ubiquitin antibodies. No α -synuclein- or ubiquitin-positive inclusions were found. Hematoxylin-eosin staining revealed no eosinophilic inclusion either (data not shown). The expression levels of α -synuclein in DJ-1 null mice were comparable with those in wild-type controls in Western blot in 5-month-old (not

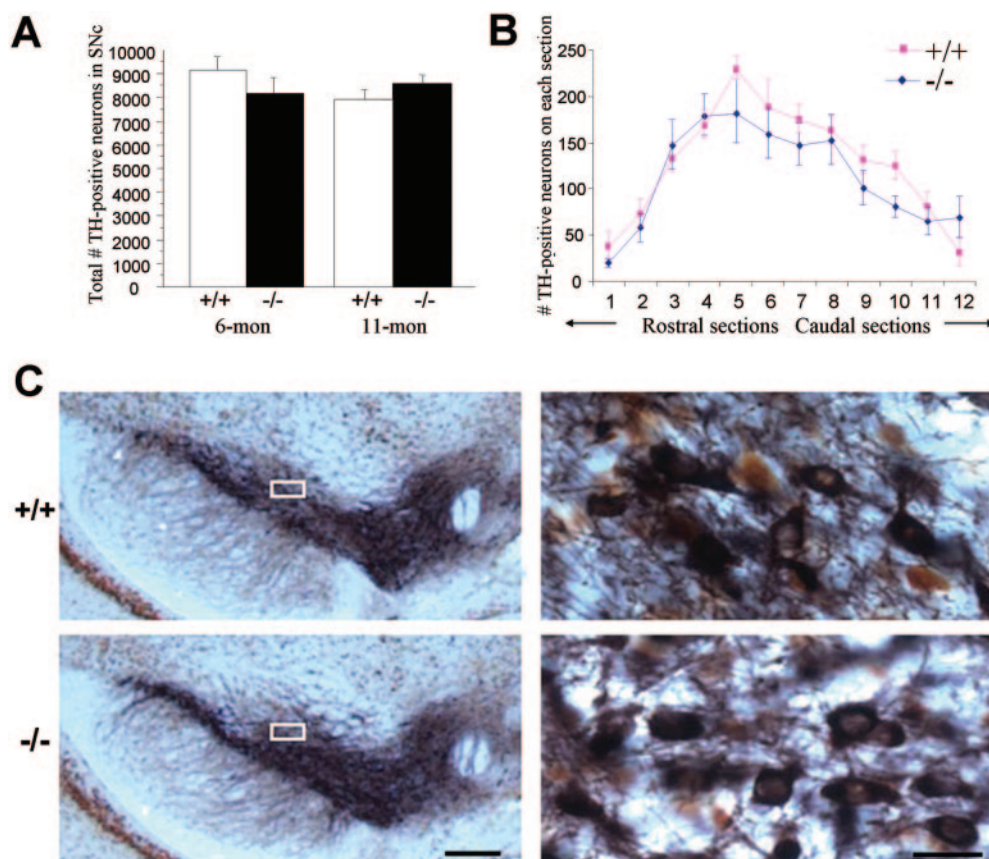


FIG. 5. No dopamine neuron loss in SNc of DJ-1 null mice. **A**, there was no obvious dopaminergic neuronal loss in 6-month- (6-mon) or 11-month-old (11-mon) DJ-1 null mice compared with wild-type controls ($n = 6$ for each genotype of each age). **B**, the distribution of dopamine neuron counts along the rostral-caudal axis throughout the SNc in 6-month-old mice. Similar distribution was seen in 11-month-old mice (data not shown). **C**, TH (black) and NeuN (brown) double staining of SNc in lower magnification (left panels) and higher magnification (right panels) from representative 6-month-old mice. Scale bar is 200 μ m for the left panels and 20 μ m for the right panels.

shown) as well as in 11-month-old mice (Fig. 7). Oxidative modification of proteins can be detected by antibodies against carbonylated proteins. Despite the potential role of DJ-1 in oxidative stress, the absence of DJ-1 did not increase carbonyl protein levels in the brains of 5-month (data not shown) and 11-month-old mice (Fig. 7).

DISCUSSION

Since the discovery that the loss-of-function mutations in DJ-1 cause an autosomal recessive form of early-onset familial PD (1), a number of studies have been published to investigate DJ-1 function and its potential role in the pathogenesis of PD. This *in vivo* study clearly indicates that the loss of DJ-1 function in mice can lead to motor deficits as well as alterations in nigrostriatal dopaminergic function.

Interestingly, the onset of motor deficits in DJ-1 null mice is age- and task-dependent. All mice appeared healthy and seemed to live a normal life at least up to age 11 months. No motor deficits could be detected in any age groups in the rotarod test. Significant motor deficits in the open field test did not become obvious until DJ-1 null mice reached 11 months of age. Importantly, the age-dependent progression of motor deficits in DJ-1 null mice further validates the potential of this mouse model as a good model for PD, given the fact that age is the single most important risk factor in this progressive neurodegenerative disease.

In contrast, significant motor deficits could be detected in DJ-1 null mice as young as 5 months old using the tape removal task. Such task dependence is in agreement with the fact that subtle motor deficits in PD patients can be detected much earlier than the occurrence of classic motor deficits of

PD (42). This could be especially true in a progressive disorder in which the affected individual could have a lengthy period to compensate for minor deficits. There have been few studies validating behavioral tasks in mice for their ability to detect mild nigrostriatal dysfunction. Tape removal may be sensitive to mild nigrostriatal dysfunction because it requires coordinated forelimb use. It is known in other rodent PD models that tasks involving forelimb use are especially sensitive in detecting subtle dopaminergic deficits (43–46). Even though the open field test is known to be sensitive to hypolocomotion often associated with hypodopaminergic function, it is not as sensitive as the tape removal task. The rotarod is commonly used in Huntington disease animal models, in cerebellum dysfunction, and in spinal cord dysfunction (47–49). However, it is a less specific and less sensitive task for dopamine system dysfunction.

It is surprising and counterintuitive that DJ-1 null mice have more tissue dopamine content, more dopamine release, as well as faster dopamine reuptake in the dorsal striatum compared with wild-type controls. The cyclic voltammetry study directly probed dopamine reuptake kinetics and the data suggested an enhancement of DAT function in DJ-1 null mice. One obvious consequence of enhanced DAT function would be elevated tissue dopamine content (due to more efficient dopamine recycling) and therefore a larger releasable pool. One relevant comparison to these conditions is the DAT knockdown mice that seem to have the opposite phenotype (50). DAT knockdown mice have decreased dopamine reuptake due to reduced DAT expression. They also have lower tissue dopamine content (due to reduced dopamine recycling) and lower dopamine release

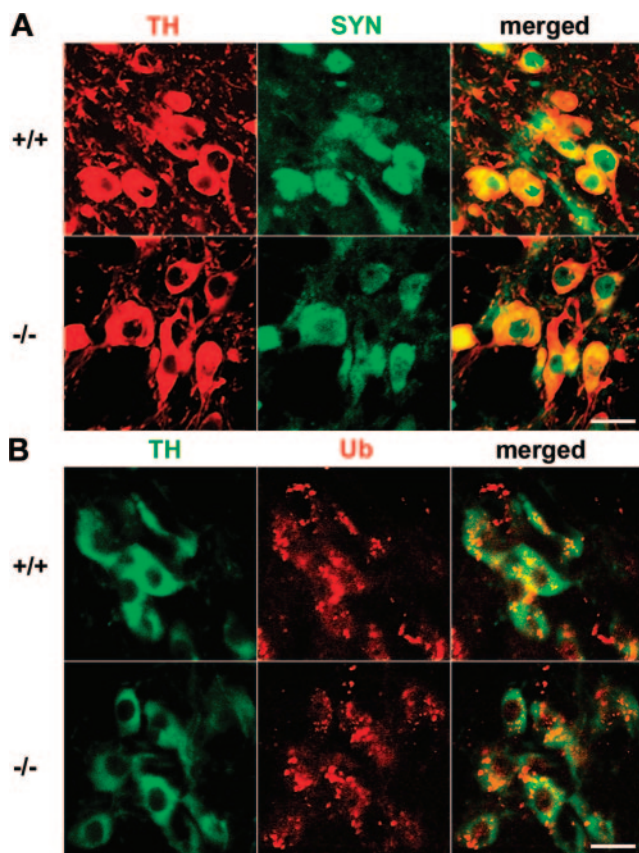


FIG. 6. No obvious neuropathology in SNc of DJ-1 null mice. Fluorescence immunostaining of SNc neurons for α -synuclein (SYN) and ubiquitin (Ub) in 11-month-old mice ($n = 3$ for each genotype) is shown. **A**, strong α -synuclein staining (green) is seen in nuclei, cytoplasm, and processes of dopaminergic neurons (labeled by TH, red). No inclusions or obvious expression level change were found in DJ-1 null mice. **B**, weak ubiquitin (Ub) staining (red, dot-like) is seen in both dopaminergic (labeled by TH, green) and non-dopaminergic cells. No inclusions or obvious expression level change were found in DJ-1 null mice. Similar results were seen in 6-month-old mice (not shown, $n = 3$ for each genotype). Scale bar is 20 μ m.

(due to a reduced releasable pool). Much more severe changes in the same direction were found in mice with complete loss of DAT function (51, 52). These decreases in dopaminergic parameters are the opposite of changes that we found in DJ-1 null mice. Importantly, DAT knockdown mice show hyperlocomotion in the open field, which is also the opposite of the behavioral deficit in DJ-1 null mice.

Furthermore, DAT function may be one of the most important factors that determine susceptibility to PD. First of all, higher tissue dopamine content is associated with increased cellular oxidative stress (53–58). Second, higher DAT function could confer vulnerability to neural toxins in the environment. Even though human genetic studies are still lacking, mice with no DAT expression or half of the normal DAT expression are much more resistant to 1-methyl-4-phenyl-1,2,3,6-tetrahydropyridine-induced Parkinsonism (59). Similarly, in *Caenorhabditis elegans*, mutations that impair DAT function make the organism less vulnerable to Parkinsonism-inducing toxins (60). Interestingly, more dopamine release and faster dopamine reuptake in DJ-1 null mice were only detected in the dorsal striatum, which is in agreement with the fact that PD affects mostly nigrostriatal DA neurons. Although we did not detect obvious elevations of DAT protein levels in DJ-1 null mice, more studies have to be conducted to determine the functional aspects of dopamine transport such as DAT compartmental expression, oligomerization, and functional modifications by DAT associated proteins (61–63).

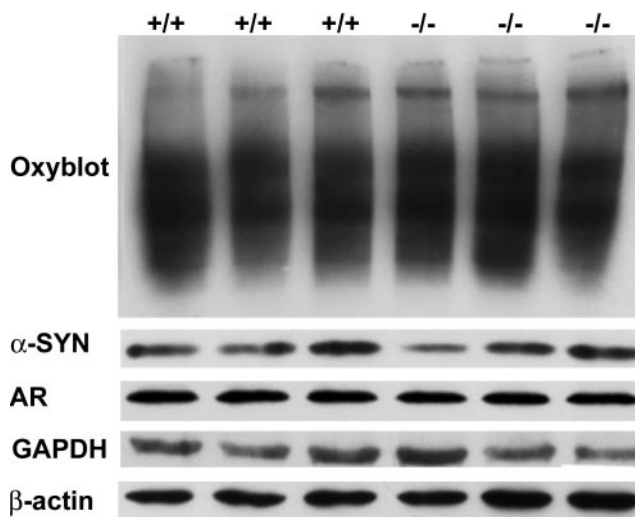


FIG. 7. Western blot analysis of brain protein levels in 11-month-old mice ($n = 6$ for each genotype). Protein levels for protein carbonyl (Oxyblot) showed comparable protein oxidation in DJ-1 null mice and wild-type controls. Western blot analysis of α -synuclein (SYN), androgen receptor (AR), and GAPDH levels did not reveal any genotype differences. Similar results were seen in 5-month-old mice (not shown, $n = 8$ for each genotype).

Even though motor deficits can be detected in DJ-1 null mice as young as 5 months of age, we did not find significant dopamine neuron loss or neuropathology in DJ-1 null mice at 6 or 11 months of age. This is in contrast to human PD patients who usually develop motor symptoms only after loss of ~50–60% dopamine neurons. There are a number of possibilities that may explain the differences between human PD patients and the mouse model. First of all, it is not clear yet whether DJ-1 linked PD patients have actual dopamine neuron loss or only functional disturbances of the dopaminergic system. 18 F-DOPA PET scan studies have shown evidence of nigrostriatal dopaminergic functional deficit in DJ-1 linked PD patients (64). However, no autopsy pathology is available yet. Second, the difficulty in detecting motor deficits in human PD patients before significant dopamine cell loss may be due to the fact that multiple behavioral compensations could happen in humans with a progressive neurodegenerative disorder. Third, neurodegenerative pathology may require a long period to manifest, whereas the life span of mice is much shorter than that of humans. Fourth, there could be intrinsic differences between mouse and human brains. For example, melanin is present in human dopaminergic neurons but not in rodents. Finally, exposure to environmental insults could be important in phenotypic expression of the genetic mutations; humans and mice are not exposed to the same type of environmental insults. Therefore, providing additional insults such as toxic exposures or other genetic mutations in the setting of DJ-1 deficiency may be necessary to manifest the full range of parkinsonian phenotypes in mouse models.

There was some suggestion of sex-specific expression of DJ-1-mediated deficits. The tape removal task showed that male DJ-1 null mice were more affected by the mutation than females. Even though one could postulate that females were not sensitive to the particular test, potential interactions between DJ-1 and the androgen receptor raise intriguing possibility of sex-specific effect of DJ-1. Earlier biochemical studies showed that DJ-1 binds to a modulator of androgen receptor PIASx, which leads to reduced repression of androgen receptor transcription activity (15, 16). In humans, a preponderance of PD in males compared with females has been noted (65), but whether DJ-1 linked PD also has a gender bias is not known yet.

Earlier studies also found that DJ-1 was reduced in rat sperm treated with sperm toxicants that cause infertility in rats (12) and that DJ-1 may play a role in fertilization in mice (13). However, we did not see any association of DJ-1 function and male fertility in our studies; there was no change of androgen receptor levels in brains of DJ-1 null mice either (Fig. 7). Another protein that was implicated in earlier studies in relation to PD and DJ-1 was GAPDH (14, 66, 67). GAPDH was found to be co-localized with α -synuclein in Lewy bodies. It was also co-purified with DJ-1 as a complex from a rat hepatoma cell line. However, we did not see any difference in GAPDH levels between DJ-1 null mice and their wild-type controls (Fig. 7).

In conclusion, the age-dependent progression of motor deficits and neurochemical changes in the nigrostriatal pathway in DJ-1 null mice provide valuable insights on the importance of DJ-1 in the pathogenesis of PD. In addition, this model provides an unprecedented opportunity to investigate the role of aging and DJ-1-related biochemical pathways in the pathogenesis of PD. Future studies will tell us whether advanced age will eventually lead to discernable neuropathology and prominent dopamine neuron loss in DJ-1 null mice.

Acknowledgments—We thank Ana Solodkin for the use of her stereology set-up; Linda Degenstein and The University of Chicago transgenic core for blastocyst injection of ES cells; Sheila Fleming, Gloria Meredith, Sangram Sisodia, Gopal Thinakaran, and Manuel Uset for their helpful discussion and advice; and Wanhao Chi, Sarah Manning, Xiaoli Xiong, Jonathan Britt, and Sehoon Choi for their expert technical assistance.

Addendum—While our paper was being reviewed, the paper by Goldberg *et al.* on DJ-1-null mice appeared in *Neuron* (Goldberg, M. S., Pisani, A., Haburcak, M., Vortherms, T. A., Kitada, T., Costa, C., Tong, Y., Martella, G., Tschertner, A., Martins, A., Bernardi, G., Roth, B. L., Pothos, E. N., Calabresi, P., and Shen, J. (2005) *Neuron* **45**, 489–496) with the main findings similar to ours. They noted behavioral deficits without dopaminergic cell loss.

REFERENCES

- Bonifati, V., Rizzu, P., van Baren, M. J., Schaap, O., Breedveld, G. J., Krieger, E., Dekker, M. C., Squitieri, F., Ibanez, P., Joosse, M., van Dongen, J. W., Vanacore, N., van Swieten, J. C., Brice, A., Meco, G., van Duijn, C. M., Oostra, B. A., and Heutink, P. (2003) *Science* **299**, 256–259
- Moore, D. J., Zhang, L., Dawson, T. M., and Dawson, V. L. (2003) *J. Neurochem.* **87**, 1558–1567
- Miller, D. W., Ahmad, R., Hague, S., Baptista, M. J., Canet-Aviles, R., McLendon, C., Carter, D. M., Zhu, P. P., Stadler, J., Chandran, J., Klinefelter, G. R., Blackstone, C., and Cookson, M. R. (2003) *J. Biol. Chem.* **278**, 36588–36595
- Macedo, M. G., Anar, B., Bronner, I. F., Cannella, M., Squitieri, F., Bonifati, V., Hoogeveen, A., Heutink, P., and Rizzu, P. (2003) *Hum. Mol. Genet.* **12**, 2807–2816
- Olzmann, J. A., Brown, K., Wilkinson, K. D., Rees, H. D., Huai, Q., Ke, H., Levey, A. I., Li, L., and Chin, L. S. (2004) *J. Biol. Chem.* **279**, 8506–8515
- Abou-Sleiman, P. M., Healy, D. G., Quinn, N., Lees, A. J., and Wood, N. W. (2003) *Ann. Neurol.* **54**, 283–286
- Hedrich, K., Djarmati, A., Schafer, N., Hering, R., Wellenbrock, C., Weiss, P. H., Hilker, R., Vieregge, P., Ozelius, L. J., Heutink, P., Bonifati, V., Schwinger, E., Lang, A. E., Noth, J., Bressman, S. B., Pramstaller, P. P., Riess, O., and Klein, C. (2004) *Neurology* **62**, 389–394
- Hering, R., Strauss, K. M., Tao, X., Bauer, A., Woitalla, D., Miez, E. M., Petrovic, S., Bauer, P., Schaible, W., Muller, T., Schols, L., Klein, C., Berg, D., Meyer, P. T., Schulz, J. B., Wollnik, B., Tong, L., Kruger, R., and Riess, O. (2004) *Hum. Mutat.* **24**, 321–329
- Gorner, K., Holtorf, E., Odoy, S., Nuscher, B., Yamamoto, A., Regula, J. T., Beyer, K., Haass, C., and Kahle, P. J. (2004) *J. Biol. Chem.* **279**, 6943–6951
- Hague, S., Rogaeva, E., Hernandez, D., Gulick, C., Singleton, A., Hanson, M., Johnson, J., Weiser, R., Gallardo, M., Ravina, B., Gwinn-Hardy, K., Crawley, A., St George-Hyslop, P. H., Lang, A. E., Heutink, P., Bonifati, V., and Hardy, J. (2003) *Ann. Neurol.* **54**, 271–274
- Nagakubo, D., Taira, T., Kitaura, H., Ikeda, M., Tamai, K., Iguchi-Ariga, S. M., and Ariga, H. (1997) *Biochem. Biophys. Res. Commun.* **231**, 509–513
- Wagenfeld, A., Yeung, C. H., Shivaji, S., Sundareswaran, V. R., Ariga, H., and Cooper, T. G. (2000) *J. Androl.* **21**, 954–963
- Okada, M., Matsumoto, K., Niki, T., Taira, T., Iguchi-Ariga, S. M., and Ariga, H. (2002) *Biol. Pharm. Bull.* **25**, 853–856
- Hod, Y., Pentyala, S. N., Whyard, T. C., and El-Maghrabi, M. R. (1999) *J. Cell. Biochem.* **72**, 435–444
- Takahashi, K., Taira, T., Niki, T., Seino, C., Iguchi-Ariga, S. M., and Ariga, H. (2001) *J. Biol. Chem.* **276**, 37556–37563
- Niki, T., Takahashi-Niki, K., Taira, T., Iguchi-Ariga, S. M., and Ariga, H. (2003) *Mol. Cancer Res.* **1**, 247–261
- Mitsumoto, A., Nakagawa, Y., Takeuchi, A., Okawa, K., Iwamatsu, A., and Takanezawa, Y. (2001) *Free Radic. Res.* **35**, 301–310
- Mitsumoto, A., and Nakagawa, Y. (2001) *Free Radic. Res.* **35**, 885–893
- Takahashi-Niki, K., Niki, T., Taira, T., Iguchi-Ariga, S. M., and Ariga, H. (2004) *Biochem. Biophys. Res. Commun.* **320**, 389–397
- Taira, T., Saito, Y., Niki, T., Iguchi-Ariga, S. M., Takahashi, K., and Ariga, H. (2004) *EMBO Rep.* **5**, 213–218
- Martinat, C., Shendelman, S., Jonason, A., Leete, T., Beal, M. F., Yang, L., Floss, T., and Abeliovich, A. (2004) *PLoS Biol.* **2**, e327
- Canet-Aviles, R. M., Wilson, M. A., Miller, D. W., Ahmad, R., McLendon, C., Bandyopadhyay, S., Baptista, M. J., Ringe, D., Petsko, G. A., and Cookson, M. R. (2004) *Proc. Natl. Acad. Sci. U. S. A.* **101**, 9103–9108
- Wilson, M. A., Collins, J. L., Hod, Y., Ringe, D., and Petsko, G. A. (2003) *Proc. Natl. Acad. Sci. U. S. A.* **100**, 9256–9261
- Tao, X., and Tong, L. (2003) *J. Biol. Chem.* **278**, 31372–31379
- Lee, S. J., Kim, S. J., Kim, I. K., Ko, J., Jeong, C. S., Kim, G. H., Park, C., Kang, S. O., Suh, P. G., Lee, H. S., and Cha, S. S. (2003) *J. Biol. Chem.* **278**, 44552–44559
- Huai, Q., Sun, Y., Wang, H., Chin, L. S., Li, L., Robinson, H., and Ke, H. (2003) *FEBS Lett.* **549**, 171–175
- Honbou, K., Suzuki, N. N., Horiuchi, M., Niki, T., Taira, T., Ariga, H., and Inagaki, F. (2003) *J. Biol. Chem.* **278**, 31380–31384
- Shendelman, S., Jonason, A., Martinat, C., Leete, T., and Abeliovich, A. (2004) *PLoS Biol.* **2**, e362
- Mouton, P. R. (2002) *Principles and Practices of Unbiased Stereology: An Introduction for Bioscientists*, The Johns Hopkins University Press, Baltimore
- Stadtman, E. R., and Oliver, C. N. (1991) *J. Biol. Chem.* **266**, 2005–2008
- Budygin, E. A., John, C. E., Mateo, Y., and Jones, S. R. (2002) *J. Neurosci.* **22**, RC222
- Phillips, P. E., Johns, J. M., Lubin, D. A., Budygin, E. A., Gainetdinov, R. R., Lieberman, J. A., and Wightman, R. M. (2003) *Brain Res.* **961**, 63–72
- Shang, H., Lang, D., Jean-Marc, B., and Kaelin-Lang, A. (2004) *Neurosci. Lett.* **367**, 273–277
- Bandyopadhyay, R., Kingsbury, A. E., Cookson, M. R., Reid, A. R., Evans, I. M., Hope, A. D., Pittman, A. M., Lashley, T., Canet-Aviles, R., Miller, D. W., McLendon, C., Strand, C., Leonard, A. J., Abou-Sleiman, P. M., Healy, D. G., Ariga, H., Wood, N. W., de Silva, R., Revesz, T., Hardy, J. A., and Lees, A. J. (2004) *Brain* **127**, 420–430
- Goldberg, M. S., Fleming, S. M., Palacino, J. J., Cepeda, C., Lam, H. A., Bhatnagar, A., Meloni, E. G., Wu, N., Ackerson, L. C., Klapstein, G. J., Gajendiran, M., Roth, B. L., Chesselet, M. F., Maidment, N. T., Levine, M. S., and Shen, J. (2003) *J. Biol. Chem.* **278**, 43628–43635
- Fleming, S. M., Salcedo, J., Fernagut, P. O., Rockenstein, E., Masliah, E., Levine, M. S., and Chesselet, M. F. (2004) *J. Neurosci.* **24**, 9434–9440
- Lowe, J., Blanchard, A., Morrell, K., Lennox, G., Reynolds, L., Billett, M., Landon, M., and Mayer, R. J. (1988) *J. Pathol.* **155**, 9–15
- Sasaki, S., Shirata, A., Yamane, K., and Iwata, M. (2004) *Neurology* **63**, 678–682
- Braak, H., and Braak, E. (2000) *J. Neurol.* **247**, Suppl. 2, II3–II10
- Spillantini, M. G., Schmidt, M. L., Lee, V. M., Trojanowski, J. Q., Jakes, R., and Goedert, M. (1997) *Nature* **388**, 839–840
- Manetto, V., Perry, G., Tabaton, M., Mulvihill, P., Fried, V. A., Smith, H. T., Gambetti, P., and Autilio-Gambetti, L. (1988) *Proc. Natl. Acad. Sci. U. S. A.* **85**, 4501–4505
- Jankovic, J., Rajput, A. H., McDermott, M. P., and Perl, D. P. (2000) *Arch. Neurol.* **57**, 369–372
- Whishaw, I. Q., Suchowersky, O., Davis, L., Sarna, J., Metz, G. A., and Pellis, S. M. (2002) *Behav. Brain Res.* **133**, 165–176
- Montoya, C. P., Campbell-Hope, L. J., Pemberton, K. D., and Dunnett, S. B. (1991) *J. Neurosci. Methods* **36**, 219–228
- Barneoud, P., Parmentier, S., Mazadier, M., Miquet, J. M., Boireau, A., Dubet, P., and Blanchard, J. C. (1995) *Neuroscience* **67**, 837–848
- Chang, J. W., Wachtel, S. R., Young, D., and Kang, U. J. (1999) *Neuroscience* **88**, 617–628
- Carter, R. J., Lione, L. A., Humby, T., Mangiarini, L., Mahal, A., Bates, G. P., Dunnett, S. B., and Morton, A. J. (1999) *J. Neurosci.* **19**, 3248–3257
- Nolan, M. F., Malleret, G., Lee, K. H., Gibbs, E., Dudman, J. T., Santoro, B., Yin, D., Thompson, R. F., Siegelbaum, S. A., Kandel, E. R., and Morozov, A. (2003) *Cell* **115**, 551–564
- Weydt, P., Hong, S. Y., Klot, M., and Moller, T. (2003) *Neuroreport* **14**, 1051–1054
- Zhuang, X., Oosting, R. S., Jones, S. R., Gainetdinov, R. R., Miller, G. W., Caron, M. G., and Hen, R. (2001) *Proc. Natl. Acad. Sci. U. S. A.* **98**, 1982–1987
- Giros, B., Jaber, M., Jones, S. R., Wightman, R. M., and Caron, M. G. (1996) *Nature* **379**, 606–612
- Jones, S. R., Gainetdinov, R. R., Jaber, M., Giros, B., Wightman, R. M., and Caron, M. G. (1998) *Proc. Natl. Acad. Sci. U. S. A.* **95**, 4029–4034
- Hastings, T. G., Lewis, D. A., and Zigmond, M. J. (1996) *Proc. Natl. Acad. Sci. U. S. A.* **93**, 1956–1961
- Ben-Shachar, D., Zuk, R., Gazawi, H., and Ljubuncic, P. (2004) *Biochem. Pharmacol.* **67**, 1965–1974
- Barzilai, A., Zilkha-Falb, R., Daily, D., Stern, N., Offen, D., Ziv, I., Melamed, E., and Shirvan, A. (2000) *J. Neural Transm. Suppl.* **60**, 59–76
- Stokes, A. H., Lewis, D. Y., Lash, L. H., Jerome, W. G., III, Grant, K. W., Aschner, M., and Vrana, K. E. (2000) *Brain Res.* **858**, 1–8
- Lotharius, J., and O'Malley, K. L. (2000) *J. Biol. Chem.* **275**, 38581–38588
- McLaughlin, B. A., Nelson, D., Erecinska, M., and Chesselet, M. F. (1998) *J. Neurochem.* **70**, 2406–2415
- Gainetdinov, R. R., Fumagalli, F., Jones, S. R., and Caron, M. G. (1997) *J. Neurochem.* **69**, 1322–1325

60. Nass, R., Hall, D. H., Miller, D. M., 3rd, and Blakely, R. D. (2002) *Proc. Natl. Acad. Sci. U. S. A.* **99**, 3264–3269
61. Torres, G. E., Carneiro, A., Seamans, K., Fiorentini, C., Sweeney, A., Yao, W. D., and Caron, M. G. (2003) *J. Biol. Chem.* **278**, 2731–2739
62. Carneiro, A. M., Ingram, S. L., Beaulieu, J. M., Sweeney, A., Amara, S. G., Thomas, S. M., Caron, M. G., and Torres, G. E. (2002) *J. Neurosci.* **22**, 7045–7054
63. Torres, G. E., Yao, W. D., Mohn, A. R., Quan, H., Kim, K. M., Levey, A. I., Staudinger, J., and Caron, M. G. (2001) *Neuron* **30**, 121–134
64. Dekker, M. C., Eshuis, S. A., Maguire, R. P., Veenma-van der Duijn, L., Pruim, J., Snijders, P. J., Oostra, B. A., van Duijn, C. M., and Leenders, K. L. (2004) *J. Neural Transm.* **111**, 1575–1581
65. Van Den Eeden, S. K., Tanner, C. M., Bernstein, A. L., Fross, R. D., Leimpeter, A., Bloch, D. A., and Nelson, L. M. (2003) *Am. J. Epidemiol.* **157**, 1015–1022
66. Tatton, N. A. (2000) *Exp. Neurol.* **166**, 29–43
67. Mazzola, J. L., and Sirover, M. A. (2002) *Neurotoxicology* **23**, 603–609

Progressive dopamine neuron loss following supra-nigral lipopolysaccharide (LPS) infusion into rats exposed to LPS prenatally

Zaodung Ling ^{a,b}, Yuanguai Zhu ^a, Chong wai Tong ^a, Joshua A. Snyder ^a,
Jack W. Lipton ^c, Paul M. Carvey ^{a,b,*}

^a Department of Pharmacology, Rush University Medical Center, Chicago, IL 60612, USA

^b Department of Neuroscience, Rush University Medical Center, Chicago, IL 60612, USA

^c Department of Psychiatry, University of Cincinnati, Cincinnati, OH, USA

Received 21 October 2005; revised 8 December 2005; accepted 12 January 2006

Available online 28 February 2006

Abstract

Toxin-induced animal models of Parkinson's disease (PD) exhibit many of the same neuroinflammatory changes seen in patients suggesting a role for inflammation in DA neuron loss. Yet, despite this inflammation, the progressive loss of DA neurons that characterizes PD is rarely seen in animals. We infused lipopolysaccharide (LPS) or saline into 7-month-old rats that had been exposed to LPS or saline prenatally and assessed them for DA neuron loss and inflammatory measures (interleukin 1 beta, tumor necrosis factor-alpha, glutathione, and activated microglia) over a period of 84 days to examine the role of pre-existing inflammation in progressive DA neuron loss. LPS infusion into both prenatal treatment groups produced neuroinflammation during the 14 days of LPS infusion that subsequently reverted toward normal over the next 70 days. In animals with pre-existing inflammation (i.e., prenatal LPS), however, the acute changes seen were attenuated, but took much longer to return to normal suggesting a prolonged inflammatory response. These inflammatory changes were consistent with the greater acute DA neuron loss seen in the prenatal saline controls and the progressive DA neuron loss seen only in the animals exposed to LPS prenatally. Interestingly, both prenatal treatment groups exhibited increases in microglia over the entire 84-day course of the study. These data suggest that pre-existing neuroinflammation prolongs the inflammatory response that occurs with a second toxic exposure, which may be responsible for progressive DA neuron loss. This provides further support for the "multiple hit" hypothesis of PD.

© 2006 Elsevier Inc. All rights reserved.

Keywords: Parkinson's disease; Interleukin-1 beta; Tumor necrosis factor-alpha; Microglia; Disease progression; Dopamine; Serotonin; Glutathione; Interleukin-10

Introduction

Numerous studies by several laboratories have reproducibly demonstrated inflammatory changes in the brains of patients with Parkinson's disease (PD) including increases in oxidized proteins (Jenner, 1998, 2003), DNA (Fukae et al., 2005; Jenner, 1998, 2003) and lipids (Gotz et al., 1990; Jenner, 1998, 2003; Knott et al., 2002; Olanow, 1990), alterations in glutathione (Gu et al., 1998; Olanow, 1990; Owen et al., 1996; Schulz et al., 2000), activation of microglia (Cho et al., 2003; Gao et al., 2003; Kim and De Vellis, 2005), and increased levels of pro-

inflammatory cytokines (Barcia and Herrero Ezquerro, 2004; Hunot and Hirsch, 2003; Mogi et al., 1996; Nagatsu et al., 2000). Although the etiology of PD is unknown, most feel that the inflammation that accompanies dopamine (DA) neuron death is responsible, at least in part, for the progressive neurodegeneration that characterizes PD. Neurotoxins used to produce animal models of PD, similarly induce inflammation, which is quite similar to that seen in the brains of patients with PD (Barcia and Herrero Ezquerro, 2004; Hunot and Hirsch, 2003; Kim and De Vellis, 2005). Yet, despite similar inflammatory states, the progressive DA neuron loss that characterizes PD rarely occurs in these animal models. This questions the role of inflammation in PD.

Several studies employing multiple DA toxin exposures revealed that animals previously exposed to neurotoxins, exhibit further, additive (Ling et al., 2004b), as well as

* Corresponding author. Department of Pharmacology, 1735 West Harrison Street (Cohn 406), Rush University Medical Center, Chicago, IL 60612, USA. Fax: +312 563 3552.

E-mail address: pcarvey@rush.edu (P.M. Carvey).

synergistic, DA neuron losses (Gao et al., 2003; Ling et al., 2004a; Thiruchelvam et al., 2003) following the second toxin exposure. These studies are consistent with the “multiple hit hypothesis” of PD, which suggests that the DA neuron losses seen in patients are a result of multiple factors, and in the cases cited above, multiple exposures to environmental DA neurotoxins. Since a single exposure to a DA neurotoxin produces neuroinflammation, but not progressive DA neuron loss, it follows that the additive and synergistic losses seen in these multiple hit studies are a consequence of additive and synergistic levels of inflammation, respectively. This further suggests that pre-existing neuroinflammation may predispose the brain to further DA neuron loss and potentially progressive loss in the weeks and months following a second exposure. Although it is possible that PD patients are continuously exposed to DA neurotoxins such as salsolinol (Naoi and Maruyama, 1999) or dieldrin (Corrigan et al., 2000; Fleming et al., 1994), it seems unlikely that acute toxin exposure, can explain progressive DA neuron loss. On the other hand, it is also possible that multiple acute toxin exposures could produce progressive DA neuron loss as a result of achieving a critical threshold of inflammation, or one that is not readily reversible. Either way, such inflammation would lead to DA neuron loss producing further inflammation leading to more DA neuron loss in a self-perpetuating fashion that leads to progressive neurodegeneration. We have now tested this hypothesis in the prenatal lipopolysaccharide (LPS) animal model of PD.

Animals exposed to LPS prenatally are born with fewer than normal DA neurons (Ling et al., 2002) and, during adulthood, exhibit several indices of neuroinflammation including increased numbers of microglia, elevations in tumor necrosis factor alpha (TNF α), increased oxidized proteins, alterations in glutathione, and Lewy-like bodies (Carvey et al., 2003; Ling et al., 2004a). Supranigral infusion of LPS also increases neuroinflammation in the brain and kills DA neurons (Liu et al., 2000). In the current study, we infused LPS supranigally into adult animals exposed to LPS prenatally and followed them for an extended period (84 days). We hoped to demonstrate progressive DA neuron loss affording the opportunity to study the inflammatory mechanisms underlying that progression. Our results demonstrate that animals exposed to LPS prenatally and then infused with LPS in midlife, do exhibit progressive DA neuron loss while analysis of DA metabolism, glutathione biochemistry, cytokine levels and microglia activation are beginning to shed some light on the mechanisms potentially responsible for this progression.

Materials and methods

Animals and prenatal LPS treatment

Ninety timed-gravid, Sprague–Dawley (Zivic-Miller, Allison Park, PA) female rats were delivered to Rush’s animal facility at gestational day 9 ± 12 h. All animals were allowed to acclimate for at least 2 days before treatment. Animals had access to food and water ad libitum and were maintained in an environmentally regulated facility for the duration of the study

(lights on 0600–1800). At gestation day 10.5, one half of the females were injected i.p. with LPS (L8274; 026:B6; Sigma) at 10,000 endotoxin units (EU)/kg body weight and the other half with vehicle (Hank’s Balanced Salt Solution [HBSS]; Sigma). Animals were allowed to deliver normally. Male offspring were weaned at postnatal (P) day 21 and housed two animals per cage. Female offspring were removed and allocated to a different study. The protocols and procedures used in these studies were approved by the Institutional Animal Care and Utilization Committee (IACUC) of Rush University Medical Center.

Animal grouping

Four different treatment groups were established using 150 pups: (1) prenatal HBSS/postnatal HBSS infusion (HBSS/HBSS); (2) prenatal HBSS/postnatal LPS infusion (HBSS/LPS); (3) prenatal LPS/postnatal HBSS infusion (LPS/HBSS); and (4) prenatal LPS/postnatal LPS infusion (LPS/LPS). Ten (or five) animals were allocated to each treatment group. At days 14 and 84, one half of each treatment group ($n = 5$) was used for biochemistry and cytokine assessments and the other half ($n = 5$) was used for immunohistochemistry. At days 3, 28, and 56, all five animals were used for biochemistry and cytokine assessments. An additional twenty pups, ten in each prenatal treatment group, were used as baseline controls (no supranigral infusion or sham surgery). They were sacrificed at baseline (7 months), and designated LPS or HBSS. In order to prevent litter effects, only one male from a given litter per prenatal treatment group was assigned to a dependent measure.

Postnatal mini-pump implantation

At 7 months of age, the offspring in each prenatal treatment group (LPS or HBSS) were randomly subdivided into two groups. One subgroup was subjected to supranigral LPS infusion via mini-pump implantation while the other half was subjected to HBSS mini-pump infusion. LPS was diluted in HBSS at 40,000 EU/ml (0.04 mg/ml). For implantation, animals were anesthetized using pentobarbital (40 mg/kg body weight). The nape of the neck and top of the head were shaved and sterilized thoroughly with Betadine. The animals were then placed in a stereotaxic frame and a skin incision was made under aseptic conditions. A burr hole was made on the right side of the head (A/P = -5.2 mm, M/L = -2.2 mm relative to bregma; D/V = -8.5 mm relative to skull) similar to the procedure previously described by Liu et al. (2000). A stainless steel cannula with tubing (Plastics One, Roanoke, VA) was inserted stereotaxically and fixed to the skull with the aid of screws and dental cement. The tubing was threaded subcutaneously to the nape of the neck and then connected to a mini-pump (Model 2002, Alzet, Cupertino, CA) pre-filled with LPS solution or HBSS. The mini-pump was inserted subcutaneously and the incision closed using silk sutures. The infusion rate of the osmotic pump was 0.5 μ l/h delivering 20 EU/h (0.02 μ g/h) for 14 days (total delivered dose estimated at 6720 EU).

Animal sacrifice

Animals in each treatment group were sacrificed at designated times following pentobarbital overdose (65 mg/kg) according to a protocol described in detail previously (Ling et al., 2002, 2004a,b). At days 0, 14, and 84, one half of the animals in each group was perfused intracardially with ice-cold saline and subsequently processed for biochemical and cytokine assessments. The other half was perfused with ice-cold saline followed by perfusion with Zamboni's fixative (7.5% saturated picric acid, 12 mM NaH₂PO₄, 88 mM Na₂HPO₄, and 4% paraformaldehyde). The brains were removed and processed for immunohistochemistry. All other animals were perfused with ice-cold saline.

Tyrosine hydroxylase and Ox-6 immunohistochemistry

Tyrosine hydroxylase (TH) is the rate-limiting enzyme for DA production in DA neurons and is widely used as an index of DA neurons. Following fixative perfusion, the brains were removed and immersed in Zamboni's fixative for two additional days at 4°C. At the end of fixation, the brains were soaked in 30% sucrose, changed twice, and subsequently cut into 40 µm coronal sections. The sections were divided into 6 series and stored in cryoprotectant (0.05 mol/l phosphate buffered saline, 30% sucrose, 30% ethylene glycol). Every sixth section was immunohistochemically processed for TH using mouse anti-rat tyrosine hydroxylase (TH) antibody (ImmunoStar, Inc. Hudson, WI; 1:20,000) as previously described (Ling et al., 2002, 2004a,b). The secondary antibody used was rat immunoglobulin anti-mouse (rat absorbed) IgG conjugated with biotin (Vector Laboratories, CA). Peroxidase conjugated avidin–biotin complex was applied following the secondary antibody. The chromogen solution used to complete the reaction consisted of 0.05% 3,3'-diaminobenzidine (DAB), 0.5% nickel sulfate, and 0.003% H₂O₂ in I/A solution (10 mM imidazole/50 mM sodium acetate) to obtain a black stain. The sections were washed, mounted on gelatin-coated slides, dehydrated through graded alcohols, cleared in xylenes, and cover-slipped with Permount. For microglial staining, OX-6 anti-major histocompatibility complex (MHC) class II primary antibody was used (1:1000; NOVUS Biologicals, Littleton, CO). The remaining steps were similar to those in the THir protocol.

Stereological cell counts

The estimation of the total number of THir neurons or OX-6ir microglia in the SN was determined using the computerized optical disector method, which allows for the stereological estimation of THir cells in the entire structure independent of size, shape, orientation, tissue shrinkage or anatomical level using StereoInvestigator software (Vu et al., 2000). The SN was anatomically identified as those cells lateral to the accessory optic track as previously described (Ling et al., 2004b). The antibody penetration throughout the whole tissue section was assessed by dissectors using an imaging capture technique. The total number (*N*) of THir or OX-6ir cells was calculated using

the formula $N = N_V \times V_{SN}$, where N_V is the numerical density and V_{SN} is the volume of the SN, as determined by Cavalieri's principle. StereoInvestigator software was also used to determine the total volume of the SN (in mm³) and the density of the cells in that volume (cell counts/mm³). THir and OX-6ir cell counts in the SN were done by an individual blinded to treatment history.

Dopamine biochemistry

DA and its metabolite homovanillic acid (HVA) as well as serotonin (5-HT) and its metabolite 5-hydroxyindole acetic acid (5-HIAA) were measured using HPLC with electrochemical detection (Koprich et al., 2003) in both left and right tissue punches. The size of each punch was 1.5 mm in diameter and about 1.8 mm in height taken from the center of each frozen striatum as previously described (Vu et al., 2000). DA, HVA, 5-HT, and 5HIAA were expressed as ng/mg tissue protein (assessed using the Bio-Rad Protein Assay Kit) and the ratios of [HVA]/[DA] and [5HIAA]/[5-HT] were used as indices of DA and 5HT activity, respectively.

Glutathione measurement

In animals processed for DA biochemistry, glutathione was assessed using the Glutathione Assay Kit (Cayman Chemical Company; Ann Arbor, MI). A single tissue punch taken adjacent to those used for DA biochemistry in the striatum, as well as a tissue punch taken from the medial compacta region of the substantia nigra (SN) lateral to the accessory optic tract, were used. The tissue punches were processed according to the manufacturer's instructions. They were placed into tubes containing 200 µl phosphate-buffered saline with 1 mM ethylene diamine tetra acetic acid (EDTA) and homogenized using a sonicator at 4°C. Tubes were centrifuged at 4°C (10,000 × *g*) and the supernatants decanted. All the samples were diluted with buffered saline to achieve equivalent protein content following protein assessment (Bio-Rad protein assay kit) and then deproteinized before glutathione assay. Total glutathione was measured using an enzymatic assay based on the manufacturer's protocol. For the GSSG levels, GSH was removed from the assay by derivatizing GSH with 2-vinylpyridine. The GSSG levels in the samples were calculated against a curve generated from the standards also treated with 2-vinylpyridine.

Cytokine assessment

The cytokine assessments were performed using rat cytokine multiplex kits (Bio-Rad, CA). Briefly, tissue punches (the size of each punch was 1.5 mm in diameter and about 1.8 mm in height) were taken and were sonicated in 200 µl lysis buffer, spun down, and debris removed. Samples were then diluted with buffer to achieve equivalent protein content (1 mg/ml). 50 µl of sample or standard was added to filter plates containing pre-coated beads for IL-1β, TNFα, and IL-10. After incubation, plates were washed using vacuum suction. The plates were then incubated with secondary antibodies conjugated with

fluorescence dye. After additional washes, the plates were processed in a Luminex 100 plate reader using Qiagen software (Valencia, CA). A standard curve was generated for each cytokine and the cytokine levels in the samples were calculated against each of these curves.

Statistical analysis

The various measures were assessed using SPSS. No statistically significant ipsilateral–contralateral differences were observed at baseline (HBSS only or LPS only). Following supranigral infusion, ipsilateral–contralateral differences were generally observed. As a result, three-way ANOVAs were performed on each side separately assessing the effects of prenatal treatment, supranigral infusion, and time of sacrifice on the dependent measures. Tukey's post hoc analyses were used to detect statistical differences among the groups using $P < 0.05$ as the threshold significance value.

Results

Tyrosine hydroxylase immunoreactive (THir) cell counts

Three-way ANOVA analysis on the THir cell counts in the ipsilateral SN revealed an overall effect ($F_{9,38} = 22.32$; $P < 0.001$) with a total of 48 animals completing the protocol (two died during the protocol). The effects of prenatal treatment ($F_{1,38} = 111.51$; $P < 0.001$) and supranigral infusion ($F_{1,38} = 31.42$; $P < 0.001$) were both significant. The effect of time was not, however, statistically significant. At baseline (day 0, Fig. 1, prior to LPS infusion), animals exposed to LPS prenatally had 27.6% fewer THir cells in the SN than those exposed

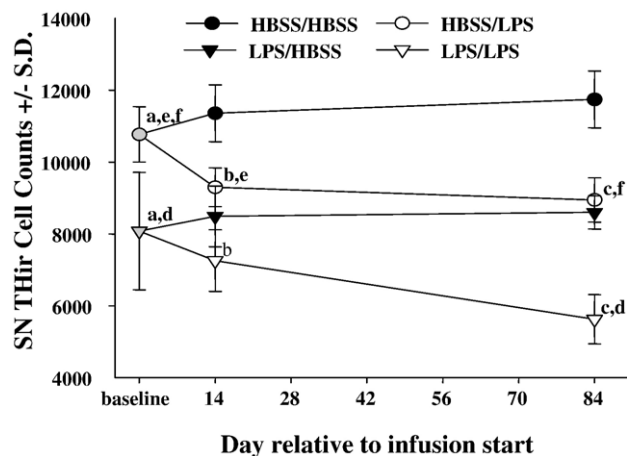


Fig. 1. Changes in tyrosine hydroxylase immunoreactive (THir) cell counts over the course of the study in 7-month-old animals exposed prenatally to Hank's Balanced Salt Solution (HBSS) or lipopolysaccharide (LPS) and infused with HBSS or LPS from days 1 to 14. (Baseline prenatal HBSS (gray circle); prenatal HBSS/postnatal HBSS infusion [HBSS/HBSS]; prenatal HBSS/postnatal lipopolysaccharide [LPS] infusion [HBSS/LPS]. Baseline prenatal LPS (gray diamond); prenatal LPS/postnatal HBSS [LPS/HBSS]; prenatal LPS/postnatal LPS infusion [LPS/LPS]). (Points which share a common letter are statistically different from one another ($P < 0.05$) and relevant to the discussion, although other statistically significant differences are present among the various points).

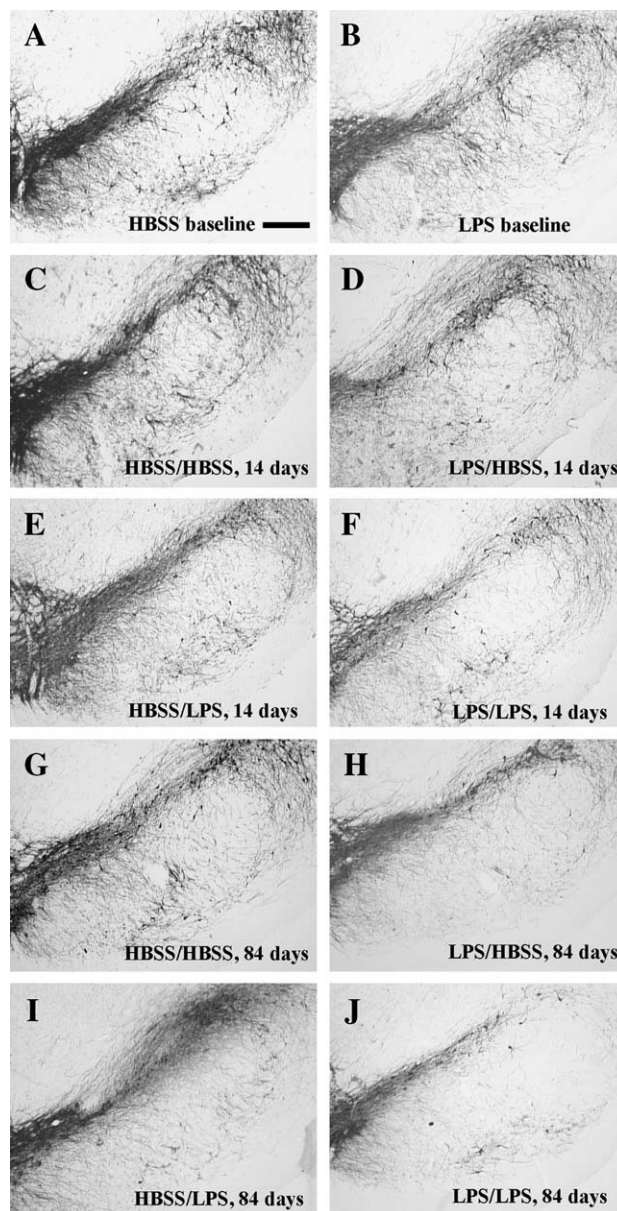


Fig. 2. Representative photomicrographs of tyrosine hydroxylase immunoreactivity in the ipsilateral (right) mesencephalon over the course of the study in 7-month-old animals exposed prenatally to Hank's Balanced Salt Solution (HBSS) or lipopolysaccharide (LPS) and infused with HBSS or LPS from days 1 to 14. (Prenatal HBSS baseline [HBSS]; prenatal HBSS/postnatal HBSS infusion [HBSS/HBSS]; prenatal HBSS/postnatal LPS infusion [HBSS/LPS]. Prenatal [LPS] baseline exposure; prenatal LPS/postnatal HBSS [LPS/HBSS]; prenatal LPS/postnatal LPS infusion [LPS/LPS]). Magnification bar = 0.25 mm.

to HBSS prenatally. The THir cell losses seen were primarily in the SN (Fig. 2B) with little overt changes seen in the ventral tegmental area (VTA) as is characteristic of this model (Ling et al., 2004b). No statistically significant differences were observed between the ipsilateral and contralateral cell counts in the SN in either prenatal group. The average baseline THir cell count in the SN of the HBSS group was $22,228 \pm 714$, which is in excellent agreement with previous publications by our group (Ling et al., 2002, 2004a,b) as well as others (German and Manaye, 1993).

Supranigral infusion of LPS produced further reductions in THir cell counts in the ipsilateral SN in both the prenatal HBSS and LPS groups. Thus, after 14 days, THir cell counts in the HBSS/LPS group were reduced by 18.2% relative to HBSS/HBSS controls, whereas after 84 days, no further significant THir cell losses were observed (25.8% loss relative to HBSS/HBSS 84 days; Figs. 1, 2E, and I). Animals in the LPS/LPS group had 14.6% fewer THir cells than the LPS/HBSS group at 14 days (Figs. 1, 2F). In contrast to the HBSS/LPS group, however, animals in the 84-day LPS/LPS group exhibited further, significant THir cell losses (34.7% reduction relative to LPS/HBSS group at 84 days; Figs. 1, 2J) yielding an overall loss of 52.2% relative to HBSS/HBSS controls. This differential effect of supranigral infusion over time and across prenatal treatment was statistically significant as reflected by the prenatal treatment vs. infusion ($F_{1,38} = 8.11$; $P < 0.01$) and the three-way ($F_{1,38} = 17.31$; $P < 0.01$) interaction statistics. Animals exposed to HBSS or LPS prenatally and infused with HBSS postnatally, did not exhibit any significant alterations in the numbers of ipsilateral THir cells over the course of the study (Fig. 1 and 2C and G) suggesting that infusion alone did not alter the cell counts. Taken together, these data suggest that animals in the LPS/LPS group exhibited continued THir cell losses during, and after LPS infusion while the HBSS/LPS animals only lost DA neurons during the period of LPS infusion.

Three-way ANOVA on the THir cell counts on the contralateral side were also statistically significant ($F_{9,38} = 15.133$; $P < 0.001$). However, the effect seen was primarily the result of prenatal treatment ($F_{1,38} = 119.72$; $P < 0.001$; Table 1). No statistically significant changes in cell sizes or SN volumes gathered during the stereological assessments were detected in any of the treatment groups (data not shown).

Microglia cell counts

Three-way ANOVAs on the OX-6ir cell counts in the SN were highly significant on both the ipsilateral ($F_{9,38} = 14.51$; $P < 0.001$) and contralateral ($F_{9,38} = 15.96$; $P < 0.001$) sides. Analysis of the ipsilateral cell counts revealed that prenatal treatment ($F_{1,38} = 16.79$; $P < 0.001$), time at sacrifice ($F_{2,38} = 10.80$; $P < 0.001$), and supranigral infusion ($F_{1,38} = 58.05$; $P < 0.001$) were all statistically significant. At baseline, the number of OX-6ir cells in animals exposed to LPS prenatally was elevated 13.96 fold relative to the cell counts seen in animals exposed to HBSS prenatally (Figs. 3 and 4A vs. B; HBSS baseline OX-6ir: 69.14 ± 24.24). Moreover, the

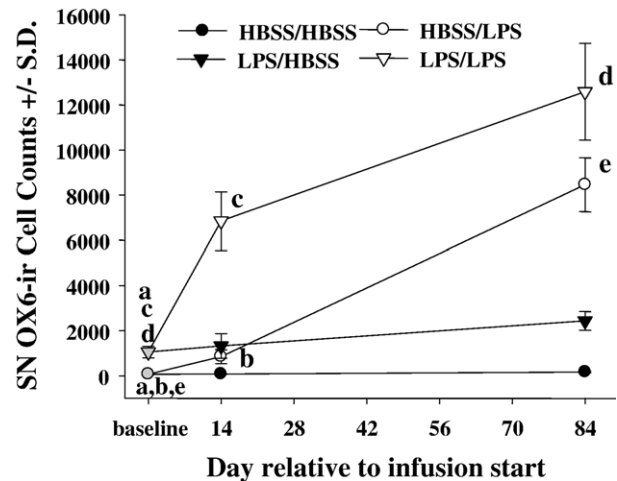


Fig. 3. Changes in OX6-ir cell counts over the course of the study in 7-month-old animals exposed prenatally to Hank's Balanced Salt Solution (HBSS) or lipopolysaccharide (LPS) and infused with HBSS or LPS from days 1 to 14. (Baseline prenatal HBSS (gray circle); prenatal HBSS/postnatal HBSS infusion [HBSS/HBSS]; prenatal HBSS/postnatal LPS infusion [HBSS/LPS]. Baseline prenatal LPS (gray diamond); prenatal LPS/postnatal HBSS [LPS/HBSS]; prenatal LPS/postnatal LPS infusion [LPS/LPS]). (Points which share a common letter are statistically different from one another ($P < 0.05$) and relevant to the discussion, although other statistically significant differences are present among the various points).

morphology of the microglia in animals exposed to LPS prenatally revealed larger cell bodies with shorter and thicker processes indicative of activated microglia (Fig. 4a vs. Fig. 4b). The numbers of these cells increased dramatically thereafter following infusion with both LPS and HBSS, but the effect was clearly larger following supranigral infusion of LPS yielding a statistically significant interaction between time and infusion ($F_{2,38} = 10.18$; $P < 0.001$). In the LPS/LPS group, the number of OX-6ir cells was increased 6.73 fold relative to LPS baseline after 14 days (Figs. 3 and 4F) and 10.10 fold after 84 days (Figs. 3 and 4J). These values reflect a 94.0 and a 141.1 fold increase, respectively, relative to the numbers of microglia seen in the HBSS group at baseline. Interestingly, many of the sections exposed to LPS prenatally and supranigral LPS infusion exhibited multiple tears at 14 days (Fig. 4F). These tears were not seen in any of the HBSS/LPS animals, nor were they evident in sections gathered from any of the animals sacrificed at 84 days and may reflect an interaction between inflammation present in the tissue and the longer duration of peroxidase needed to develop the OX-6ir stain.

In animals exposed to HBSS prenatally and supranigral LPS infusion, the average number of OX-6ir cells at 14 days increased 11.7 fold relative to baseline (Figs. 3 and 4C) and by 84 days, increased 116.18 fold (Figs. 3 and 4G). The increases seen in OX-6ir cell counts in any of the LPS infusion groups were primarily the result of the LPS and not just cannulation and HBSS infusion since the OX-6ir cell counts at 84 days in the HBSS/HBSS group were only increased 2.31 fold relative to baseline while the LPS/HBSS group exhibited only a 3.12 fold increase. Regardless, supranigral infusion of either HBSS or LPS led to morphological changes in the microglia indicative of activation (i.e., shorter processes and thicker cell bodies [Fig. 4]).

Table 1

Prenatal exposure	Baseline	Postnatal infusion	Days relative to baseline	
			Day 14	Day 84
HBSS	11,769 ± 830*	HBSS	11,242 ± 836	11,754 ± 842
		LPS	11,422 ± 621	10,573 ± 1116
LPS	7559 ± 2267*	HBSS	8764 ± 1098*	8852 ± 524*
		LPS	9224 ± 626*	8309 ± 781*

Footnote: Contralateral THir cell counts in SN area ± standard deviation (* indicates statistical difference relative to THir cell count in the animals prenatally exposed to HBSS baseline (♦), $P < 0.05$).

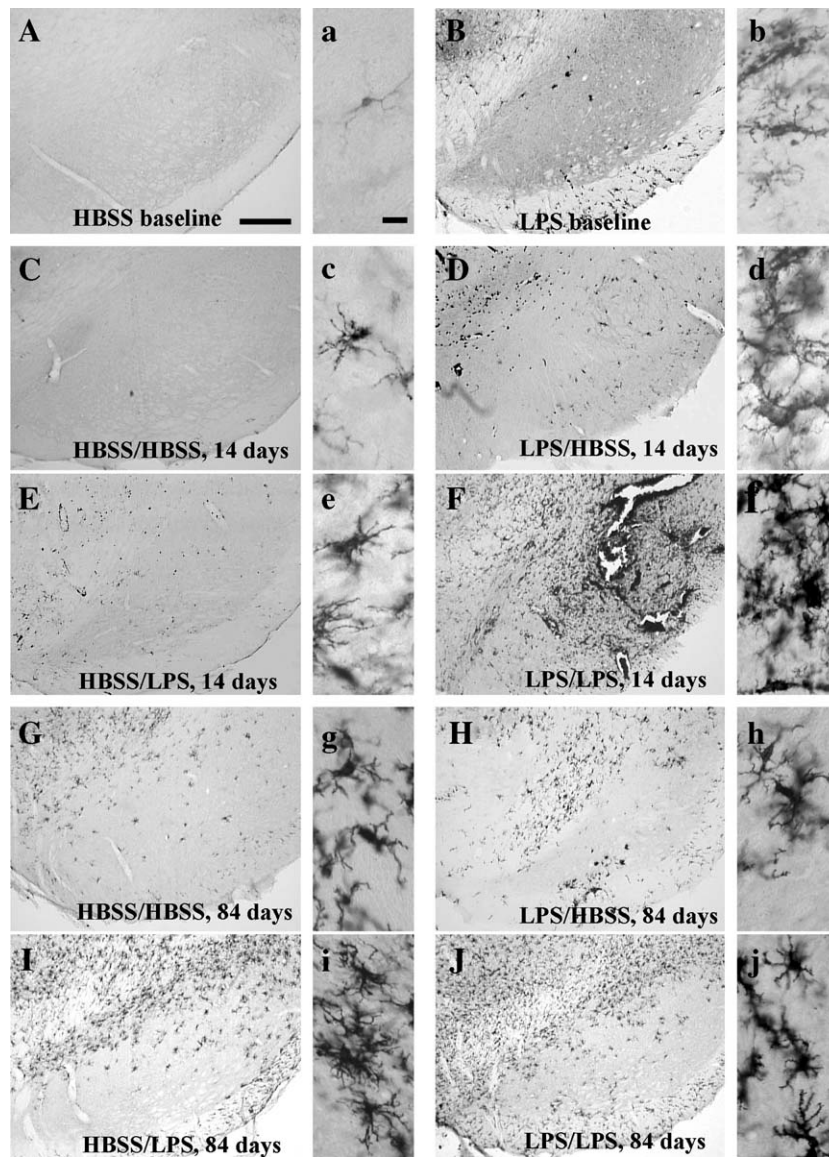


Fig. 4. Representative photomicrographs of OX6 immunoreactive microglia in the ipsilateral (right) mesencephalon over the course of the study in 7-month-old animals exposed prenatally to Hank's Balanced Salt Solution (HBSS) or lipopolysaccharide (LPS) from days 1 to 14. Capital letters depict the whole mesencephalon (magnification bar = 0.25 mm) whereas small matching letters depict the morphology of the microglia taken from the matching section (magnification bar = 25 μ m). Note that typical microglia in the HBSS controls prior to any infusion have small cell bodies with long, thin and mostly unramified processes (a). With activation, the cell bodies become larger and the processes are thicker and more ramified and sometimes amorphous (i). (Prenatal Hank's Balanced Salt Solution [HBSS]; prenatal HBSS/postnatal HBSS infusion [HBSS/HBSS]; prenatal HBSS/postnatal lipopolysaccharide [LPS] infusion [HBSS/LPS]. Prenatal lipopolysaccharide [LPS] exposure; prenatal LPS/postnatal HBSS [LPS/HBSS]; prenatal LPS/postnatal LPS infusion [LPS/LPS]).

Similar, although less dramatic effects were seen in the contralateral SN where there were overall, fewer OX-6ir cells relative to the ipsilateral SN (data not shown). As was true in the ipsilateral SN, the number of OX-6ir cells at baseline in animals exposed to LPS prenatally was significantly elevated (16.63 fold) relative to the HBSS group. This difference increased insignificantly after 14 days of supranigral LPS infusion, whereas by 84 days, it had increased significantly (1.96 fold increase relative to LPS at baseline and 32.64 fold increase relative to HBSS at baseline). In contrast, the supranigral LPS infusion into the opposite SN in the animals exposed to HBSS prenatally increased the number of OX-6ir cells relative to HBSS at baseline only 3.95 fold after 84 days. HBSS infusion

into the opposite hemisphere did not have a significant effect on contralateral OX-6ir cell counts in either prenatal group.

Striatal DA biochemistry

Three-way ANOVA revealed an overall effect on ipsilateral striatal DA ($F_{21,88} = 6.47$; $P < 0.001$) with a total of 120 animals completing the protocol (no animals died in these groups). The effects of prenatal treatment ($F_{1,88} = 54.06$; $P < 0.001$), supranigral infusion ($F_{1,88} = 31.57$; $P < 0.001$), and time at sacrifice ($F_{5,88} = 3.17$; $P < 0.05$) were all statistically significant (Fig. 5A). At baseline, striatal DA levels in animals prenatally exposed to LPS were 14.5% reduced relative to the prenatal

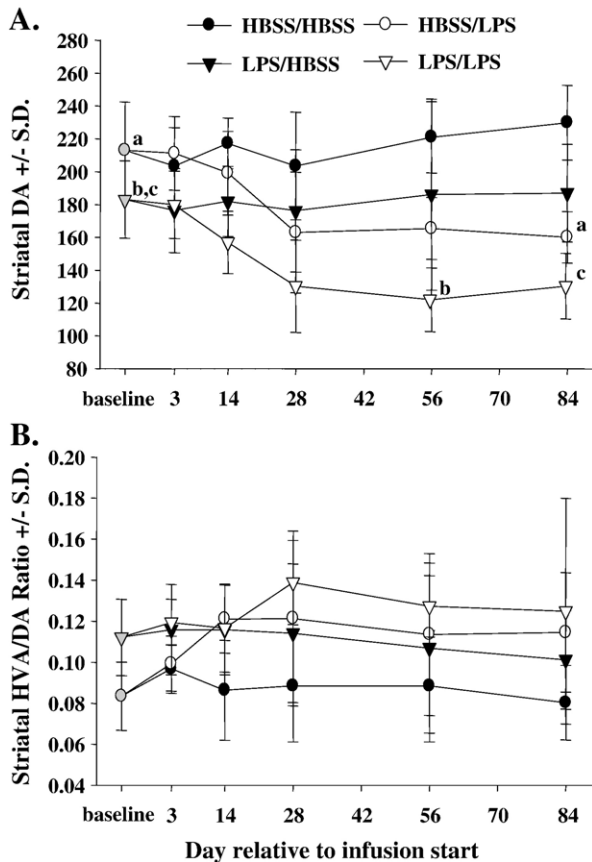


Fig. 5. Changes in striatal dopamine (DA; A) and DA activity ([homovanillic acid (HVA)]/[DA]; B) in tissue punches over the course of the study in 7-month-old animals exposed prenatally to Hank's Balanced Salt Solution (HBSS) or lipopolysaccharide (LPS) and infused with HBSS or LPS from days 1 to 14. (Baseline prenatal HBSS (gray circle); prenatal HBSS/postnatal HBSS infusion [HBSS/HBSS]; prenatal HBSS/postnatal LPS infusion [HBSS/LPS]. Baseline prenatal LPS (gray diamond); prenatal LPS/postnatal HBSS [LPS/HBSS]; prenatal LPS/postnatal LPS infusion [LPS/LPS]). (Points which share a common letter are statistically different from one another ($P < 0.05$) and relevant to the discussion, although other statistically significant differences are present among the various points).

HBSS baseline group (213.04 ± 29.40 ng/mg protein). Supranigral infusion of LPS into both prenatal treatment groups reduced DA levels to approximately 75% of their respective baselines in a parallel fashion by 28 days, after which, they remained at that level through to the end of the study. Supranigral HBSS infusion did not produce significant alterations in the ipsilateral DA content in the striatum in either of the two prenatal treatment groups. In addition, supranigral infusion of either HBSS or LPS had no statistically significant effects on contralateral striatal DA over time, although the effects of prenatal treatment were significant ($F_{1,88} = 63.58$; $P < 0.001$; data not shown).

The HVA/DA ratio is used to reflect DA activity (the release of DA in a structure such that an increase in the ratio reflects compensatory increased release in the face of reduced DA signaling (D'astous et al., 2003; Thiblin et al., 1999; Yurek et al., 1998; Zigmond et al., 2002)). Three-way ANOVA revealed an overall statistically significant effect in the ipsilateral

striatum ($F_{21,88} = 5.35$; $P < 0.001$) as a result of prenatal exposure ($F_{1,88} = 41.88$; $P < 0.001$) and supranigral infusion ($F_{1,88} = 29.82$; $P < 0.001$; Fig. 5B). At baseline, the HVA/DA ratio in the HBSS group was 0.083 which is a value typical of adult rats (Pereira et al., 2004; Zigmond et al., 2002). After 84 days, this ratio was increased by 37% as a result of supranigral LPS infusion. The baseline ratio in the animals exposed to LPS prenatally was 0.112 reflecting a 35%, statistically significant ($P < 0.05$) increase relative to HBSS controls. This ratio increased an additional 11.6% over the course of the 84 days in the ipsilateral side as a result of supranigral LPS infusion yielding an overall increase in this index of DA activity of 51% relative to HBSS animals at baseline. The changes in DA activity across the time points studied in both groups were roughly parallel although the effects over time were not statistically significant ($P = 0.064$), likely due to the large variances. No statistically significant interactions were observed. As was true for the DA data, there were no statistically significant effects of supranigral infusion over time in the contralateral striatum (data not shown).

The three-way ANOVAs on the ipsilateral striatal serotonin data detected overall significant differences in 5HT ($F_{21,88} = 4.51$; $P < 0.001$; Fig. 6A) and the 5HIAA/5HT ratio ($F_{21,88} = 7.51$; $P < 0.001$; Fig. 6B). For 5HT, only the effects of time were statistically significant ($F_{5,88} = 6.33$; $P < 0.001$). At baseline, 5HT levels in the ipsilateral striata of the LPS animals were 30.7% reduced relative to animals prenatally exposed to HBSS (4.4 ± 0.83 ng/mg protein) although this effect was not statistically significant. At 84 days 5HT levels in the LPS/LPS animals were approximately the same (35.0% reduced relative to HBSS) suggesting that LPS supranigral infusion had little effect on 5HT (Fig. 6A). In contrast, 5HT levels in the HBSS/LPS group were reduced 43.2% at 84 days relative to baseline suggesting that supranigral infusion did affect 5HT in control animals as reflected in the statistically significant interaction between prenatal treatment and time ($F_{5,88} = 5.68$; $P < 0.001$). Interestingly, the effects on 5HT in the contralateral striata were similar (data not shown).

Overall, the changes in 5HT activity were less pronounced than seen in levels of striatal 5HT or DA activity. At baseline, the 5HIAA/5HT ratio was elevated only 11% relative to controls (HBSS animals at baseline: HIAA/5HT = 1.52 ± 0.10) in the animals exposed to LPS prenatally. Unlike DA activity which increased over time in all LPS infusion groups, the 5HT activity ratio was decreased by 9% in the LPS/LPS group and by 8.1% in the HBSS/LPS group relative to their respective baselines resulting in a significant interaction between time and supranigral infusion in the three-way ANOVA ($F_{4,88} = 3.05$; $P < 0.05$).

Striatal and nigral glutathione

Reduced glutathione (GSH) assists in neutralizing reactive oxygen species through glutathione peroxidase to yield oxidized glutathione (GSSG) which is then converted back to GSH by glutathione reductase. The amount of GSH thus serves as an index of antioxidant reserve and the ratio of GSH/GSSG

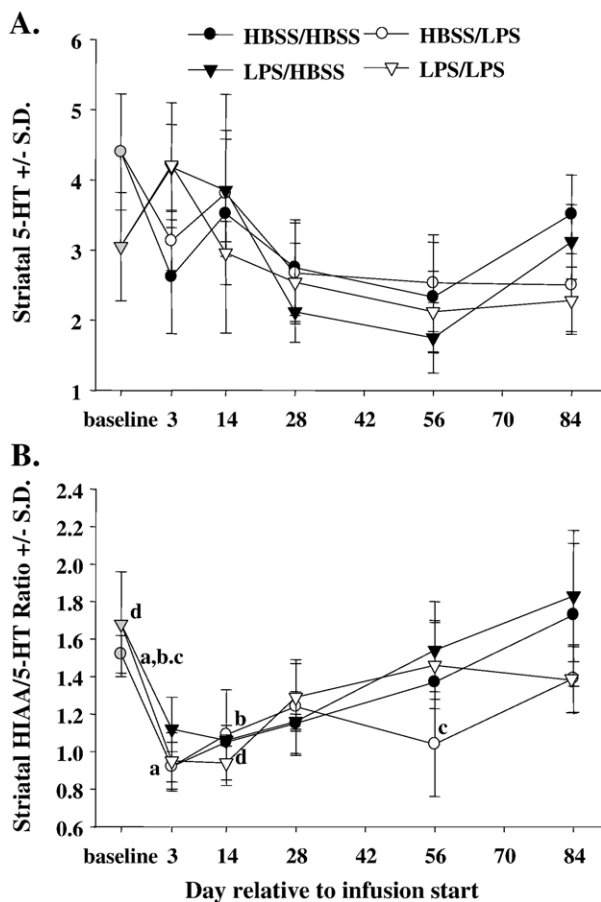


Fig. 6. Changes in striatal serotonin (5HT; A) and 5HT activity ([5-hydroxyindoleacetic acid (5HIAA)]/[5HT]; B) in tissue punches over the course of the study in 7-month-old animals exposed prenatally to Hank's Balanced Salt Solution (HBSS) or lipopolysaccharide (LPS) and infused with HBSS or LPS from days 1 to 14. (Baseline prenatal HBSS (gray circle); prenatal HBSS/postnatal HBSS infusion [HBSS/HBSS]; prenatal HBSS/postnatal LPS infusion [HBSS/LPS]. Baseline prenatal LPS (gray diamond); prenatal LPS/postnatal HBSS [LPS/HBSS]; prenatal LPS/postnatal LPS infusion [LPS/LPS]). (Points which share a common letter are statistically different from one another ($P < 0.05$) and relevant to the discussion, although other statistically significant differences are present among the various points).

reflects the relative amount of detoxification occurring. Alterations in glutathione are considered one of the earliest markers of DA neuron loss (Jenner, 1993; Owen et al., 1996).

Three-way ANOVA on the GSH/GSSG ratio revealed an overall statistically significant effect ($F_{21,88} = 5.46$; $P < 0.001$) where all three factors were also statistically significant (prenatal treatment, $F_{1,88} = 14.56$; $P < 0.001$; supranigral infusion, $F_{1,88} = 29.74$; $P < 0.001$ and time, $F_{5,88} = 5.35$; $P < 0.001$). The GSH/GSSG ratio in the SN at baseline in animals exposed to LPS prenatally was reduced 25.8% relative to animals exposed to HBSS prenatally (Fig. 7A; HBSS animals at baseline: 47.44 ± 3.73). Three days into the supranigral LPS infusion, this ratio decreased to 49.6% of baseline control and only partially recovered to the pre-infusion level at day 84 where the GSH/GSSG ratio was still reduced by 39.3% relative to controls. Supranigral LPS infusion into animals exposed to HBSS prenatally decreased the GSH/GSSG ratio by 35.2% at 3 days

into the infusion and this ratio remained reduced for the duration of the study exhibiting only partial recovery at 84 days relative to baseline (28.7% reduced). It is important to note that the infusion of HBSS produced a less dramatic, albeit observable, effect on this ratio in both prenatal treatment groups suggesting that mechanical perturbation and HBSS infusion produced some oxidant stress.

In the striatum, three-way ANOVA also revealed an overall statistically significant effect on the GSH/GSSG ratio on the ipsilateral side ($F_{21,88} = 3.43$; $P < 0.001$; Fig. 7B), but among the three factors tested, only the effects of prenatal treatment were statistically significant ($F_{1,88} = 49.76$; $P < 0.001$). The reduction in the ipsilateral ratio in animals exposed to LPS prenatally was primarily the result of statistically significant increases in the levels of GSSG at baseline (41.5% relative to control), whereas the GSH levels in these animals were only elevated by 7.3% (data not shown).

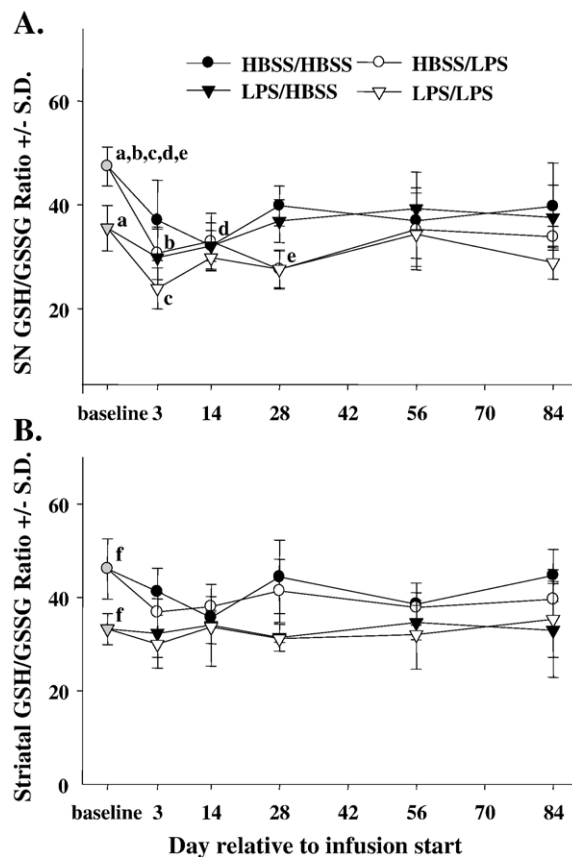


Fig. 7. Changes in the ratio of reduced glutathione (GSH) to oxidized glutathione (GSSG) in tissue punches taken from the substantia nigra (SN; A) and striatum (B) over the course of the study in 7-month-old animals exposed prenatally to Hank's Balanced Salt Solution (HBSS) or lipopolysaccharide (LPS) and infused with HBSS or LPS from days 1 to 14. (Baseline prenatal HBSS (gray circle); prenatal HBSS/postnatal HBSS infusion [HBSS/HBSS]; prenatal HBSS/postnatal LPS infusion [HBSS/LPS]; Baseline prenatal LPS (gray diamond); prenatal LPS/postnatal HBSS [LPS/HBSS]; prenatal LPS/postnatal LPS infusion [LPS/LPS]). (Points which share a common letter are statistically different from one another ($P < 0.05$) and relevant to the discussion, although other statistically significant differences are present among the various points).

The effects of treatment on contralateral GSH, GSSG, total glutathione, and GSH/GSSG in both the striatum and the SN, were unaffected or only mildly affected over the course of the study (data not shown). In the contralateral SN and striatum, the GSH/GSSG ratio was significantly lower in animals exposed to LPS prenatally as was GSSG. In addition, there was a general reduction in the GSH/GSSG during the early phases of infusion of both LPS and HBSS probably reflecting injury in the ipsilateral SN. In all the animals, regardless of prenatal treatment or supranigral infusion, no changes in total glutathione were observed suggesting that induction did not occur. The total glutathione levels in the striatum and the SN were approximately equivalent ($\sim 1.3 \mu\text{M/g}$ wet tissue weight). Glutathione changes were not observed in the cerebellum regardless of prenatal treatment or supranigral infusion.

Striatal and nigral cytokine assessment

The cytokines $\text{TNF}\alpha$, $\text{IL-1}\beta$, and IL-10 were assessed in tissue punches from the ipsilateral and contralateral SNs and striata of each animal. Since both inflammatory and anti-inflammatory cytokines are likely involved with neurodegenerative changes in the DA system, we also evaluated the ratio of $[\text{TNF}\alpha] + [\text{IL-1}\beta]/[\text{IL-10}]$ to assess the overall status of pro- and anti-inflammatory cytokines. The baseline values (pg/mg protein) of each cytokine differed across the three cytokines and simply making a ratio of their absolute levels would therefore not appropriately reflect the relative contribution each made to the ratio since any changes seen would reflect most, the levels of the cytokine with the largest absolute value (i.e., IL-10 26.54 pg/mg protein at baseline). We therefore expressed each cytokine as a percentage of its respective baseline for visual presentation, although the statistical analyses were performed on the raw values.

Supranigral infusion of LPS dramatically increased the ratio of $[\text{TNF}\alpha] + [\text{IL-1}\beta]/[\text{IL-10}]$ in the ipsilateral SN suggesting an overall increase in inflammation (Fig. 8A). Three-way ANOVA on the un-adjusted cytokine levels (raw numbers) revealed an overall effect $F_{21,88} = 62.32$; $P < 0.001$. Both time at sacrifice ($F_{5,88} = 93.68$; $P < 0.001$) and supranigral infusion ($F_{1,88} = 347.40$; $P < 0.001$) were significantly affected. However, the effect of prenatal treatment was not, suggesting that this ratio was not statistically altered by LPS or HBSS prenatal exposure. The cytokine ratio increased almost 100 fold after 3 days of LPS infusion in the animals exposed to HBSS prenatally and returned to baseline by 28 days. In contrast, the ratio after 3 days of LPS infusion into animals exposed to LPS prenatally was only increased 40 fold, but remained elevated, relative to baseline, through 56 days and only returned toward baseline at the end of the study. Similar statistically significant patterns of change were seen in the contralateral SN ($F_{21,88} = 22.59$; $P < 0.001$); data not shown), although the magnitudes were significantly lower relative to the ipsilateral side. Thus, supranigral LPS infusion into animals exposed to HBSS prenatally increased the $[\text{TNF}\alpha] + [\text{IL-1}\beta]/[\text{IL-10}]$ ratio over the first 14 days with a rapid return to baseline. The peak

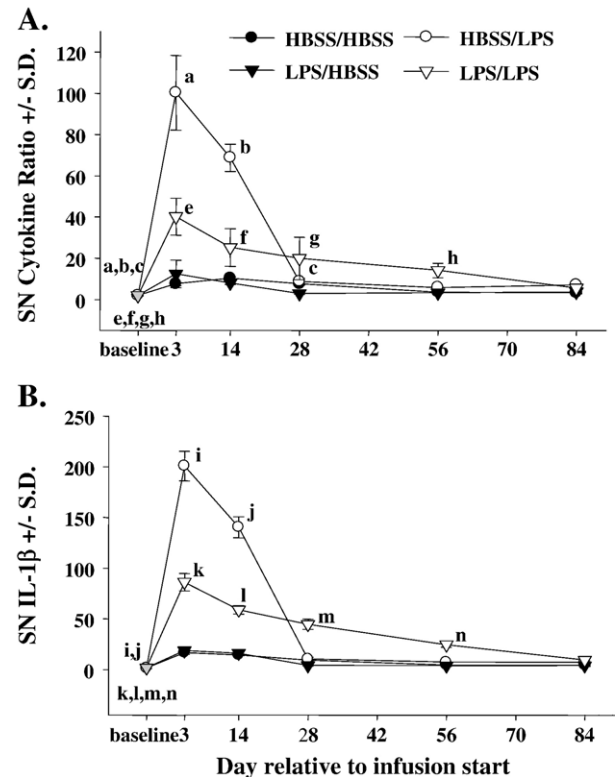


Fig. 8. Changes in the ratio of proinflammatory cytokines ($[\text{TNF-}\alpha + \text{IL-1}\beta]$) to the anti-inflammatory cytokine $[\text{IL-10}]$ (A) and the levels of $\text{IL-1}\beta$ (B) in tissue punches taken from the substantia nigra (SN) over the course of the study in 7-month-old animals exposed prenatally to Hank's Balanced Salt Solution (HBSS) or lipopolysaccharide (LPS) and infused with HBSS or LPS from days 1 to 14. (Baseline prenatal HBSS (gray circle); prenatal HBSS/postnatal HBSS infusion [HBSS/HBSS]; prenatal HBSS/postnatal LPS infusion [HBSS/LPS]. Baseline prenatal LPS (gray diamond); prenatal LPS/postnatal HBSS [LPS/HBSS]; prenatal LPS/postnatal LPS infusion [LPS/LPS]). (Points which share a common letter are statistically different from one another ($P < 0.05$) and relevant to the discussion, although other statistically significant differences are present among the various points).

increase observed was again at 3 days, but the ratio only increased 9.6 fold relative to baseline, more than 10 times less than that seen in the ipsilateral SN. The 3-day increases in the LPS/LPS animals were attenuated relative to the HBSS/LPS group, but remained elevated until day 56. Time at sacrifice ($F_{5,88} = 66.74$; $P < 0.001$) and supranigral infusion ($F_{1,88} = 61.920$; $P < 0.001$) were again the only two factors that were statistically significant. Supranigral infusion had even fewer effects on the cytokine ratios in the ipsilateral and contralateral striata (data not shown) where the effects seen were far less pronounced, although still statistically significant. Thus, the greatest change seen was in the ipsilateral striatum where the maximum magnitude of change (55%) was after 3 days of supranigral infusion of LPS into animals exposed to HBSS prenatally. The cytokine ratio in the cerebellum was not statistically altered by prenatal treatment or supranigral infusion (data not shown).

Among the individual cytokines, $\text{IL-1}\beta$ was most affected (Fig. 8B). Three-way ANOVA revealed a highly significant overall effect ($F_{21,88} = 602.58$; $P < 0.001$). Moreover, prenatal

treatment ($F_{1,88} = 249.02$; $P < 0.001$), post-natal infusion ($F_{1,88} = 2,890.60$; $P < 0.001$) and time at sacrifice ($F_{5,88} = 828.59$; $P < 0.001$) as well as all interactions were statistically significant. In the ipsilateral SN, baseline levels of IL-1 β (2.00 ± 0.08 pg/mg protein) increased almost 152 fold by 3 days in animals infused with LPS and exposed to HBSS prenatally. IL-1 β levels rapidly returned to normal after cessation of the LPS infusion and were back at baseline by 28 days. In contrast, animals exposed to LPS prenatally exhibited a 61.5 fold peak increase after 3 days, but unlike the levels seen in the HBSS/LPS animals, the levels only gradually returned to baseline over 84 days. In the contralateral SN the magnitude of the changes seen were dramatically reduced revealing a maximum change of an 11 fold increase that peaked after 3 days in the HBSS/LPS group, but was back to baseline by 28 days (data not shown). No changes were detected in the cerebellum (data not shown).

Three-way ANOVA revealed an overall effect on ipsilateral TNF α levels in both the SN ($F_{21,88} = 14.46$; $P < 0.001$) and the striatum ($F_{21,88} = 14.80$; $P < 0.001$) as well. In both tissues, prenatal treatment, supranigral infusion, and age at sacrifice all had significant effects. In the SN, animals exposed to LPS prenatally had TNF α levels that were 39.8% elevated relative to animals exposed to HBSS prenatally (Fig. 9A; HBSS animals at baseline: 3.16 ± 0.25 pg/mg protein). This difference increased to a peak level that was 133% elevated relative to control values at 3 days as a result of supranigral LPS perfusion and returned toward baseline after 84 days (54% increased). Animals exposed to HBSS prenatally exhibited a similar pattern of change in TNF α protein levels over the course of the study. Thus, supranigral LPS infusion increased TNF α by 89.2% at 3 days followed by a return toward normal over the remainder of the study. As was true of the changes seen in TNF α levels in the LPS/LPS group, the TNF α levels never completely returned to baseline, and, at 84 days, were still 39% increased relative to baseline. TNF α levels in the ipsilateral striatum followed a similar pattern, although overall, the changes seen were not nearly as large as those in the SN (Fig. 9B). Thus, at baseline, TNF α levels in animals exposed to prenatal LPS were 40% higher than controls (3.24 ± 0.31 pg/mg protein), the levels increased to a peak 3 days into supranigral infusion of LPS, and returned to baseline after 84 days. TNF α levels in the ipsi- and contra-lateral striata and SNs increased transiently in response to HBSS infusion regardless of prenatal exposure and returned to baseline at 84 days. TNF α levels in the cerebellum were not significantly changed by either prenatal exposure or supranigral infusion over the course of the study.

Among the cytokines, IL-10 was the least affected by prenatal LPS or supranigral LPS infusion. Three-way ANOVA on the IL-10 levels in the ipsilateral SN were, overall, statistically significant ($F_{21,88} = 25.93$; $P < 0.001$) as a result of significant effects of prenatal treatment ($F_{1,88} = 95.10$; $P < 0.001$), supranigral infusion ($F_{1,88} = 9.830$; $P < 0.001$), and time at sacrifice ($F_{5,88} = 32.54$; $P < 0.001$). The baseline levels of IL-10 in animals exposed to LPS prenatally were reduced by 10% relative to controls (27.12 ± 3.00 pg/mg protein). In addition, LPS prenatal exposure was associated with an

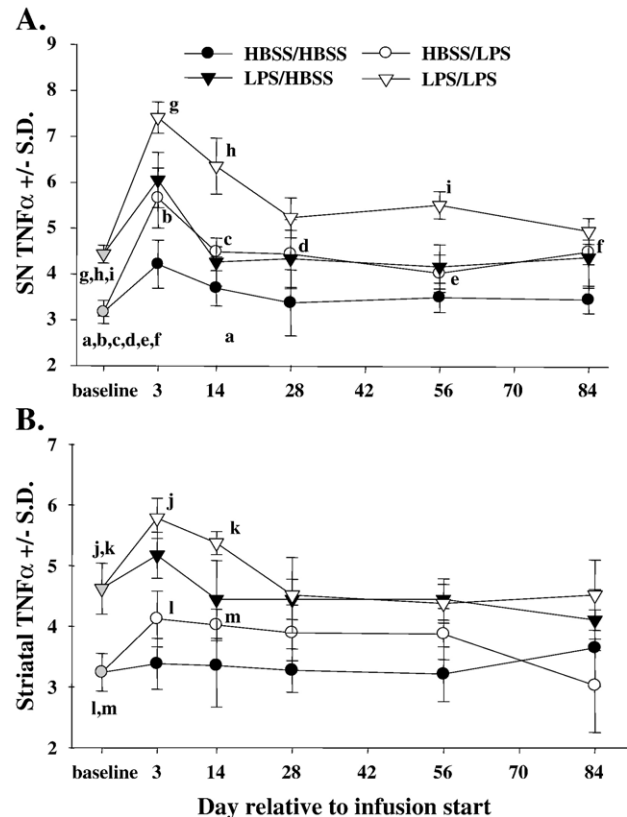


Fig. 9. Changes in TNF α in tissue punches taken from the substantia nigra (SN; A) or the striatum (B) over the course of the study in 7-month-old animals exposed prenatally to Hank's Balanced Salt Solution (HBSS) or lipopolysaccharide (LPS) and infused with HBSS or LPS from days 1 to 14. (Baseline prenatal HBSS (gray circle); prenatal HBSS/postnatal HBSS infusion [HBSS/HBSS]; prenatal HBSS/postnatal LPS infusion [HBSS/LPS]; Baseline prenatal LPS (gray diamond); prenatal LPS/postnatal HBSS [LPS/HBSS]; prenatal LPS/postnatal LPS infusion [LPS/LPS]). (Points which share a common letter are statistically different from one another ($P < 0.05$) and relevant to the discussion, although other statistically significant differences are present among the various points).

attenuated increase, relative to controls, in response to supranigral LPS or HBSS infusion. Similar statistically significant effects were also seen in the contralateral SN ($F_{21,88} = 24.32$; $P < 0.001$), whereas no significant changes were seen in any of the three factors in the ipsi- or contra-lateral striata, or in the cerebellum.

Discussion

The results from this study demonstrate that a second inflammatory challenge (LPS), to a SN that is already inflamed because of prenatal LPS exposure, produces progressive loss of DA neurons. These results not only support the multiple hit hypothesis of PD, but also suggest that the progressive loss of DA neurons that characterizes PD may be a consequence of an altered inflammatory response produced by a prior toxin exposure. Thus, in normal animals, supranigral infusion of LPS for 14 days produced THir cell losses in the SN at 14 days, but no further losses over the remaining 70 days of the study. As

expected, supranigral infusion of LPS into control animals produced significant increases in the inflammatory indices measured, which in some cases, were more pronounced than those seen in the LPS/LPS animals. With the notable exception of the increases in numbers of activated microglia, however, these indices reverted toward normal within 28 days. Animals exposed to LPS prenatally, on the other hand, had, in most cases, an attenuated acute inflammatory response to supranigral LPS infusion, but the duration of that response was markedly prolonged, relative to controls, and associated with progressive DA neuron loss. Since animals exposed to LPS prenatally had higher levels of TNF α , increased numbers of activated microglia, and a lower ratio of GSH/GSSG relative to controls at baseline, it is possible that this pre-existing neuroinflammation altered the second inflammatory response in such a way that it produced progressive DA neuron loss. Taken together, these data are consistent with the notion that multiple, sequential inflammatory challenges, produce an inflammatory response that subsides more slowly than that seen following a single toxic exposure. The extended duration of the inflammatory response seen in the “multiple hit” model may then lead to further neuron losses, which might explain the progressive degeneration of DA neurons that characterizes PD.

Numerous environmental toxins kill DA neurons *in vivo* and this death generally occurs over a short period (Fearnley and Lees, 1991; Jackson-Lewis et al., 1995). In contrast, progressive and extended loss of DA neurons is an important characteristic of PD. Therefore, if an environmental toxin does participate in the pathogenesis of PD, then progressive loss of DA neurons should occur in toxin-induced animal models of PD. Yet, supranigral infusion of LPS (Gao et al., 2003), paraquat with maneb (Thiruchelvam et al., 2003), and long-term, low-dose MPTP exposure in non-human primates (Brownell et al., 1998) are the only three reports we are aware of, that showed continued THir cell loss in the months following withdrawal from the toxin. Acute exposure to epoxomicin, or its synthetic analog, similarly produced progressive DA neuron loss following discontinuation of exposure, although the animals were only studied for an additional 6 weeks (McNaught et al., 2004). Thus, the majority of toxins used to produce PD-like lesions reproduce the neuroinflammation, but not the progressive loss of DA neurons seen in PD. This failure to exhibit progression could be the result of several factors including age at exposure, exposing animals for too short a period, or simply that the toxin used does not produce the same pathophysiological changes as those seen in patients. Alternatively, the levels of inflammation achieved in these models may quickly subside preventing further DA neuron death and even allowing recovery. Indeed, many neurotoxins produce acute DA neuron losses and then partial recovery of those losses in the weeks and months following exposure (Bezard et al., 2001; Jakowec and Petzinger, 2004). If neuroinflammation, which usually subsides over time, is indeed responsible for the progressive loss of DA neurons, then a mechanism for perpetuating such inflammation must exist, or alternatively, it reaches a critical threshold where homeostatic mechanisms are overwhelmed. This would then suggest that the majority of toxins studied might produce a

progressive DA neuron loss if the brain were predisposed due to pre-existing inflammation as was true in the animals in the present study.

Prior to supranigral infusion, animals exposed to LPS prenatally had 28% fewer THir cells in their SNs. In addition to THir cell loss, the prenatal LPS animals at baseline had reduced striatal DA and increased DA activity, increased numbers of activated microglia, increased levels of TNF α and normal levels of IL-1 β relative to controls. These findings are similar to those reported previously (Carvey et al., 2003; Ling et al., 2002, 2004a,b) and supports the hypothesis that prenatal exposure to LPS produces a life-long state of neuroinflammation associated with reduced DA function. However, the changes in glutathione biochemistry and 5HT reported here broaden the similarities between the prenatal LPS animal model and PD. Thus, the reduced levels of GSH and GSH/GSSG ratio as well as the slightly reduced levels of 5HT seen in the striata of animals exposed to LPS prenatally, are similar to those described in patients with PD (Hesselink, 1993; Jenner et al., 1983). These changes further reinforce our contention that exposure to LPS *in utero*, which commonly occurs during pregnancy complicated by bacterial vaginosis, serves as a risk factor for PD (Ling et al., 2002). The reason for the perpetual inflammatory state and reductions in DA function in these animals is currently unknown and under active investigation.

Following exposure to LPS, both prenatal treatment groups exhibited parallel increases in TNF α . Thus, in the SN ipsilateral to the LPS infusion, both groups showed peak increases of TNF α 3 days into supranigral LPS infusion, which returned only partially to their respective baseline levels at the end of the study. Since TNF α kills DA neurons in tissue culture (McGuire et al., 2001) and following supranigral infusion (Carvey et al., 2005), the elevated levels of TNF α in the HBSS/LPS group should have produced progressive DA neuron loss, but this was not shown. Thus, it is unlikely that TNF α is responsible for the progressive DA neuronal loss seen in our experiments.

Supranigral LPS infusion also produced dramatic increases in IL-1 β in both prenatal treatment groups (50 to 152 fold increases relative to the respective baseline). IL-1 β has also been shown to reduce DA neurons when given to newborns (Kabiersch et al., 1998) or following supranigral infusion into adults (Carvey et al., 2005). Indeed, of all the inflammatory indices evaluated, the changes in IL-1 β were most affected by treatment and similar to the patterns of change seen in THir cell counts. Thus, in the HBSS/LPS group, IL-1 β levels increased much more dramatically during LPS infusion than seen in the LPS/LPS group. However, the high levels in the HBSS/LPS group reverted rapidly back to baseline after discontinuation of LPS exposure, whereas IL-1 β reverted very slowly in the LPS/LPS animals. The larger acute increases in IL-1 β in the HBSS/LPS group might explain the greater DA neuron losses seen in that group at 14 days while the rapid reversion to normal might account for the absence of further DA neuron loss over the next 70 days. However, in the LPS/LPS group IL-1 β levels remained elevated well

beyond the discontinuation of LPS infusion in association with progressive THir cell loss. Thus, in animals with an elevated baseline level of neuroinflammation, both the acute response to LPS infusion and the rate at which it normalized following discontinuation of LPS infusion were altered. Since the acute increases in IL-1 β in the LPS/LPS animals were attenuated compared with the HBSS/LPS group, it cannot be argued that it was a greater inflammatory response in the LPS/LPS group that was responsible for the progressive loss seen. Indeed, a “blunted” inflammatory response to a second challenge with LPS has been extensively studied and known for years (Li et al., 2000; Mathison et al., 1990), although the responsible mechanism is not understood (Fan and Cook, 2004). Rather, what changed was the duration of the IL-1 β response. Since this prolonged response occurred during the interval of progressive DA neuron loss, IL-1 β may participate in disease progression.

It is important to note, however, that anti-inflammatory cytokines counteract the proinflammatory cytokines during inflammation (Kremlev and Palmer, 2005; Strle et al., 2001). Indeed, IL-10 levels did increase because of LPS infusion in both prenatal treatment groups, and although the increases seen in the prenatal LPS animals were less dramatic than in the prenatal HBSS group, the differences were not statistically significant. Alterations in IL-10 therefore do not appear to explain the differences in THir cell losses across the two prenatal treatment groups infused with LPS.

Examination of each individual cytokine likely does not adequately reflect the entire inflammatory environment, so we attempted to generate a cytokine inflammatory index by expressing the absolute level of each cytokine as a percent of its baseline and then generated a pro-/anti-inflammatory ratio ($[\text{TNF}\alpha] + [\text{IL-1}\beta]/[\text{IL10}]$). The changes seen in this ratio over the course of the experiment were, not surprisingly, similar to IL-1 β since this cytokine changed so dramatically over the course of the study and therefore contributed most to the generated ratio. Regardless, this ratio increased 50 fold acutely then quickly reverted to normal in control animals following supranigral infusion. In the prenatal LPS group, the ratio increased significantly less and only gradually returned toward normal after 84 days. This matched the pattern of changes seen in THir cell counts in both prenatal treatment groups. Using an overall index of inflammation that incorporates both inflammatory and anti-inflammatory factors therefore seems to be a valid index of neuroinflammation that can predict DA neuron changes.

We also examined the numbers of activated microglia by assessing OX-6ir cells. OX-6 binds to the MHC class II of receptors on monocytes and expression of this antigen in brain suggests microglial activation (Cho et al., 2003; Ng and Ling, 2001; Tomas-Camardiel et al., 2004). Activated microglia release a number of pro-inflammatory cytokines as well as other inflammatory mediators (Chianella et al., 1999; Cho et al., 2003; Kim and De Vellis, 2005; Mcgeer et al., 1988; Ng and Ling, 2001). The baseline OX-6ir cell counts in the LPS animals were markedly elevated relative to controls and consistent with the increased levels of TNF α seen in these animals. Ox-6ir cell

counts increased dramatically thereafter as a result of LPS infusion, increasing 151 fold relative to baseline at 84 days. However, animals exposed to HBSS prenatally and supranigral LPS infusion exhibited a similar pattern of increase, although the absolute numbers were significantly lower (116 fold increase relative to baseline). Yet, the HBSS/LPS animals failed to exhibit progressive DA neuron loss. Obviously, the increased numbers of OX-6ir cells were not responsible for the THir cell losses seen since small, yet significant, increases in OX-6ir cells were also seen in animals infused with HBSS that did not exhibit any THir cell loss. The changes in microglia observed therefore do not seem to explain the progressive losses of THir cells observed.

Given that microglia are known to release TNF α and IL-1 β upon activation, it was surprising to discover that the significant increases in OX-6ir cells did not correlate well with cytokine production. Thus, following discontinuation of LPS infusion, the number of microglia continued to increase while both TNF α and IL-1 β decreased. The presence of activated microglia is presumed to reflect the inflammatory state of neural tissue. However, the results presented here suggest otherwise, at least in terms of pro-inflammatory cytokine production. It is possible that other markers of activated microglia such as OX-42 or ED-1 (Chianella et al., 1999) would better correlate with pro-inflammatory cytokine levels. Regardless, this finding suggests that increased numbers of activated microglia do not necessarily indicate increased proinflammatory cytokine production.

Gao et al. (2003) demonstrated that supranigral LPS infusion also increased the numbers of activated microglia (OX-42ir cells). They also showed that microglia activation preceded a progressive DA neuron loss that occurred over several months. However, by comparison, their THir cell losses were significantly larger. The apparent increased susceptibility in their study could reflect rat strain differences (Fisher 344 vs. Sprague–Dawley). They also used a different lot of *E. coli* LPS, and we have previously noted that the number of EU/mg endotoxin can vary dramatically between lots (unpublished observation). Thus, it is possible that they were delivering comparatively more EU/kg, which could explain the differences in magnitude seen between their study and ours. If this were the case, the greater degree of inflammation a larger dose would have produced would explain the progressive loss seen in their animals whereas our control animals failed to exhibit progressive THir cell losses. In addition, the use of a different marker for activated microglia might also explain some of the differences between Gao et al.’s study and ours. Although the differences between their results and ours require further investigation, both studies provide data indicating that inflammation precedes and contributes to progressive neuron loss.

One final inflammatory index that could help to explain the differences in LPS infusion-induced progression between the two prenatal treatment groups is the ratio of GSH/GSSG. This ratio reflects the level of oxidant stress present in a tissue (Owen et al., 1996; Schulz et al., 2000). Consistent with our previous results showing increased protein oxidation in animals exposed

to LPS prenatally (Ling et al., 2004a), the GSH/GSSG ratio in the ipsilateral SN of the LPS group was reduced 25.2% relative to animals exposed to HBSS prenatally. Supranigral LPS infusion significantly reduced this ratio further in both prenatal treatment groups yielding a peak reduction in the LPS/LPS group at 3 days of 49.6% of normal. Interestingly, the ratios in both prenatal treatment groups reverted only partially back to normal after 84 days, and remained reduced relative to control and their respective baselines in both treatment groups. If indeed the GSH/GSSG ratio is an index of oxidant stress which contributes to progressive neuron loss, then both supranigral infusion groups were still exhibiting oxidant stress 70 days following discontinuation of LPS perfusion which should be associated with further DA neuron loss. This was not the case, however. Moreover, as was true with many of the other inflammatory indices, the patterns of change in this ratio during and after LPS infusion were parallel between the two prenatal treatment groups thereby failing to explain the progressive THir cell loss in the animals exposed to LPS prenatally. Finally, the GSH levels in the LPS/LPS ipsilateral SN after 84 days were only reduced by 9.2% relative to controls at baseline. This indicates that there was plenty of free radical detoxification reserve remaining suggesting that the ability of the glutathione system to handle reactive oxygen species burden was not overwhelmed.

Taken together, the results from the present study suggest that pre-existing neuroinflammation contributes to progressive DA neuron loss following a second inflammatory challenge with LPS. The mechanism(s) responsible for this progression may involve changes in IL-1 β , although a host of other inflammatory mediators that were not evaluated here could also be involved. Although it is possible that a second exposure to an inflammogen could produce an overall level of inflammation that reaches some critical threshold that precludes reversal, this does not appear to be the case in the present study since LPS infusion into a normal SN, produced in some cases, a greater inflammatory response. It therefore seems more likely that pre-existing inflammation somehow changes the response to a subsequent inflammatory challenge such that the duration of that inflammatory change is prolonged as suggested here, or changed in some other unknown manner. Regardless of the mechanism involved, the data from the present study are consistent with notion that PD, beside the genetic factors, is a consequence of multiple exposures to environmental toxins. Whether or not this altered inflammatory response is unique to prenatal LPS and postnatal LPS infusion or is a universal consequence of multiple toxin exposures is currently being examined. Understanding the interactions of these “multiple hits” may lead to a better understanding of the mechanisms responsible for disease progression in PD.

Acknowledgments

This project was supported by a grant from the Michael J. Fox Foundation. Additional support for the laboratory was provided by NINDS NS045316, NIEHS 012307, and USARMRA W81XWH-04-01-0365.

References

- Barcia, G.C., Herrero Ezquerro, M.T., 2004. [Inflammation and Parkinson's disease]. *Rev. Neurol.* 38, 545–553.
- Bezard, E., Dovero, S., Prunier, C., Ravenscroft, P., Chalon, S., Guilloteau, D., Crossman, A.R., Bioulac, B., Brotchie, J.M., Gross, C.E., 2001. Relationship between the appearance of symptoms and the level of nigrostriatal degeneration in a progressive 1-methyl-4-phenyl-1,2,3,6-tetrahydropyridine-lesioned macaque model of Parkinson's disease. *J. Neurosci.* 21, 6853–6861.
- Brownell, A.L., Jenkins, B.G., Elmaleh, D.R., Deacon, T.W., Speelman, R.D., Isacson, O., 1998. Combined PET/MRS brain studies show dynamic and long-term physiological changes in a primate model of Parkinson disease. *Nat. Med.* 4, 1308–1312.
- Carvey, P.M., Chang, Q., Lipton, J.W., Ling, Z., 2003. Prenatal exposure to the bacteriotxin lipopolysaccharide leads to long-term losses of dopamine neurons in offspring: a potential, new model of Parkinson's disease. *Front. Biosci.* 8, s826–s837.
- Carvey, P.M., Chen, E.Y., Lipton, J.W., Tong, C.W., Chang, Q.A., Ling, Z.D., 2005. Intra-parenchymal injection of tumor necrosis factor- α and interleukin 1- β produces dopamine neuron loss in the rat. *J. Neural Transm.* 112, 601–612.
- Chianella, S., Semprevivo, M., Peng, Z.C., Zaccaro, D., Bentivoglio, M., Grassi-Zucconi, G., 1999. Microglia activation in a model of sleep disorder: an immunohistochemical study in the rat brain during *Trypanosoma brucei* infection. *Brain Res.* 832, 54–62.
- Cho, B.P., Sugama, S., Shin, D.H., Degiorgio, L.A., Kim, S.S., Kim, Y.S., Lim, S.Y., Park, K.C., Volpe, B.T., Cho, S., Joh, T.H., 2003. Microglial phagocytosis of dopamine neurons at early phases of apoptosis. *Cell. Mol. Neurobiol.* 23, 551–560.
- Corrigan, F.M., Wienburg, C.L., Shore, R.F., Daniel, S.E., Mann, D., 2000. Organochlorine insecticides in substantia nigra in Parkinson's disease. *J. Toxicol. Environ. Health, Part A* 59, 229–234.
- D'astous, M., Morissette, M., Tanguay, B., Callier, S., 2003. Dehydroepiandrosterone (DHEA) such as 17 β -estradiol prevents MPTP-induced dopamine depletion in mice. *Synapse* 47, 10–14.
- Fan, H., Cook, J.A., 2004. Molecular mechanisms of endotoxin tolerance. *J. Endotoxin. Res.* 10, 71–84.
- Fearnley, J.M., Lees, A.J., 1991. Ageing and Parkinson's disease: substantia nigra regional selectivity. *Brain* 114 (Pt. 5), 2283–2301.
- Fleming, L., Mann, J.B., Bean, J., Briggles, T., 1994. Parkinson's disease and brain levels of organochlorine pesticides. *Ann. Neurol.* 36, 100–103.
- Fukae, J., Takanashi, M., Kubo, S., Nishioka, K., Nakabeppu, Y., Mori, H., Mizuno, Y., Hattori, N., 2005. Expression of 8-oxoguanine DNA glycosylase (OGG1) in Parkinson's disease and related neurodegenerative disorders. *Acta Neuropathol. (Berl.)* 109, 256–262.
- Gao, H.M., Liu, B., Zhang, W., Hong, J.S., 2003. Synergistic dopaminergic neurotoxicity of MPTP and inflammatory lipopolysaccharide: relevance to the etiology of Parkinson's disease. *FASEB J.* 17, 1957–1959.
- German, D.C., Manaye, K.F., 1993. Midbrain dopaminergic neurons (nuclei A8, A9, and A10): three-dimensional reconstruction in the rat. *J. Comp. Neurol.* 331, 297–309.
- Gotz, M.E., Freyberger, A., Riederer, P., 1990. Oxidative stress: a role in the pathogenesis of Parkinson's disease. *J. Neural Transm., Suppl.* 29, 241–249.
- Gu, M., Owen, A.D., Toffa, S.E., Cooper, J.M., Dexter, D.T., Jenner, P., Marsden, C.D., Schapira, A.H., 1998. Mitochondrial function, GSH and iron in neurodegeneration and Lewy body diseases. *J. Neurol. Sci.* 158, 24–29.
- Hesselink, J.M., 1993. Serotonin and Parkinson's disease. *Am. J. Psychiatry* 150, 843–844.
- Hunot, S., Hirsch, E.C., 2003. Neuroinflammatory processes in Parkinson's disease. *Ann. Neurol.* 53 (Suppl. 3), S49–S58.
- Jackson-Lewis, V., Jakowec, M., Burke, R.E., Przedborski, S., 1995. Time course and morphology of dopaminergic neuronal death caused by the neurotoxin 1-methyl-4-phenyl-1,2,3,6-tetrahydropyridine. *Neurodegeneration* 4, 257–269.
- Jakowec, M.W., Petzinger, G.M., 2004. 1-methyl-4-phenyl-1,2,3,6-tetrahydropyridine-lesioned model of parkinson's disease, with emphasis on mice and nonhuman primates. *Comp. Med.* 54, 497–513.

- Jenner, P., 1993. Altered mitochondrial function, iron metabolism and glutathione levels in Parkinson's disease. *Acta Neurol. Scand., Suppl.* 146, 6–13.
- Jenner, P., 1998. Oxidative mechanisms in nigral cell death in Parkinson's disease. *Mov. Disord.* 13 (Suppl. 1), 24–34.
- Jenner, P., 2003. Oxidative stress in Parkinson's disease. *Ann. Neurol.* 53 (Suppl. 3), S26–S36.
- Jenner, P., Sheehy, M., Marsden, C.D., 1983. Noradrenaline and 5-hydroxytryptamine modulation of brain dopamine function: implications for the treatment of Parkinson's disease. *Br. J. Clin. Pharmacol.* 15 (Suppl. 2), 277S–289S.
- Kabiersch, A., Furukawa, H., Besedovsky, H.O., 1998. Administration of interleukin-1 at birth affects dopaminergic neurons in adult mice. *Ann. N. Y. Acad. Sci.* 840, 123–127.
- Kim, S.U., De Vellis, J., 2005. Microglia in health and disease. *J. Neurosci. Res.* 81, 302–313.
- Knott, H.M., Baoutina, A., Davies, M.J., Dean, R.T., 2002. Comparative time-courses of copper-ion-mediated protein and lipid oxidation in low-density lipoprotein. *Arch. Biochem. Biophys.* 400, 223–232.
- Koprich, J.B., Campbell, N.G., Lipton, J.W., 2003. Neonatal 3,4-methylenedioxymethamphetamine (ecstasy) alters dopamine and serotonin neurochemistry and increases brain-derived neurotrophic factor in the forebrain and brainstem of the rat. *Brain Res. Dev. Brain Res.* 147, 177–182.
- Kremlev, S.G., Palmer, C., 2005. Interleukin-10 inhibits endotoxin-induced proinflammatory cytokines in microglial cell cultures. *J. Neuroimmunol.* 162, 71–80.
- Li, L., Cousart, S., Hu, J., McCall, C.E., 2000. Characterization of interleukin-1 receptor-associated kinase in normal and endotoxin-tolerant cells. *J. Biol. Chem.* 275, 23340–23345.
- Ling, Z., Gayle, D.A., Ma, S.Y., Lipton, J.W., Tong, C.W., Hong, J.S., Carvey, P.M., 2002. In utero bacterial endotoxin exposure causes loss of tyrosine hydroxylase neurons in the postnatal rat midbrain. *Mov. Disord.* 17, 116–124.
- Ling, Z., Chang, Q.A., Tong, C.W., Leurgans, S.E., Lipton, J.W., Carvey, P.M., 2004a. Rotenone potentiates dopamine neuron loss in animals exposed to lipopolysaccharide prenatally. *Exp. Neurol.* 190, 373–383.
- Ling, Z.D., Chang, Q., Lipton, J.W., Tong, C.W., Landers, T.M., Carvey, P.M., 2004b. Combined toxicity of prenatal bacterial endotoxin exposure and postnatal 6-hydroxydopamine in the adult rat midbrain. *Neuroscience* 124, 619–628.
- Liu, B., Jiang, J.W., Wilson, B.C., Du, L., Yang, S.N., Wang, J.Y., Cao, G.C., Hong, X.D., 2000. Systemic infusion of naloxone reduces degeneration of rat substantia nigral dopaminergic neurons induced by intranigral injection of lipopolysaccharide. *J. Pharmacol. Exp. Ther.* 295, 125–132.
- Mathison, J.C., Virca, G.D., Wolfson, E., Tobias, P.S., Glaser, K., Ulevitch, R.J., 1990. Adaptation to bacterial lipopolysaccharide controls lipopolysaccharide-induced tumor necrosis factor production in rabbit macrophages. *J. Clin. Invest.* 85, 1108–1118.
- McGeer, P.L., Itagaki, S., Boyes, B.E., McGeer, E.G., 1988. Reactive microglia are positive for HLA-DR in the substantia nigra of Parkinson's and Alzheimer's disease brains. *Neurology* 38, 1285–1291.
- McGuire, S.O., Ling, Z.D., Lipton, J.W., Sortwell, C.E., Collier, T.J., Carvey, P.M., 2001. Tumor necrosis factor alpha is toxic to embryonic mesencephalic dopamine neurons. *Exp. Neurol.* 169, 219–230.
- McNaught, K.S., Perl, D.P., Brownell, A.L., Olanow, C.W., 2004. Systemic exposure to proteasome inhibitors causes a progressive model of Parkinson's disease. *Ann. Neurol.* 56, 149–162.
- Mogi, M., Harada, M., Narabayashi, H., Inagaki, H., Minami, M., Nagatsu, T., 1996. Interleukin (IL)-1 beta, IL-2, IL-4, IL-6 and transforming growth factor-alpha levels are elevated in ventricular cerebrospinal fluid in juvenile parkinsonism and Parkinson's disease. *Neurosci. Lett.* 211, 13–16.
- Nagatsu, T., Mogi, M., Ichinose, H., Togari, A., 2000. Cytokines in Parkinson's disease. *J. Neural* 143–151.
- Naoi, M., Maruyama, W., 1999. N-methyl (R)salsolinol, a dopamine neurotoxin, in Parkinson's disease. *Adv. Neurol.* 80, 259–264.
- Ng, Y.K., Ling, E.A., 2001. Microglial reaction in focal cerebral ischaemia induced by intra-carotid homologous clot injection. *Histol. Histopathol.* 16, 167–174.
- Olanow, C.W., 1990. Oxidation reactions in Parkinson's disease. *Neurology* 40 (Suppl. 7).
- Owen, A.D., Schapira, A.H., Jenner, P., Marsden, C.D., 1996. Oxidative stress and Parkinson's disease. *Ann. N. Y. Acad. Sci.* 786, 217–223.
- Pereira, F.C., Santos, S.D., Ribeiro, C.F., Ali, S.F., Macedo, T.R., 2004. A single exposure to morphine induces long-lasting hyporeactivity of rat caudate putamen dopaminergic nerve terminals. *Ann. N. Y. Acad. Sci.* 1025, 414–423.
- Schulz, J.B., Lindenau, J., Seyfried, J., Dichgans, J., 2000. Glutathione, oxidative stress and neurodegeneration. *Eur. J. Biochem.* 267, 4904–4911.
- Strle, K., Zhou, J.H., Shen, W.H., Broussard, S.R., Johnson, R.W., Freund, G.G., Dantzer, R., Kelley, K.W., 2001. Interleukin-10 in the brain. *Crit. Rev. Immunol.* 21, 427–449.
- Thiblin, I., Finn, A., Ross, S.B., Stenfors, C., 1999. Increased dopaminergic and 5-hydroxytryptaminergic activities in male rat brain following long-term treatment with anabolic androgenic steroids. *Br. J. Pharmacol.* 126, 1301–1306.
- Thiruchelvam, M., McCormack, A., Richfield, E.K., Baggs, R.B., Tank, A.W., 2003. Age-related irreversible progressive nigrostriatal dopaminergic neurotoxicity in the paraquat and maneb model of the Parkinson's disease phenotype. *Eur. J. Neurosci.* 18, 589–600.
- Tomas-Camardiel, M., Rite, I., Herrera, A.J., De Pablos, R.M., Cano, J., Machado, A., Venero, J.L., 2004. Minocycline reduces the lipopolysaccharide-induced inflammatory reaction, peroxynitrite-mediated nitration of proteins, disruption of the blood–brain barrier, and damage in the nigral dopaminergic system. *Neurobiol. Dis.* 16, 190–201.
- Vu, T.Q., Ling, Z.D., Ma, S.Y., Robie, H.C., Tong, C.W., Chen, E.Y., Lipton, J.W., Carvey, P.M., 2000. Pramipexole attenuates the dopaminergic cell loss induced by intraventricular 6-hydroxydopamine. *J. Neural Transm.* 107, 159–176.
- Yurek, D.M., Hipkens, S.B., Hebert, M.A., Gash, D.M., Gerhardt, G.A., 1998. Age-related decline in striatal dopamine release and motoric function in brown Norway/Fischer 344 hybrid rats. *Brain Res.* 791, 246–256.
- Zigmond, M.J., Hastings, T.G., Perez, R.G., 2002. Increased dopamine turnover after partial loss of dopaminergic neurons: compensation or toxicity? *Parkinsonism Relat. Disord.* 8, 389–393.

REVIEW

Progressive Dopamine Neuron Loss in Parkinson's Disease: The Multiple Hit Hypothesis

Paul M. Carvey,*† Ashok Punati,* and Mary B. Newman*†

*Department of Pharmacology, Rush University Medical Center, Chicago, IL, USA

†Department of Neuroscience Program, Rush University Medical Center, Chicago, IL, USA

Animal models have been an essential tool for researchers and clinicians in their efforts to study and treat Parkinson's disease (PD). Thus, the various ways 6-hydroxydopamine is employed, the use of MPTP in rodents and nonhuman primates, the prenatal exposure to bacterial endotoxin, the postnatal exposure to environmental toxins such as paraquat and rotenone, the assessment of dopamine (DA) neurons in genetic knockout mouse, and even the behavioral analysis of fruit flies and worms have added significantly to our knowledge base of PD—or have they? Are these animal models manifesting a true model of PD? Have the 7786 published studies (to date) on PD with animal models led to a clearer understanding of its etiology, treatment, or progression? In this review we critically assess this question. We begin with a succinct history of the major contributions, which have led to the current animal models of PD. We then evaluate the primary issue of the progressive loss of DA neurons, which, except for a few studies, has not been addressed in animal models of PD, even though this is the major pathological characteristic of the disease. Lastly, we discuss the possibility that more than one risk factor for PD may be necessary to develop an animal model that shows synergy—the progressive loss of DA neurons. Thus, the multiple hit hypothesis of PD—that is, the effect of more than one risk factor—may be the start of new era in animal models of PD that is one step closer to mimicking the pathology of PD in humans.

Key words: Parkinson's disease Dopamine neurons Progression Multiple hit hypothesis

PARKINSON'S DISEASE

James Parkinson first systematically described the symptoms of Parkinson's disease (PD) in the early 1800s, which he labeled the “shaking palsy.” The cardinal features of PD are tremor, rigidity, brady-/akinesia, and postural instability. Approximately 40,000 people in the US are diagnosed with PD every day, and over 1 million Americans have this disease. The daily cost is estimated at \$66 million, including direct and indirect costs such as the inability to work and medical/long-term care (75). PD is the second most prevalent neurodegenerative disease next to Alzheimer's disease. No cure currently exists.

The symptoms of PD do not develop until there is an estimated 70–80% reduction in the dopamine (DA) content of the caudate and putamen (striatum) associated

with an estimated 50–60% loss of DA neurons in the substantia nigra pars compacta (SNpc) (2,26,81). Idiopathic PD generally develops after the age of 60. However, patients younger than 40 years of age have been identified, and many have been shown to have one of several genetic mutations, suggesting that early onset PD may be familial (18,41,69,88). PD is a progressive neurodegenerative disease. When first diagnosed, most patients exhibit mild unilateral symptoms that inexorably progress to bilateral debilitating signs and symptoms that require full-time nursing care in late-stage disease. To date there is no proven strategy to stop or slow the progression of PD. However, significant advancements in alleviating the symptoms of PD using drug therapy and surgical procedures have evolved. The most widely used treatment is levodopa, a DA precursor that is transported across the blood–brain barrier (BBB). Although

Received February 7, 2006; final acceptance February 13, 2006.

Address correspondence to Paul M. Carvey, Ph.D., Chairman, Department of Pharmacology, Rush University Medical Center, Cohn Research Building, Suite 406, 1735 W. Harrison Street, Chicago, IL 60612, USA. Tel: 312-563-2563; Fax: 312-563-3552; E-mail: pcarvey@rush.edu

levodopa markedly improves symptoms in most PD patients, it is clearly not a cure and its effectiveness diminishes over time (36,37).

The transplantation of human embryonic ventral mesencephalic (VM) tissue has shown encouraging results in some patients with PD (38,44,74). However, there are limitations to the use of fetal donor tissue (43) along with a loss of benefits following withdrawal from immunosuppressive therapy, and some patients have experienced graft-induced dyskinesias [for review see (71)].

Studies employing animal models as well as patient studies are now indicating that a complex set of factors occurring over long periods likely contribute to PD. Pathogenesis of PD is accompanied by changes in multiple neuronal systems and immune responses against a background of genetic predispositions and innate characteristics that interact with environmental toxins. Animal models have helped to establish many of the hallmark characteristics of PD (Table 1), and some of the models exhibit multiple characteristics of the human disease (Table 2). However, it is fair to say that very few models have looked at more than one of these characteristics, focusing rather on the DA system alone. This dopaminocentric perspective restricts our perspective on PD causation and implies that only DA is involved in the pathogenesis of PD. Moreover, many studies focus on the

acute loss of DA neurons produced by DA neurotoxins. Do we really think that constipation or the degeneration in the locus coeruleus (LC) is solely a consequence of DA neuron loss? This focus on acute DA neuron loss is based on the misguided notion that understanding acute DA neuron loss will help us to treat PD patients and understand their disease. When patients arrive in the clinic, they already have significant DA neuron loss. They seek therapies that will slow the progression and that will inexorably condemn them to late-stage disease. Yet very few studies have ever addressed the issue of progression. In this review, we will provide a brief history of PD animal models from the perspective of disease progression. We hope to effectively argue that animal models need to begin to examine the mechanisms underlying progressive DA neuron loss, and that progression most likely occurs following exposure to multiple risk factors including environmental toxins, genetic alterations, and aging, as codified under the multiple hit hypothesis of PD.

ANIMAL MODELS OF PD

A half a century after James Parkinson's essay, the prominent French neurologist Jean Martin Charcot (1865) elaborated on Parkinson's clinical report and named the disease after James Parkinson (17). Using the clinico-anatomic method, Charcot and others were able to distinguish PD from multiple sclerosis and other neurological disorders (40). Even during the 19th century, animals were considered a possible means to study PD. In Charcot's writings, he discusses a Germanic group headed by Henie and Volkman who reported on the tremorigenic properties of nicotine in the frog (17), which represents the first animal studies we were able to identify concerning PD. Indeed, very few studies were performed on animals for several decades, despite the appreciation of the prevalence of the disease.

Between Charcot's naming the disease and the discovery of reserpine, we were only able to identify a few studies on PD, most of which used neurosurgical ablation. Typical of those studies was a stereotaxic ablation, using the newly developed Horsley-Clark apparatus, to induce electrolytic lesions in the mammillary bodies and the third nerve of cats performed by Ranson and Ingram in 1932, which produced a cataleptic-like rigidity (82). One of the first animal models of PD was most likely found in the 1930s when the Raowolfian alkaloid, reserpine, now known to be a vesicular monoamine transporter inhibitor, was shown to induce PD-like symptoms. Kline in 1954 probably published the first report on reserpine in which his interest in this drug came after reading an article in the *New York Times* on an Indian physician use of a herbal root to treat mental illness (50). Reserpine induced a parkinsonism-like syndrome in some

Table 1. Pathological Signs and Symptoms Seen in Parkinson's Disease

-
1. Progressive degeneration of DA neurons of the SNpc
 2. Formation of fibrillar cytoplasmic inclusions—Lewy bodies
 - a. with ubiquitin
 - b. with alpha'synuclein aggregates
 3. Reduced striatal DA with increased DA activity (HVA/DA)
 - a. reductions in brain serotonin
 4. Neuroinflammation
 - a. activated microglia
 - b. possible astrocytosis
 - c. increased proinflammatory cytokines (TNF- α and IL-1 β)
 5. Oxidative stress
 - a. formation or accumulation of numerous reactive oxygen species (ROS)
 - b. presence of oxidized proteins
 - c. presence of oxidized lipids
 6. Behavioral deficits
 - a. motor deficits
 - b. cognitive disorders
 7. Degenerative changes in other brain areas
 - a. locus ceruleus (LC)
 - b. dorsal motor nucleus of the vagus
 - c. reductions of DA in several cortical areas
 8. Numerous peripheral problems
 - a. constipation
 - b. blood pressure fluctuations
-

Table 2. Comparison of Human PD Characteristics With Animal Models

Characteristics	Animal Models				
	6-OHDA	MPTP	Herbicides	Prenatal LPS	Genetic Models
Progression	no	no	no	some	yes
Inclusions Lewy bodies	no	no	yes (rotenone)	yes	yes
Striatal DA changes	yes	yes	yes	yes	limited
Neuroinflammation	yes	yes	yes	yes	yes
Free radicals	yes	yes	yes	yes	yes
Behavioral changes	limited	yes	yes	limited	limited
Loss in other areas of brain	LC	not evaluated	not evaluated	LC, serotonin	not evaluated
Peripheral characteristics	not evaluated	not evaluated	not evaluated	not evaluated	not evaluated

patients as well as depression. Rats injected with the drug showed reduced locomotion, hunched posture, tremors, and rigidity, after which reserpine quickly became a model for PD. Thus, reserpine not only laid the foundation for eventual studies into the cause of depression, but for PD as well.

In 1953 Delay and Deniker introduced the drug chlorpromazine (ostensibly an antihistamine) and thought it would be helpful in schizophrenia due to its calming effect on animals and its ability to attenuate amphetamine's psychoactive effects (28). At higher doses, it produced neuroleptosis with rigidity (cogwheeling) and paucity of movement (hypokinesia). This Parkinson-like syndrome is similar to encephalitis lethargica and today is broadly taught as drug-induced parkinsonism. In attempting to identify the cause of these symptoms, animals were used to compare the effects of reserpine and chlorpromazine (27). However, lacking a clear understanding of DA and its role in the brain precluded any useful study. Even though in 1938 the enzyme, DOPA decarboxylase, in the mammalian tissue was identified by Holtz and shown to be responsible for converting levodopa to DA (42), it was not until 1957 that Montagu discovered DA in the brain (66). In the same year in Sweden, Carlsson determined that the parkinsonism-like effects of reserpine could be reversed by injections of levodopa and that DA levels in the brain were reduced by reserpine and restored to normal by levodopa (14). Anticholinergics (atropine and scopolamine), among the few anti-PD drugs then in existence, were assessed in these models with little or varied success. However, in 1960 Ehringer and Hornykiewicz demonstrated DA deficiency in the brains of PD patients (29) and the next year Birkmayer and Hornykiewicz delivered levodopa intravenously to treat PD (9). Then in 1969, Cotzias established a rational treatment strategy for PD patients using levodopa (24), and the FDA approved it for use in patients in 1970. The link between PD and DA and levodopa's ability to reverse the motor effects of reserpine

thus solidified the notion that animal models could be useful in studying PD.

THE 6-HYDROXYDOPAMINE MODEL OF PD

The 6-hydroxydopamine (6-OHDA) model truly formalized the use of animals in PD research. For almost 20 years, it was the most commonly used PD model and is still used widely today. There are 6404 citations on the use of 6-OHDA in general and 1159 citations using key words 6-OHDA and PD in animals according to PubMed. It is the second most cited animal model after 1-methyl-4-phenyl-1,2,3,6 tetrahydropyridine (MPTP). 6-OHDA as a DA neurotoxin is a hydroxylated analogue of the endogenous neurotransmitter dopamine that produces DA neuron degeneration both in vitro and in vivo [for review see (10)]. Senoh and colleagues (1959) were the first to report its isolation (85,86), and Porter and colleagues (1963) were the first to use it in animals when they showed that it depleted norepinephrine (NE) in the heart (78). Its first use was thus as a NE neurotoxin. In 1968, Ungerstedt demonstrated that unilateral depletion of DA occurred after unilateral 6-OHDA injection into the medial forebrain bundle (95). This not only allowed the animal to serve as its own control by comparing contra- and ipsilateral sides, but laid the groundwork for the widely used rotational model where direct-acting DA agonists produced contralateral rotation following the development of denervation hypersensitivity and indirect-acting agonists produced ipsilateral rotation caused by increasing contralateral release of DA.

In 1970, Iversen demonstrated that 6-OHDA entered catecholamine neurons through DA reuptake sites (45, 46), and since then it has been shown to induce oxidant stress and/or mitochondrial dysfunction as a complex I inhibitor. 6-OHDA has been found in both the human and rat brain, suggesting it may form endogenously (25). Although it was first used by Porter and colleagues as a systemic toxin (78), it only enters the brain in very

young animals lacking a BBB. In older animals, systemic delivery produces a peripheral sympathectomy and adult animals treated with 6-OHDA may be useful in providing insight into the peripheral characteristics of PD, including constipation and regulation of blood pressure.

Since its discovery as a DA neurotoxin, the experimental protocol to create PD in the rat brain has expanded to include injection of 6-OHDA unilaterally into the striatum and substantia nigra. 6-OHDA can also be delivered intracerebroventricularly (ICV) to produce a bilateral loss of catecholamine cells, as first shown by Uretsky and Iversen (96). ICV injection leads to degeneration of DA and NE cells. Because of its ability to produce both DA and NE depletion following ICV injection, desipramine, a NE reuptake inhibitor, is generally given to protect NE cells. However, in PD patients, the loss of NE neurons in the LC may be partially responsible for both the onset and progression of damage to DA neurons (5). Thus, concurrent LC lesions in 6-OHDA-injected animals worsen the 6-OHDA-induced nigrostriatal DA toxicity (34,61). This suggests that desipramine should not be used to protect the NE neurons in the 6-OHDA model of PD because PD exhibits both SN and LC degeneration.

Numerous characteristics of the PD brain are produced by 6-OHDA (Table 2). Thus, it produces DA neuron loss and all of the inflammatory characteristics normally seen in PD. It does produce a behavioral syndrome that can be used to assess DA function, but actual PD-like symptoms are not seen. No one we are aware of has evaluated the peripheral characteristics of this model in animals to determine whether they exhibit alterations in blood pressure or exhibit constipation. Furthermore, the animals do not exhibit inclusion bodies nor do they exhibit a progressive DA neuron loss following treatment.

THE MPTP MODEL OF PD

MPTP is the most used neurotoxin in animal models of PD. There are currently 1526 citations exhibiting the key words MPTP and PD in animals at this writing according to PubMed. MPTP is one of the few neurotoxins discovered in humans first. The initial reported instance of human exposure to MPTP was in 1976 when a chemistry student self-administered a meperidine analogue he was trying to synthesize. He apparently rushed the synthesis, generating a batch contaminated with MPTP (47). Despite the magnitude of this discovery, it did not generate considerable attention until the team led by Bill Langston described a group of patients in Northern California where seven heroin users were identified in emergency rooms with signs and symptoms remarkably similar to PD (51,52). The events surrounding this discovery, revealing how science met forensics, was detailed in the

book *The Case of the Frozen Addict* (53). It is assumed that synthesis errors similar to those made in 1976 were responsible for a batch of synthetic meperidine contaminated with MPTP that got out onto the streets, affecting a large cohort of patients.

MPTP is not the actual toxin, but rather a protoxin that is catabolized to 1-methyl-4-phenyl-2,3-dihydropyridinium (MPDP) within nondopaminergic cells by MAO-B, after which it is oxidized to form 1-methyl-4-phenyl-pyridinium (MPP⁺) (73), which, like 6-OHDA, is an excellent substrate for the DA transporter (80). Once inside the cell it accumulates in mitochondria where it inhibits complex I.

The use of MPTP to induce animal models of PD gained wide popularity because it was known to produce a syndrome in humans that resembled PD and because of its ease of use (35,51,79,80). MPTP causes an acute loss of DA neurons within the first 3 days after systemic administration. After the initial reduction in DA cells through 10 days, no further loss is seen unless exposure is continued, and in some cases there is a recovery of initially lost DA neurons (1,39,61,83,94). Animals treated with MPTP exhibit many of the characteristics of PD including similar behavioral abnormalities (Table 2). However, MPTP animals have not been evaluated for peripheral characteristics, they do not show formation of inclusion bodies, and, most importantly, they do not exhibit progressive loss.

PESTICIDES AND HERBICIDES AND PD ANIMAL MODELS

Exposure to pesticides and herbicides has long been suggested as a risk factor for PD. The initial discovery by Langston of MPTP (51–53) laid the groundwork for what eventually became known as the environmental hypothesis of PD. This hypothesis has been reinforced by numerous subsequent reports suggesting that environmental agents produce DA neuron loss in animals. Thus, rotenone (6,87), paraquat (3,20,57,58), the fungicide maneb (90,91), and dieldrin (48,84) have all been shown to produce DA neuron loss in animals. Some of these toxins have even been associated with PD in patients (32,63) while Corrigan and colleagues detected levels of dieldrin in the brains of PD patients (21).

The major attraction of these models is their potential as a naturally occurring animal model of PD. Because humans are exposed to them through the environment, it is easy to assume that they could contribute to PD. However, only rotenone is found naturally while the others are synthetic. These studies can be criticized because one is hard-pressed to determine how synthetic molecules could have contributed to PD development prior to the 20th century. It is important to recognize, however, that numerous substituted pyridinium compounds

with structures similar to MPTP and paraquat are found in nature (64,65).

These DA toxins produce many of the characteristics of PD (Table 2). Rotenone in particular was the first toxin to produce a Lewy-like body. In addition, DA neuron loss, the biochemical characteristics in the striatum, along with inflammation and locomotor alterations have been well studied in many of these models. However, the involvement of other areas of the brain and peripheral changes have not been assessed and, again, progressive DA neuron loss has not been seen.

THE PRENATAL LPS MODEL

In 2001, we inadvertently stumbled onto a new animal model of PD. We discovered that exposing gravid female rats to the bacteriotoxin lipopolysaccharide (LPS) during a critical window of vulnerability led to the birth of her offspring with fewer than normal DA neurons (55). These animals exhibit numerous characteristics of PD including all the inflammatory measures, behavioral changes, and inclusion bodies (15,54,56). These animals also show alterations in striatal serotonin (unpublished observation) and loss of cell bodies in the LC (72). We have not yet evaluated peripheral changes in these animals, and life-long studies just completed show only minor progressive losses of DA neurons (unpublished observation). One of the appealing elements of this model is the fact that the low doses of LPS used to generate the model are similar to those seen in pregnant women with bacterial vaginosis (15). Thus, individuals born to a mother with bacterial vaginosis during the first trimester would be naturally exposed to LPS, raising the possibility that this risk factor occurs naturally.

THE GENETIC MODELS OF PD

Although numerous reports of PD running in families led to linkage studies and a search for a genetic basis of so-called familial PD, it was the report by Polymeropoulos and colleagues that generated a dramatic change in the animal model of PD literature (77). Their discovery that a mutation in the gene encoding the protein alpha-synuclein led to a veritable explosion of studies looking for other familial genetic defects and their expression in animal models (67). Because alpha-synuclein was present in Lewy bodies, and no animal model up to that time had shown the formation of inclusion bodies, genetic alterations raised the specter that the widespread belief that environmental toxins caused PD were misguided. As important as this observation was, it soon became clear that the vast majority of PD patients did not exhibit these gene defects, forcing the Parkinson community to again look for alternative hypotheses. These findings did lead many investigators to study gene mutations similar to those in patients in animals. To

date, however, only overexpression of human alpha-synuclein or its mutated form has produced any type of significant DA neuron loss (49,93). Regardless, studies in *Drosophila* (30) and *Caenorhabditis elegans* (70) have contributed significantly to our understanding of the role genes play in PD. In particular, the original study by Polymeropoulos and colleagues and those that followed have pointed to a role for abnormal proteosomal processing in familial PD (89), and the possibility that protein toxicity underlies the pathogenesis of all PD should be considered.

PROGRESSION IN PD

As of this writing, there are 7786 published studies that use animals to study PD (Fig. 1) and these studies focus almost exclusively on inducing or preventing DA neuron loss during, or immediately following, an acute toxin exposure (Fig. 2). As originally conceptualized by Donald Calne and Bill Langston, the so-called Calne-Langston hypothesis asserts that an environmental toxin kills off a percentage of DA neurons and then the normal age-related decline of DA neurons eventually brings the patient to the symptom threshold (12). Today we know that the pattern of DA neuron loss produced by aging is primarily homogeneous throughout the mid-brain and inconsistent with the loss of DA neurons in the lateral SN and its ventral tier that characterizes the PD brain (31). This brings into question the possibility that normal age-related DA neuron loss, by itself, could lead to PD, although it is possible that a toxin that produces this pattern of loss together with normal aging could create such a pattern. In addition, it is now presumed that the rate of DA neuron loss in PD patients is not linear as depicted by Calne and Langston, but rather exponential (Fig. 3) with the start of the cell loss estimated at approximately 7 years prior to symptom expression (68). Thus, although 6-OHDA, MPTP, rotenone, paraquat, and the endotoxin LPS produce PD-like characteristics, these toxins fail to produce progressive DA neuron loss. So even though these animal models have lent considerable insight into the causes of DA neuron death, they have done little to help us understand the progressive DA neuron loss that characterizes PD, which, in the final analysis, is largely responsible for the debilitating aspects of this neurodegenerative disease. This not only questions the role of inflammation in PD, but also fails to support the widely held assertion that PD is, in part, a consequence of environmental toxins.

There have been but a few attempts to produce progression in models of PD. Bezard and colleagues administered MPTP chronically (0.2 mg/kg, IV) for approximately 15 days to cynomolgus monkeys (8). These animals reached full parkinsonism at day 22, and when challenged with levodopa, motor abnormalities were al-

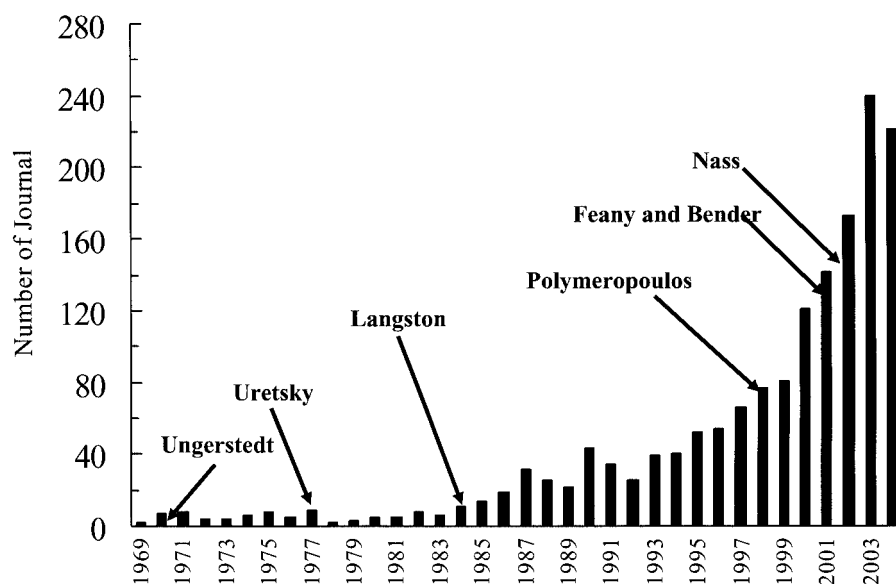


Figure 1. A time graph of animal studies (7786 citations). The major contributions leading to the animal models we use today are written within the article; here the contributors are listed chronologically. The number of published reports, across time, using animals to study PD is depicted in the graph.

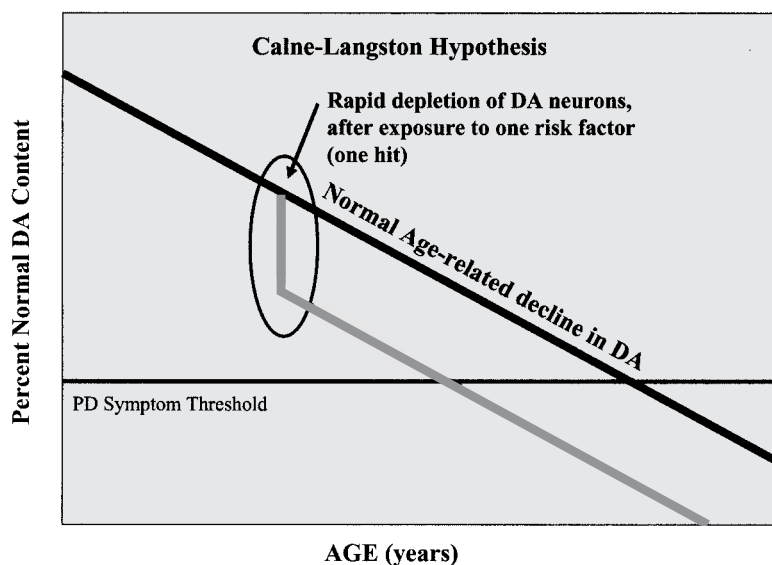


Figure 2. Illustration of the Calne-Langston hypothesis. The diagram depicts the most commonly thought explanation for idiopathic PD. During human life span there is a normal gradual decrease in DA neurons (solid black line). However, in PD after the exposure to one risk factor an acute rapid decrease followed by the progressive loss of DA neurons throughout the remainder of life is seen (solid gray line). This loss continues, mostly goes unnoticed, until the DA cells loss reaches the threshold where PD symptoms are realized. The majority of research, thus far, on PD focuses on the period of rapid loss for DA neurons (oval black circle), and the current animal models using one risk factor (one hit) mimic this scenario.

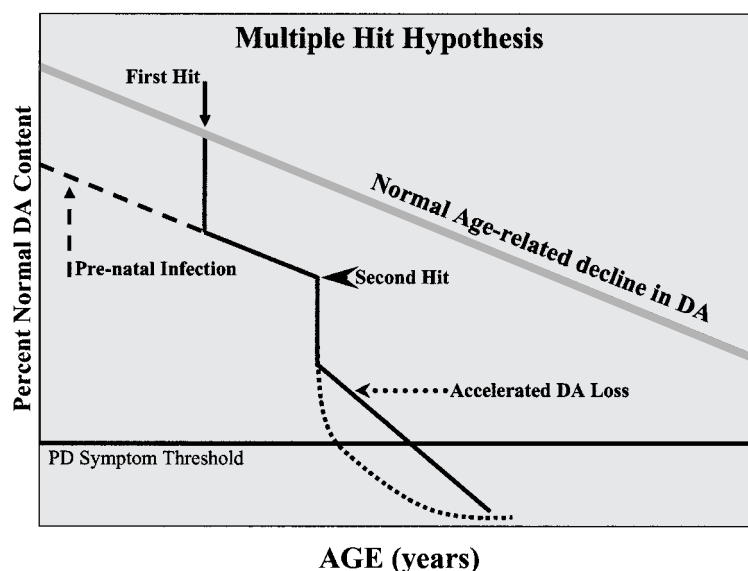


Figure 3. Illustration of the “multiple hit hypothesis.” In this model, we suggest that more than multiple risk factors (multiple hits) may be necessary to create the progressive loss of DA neurons. Again, there is the normal DA neuron loss that occurs during aging (solid gray line). However, in this model the first hit (a risk factor) may come before birth. Such would be the case for either a prenatal infection (dashed black arrow) or a genetic mutation. When the first hit occurs before birth there is more than likely a deficiency in the dopaminergic system upon birth or a yet identified deficiency, thus creating an underlying susceptibility to a second hit or risk factor (e.g., we have shown that rats prenatally exposed to LPS are born with few DA neurons and an altered innate immune system, making them more susceptible to a second hit). Alternatively, the first hit may occur later in life (solid black arrow) in which there is a substantial decrease in DA neurons that compromises the dopaminergic system, but does not reach threshold. Therefore, the second hit (black arrowhead) results in another acute loss of DA neurons followed by the progressive loss. The continuation of the progressive loss may be a linear loss (solid black line), as suggested by Calne and Langston, or exponential in which a greater number of DA neurons (dotted curve) are lost before reaching threshold.

leviated. No recovery was noted throughout the study. Although there was a substantial loss of DA neurons (90% depletion) in the SNc, this measure was only obtained at the end of the experiment (2 months after the first injection). The authors suggested progression occurred in this model because of the gradual onset of motor deficits during the presymptomatic period. This could be true for onset of behavioral deficits, but for progression in the loss of DA neurons, cell depletion would need to be determined at several times after treatment initiation.

Bezard et al. investigated progressive DA neuron loss in mice given a chronic low dose of MPTP in which they delivered 4 mg/kg, IP, of MPTP for 20 days and assessed the brains at various times. The authors reported two phases of DA cell loss. First, there was a significant, rapid reduction of DA neurons that started on day 2 and continued through the 14th injection, while a second phase continued from day 15 to 20 (the last day of the injection), stabilizing thereafter (7). The main

problem in this study was the continued presence of the DA neurotoxin. Unless we assume that the patient is being continuously exposed to the toxin, it was clear that progressive DA neuron loss did not continue after completion of the exposure. Another study by Brownell et al. also looked at low-dose, intermittent (every other week) chronic MPTP exposure in monkeys. These animals exhibited progressive loss of DA signal in the striatum through 18 months of continued treatment. However, these animals continued to exhibit further losses for 6 months following discontinuation of MPTP treatment and were stable thereafter (11). This suggests that long-term continuous exposure can lead to some progression after discontinuation of treatment. However, this model does not reveal the exponential DA neuron loss that seems to occur in PD patients.

One additional study used a combination of MPTP and probenecid, a drug used to remove excess uric acid, in which the neurotoxicity was enhanced by reducing MPTP and its metabolites from clearing the kidney and

brain (76). MPTP (25 mg/kg, SC) and probenecid (250 mg/kg, IP) were coadministered twice a week for 5 weeks to mice. Animals were assessed at various times after the last injection up to 24 weeks. Initially there was a loss of DA neurons; however, by 6 months there was partial recovery of DA neurons. In PD progressive loss of DA neurons continues until the end of life; therefore this model does not reflect true progression.

Taken together, the studies by Bezard and Brownell imply that continuous exposure may produce a form of progressive DA neuron loss. However, the implication is either continuous or long-term exposure to the toxin. Although this is possible given that well water contaminated with insecticides and herbicides is implicated in PD (33), it seems unlikely in most cases of idiopathic PD. Alternatively, acute or short-term exposure to a DA neurotoxin could kill DA neurons, leading to the formation of endogenous toxins such as salsolinol (59). However, this also seems unlikely because the traditional toxins MPTP or 6-OHDA, alone, which would also be expected to produce substituted quinines, do not produce progressive loss. Acute exposure to epoxomicin, or its synthetic analog, is touted as producing progressive DA neuron loss following discontinuation of exposure. However, the animals were only studied for 6 weeks (62), which is not nearly enough time to determine progression, and there have been significant problems with the reproducibility of the study (60). Indeed, studies of acute toxin exposure reveal partial recovery of the initial DA cell loss (1,39,61,83,94). Recovery from cell loss suggests that acute toxin exposure suppressed the DA phenotype (usually assessed by immunocytochemically staining for tyrosine hydroxylase) followed by reinstatement of function through several unknown compensatory processes. Thus, data demonstrating progressive DA neuron loss following a single toxin exposure are rare in the literature. This raises the question: are investigators simply not studying the phenomenon or does exposure to a neurotoxin not produce progressive DA neuron loss?

THE MULTIPLE HIT HYPOTHESIS OF PD

The sequential or simultaneous interaction of more than one PD risk factor (more than one hit) is embodied in the multiple hit hypothesis of PD (Fig. 3). This hypothesis argues that multiple risk factors, including genetic predisposition, toxin exposure, aging, and potentially other unknown factors, interact to produce PD. We have known for more than two decades that the nigrostriatal DA system possesses a host of compensatory mechanisms that maintain normal motor function despite significant losses of DA neurons in the SN (13). These same compensatory mechanisms likely overcome the effects of a single administered toxin or genetic de-

fect in animals. Conceptually, if a DA neuron were insulted by more than one toxin acting through different mechanisms, the range of possible compensatory mechanisms would be reduced, potentially leading to a progressive DA cell loss. Cory-Slechta suggested that when there are multiple risk factors, the system can no longer "homeostatically reregulate itself," thus leading to damage (22,23). We have been testing the concept in the prenatal LPS animal model.

In two similar studies we challenged prenatal LPS animals with 6OHDA (56) or rotenone (54). Prenatal LPS or saline was delivered at embryonic day 10.5. 6-OHDA (150 µg, ICV) or vehicle was administered at 2 months and rotenone or vehicle was administered (intracarotid) at 15 months. In both studies, the rats were sacrificed 2 months following the adult toxin exposure. In the 6-OHDA study, a clear additive loss of DA neurons was seen. However, in the rotenone study, interaction of prenatal LPS and postnatal rotenone produce a highly significant synergistic DA cell loss. This finding is reminiscent of the "silent toxicity" described by Thiruchelvam et al., where they observed a synergistic DA cell loss in response to paraquat after 6 months in animals that had been exposed to maneb perinatally (92). The prenatal LPS study with rotenone and the study with paraquat and maneb suggest that compensatory processes are more compromised following multiple exposures to DA neurotoxins.

We have also recently shown that prenatal LPS animals exposed at 7 months to 14 days of supranigral LPS infusion (20 EU/h, total delivered dose estimated at 6720 EU), exhibited progressive DA neuron loss (16). LPS infusion killed an equivalent number of DA neurons on the ipsilateral side of the SN in both the LPS and saline prenatal groups at day 14. However, the prenatal LPS animals infused with LPS continued to exhibit further DA neuron loss over the 84-day course of the experiment, whereas the prenatal saline and LPS-infused animals did not. These data suggests that multiple hits with the same toxin can produce progressive DA neuron loss.

In a second study, we challenged controls and animals treated with LPS prenatally with 6-OHDA at 2 months and evaluated one half of them at 4 months and the other half at 17 months (16). The control animals (SAL/SAL) showed slight age-related reductions in DA cell counts over their lives. 6-OHDA-challenged saline animals exhibited a 29% DA neuron loss at 4 months and only exhibited a 2% DA neuron loss in the next 13 months. In contrast, prenatal LPS animals challenged with 6-OHDA at 2 months exhibited a 20% DA neuron loss at 4 months with significant progression of DA cell loss over the next 13 months. Thus, the LPS/6-OHDA animals sacrificed at 17 months had DA neuron counts

that were only 44% of normal, revealing an additional 12% loss from baseline at 4 months. These data suggest that multiple hits with different toxins (i.e., prenatal LPS and postnatal 6-OHDA) are associated with progression. These progressive losses in the two models may have been more pronounced had we extended the protocols until the animals were older, given that compensatory processes are markedly attenuated in aged animals (19).

In another series of studies, Cory-Slechta and colleagues showed results similar to ours using different combinations of DA toxins. Mice were administered 10 mg/kg of the herbicide paraquat, 30 mg/kg of the fungicide maneb, or both twice a week for 3 weeks and DA neurons were assessed at 6 weeks and 5 and 18 months. The combination of paraquat and maneb produced greater DA cell loss across time than their age-matched controls, and more than the paraquat-alone-treated mice. The paraquat- and maneb-treated groups showed progressive DA neuron loss (91). In a second study, maneb was administered during gestational days 10–17 at 1 mg/kg, SC, and pups were then challenged at 7–8 weeks of age with 5 mg/kg of paraquat or 30 mg/kg maneb daily for 8 days. The animals were assessed after an additional 7 days (week 9). Only the male mice prenatally treated with maneb and postnatally treated with paraquat showed significant reductions in locomotor activity at 9 weeks as well as reduction in levels of DA and DOPAC. Moreover only the male mice showed significant loss of DA neurons in the SN (4). In a final study, the results showed mice overexpressing the double-mutant form of human alpha-synuclein exhibited synergistic DA neuron losses following exposure to paraquat and maneb. They concluded that overexpression of human alpha-synuclein had adverse effects on DA neurons and that due to the interaction of the human alpha-synuclein mutations, ageing, and exposure to pesticides combined to produce greater cell loss than any of the individual risk factors alone (93). These data suggest that combining a genetic risk factor and environmental toxin can also combine to produce at least synergistic and perhaps progressive DA neuron loss consistent with the multiple hit hypothesis.

SUMMARY

Despite the significant contribution animal models have made to our understanding of PD, we still have a long way to go. Research performed, to date, has been highly dopamino-centric, focusing almost exclusively on acute DA neuron losses and the mechanisms surrounding their death. Although these studies have aided the development of new drugs, therapies, and treatments, they have not focused on progressive DA neuron loss. Therefore, from the patients' perspective, we know very little if anything about the mechanisms that produce this

progressive loss, thus obviating our ability to develop therapies that slow or stop progression. Recent studies suggest that our focus on only one risk factor at a time is misguided. Given this, and aside from the studies of Brownell where a single toxin was administered numerous times, no single hit study we are aware of has produced progression. In contrast, the synergistic losses seen following multiple hits and our preliminary indication that multiple hits can produce progression argues that multiple hits are necessary to produce progressive loss of DA neurons. Understanding the mechanism(s) responsible for these synergistic and progressive losses may provide critical insight into the alteration in the compensatory environment within the nigrostriatal system. Moreover, logic dictates that humans are not just exposed to single risk factor, but rather, combinations of risk factors that occur at various times during their lives. Developing animal models based on multiple hits seems like the next logical step in the evolution of animal models for PD.

ACKNOWLEDGMENTS: *Our studies included in this review were support by NINDS NS045316, NIEHS 012307, USARMRA W81XWH-04-01-0365, and a grant from the Michael J. Fox Foundation. The authors would like to especially thank Dr. Thonar for his translation of the Charcot paper.*

REFERENCES

1. Albanese, A.; Granata, R.; Gregori, B.; Piccardi, M. P.; Colosimo, C.; Tonali, P. Chronic administration of 1-methyl-4-phenyl-1,2,3,6-tetrahydropyridine to monkeys: Behavioural, morphological and biochemical correlates. *Neuroscience* 55:823–832; 1993.
2. Antonini, A.; Moresco, R. M.; Gobbo, C.; De Notaris, R.; Panzacchi, A.; Barone, P.; Bonifati, V.; Pezzoli, G.; Fazio, F. Striatal dopaminergic denervation in early and late onset Parkinson's disease assessed by PET and the tracer [11C]FECIT: Preliminary findings in one patient with autosomal recessive parkinsonism (Park2). *Neurol. Sci.* 23(Suppl. 2):S51–52; 2002.
3. Barbeau, A.; Dallaire, L.; Buu, N. T.; Poirier, J.; Rucinska, E. Comparative behavioral, biochemical and pigmentary effects of MPTP, MPP+ and paraquat in *Rana pipiens*. *Life Sci.* 37:1529–1538; 1985.
4. Barlow, B. K.; Richfield, E. K.; Cory-Slechta, D. A.; Thiruchelvam, M. A fetal risk factor for Parkinson's disease. *Dev. Neurosci.* 26:11–23; 2004.
5. Bertrand, E.; Lechowicz, W.; Szpak, G. M.; Dymecki, J. Qualitative and quantitative analysis of locus coeruleus neurons in Parkinson's disease. *Folia Neuropathol.* 35:80–86; 1997.
6. Betarbet, R.; Sherer, T. B.; MacKenzie, G.; Garcia-Osuna, M.; Panov, A. V.; Greenamyre, J. T. Chronic systemic pesticide exposure reproduces features of Parkinson's disease. *Nat. Neurosci.* 3:1301–1306; 2000.
7. Bezard, E.; Dovero, S.; Bioulac, B.; Gross, C. E. Kinetics of nigral degeneration in a chronic model of MPTP-treated mice. *Neurosci. Lett.* 234:47–50; 1997.
8. Bezard, E.; Imbert, C.; Deloire, X.; Bioulac, B.; Gross, C. E. A chronic MPTP model reproducing the slow evolu-

- tion of Parkinson's disease: Evolution of motor symptoms in the monkey. *Brain Res.* 766:107–112; 1997.
9. Birkmayer, W.; Hornykiewicz, O. Der 1-3,4-dioxyphenylalanin (dopa)-effekt bei der parkinson-akinese. *Wien. Klin. Wochenschr.* 73:787–788; 1961.
 10. Blum, D.; Torch, S.; Lambeng, N.; Nissou, M.; Benabid, A. L.; Sadoul, R.; Verna, J. M. Molecular pathways involved in the neurotoxicity of 6-OHDA, dopamine and MPTP: Contribution to the apoptotic theory in Parkinson's disease. *Prog. Neurobiol.* 65:135–172; 2001.
 11. Brownell, A. L.; Jenkins, B. G.; Elmaleh, D. R.; Deacon, T. W.; Speelman, R. D.; Isacson, O. Combined PET/MRS brain studies show dynamic and long-term physiological changes in a primate model of Parkinson disease. *Nat. Med.* 4:1308–1312; 1998.
 12. Calne, D. B.; Langston, J. W. Aetiology of Parkinson's disease. *Lancet* 2:1457; 1983.
 13. Calne, D. B.; Zigmond, M. J. Compensatory mechanisms in degenerative neurologic diseases. Insights from parkinsonism. *Arch. Neurol.* 48:361–363; 1991.
 14. Carlsson, A.; Lindqvist, M.; Magnusson, T. 3,4-Dihydroxyphenylalanine and 5-hydroxytryptophan as reserpine antagonists. *Nature* 180:1200; 1957.
 15. Carvey, P. M.; Chang, Q.; Lipton, J. W.; Ling, Z. Prenatal exposure to the bacteriotoxin lipopolysaccharide leads to long-term losses of dopamine neurons in offspring: A potential, new model of Parkinson's disease. *Front. Biosci.* 8:s826–837; 2003.
 16. Carvey, P. M.; Zhu, Y.; Snyder, J. A.; Newman, M. B.; Ling, Z. Progressive loss of dopamine (DA) neurons in the brains of prenatal LPS-exposed rats receiving postnatal supranigral LPS infusion. I. effects on cytokines. *Soc. Neurosci. Abstr.* 663.4; 2005.
 17. Charcot, J. M.; Vulpian, A. Revue clinique de la paralysie agitante: III, Queique mots concernant la physiologiepathologique de la paralysie agitante at du tremblement en general. *Gaz. Hedbomadaire* 9:56–59; 1862.
 18. Clarimon, J.; Johnson, J.; Dogu, O.; Horta, W.; Khan, N.; Lees, A. J.; Hardy, J.; Singleton, A. Defining the ends of Parkin exon 4 deletions in two different families with Parkinson's disease. *Am. J. Med. Genet. B. Neuropsychiatr. Genet.* 133:120–123; 2005.
 19. Collier, T. J.; Dung Ling, Z.; Carvey, P. M.; Fletcher-Turner, A.; Yurek, D. M.; Sladek, Jr., J. R.; Kordower, J. H. Striatal trophic factor activity in aging monkeys with unilateral MPTP-induced parkinsonism. *Exp. Neurol.* 191(Suppl. 1):S60–67; 2005.
 20. Corasaniti, M. T.; Strongoli, M. C.; Rotiroli, D.; Bagetta, G.; Nistico, G. Paraquat: A useful tool for the in vivo study of mechanisms of neuronal cell death. *Pharmacol. Toxicol.* 83:1–7; 1998.
 21. Corrigan, F. M.; Murray, L.; Wyatt, C. L.; Shore, R. F. Diorthosubstituted polychlorinated biphenyls in caudate nucleus in Parkinson's disease. *Exp. Neurol.* 150:339–342; 1998.
 22. Cory-Slechta, D. A.; Thiruchelvam, M.; Barlow, B. K.; Richfield, E. K. Developmental pesticide models of the Parkinson disease phenotype. *Environ. Health Perspect.* 113:1263–1270; 2005.
 23. Cory-Slechta, D. A.; Thiruchelvam, M.; Richfield, E. K.; Barlow, B. K.; Brooks, A. I. Developmental pesticide exposures and the Parkinson's disease phenotype. *Birth Defects Res. A Clin. Mol. Teratol.* 73:136–139; 2005.
 24. Cotzias, G. C.; Papavasiliou, P. S.; Gellene, R. Modification of parkinsonism—chronic treatment with L-dopa. *N. Engl. J. Med.* 280:337–345; 1969.
 25. Curtis, D. R.; Johnston, G. A. Amino acid transmitters in the mammalian central nervous system. *Ergeb. Physiol.* 69:97–188; 1974.
 26. Damier, P.; Hirsch, E. C.; Agid, Y.; Graybiel, A. M. The substantia nigra of the human brain. II. Patterns of loss of dopamine-containing neurons in Parkinson's disease. *Brain* 122(Pt. 8):1437–1448; 1999.
 27. Delay, J.; Deniker, P. Comparison of reserpine and chlorpromazine. *Arch. Psicol. Neurol. Psichiatr.* 17:631–633; 1956.
 28. Delay, J.; Deniker, P. Neuroleptic effects of chlorpromazine in therapeutics of neuropsychiatry. *Int. Rec. Med. Gen. Pract. Clin.* 168:318–326; 1955.
 29. Ehringer, H.; Hornykiewicz, O. Distribution of noradrenaline and dopamine in the human brain and their behavior in diseases of the extrapyramidal system. *Klin. Wochenschr.* 38:1236–1239; 1960.
 30. Feany, M. B.; Bender, W. W. A *Drosophila* model of Parkinson's disease. *Nature* 404:394–398; 2000.
 31. Fearnley, J. M.; Lees, A. J. Ageing and Parkinson's disease: Substantia nigra regional selectivity. *Brain* 114(Pt. 5):2283–2301; 1991.
 32. Ferraz, H. B.; Bertolucci, P. H.; Pereira, J. S.; Lima, J. G.; Andrade, L. A. Chronic exposure to the fungicide maneb may produce symptoms and signs of CNS manganese intoxication. *Neurology* 38:550–553; 1988.
 33. Firestone, J. A.; Smith-Weller, T.; Franklin, G.; Swanson, P.; Longstreth, Jr., W. T.; Checkoway, H. Pesticides and risk of Parkinson disease: A population-based case-control study. *Arch. Neurol.* 62:91–95; 2005.
 34. Fornai, F.; Bassi, L.; Torracca, M. T.; Scalori, V.; Corsini, G. U. Norepinephrine loss exacerbates methamphetamine-induced striatal dopamine depletion in mice. *Eur. J. Pharmacol.* 283:99–102; 1995.
 35. Forno, L. S.; DeLanney, L. E.; Irwin, I.; Langston, J. W. Similarities and differences between MPTP-induced parkinsonism and Parkinson's disease. *Neuropathologic considerations.* *Adv. Neurol.* 60:600–608; 1993.
 36. Freed, C. R.; Breeze, R. E.; Rosenberg, N. L.; Schneck, S. A.; Kriek, E.; Qi, J. X.; Lone, T.; Zhang, Y. B.; Snyder, J. A.; Wells, T. H.; et al. Survival of implanted fetal dopamine cells and neurologic improvement 12 to 46 months after transplantation for Parkinson's disease. *N. Engl. J. Med.* 327:1549–1555; 1992.
 37. Freed, C. R.; Leehey, M. A.; Zawada, M.; Bjugstad, K.; Thompson, L.; Breeze, R. E. Do patients with Parkinson's disease benefit from embryonic dopamine cell transplantation? *J. Neurol.* 250(Suppl. 3):III44–46; 2003.
 38. Hagell, P.; Schrag, A.; Piccini, P.; Jahanshahi, M.; Brown, R.; Rehnckrona, S.; Widner, H.; Brundin, P.; Rothwell, J. C.; Odin, P.; Wenning, G. K.; Morrish, P.; Gustavii, B.; Björklund, A.; Brooks, D. J.; Marsden, C. D.; Quinn, N. P.; Lindvall, O. Sequential bilateral transplantation in Parkinson's disease: Effects of the second graft. *Brain* 122(Pt. 6):1121–1132; 1999.
 39. Hallman, H.; Lange, J.; Olson, L.; Stromberg, I.; Jonsson, G. Neurochemical and histochemical characterization of neurotoxic effects of 1-methyl-4-phenyl-1,2,3,6-tetrahydropyridine on brain catecholamine neurones in the mouse. *J. Neurochem.* 44:117–127; 1985.
 40. Hartemann-Heurtier, A.; Van, G. H.; Grimaldi, A. The Charcot foot. *Lancet* 360:1776–1779; 2002.

41. Hofer, A.; Berg, D.; Asmus, F.; Niwar, M.; Ransmayr, G.; Riemenschneider, M.; Bonelli, S. B.; Steffebauer, M.; Ceballos-Baumann, A.; Haussermann, P.; Behnke, S.; Kruger, R.; Prestel, J.; Sharma, M.; Zimprich, A.; Riess, O.; Gasser, T. The role of alpha-synuclein gene multiplications in early-onset Parkinson's disease and dementia with Lewy bodies. *J. Neural Transm.* 112:1249–1254; 2005.
42. Holtz, P.; Heise, R.; Ludtke, K. Fermentativer Abbau von l-dioxyphenylalanin (dopa) durch Niere. *Naunyn-Schmiedeberg's Arch. Exp. Pathol. Pharmacol.* 191:87–118; 1938.
43. Isacson, O.; Bjorklund, L.; Pernaute, R. S. Parkinson's disease: Interpretations of transplantation study are erroneous. *Nat. Neurosci.* 4:553; 2001.
44. Isacson, O.; Costantini, L.; Schumacher, J. M.; Cicchetti, F.; Chung, S.; Kim, K. Cell implantation therapies for Parkinson's disease using neural stem, transgenic or xenogeneic donor cells. *Parkinsonism Relat. Disord.* 7:205–212; 2001.
45. Iversen, L. L. Inhibition of catecholamine uptake by 6-hydroxydopamine in rat brain. *Eur. J. Pharmacol.* 10:408–410; 1970.
46. Iversen, L. L. Neuronal uptake processes for amines and amino acids. *Adv. Biochem. Psychopharmacol.* 2:109–132; 1970.
47. Jackson-Lewis, V.; Smeyne, R. J. From man to mouse: The MPTP model of Parkinson disease. In: *Animal models of movement disorders*. New York: Elsevier Science; 2005:149–160.
48. Kanthasamy, A. G.; Kitazawa, M.; Kanthasamy, A.; Anantharam, V. Dieldrin-induced neurotoxicity: Relevance to Parkinson's disease pathogenesis. *Neurotoxicology* 26:701–719; 2005.
49. Kirik, D.; Rosenblad, C.; Burger, C.; Lundberg, C.; Johansen, T. E.; Muzyczka, N.; Mandel, R. J.; Björklund, A. Parkinson-like neurodegeneration induced by targeted overexpression of alpha-synuclein in the nigrostriatal system. *J. Neurosci.* 22:2780–2791; 2002.
50. Kline, N. Use of rauwolfia serpentina benth in neuropsychiatric conditions. *Ann. NY Acad. Sci.* 59:107–132; 1954.
51. Langston, J. W. MPTP neurotoxicity: An overview and characterization of phases of toxicity. *Life Sci.* 36:201–206; 1985.
52. Langston, J. W.; Ballard, P.; Tetrud, J. W.; Irwin, I. Chronic Parkinsonism in humans due to a product of meperidine-analog synthesis. *Science* 219:979–980; 1983.
53. Langston, J. W.; Palfreman, J. The case of the frozen addicts. New York: Pantheon Books; 1995.
54. Ling, Z.; Chang, Q. A.; Tong, C. W.; Leurgans, S. E.; Lipton, J. W.; Carvey, P. M. Rotenone potentiates dopamine neuron loss in animals exposed to lipopolysaccharide prenatally. *Exp. Neurol.* 190:373–383; 2004.
55. Ling, Z.; Gayle, D. A.; Ma, S. Y.; Lipton, J. W.; Tong, C. W.; Hong, J. S.; Carvey, P. M. In utero bacterial endotoxin exposure causes loss of tyrosine hydroxylase neurons in the postnatal rat midbrain. *Mov. Disord.* 17:116–124; 2002.
56. Ling, Z. D.; Chang, Q.; Lipton, J. W.; Tong, C. W.; Landers, T. M.; Carvey, P. M. Combined toxicity of prenatal bacterial endotoxin exposure and postnatal 6-hydroxydopamine in the adult rat midbrain. *Neuroscience* 124:619–628; 2004.
57. Liou, H. H.; Chen, R. C.; Tsai, Y. F.; Chen, W. P.; Chang, Y. C.; Tsai, M. C. Effects of paraquat on the substantia nigra of the wistar rats: Neurochemical, histological, and behavioral studies. *Toxicol. Appl. Pharmacol.* 137:34–41; 1996.
58. Liou, H. H.; Tsai, M. C.; Chen, C. J.; Jeng, J. S.; Chang, Y. C.; Chen, S. Y.; Chen, R. C. Environmental risk factors and Parkinson's disease: A case-control study in Taiwan. *Neurology* 48:1583–1588; 1997.
59. Maruyama, W.; Takahashi, T.; Minami, M.; Takahashi, A.; Dostert, P.; Nagatsu, T.; Naoi, M. Cytotoxicity of dopamine-derived 6,7-dihydroxy-1,2,3,4-tetrahydroisoquinolines. *Adv. Neurol.* 60:224–230; 1993.
60. Mathur, B. N.; Neely, M. D.; Zhang, Y.; Deutch, A. Y. Failure of systemic administration of the proteasome inhibitor z-lle-glu(otbu)-ala-leu-al (PSI) to induce parkinsonism. *Soc. Neurosci. Abstr.* 426.11; 2005.
61. Mavridis, M.; Degryse, A. D.; Lategan, A. J.; Marien, M. R.; Colpaert, F. C. Effects of locus coeruleus lesions on parkinsonian signs, striatal dopamine and substantia nigra cell loss after 1-methyl-4-phenyl-1,2,3,6-tetrahydropyridine in monkeys: A possible role for the locus coeruleus in the progression of Parkinson's disease. *Neuroscience* 41:507–523; 1991.
62. McNaught, K. S.; Perl, D. P.; Brownell, A. L.; Olanow, C. W. Systemic exposure to proteasome inhibitors causes a progressive model of Parkinson's disease. *Ann. Neurol.* 56:149; 2004.
63. Meco, G.; Bonifati, V.; Vanacore, N.; Fabrizio, E. Parkinsonism after chronic exposure to the fungicide maneb (manganese ethylene-bis-dithiocarbamate). *Scand. J. Work Environ. Health* 20:301–305; 1994.
64. Michel, P. P.; Dandapani, B. K.; Efange, S. M.; Hefti, F. Potential environmental neurotoxins related to 1-methyl-4-phenylpyridinium: Selective toxicity of 1-methyl-4-(4'-acetamidophenyl)-pyridinium and 1-methyl-4-cyclohexylpyridinium for dopaminergic neurons in culture. *Exp. Neurol.* 108:141–150; 1990.
65. Michel, P. P.; Dandapani, B. K.; Sanchez-Ramos, J.; Efange, S.; Pressman, B. C.; Hefti, F. Toxic effects of potential environmental neurotoxins related to 1-methyl-4-phenylpyridinium on cultured rat dopaminergic neurons. *J. Pharmacol. Exp. Ther.* 248:842–850; 1989.
66. Montagu, K. A. Catechol compounds in rat tissues and in brains of different animals. *Nature* 180:244–245; 1957.
67. Morris, H. R. Genetics of Parkinson's disease. *Ann. Med.* 37:86–96; 2005.
68. Morrish, P. K.; Rakshi, J. S.; Bailey, D. L.; Sawle, G. V.; Brooks, D. J. Measuring the rate of progression and estimating the preclinical period of Parkinson's disease with [¹⁸F]dopa PET. *J. Neurol. Neurosurg. Psychiatry* 64:314–319; 1998.
69. Mueller, J. C.; Fuchs, J.; Hofer, A.; Zimprich, A.; Lichtner, P.; Illig, T.; Berg, D.; Wullner, U.; Meitinger, T.; Gasser, T. Multiple regions of alpha-synuclein are associated with Parkinson's disease. *Ann. Neurol.* 57:535–541; 2005.
70. Nass, R.; Miller, D. M.; Blakely, R. D. *C. elegans*: A novel pharmacogenetic model to study Parkinson's disease. *Parkinsonism Relat. Disord.* 7:185–191; 2001.
71. Newman, M. B.; Freeman, T. B.; Davis, C. D.; Sanberg, P. R. Neural stem cells for cellular therapy in humans. In Bottenstein, J. E., ed. *Neural stem cells: Development and transplantation*. Boston: Kluwer Academic Publishers; 2003:379–412.

72. Newman, M. B.; Ling, Z. D.; Tong, C.; Punati, A. K.; Carvey, P. M. Norepinephrine may contribute to the progression of Parkinson's disease by microglia regulation. *Soc. Neurosci. Abstr.* 31:11; 2005.
73. Nicklas, W.; Vyas, I.; Heikkila, R. Inhibition of NADH-linked oxidation in brain mitochondria by 1-methyl-4-henylpyridine, a metabolite of the nerotonis, 1-methyl-1,2,3,6-tetrahydro-pyridine. *Life Sci.* 36:2503–2508; 1985.
74. Olanow, C. W.; Kordower, J. H.; Freeman, T. B. Fetal nigral transplantation as a therapy for Parkinson's disease. *Trends Neurosci.* 19:102–109; 1996.
75. PDF: Parkinson's Disease Foundation: General Parkinson's disease facts. http://www.pdf.org/Publications/fact_sheets.cfm; 2005.
76. Petroske, E.; Meredith, G. E.; Callen, S.; Totterdell, S.; Lau, Y. S. Mouse model of Parkinsonism: A comparison between subacute MPTP and chronic MPTP/probenecid treatment. *Neuroscience* 106:589–601; 2001.
77. Polymeropoulos, M. H.; Lavedan, C.; Leroy, E.; Ide, S. E.; Dehejia, A.; Dutra, A.; Pike, B.; Root, H.; Rubenstein, J.; Boyer, R.; Stenroos, E. S.; Chandrasekharappa, S.; Athanassiadou, A.; Papapetropoulos, T.; Johnson, W. G.; Lazzarini, A. M.; Duvoisin, R. C.; Di Iorio, G.; Golbe, L. I.; Nussbaum, R. L. Mutation in the alpha-synuclein gene identified in families with Parkinson's disease. *Science* 276:2045–2047; 1997.
78. Porter, C. C.; Totaro, J. A.; Stone, C. A. Effect of 6-hydroxydopamine and some other compounds on the concentration of norepinephrine in the hearts of mice. *J. Pharmacol. Exp. Ther.* 140:308–316; 1963.
79. Przedborski, S.; Jackson-Lewis, V.; Yokoyama, R.; Shibata, T.; Dawson, V. L.; Dawson, T. M. Role of neuronal nitric oxide in 1-methyl-4-phenyl-1,2,3,6-tetrahydropyridine (MPTP)-induced dopaminergic neurotoxicity. *Proc. Natl. Acad. Sci. USA* 93:4565–4571; 1996.
80. Przedborski, S.; Vila, M. The 1-methyl-4-phenyl-1,2,3,6-tetrahydropyridine mouse model: A tool to explore the pathogenesis of Parkinson's disease. *Ann. NY Acad. Sci.* 991:189–198; 2003.
81. Ransmayr, G.; Seppi, K.; Donnemiller, E.; Luginger, E.; Marksteiner, J.; Riccabona, G.; Poewe, W.; Wenning, G. K. Striatal dopamine transporter function in dementia with Lewy bodies and Parkinson's disease. *Eur. J. Nucl. Med.* 28:1523–1528; 2001.
82. Ranson, S. W.; Ingram, W. R. Catalepsy caused by lesions between the mammillary bodies and III nerve in the cat. *Am. J. Physiol.* 101:690; 1932.
83. Ricaurte, G. A.; Langston, J. W.; Delanney, L. E.; Irwin, I.; Peroutka, S. J.; Forno, L. S. Fate of nigrostriatal neurons in young mature mice given 1-methyl-4-phenyl-1,2,3,6-tetrahydropyridine: A neurochemical and morphological reassessment. *Brain Res.* 376:117–124; 1986.
84. Sanchez-Ramos, J.; Facca, A.; Basit, A.; Song, S. Toxicity of dieldrin for dopaminergic neurons in mesencephalic cultures. *Exp. Neurol.* 150:263–271; 1998.
85. Senoh, S.; Creveling, C. R.; Udenfriend, S.; Witkop, B. Chemical, enzymatic and metabolic studies on the mechanism of oxidation of dopamine. *J. Am. Chem. Soc.* 81: 6236–6240; 1959.
86. Senoh, S.; Witkop, B.; Creveling, C. R.; Udenfriend, S. 2,4,5-tr-hydroxyphenetylamine, a new metabolite of 3,4-dihydroxyphenetylamine. *J. Am. Chem. Soc.* 81:1768–1769; 1959.
87. Singer, T. P.; Ramsay, R. R. The reaction sites of rotenone and ubiquinone with mitochondrial NADH dehydrogenase. *Biochim. Biophys. Acta* 1187:198–202; 1994.
88. Sinha, R.; Racette, B.; Perlmuter, J. S.; Parsian, A. Prevalence of parkin gene mutations and variations in idiopathic Parkinson's disease. *Parkinsonism Relat. Disord.* 11:341–347; 2005.
89. Snyder, H.; Wolozin, B. Pathological proteins in Parkinson's disease: focus on the proteasome. *J. Mol. Neurosci.* 24:425–442; 2004.
90. Thiruchelvam, M.; Brockel, B. J.; Richfield, E. K.; Baggs, R. B.; Cory-Slechta, D. A. Potentiated and preferential effects of combined paraquat and maneb on nigrostriatal dopamine systems: Environmental risk factors for Parkinson's disease? *Brain Res.* 873:225–234; 2000.
91. Thiruchelvam, M.; McCormack, A.; Richfield, E. K.; Baggs, R. B.; Tank, A. W.; Di Monte, D. A.; Cory-Slechta, D. A. Age-related irreversible progressive nigrostriatal dopaminergic neurotoxicity in the paraquat and maneb model of the Parkinson's disease phenotype. *Eur. J. Neurosci.* 18:589–600; 2003.
92. Thiruchelvam, M.; Richfield, E. K.; Goodman, B. M.; Baggs, R. B.; Cory-Slechta, D. A. Developmental exposure to the pesticides paraquat and maneb and the Parkinson's disease phenotype. *Neurotoxicology* 23:621–633; 2002.
93. Thiruchelvam, M. J.; Powers, J. M.; Cory-Slechta, D. A.; Richfield, E. K. Risk factors for dopaminergic neuron loss in human alpha-synuclein transgenic mice. *Eur. J. Neurosci.* 19:845–854; 2004.
94. Ueki, A.; Chong, P. N.; Albanese, A.; Rose, S.; Chivers, J. K.; Jenner, P.; Marsden, C. D. Further treatment with MPTP does not produce parkinsonism in marmosets showing behavioural recovery from motor deficits induced by an earlier exposure to the toxin. *Neuropharmacology* 28:1089–1097; 1989.
95. Ungerstedt, U. 6-Hydroxy-dopamine induced degeneration of central monoamine neurons. *Eur. J. Pharmacol.* 5: 107–110; 1968.
96. Uretsky, N. J.; Iversen, L. L. Effects of 6-hydroxydopamine on catecholamine containing neurones in the rat brain. *J. Neurochem.* 17:269–278; 1970.

available at www.sciencedirect.comwww.elsevier.com/locate/brainresBRAIN
RESEARCH

Research Report

Age-related changes in glutathione and glutathione-related enzymes in rat brain

Yuanguai Zhu^{a,b}, Paul M. Carvey^a, Zhaodung Ling^{a,c,*}^aDepartment of Pharmacology, Rush University Medical Center, 1735 West Harrison Street, Chicago, IL 60612, USA^bFujian Institute of Geriatrics, Union Hospital, Fujian Medical University, Fuzhou, Fujian 350004, China^cDivision of Mental Health and Substance Abuse Research, National Health Research Institutes, Taiwan

ARTICLE INFO

Article history:

Accepted 17 March 2006

Available online 2 May 2006

Keywords:

Aging

Glutathione

 γ -glutamylcysteine synthetase

Oxidative stress

Rat

Abbreviations:

 γ -GC, γ -glutamylcysteineGCS, γ -glutamylcysteine synthetase

GPx, glutathione peroxidase

GR, glutathione reductase

GS, glutathione synthetase

GSH, glutathione

GSSG, glutathione disulfide

GST, glutathione S-transferase

 γ -GT, γ -glutamyl transpeptidase

LPO, lipid peroxide

NDA,

2,3-naphthalenedicarboxyaldehyde

PBS, phosphate-buffered saline

ROS, reactive oxygen species

SSA, 5-sulfosalicylic acid

ABSTRACT

The most reliable and robust risk factor for some neurodegenerative diseases is aging. It has been proposed that processes of aging are associated with the generation of reactive oxygen species and a disturbance of glutathione homeostasis in the brain. Yet, aged animals have rarely been used to model the diseases that are considered to be age-related such as Parkinson's or Alzheimer's disease. This suggests that the results from these studies would be more valuable if aged animals were used. The present study was designed to provide insight into the glutathione redox state in young and aged rat siblings of both genders by studying the enzyme activities related to glutathione synthesis, cycling, and usage. The results suggested a significant age-related reduction of reduced glutathione (GSH) level in all brain regions examined, associated with an increase of GSH oxidation to glutathione disulfide (GSSG) and decrease of the GSH/GSSG ratio. These changes were accompanied by diminished γ -glutamylcysteine synthetase activity in de novo glutathione synthesis and increased lipid peroxidation. In addition, these changes were associated with increased enzyme activities related to the GSH usage (glutathione peroxidase, γ -glutamyl transpeptidase, and glutathione S-transferase). The results indicate that aged animals are likely more vulnerable to oxidative stress and insinuate the roles of aged animals in modeling age-related neurodegeneration diseases.

© 2006 Elsevier B.V. All rights reserved.

* Corresponding author. Department of Pharmacology, 1735 West Harrison Street, Suite 410, Chicago, IL 60612, USA. Fax: +1 312 563 3552.
E-mail address: 950108@nhri.org.tw (Z. Ling).

1. Introduction

Oxidative stress, an unavoidable consequence in the metabolism of oxygen in aerobic cells, is a major factor in the aging process and in the course of many chronic diseases associated with aging (Ames et al., 1993). There is substantial evidence that aging is one of the most robust and significant risk factors for age-related neurodegenerative diseases, such as Parkinson's disease (Olanow and Tatton, 1999). In study of such diseases, however, young animals, which do not display characteristics found in the central nervous system of older animals, are often used to model the age-related diseases (Vu et al., 2000; Brown et al., 2005; Ossowska et al., 2005).

Aging-related changes in the brain include reduction of trophic supports (Ling et al., 2000; Sortwell et al., 2001), decreased proteasomal enzyme activities (Gray et al., 2003; Zeng et al., 2005), mitochondrial dysfunction (Hampton, 2005), change into more pro-inflammatory environment (Gayle et al., 1999), and, more importantly, aging is associated with an increase in reactive oxygen species (ROS) (Ames et al., 1993).

Glutathione (GSH) is the most abundant non-protein thiol that buffers ROS in the brain tissue (Dringen et al., 2000). It eliminates H_2O_2 and organic peroxides by glutathione peroxidases (GPx) (Meister, 1988). GSH also transports amino acids across the cellular membrane by the γ -glutamyl cycle and detoxifies foreign agents by glutathione S-transferase (GST) (Meister, 1988). Normal levels of glutathione are maintained by de novo glutathione synthesis and the salvage pathway. GSH is comprised of three amino acids, glutamate, cysteine, and glycine. The first enzyme in de novo synthesis is γ -glutamylcysteine synthetase (GCS) that catalyzes glutamate and cysteine to form γ -glutamylcysteine. γ -Glutamylcysteine and glycine form GSH by second enzyme glutathione synthetase (GS). During detoxification, ROS are reduced by GPx at the expense of GSH to form glutathione disulfide (GSSG). GSH is regenerated by redox recycling, in which GSSG is reduced to GSH by glutathione reductase (GR) with a consumption of one NADPH. During transportation of amino acids into mammalian cells, one GSH is lost for each amino acid transported, but it can be restored by the salvage pathways including recovery of cysteine and de novo GSH synthesis. These salvage pathways maintain homeostasis of glutathione system (Griffith et al., 1978; Dickinson and Forman, 2002).

The aims of the present study were to define the levels of glutathione (GSH and GSSG) and GSH-related enzymes activities of aged rats in both genders and compare them with those found in young littermates. The results reveal relatively complete view of glutathione system in conjunction with lipid peroxidation and provide useful information for those who may use aged rats to study neurodegenerative diseases such as Parkinson's disease. Our findings also highlight the role of GCS in maintaining GSH homeostasis in the rat brain.

2. Results

2.1. Age-related changes in GSH and GSSG in rat brain

To gauge glutathione levels in the brain, GSH and GSSG were determined in the frontal cortex, striatum, midbrain, and

cerebellum. Overall, aging caused GSH reduction in all brain regions examined ($F_{1,76} = 93.34$, $P < 0.001$). These age-related changes in GSH level equally occurred in both genders ($F_{1,76} = 0.12$, $P = 0.73$). As shown in Fig. 1A, in the midbrain of aged male rats, there was a $25 \pm 4\%$ decrease in GSH level when compared with the young rats ($P < 0.01$). GSH was also reduced in three other regions in both genders when compared with the young rats (Fig. 1A).

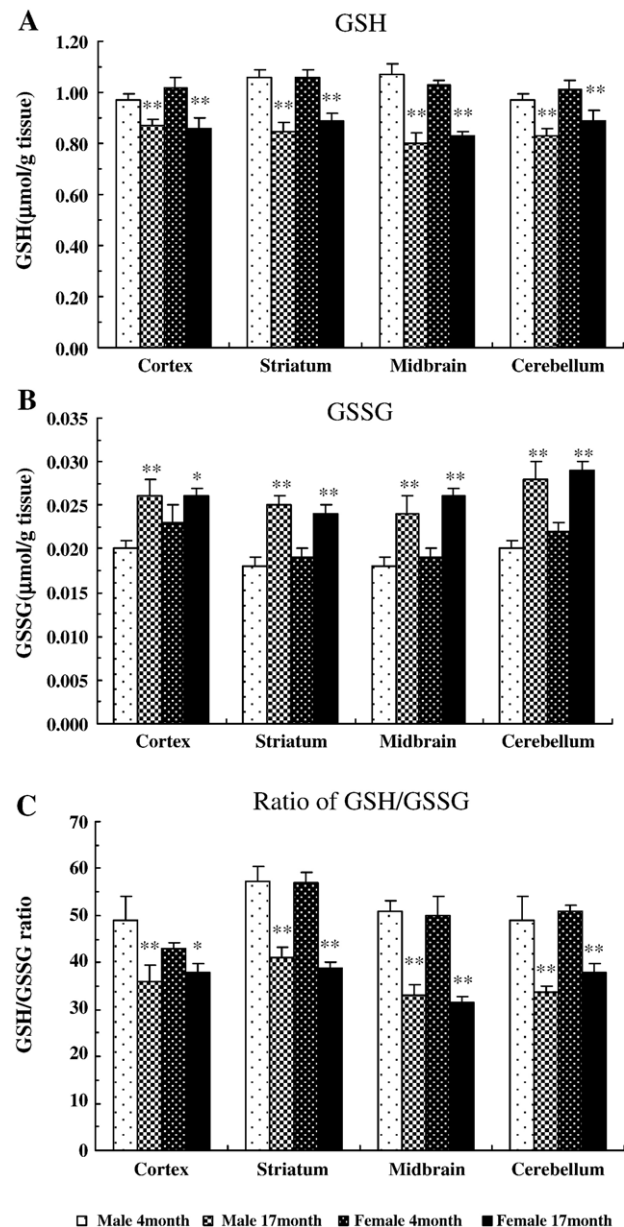


Fig. 1 – The levels of reduced glutathione (GSH), glutathione disulfide (GSSG), and GSH/GSSG ratio in rat regional brain tissues. GSH and GSSG were measured in cortex, striatum, midbrain, and cerebellum of male and female rats at 4 and 17 months of age. (A) GSH, (B) GSSG, and (C) ratio of GSH over GSSG. Data are the means \pm SEM from 5 animals in each group. * $P < 0.05$, ** $P < 0.01$ compared with the corresponding young group.

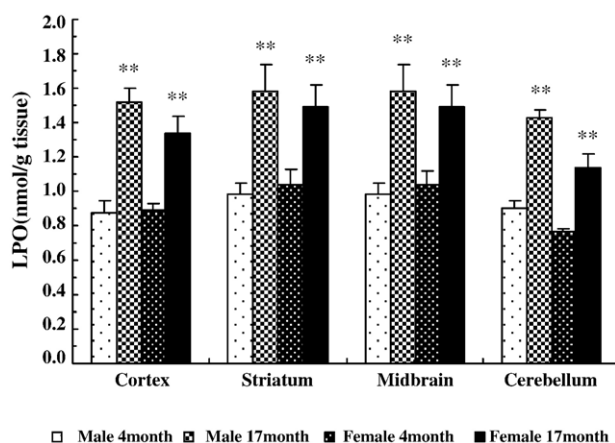


Fig. 2 – The levels of lipid peroxide (LPO) in rat brain tissues. LPO was measured in cortex, striatum, midbrain, and cerebellum of male and female rats at 4 and 17 months of age. Data are the means \pm SEM from 5 animals in each group. ** $P < 0.01$ compared with the corresponding young group.

When GSH is oxidized by GPx to form GSSG, GSSG level is increased, and the GSH/GSSG ratio is proportionately decreased. As shown in Figs. 1B and C, there was a significant increase in the GSSG level and a decrease in the GSH/GSSG ratio in aged rat brains compared with the young brains in all

regions examined ($P < 0.05$). In particular, there was a 20% to 35% decline in the GSH/GSSG ratio in aged animals compared with the young rats. As was true for GSH, the age effects on GSSG level and GSH/GSSG ratio were equivalent in both genders.

2.2. Age-related changes of lipid peroxide (LPO) in rat brain

To evaluate the possible consequences of oxidative stress in the brain, lipid peroxide was measured in different regions of brain. As shown in Fig. 2, there were significant increases in LPO production in cortex (male $64 \pm 9\%$ and female $51 \pm 8\%$), striatum (male $61 \pm 8\%$ and female $44 \pm 9\%$), midbrain (male $61 \pm 9\%$ and female $44 \pm 8\%$), and cerebellum (male $64 \pm 11\%$ and female $51 \pm 6\%$) compared with the respective regions in young rats ($P < 0.01$). In addition, two-way ANOVA showed that the effect of age on LPO was independent of gender in all regions examined ($F_{1,76} = 0.38$, $P = 0.59$).

2.3. Age-related changes in de novo GSH synthesis and GCS protein expression in rat brain

To determine whether GCS or GS was affected by age, GCS and GS activities were measured in the brain tissues. Overall, aging caused an increase in GCS activity in all brain regions examined ($F_{1,76} = 117.55$, $P < 0.001$). However, as summarized

Table 1 – Summary of enzyme activities related to glutathione metabolism in rat brain

Enzyme	Gender	Age (month)	Cortex	Striatum	Midbrain	Cerebellum
GCS	M	4	0.78 \pm 0.05	0.78 \pm 0.03	0.93 \pm 0.06	0.95 \pm 0.04
		17	0.63 \pm 0.05*	0.70 \pm 0.04*	0.65 \pm 0.03**	0.79 \pm 0.04**
	F	4	0.81 \pm 0.04	0.87 \pm 0.06	0.96 \pm 0.06	0.92 \pm 0.04
GS	M	4	0.65 \pm 0.05**	0.60 \pm 0.02**	0.73 \pm 0.05**	0.75 \pm 0.04**
		17	0.62 \pm 0.02	0.71 \pm 0.07	0.68 \pm 0.04	0.63 \pm 0.07
	F	4	0.56 \pm 0.03	0.63 \pm 0.05	0.61 \pm 0.05	0.65 \pm 0.02
GR	M	4	0.68 \pm 0.04	0.76 \pm 0.04	0.86 \pm 0.05	0.70 \pm 0.04
		17	0.55 \pm 0.08	0.68 \pm 0.02	0.71 \pm 0.05*	0.65 \pm 0.03
	F	4	4.86 \pm 0.33	4.48 \pm 0.55	4.14 \pm 0.32	3.76 \pm 0.34
GPx	M	4	5.96 \pm 0.23**	5.92 \pm 0.19**	6.12 \pm 0.53** Δ	5.20 \pm 0.45**
		17	4.11 \pm 0.44	3.91 \pm 0.46	3.75 \pm 0.23	3.89 \pm 0.52
	F	4	4.90 \pm 0.20*	5.36 \pm 0.30	6.36 \pm 0.39** Δ	5.45 \pm 0.22
γ -GT	M	4	7.51 \pm 0.62	7.70 \pm 0.63	8.27 \pm 0.46	7.70 \pm 0.57
		17	9.41 \pm 0.82*	10.10 \pm 0.12**	10.96 \pm 0.33** Δ	9.31 \pm 0.94**
	F	4	7.81 \pm 0.14	6.11 \pm 0.24	8.87 \pm 1.00	7.95 \pm 0.50
GST	M	4	8.78 \pm 0.71*	10.20 \pm 0.21**	10.97 \pm 0.24** Δ	9.71 \pm 0.45**
		17	0.52 \pm 0.06	0.75 \pm 0.06	0.65 \pm 0.04	0.66 \pm 0.10
	F	4	0.86 \pm 0.08**	1.15 \pm 0.15**	1.02 \pm 0.09**	0.97 \pm 0.05**
	M	4	0.62 \pm 0.04	0.71 \pm 0.05	0.78 \pm 0.05	0.66 \pm 0.06
		17	0.98 \pm 0.12**	1.16 \pm 0.09**	1.15 \pm 0.14**	1.07 \pm 0.04**
	F	4	9.38 \pm 0.37	8.31 \pm 0.45	8.68 \pm 0.23	10.50 \pm 0.42
	M	4	12.02 \pm 0.79**	10.90 \pm 0.52**	10.57 \pm 0.46**	13.10 \pm 0.34**
		17	9.00 \pm 0.43	7.59 \pm 0.51	7.59 \pm 0.51	8.70 \pm 0.58
	F	4	10.70 \pm 0.81*	9.96 \pm 0.25**	10.10 \pm 0.42**	10.41 \pm 0.75** Δ

GCS: γ -glutamylcysteine synthetase; GS: glutathione synthetase; GR: glutathione reductase; GPx: glutathione peroxidase; γ -GT: γ -glutamyl transpeptidase; GST: glutathione S-transferase; M: male; F: female. All the enzyme activities are expressed as nmol/min/mg protein. Data are means \pm SEM from 5 animals in each group.

* $P < 0.05$, significant changes compared with the corresponding region in the same gender.

** $P < 0.01$, significant changes compared with the corresponding region in the same gender.

†† $P < 0.01$, significant change compared with the corresponding region in opposite gender.

Δ $P < 0.05$, significant changes compared with other brain regions in the same age/same gender.

in Table 1, a pronounced decrease in GCS activity was observed in the midbrain of rats at 17 months of age (by $30 \pm 7\%$ in male and $21 \pm 5\%$ in female, respectively). In the cortex, striatum, and cerebellum, the change was less dramatic but still statistically significant (Table 1). The effect of age on GCS activity was independent of gender in all regions examined ($F_{1,76} = 0.82$, $P = 0.37$). In contrast, there were no age- or gender-associated changes in GS activity in rat brain except in the midbrain of female rats with a significant decrease relative to the midbrain of young females ($P < 0.05$).

Structurally, GCS is composed of heavy and light subunits (GCS-HS and GCS-LS), which are dissociated under reducing conditions and can be detected with specific antibodies (Yan and Meister, 1990). Western blot and band density analysis data showed that there were no significant changes of GCS-HS protein amount among young and aged male and female rats in the four regions examined (Figs. 3A, C). However, the amount of GCS-LS was significantly decreased in all regions of the aged animals compared with the young rats ($P < 0.05$), although the changes were not the same across all regions examined (Figs. 3B, D).

Overall, there was no significant difference between male and female groups when region and gender were used as two factors in the two-way ANOVA on GCS-LS. However, post hoc analysis in one-way ANOVA indicated a male and female GCS-LS difference in midbrain of 4-month-old animals. Similarly,

there was a male and female GCS-LS difference in the striatum of 17-month-old animals. These differences were not seen in other regions suggesting regional effects. Pearson 2-tailed test showed significant correlation between GCS activity and GCS-LS protein levels ($r^2 = 0.595$, $P < 0.01$).

2.4. Age-related changes in GR activity in rat brain

GR participates in glutathione redox cycling by converting GSSG back to GSH. As summarized in Table 1, GR activity was increased in both male or female aged brains compared with the young male or female rat brains, respectively ($P < 0.05$). The most prominent increase in GR activity was seen in the midbrain of the aged rats, although other regions also displayed increases in GR activities ($P < 0.05$). In addition, the effect of age on GR activity was independent of gender in all regions examined ($F_{1,76} = 0.96$, $P = 0.33$).

2.5. Age-related changes of GPx, γ -glutamyl transpeptidase (γ -GT), and GST activity in rat brain

GPx, γ -GT, and GST are important GSH-using enzymes and play important roles in maintaining GSH homeostasis and tissue detoxification. As summarized in Table 1, all these enzyme activities were significantly increased in both male or female aged rat brains compared with the young animals in all

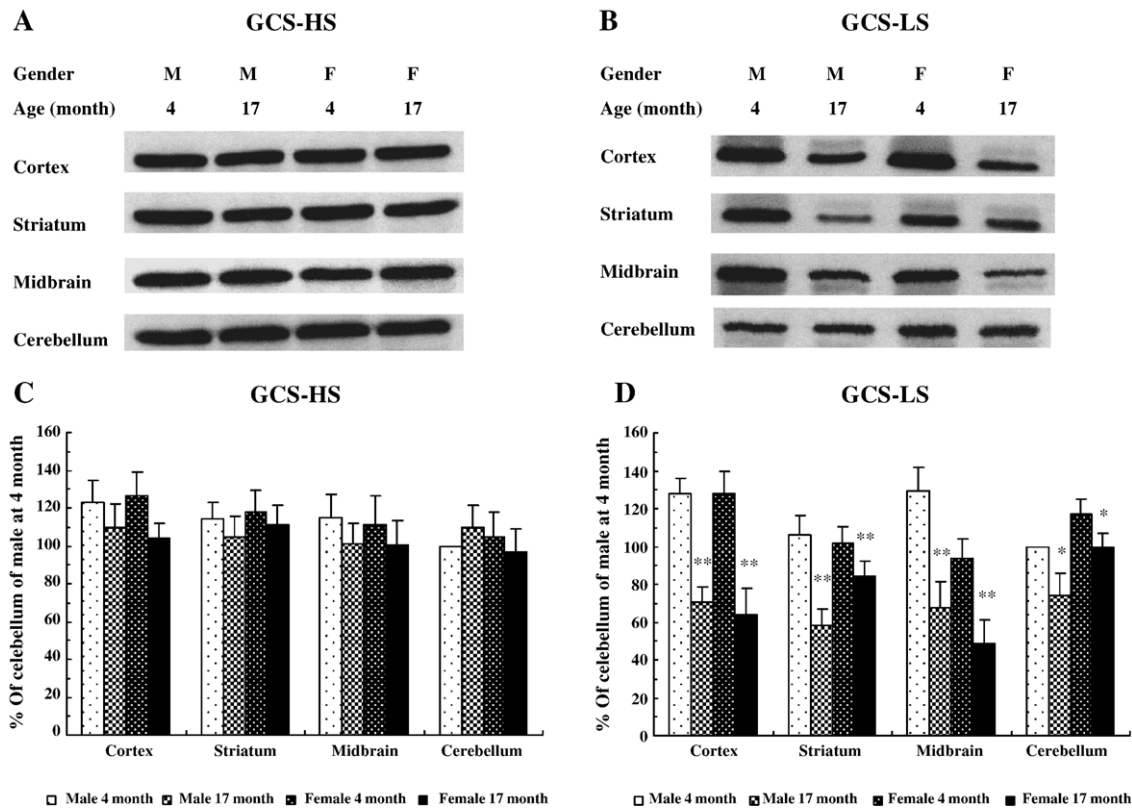


Fig. 3 – The subunits of γ -glutamylcysteine synthetase (GCS) protein in rat brain tissues. Heavy subunit of GCS (GCS-HS) and light subunit of GCS (GCS-LS) were immunoblotted for cortex, striatum, midbrain, and cerebellum of male and female rats at 4 and 17 months of age. A and B were representative Western blot images for GCS-HS (A) and GCS-LS (B). C (GCS-HS) and D (GCS-LS) represent percent of optical density of immunoblot bands relative to the band density in cerebellum in male rat at 4 months of age. Data are the means \pm SEM from 5 animals in each group. * $P < 0.05$; ** $P < 0.01$ compared with the corresponding young group.

brain regions examined ($P < 0.05$). However, GPx activity was significantly higher in the midbrain compared with other regions ($P < 0.05$). In addition, the effect of age on these enzyme activities did not depend on gender in all regions examined.

3. Discussion

Increasing evidences suggest that the excessive production of free radicals in brain, and the imbalance between oxidative species and antioxidant defenses is related to aging and the pathogenesis of neurodegenerative diseases (Schulz et al., 2000; Kasapoglu and Ozben, 2001). Glutathione redox cycling is an extremely important system in cellular free radical detoxification. Glutathione homeostasis is maintained by de novo glutathione synthesis and redox cycling. In order to realize how aging may alter this system, we measured reduced and oxidized glutathione in multiple regions of brain, we also assessed activities of those enzymes involved in de novo glutathione synthesis, glutathione redox cycling, and glutathione consumption in the same tissues. Thus, results of this study firstly reveal a relatively complete view of glutathione metabolism in young and aged rat brains of both genders, which provides useful information for those who may use aged rats to study neurodegenerative diseases, such as Parkinson's disease.

3.1. Age effects on GSH, GSSG, and GSH/GSSG ratio in rat brain

GSH is present in the brain in millimolar concentrations (Dringen et al., 2000). However, reports on the GSH level among various brain areas are inconsistent (Chen et al., 1989; Abbott et al., 1990; Hussain et al., 1995). In the present study, GSH level was similar in all brain tissues examined (cortex, striatum, midbrain, and cerebellum) regardless of genders. This is in agreement with Liu's (2002) study, in which there were no significant variations of GSH levels in cortex, cerebellum, and hippocampus of 3-month-old Fisher 344 rats. However, Abbott et al. (1990) and Kang et al. (1999) reported that the levels of GSH in 4-month-old mouse brain varied from region to region with cortex > cerebellum > hippocampus > striatum > substantia nigra. This discrepancy could be due to the use of different species (rats versus mice) or differences in animal housing or other environmental conditions. In stressful conditions (Bottje et al., 1998) or in the mild pathological conditions (Maher, 2005), animals may show elevations in GSH levels in tissues or organs that are targets of such insults. Nevertheless, our data suggests that GSH is homogeneous across the midbrain, striatum, cortex, and cerebellum in both male and female Sprague–Dawley rats within the same age group.

An age-associated decline in GSH level has been reported in the brain tissue of various species (Chen et al., 1989; Liu, 2002; Kim et al., 2003), which are consistent overall with the findings of current study. Increases in GSSG were significant in all four brain regions of the aged rats. The decrease in GSH level and increase in GSSG level in aged rats produces a significant decrease in the GSH/GSSG ratio, which is often used to indicate the redox state within the tissue (Dringen et al.,

2000; Lin et al., 2002; Samuele et al., 2005). In previous studies, the ratios of GSH/GSSG spread from 7 to 200 (Lin et al., 2002; Lipton et al., 2003; Samuele et al., 2005). The ratios in this study (31 to 57) are clearly within this range. Among the factors that may contribute to this range are strain of rat, age, tissue preparation, and the methodology that was employed to assess GSH and GSSG (Lin et al., 2002; Lipton et al., 2003; Samuele et al., 2005). In the present study, the reduction in GSH/GSSG ratio in aged rats suggested a deficiency in the aged brains to detoxify the ROS, which normally occurs in the brain (Dringen et al., 2000), or resulting from neurotoxin insults.

3.2. Lipid peroxidation in aged rat brain

Quantification of lipid peroxidation is widely used to indicate oxidative injury in diseases (Porter et al., 1995; Halliwell, 1996). We observed a significant increase in LPO production in the brains of aged animals consistent with the recent report by Subathra et al. (2005). Lipid peroxidation is a complex process, and polyunsaturated fatty acids are readily susceptible to autoxidation. The results of this study have led us to believe that deficiency of non-protein thiol is an important, but not an exclusive factor, in aging-related brain injury as indicated by increases in LPO and GSSG productions.

3.3. Age effects on glutathione-related enzymes activities in rat brain

The mechanisms underlying the age-related decline in the GSH level are not well understood. It may result from the reduction in de novo glutathione synthesis. We assessed two de novo synthetic enzyme activities, GCS and GS. Significant reductions in GCS but not in GS activities were observed. Therefore, GCS is more likely responsible for the reduction in GSH level. Recently, Liu and Choi (2000) reported that an age-associated decline in GCS gene expression was accompanied by a decline in total GSH level in aged rats. This suggests that decrease in de novo GSH synthesis may be responsible for the age-associated decrease in GSH content.

GCS catalyzes the first reaction in de novo GSH synthesis. Mammalian GCS is a heterodimer consisting of a catalytic heavy subunit (GCS-HS, 73 kDa) and a regulatory light subunit (GCS-LS, 31 kDa), which are encoded by different genes and are dissociated under reducing conditions (Yan and Meister, 1990; Huang et al., 1993). GCS-HS exhibits all of the catalytic activity of the isolated enzyme (Seelig et al., 1984). GCS-LS is enzymatically inactive but plays an important regulatory function by lowering the K_m of GCS for glutamate and raising the K_i for GSH (Huang et al., 1993). Regulation of GCS-LS gene expression appears to be critical for GSH homeostasis. Kang et al. (1999) found that GCS activity is highly correlated with GCS-LS mRNA levels in different brain regions. In addition, the activity of GCS is also under post-translational regulation by protein kinases. In 1996, Sun et al. (1996) first reported that GCS was phosphorylated by protein kinase A (PKA), protein kinase C (PKC), and Ca^{2+} /calmodulin-dependent kinase (CMK). This suggests that phosphorylation or dephosphorylation may represent an important regulatory mechanism of GCS activity. In the present study, protein analysis for the subunit of GCS showed that there were no changes in the GCS-HS

protein in aged rats compared with young rats. In contrast, a reduction of GCS-LS protein in old rats was seen in all regions observed, which is consistent with another report (Liu, 2002). The fact that these two proteins are translated from two distinct genes and regulated differently in various tissues under physiological conditions (Gipp et al., 1995; Liu et al., 1998) may explain why we observed a difference in translational levels between GCS-HS (no change in aged animals, Figs. 3A, C) and GCS-LS (decreased in aged animals, Figs. 3B, D).

GR was found increased in midbrain particularly in the midbrain of older animals. This is likely resulted from the fact that midbrain contains high level of dopamine which is not sequestered in synaptic vesicles, promoting a higher turnover of dopamine which produces hydroxyl radicals, and hydrogen peroxide. During aging, this turnover becomes more prominent (Ling et al., 2000) which depletes more GSH to cause a greater increase in GSSG, thus stimulating an increase in GR to remove excess GSSG. However, whether increase in GR activity reciprocally down-regulates GCS-LS activity in de novo GSH synthesis is not clear. GSH is a product of both de novo synthesis and glutathione redox cycling. GSH is a nonallosteric feedback inhibitor of the GCS enzyme (Richman and Meister, 1975). In the presence of thiols like GSH, the disulfide bridge connecting the heavy and light subunits of GCS heterodimer is reduced, leading to a conformational change within the substrate-binding site of GCS-HS. The relaxed substrate-binding site can accommodate tripeptides like GSH with greater affinity, thereby inhibiting substrate binding leading to decreased synthesis of GSH (Richman and Meister, 1975). However, in the aged group, this did not seem the case since GSH, as an inhibitor for GCS activity, was reduced significantly regardless of an increase in GR activity. This seems to support a view that GCS activity is independently affected by aging process.

GSH is transported from the intracellular space to extracellular space by glutathione transporter. Peroxides and other oxidative species are disposed from cells through this transporter. Such reactions result in a loss of GSH involving the conversion of GSH to GSSG by GPx. GPx activity appears to be increased in aged brain (Carrillo et al., 1992). In the present study, GPx was significantly increased in all four brain regions of aged rats compared to the young rats regardless of genders, demonstrating an adaptive enzymatic alteration in the aged rats secondary to the increase of oxidative stress, as evidenced by the increase in LPO.

GST is another detoxification enzyme which catalyzes the glutathione moiety to a great variety of acceptor molecules including toxins, organic hydroperoxides, and lipid peroxides to form conjugates. These conjugates are degraded in the γ -glutamyl cycle. In one study, GST activity was 1.7-fold increased in the brains of 9-month-old rats compared with those of 5-week-old rats (Kim et al., 2003). In our current study, GST was increased significantly in all brain regions examined in aged male or female rats. Like the elevation of GPx activity, GST is assumed to respond to aging as an adaptive mechanism secondary to increases of oxidative stress.

γ -GT initiates the degradation of extracellular GSH by catalyzing the transfer of the γ -glutamyl moiety from GSH onto an acceptor molecule, usually an amino acid, to form γ -glutamyl-amino acid and cysteinylglycine, which then is

broken down by dipeptidase to produce free cysteine for reuse. Because of its degradative function, increases in γ -GT activity would theoretically lead to a decrease in GSH level. In fact, Sian et al. (1994) have reported that the decrease in GSH in the substantia nigra in Parkinson's disease was due to an increase in γ -GT activity. In the present study, the increase of γ -GT activity was 30 to 40% higher in aged animals relative to the young animals regardless of brain region or gender, suggesting an excessive degradative metabolism of GSH in the aged brains.

3.4. Gender effect on glutathione metabolism in rat brain

The present study showed that the aged-associated changes in GSH, GSSG, and GSH/GSSG ratio, as well as GSH-related enzyme activities were gender-independent with an exception of GST in female cerebellum (Table 1). These findings differed from a report by Wang et al. (2003), which showed that male mice had a more dramatic age-associated change in GSH level than did female mice. The discrepancy may be associated with the animal species (mouse vs. rat) and the subject selection. In the present study, male and female pups were siblings and only one male or female pup was allowed to be assigned into an age group to avoid litter effects. In addition, dividing siblings into young and aged groups also allowed better comparisons cross two time points. This setting might explain why there were no gender-associated variation in GSH and GSH-related enzyme activities in the present study.

Another exception was the gender effect on GCS-LS protein expression. Difference was seen only in midbrain (lower in aged female group) and striatum (lower in aged male group). These differences were not seen in other regions of both young and aged groups suggesting regional effects. The mechanism underlying such differences was not clear and warrants further investigation. However, the differential post-translational regulation among regions may play a role (Sun et al., 1996). The positive correlation between GCS-LS protein levels (Fig. 3D) and GCS activity levels (Table 1) was in agreement with a report by Kang et al. (1999) who found that GCS activity is highly correlated with GCS-LS mRNA levels in different brain regions.

In conclusion, data from this study indicated that the aging-associated GSH decline was accompanied by an increase in oxidative load in the aged rat brains. Data also demonstrated that the age-associated GSH decline was due to both the reduction of GCS-mediated de novo GSH synthesis and the increase of consumption in aged brain. This study provides invaluable data for modeling diseases with neurodegenerative nature, especially age-related diseases such as PD.

4. Experimental procedures

4.1. Chemicals and reagents

2,3-Naphthalenedicarboxyaldehyde (NDA), GSH, γ -glutamyl-cysteine, ATP, 5-sulfosalicylic acid (SSA), L-glutamic acid, L-cysteine, L-serine, glycylglycine, protease inhibitor cocktail, and other analytical grade reagents were purchased from Sigma Chemical Co. (St. Louis, MO). γ -Glutamyl-7-amino-4-

methyl-coumarin (γ -glutamyl-AMC) was from Bachem Bioscience (Torrance, CA). AMC was from Anaspec (San Jose, CA). Assay kits for GSH, GPx, GR, GST, and LPO were from Cayman Chemical (Ann Arbor, MI). Rabbit anti-GCS-HS was from Abcam Inc (Cambridge, MA), and rabbit GCS-LS was a generous gift from Dr. Terrance J. Kavanagh (University of Washington and Bristol-Myers Squibb Company, Seattle, Washington).

4.2. Animals

All animal protocols in the present study were approved by the Institutional Animal Care and Utilization Committee (IACUC) of Rush University and met the guidelines of the Council on Accreditation of the Association for Assessment and Accreditation of Laboratory Animals Care (AAALAC).

Timed-gravid female Sprague–Dawley rats (Zivic-Miller, Allison Park, PA) were purchased at embryonic day 9 (E9) and maintained in an environmentally regulated animal facility. Females were housed individually, and all pups were born normally at E22. The offspring were weaned at postnatal day 21, and the dams were sacrificed. Only one male or female from each of five litters was assigned to the 4- and 17-month groups to avoid litter effect. After 4 and 17 months, the pups were anesthetized using sodium pentobarbital (Sigma, 60 mg/kg, i.p.) and perfused transcardially with ice-cold saline. The brains were quickly removed and frozen in 2-methylbutane and stored at -80°C for less than 2 months for further analyses.

4.3. Preparation of brain homogenates

The brains were dissected while still frozen as previously described (Ling et al., 2004). The striatum, midbrain, frontal cortex and cerebellum were isolated and weighted. The tissues were homogenized with an ultrasonic dismembrator (Biologics Inc, Gainesville, Virginia) for 12 rapid pulses in ice-cold 0.1 M phosphate-buffered saline (PBS, pH 7.4) containing 0.1 mM EDTA. The homogenates were centrifuged at $14,000 \times g$ for 30 min at 4°C , and the supernatants were collected for different analyses. Protein concentrations were determined using the Bio-Rad (Hercules, CA) DC protein assay kit using bovine serum albumin as a standard.

4.4. Measurement of GSH and GSSG

Reduced glutathione (GSH) and GSSG concentrations were measured by a commercial kit supplied by Cayman Chemical. This kit utilizes an optimized enzymatic GR recycling method for quantification of GSH (Baker et al., 1990). Briefly, 100 μl of brain homogenate was added to an equal volume of the metaphosphoric acid and then centrifuged at $2000 \times g$ for 2 min to remove protein. Then, 50 μl of 4 M triethanolamine was added for each milliliter of homogenate to increase the pH. For total GSH assay, 50 μl of sample was added to 150 μl of a reaction mixture containing 0.4 M 2-(*N*-morpholino) ethanesulfonic acid, 0.1 M phosphate (pH 6.0), 2 mM EDTA, 0.24 mM NADPH, 0.1 mM 5,5'-dithiobis-2-nitrobenzoic acid (DTNB), and 0.1 unit GR. The reaction was carried out at 37°C for 25 min, and then total glutathione was determined by absorbance at 412 nm using GSSG as standard. For the measurement of

GSSG, GSH was removed from the reaction by adding 10 μl of 1 M 2-vinylpyridine solution for each milliliter of homogenate. Then, the remaining GSSG in the reaction was quantified as total GSH assay. The amount of reduced GSH was obtained by subtracting GSSG from total glutathione. Each sample was assessed in duplicates, and the levels of GSH and GSSG were expressed as $\mu\text{mol/g}$ tissue. The ratio of GSH over GSSG was used to indicate redox status that inferences the detoxification capacity.

4.5. LPO measurement

Lipid peroxidation results in a formation of LPO that can therefore be used to indicate the levels of lipid peroxidation in tissue. LPO was quantified with the Cayman's LPO assay kit. This kit measures hydroperoxides directly utilizing the redox reactions with ferrous ions (Mihaljevic et al., 1996). Briefly, 100 μl of brain homogenate was added to an equal volume of saturated methanol and 1 ml of cold chloroform. The mixture was mixed thoroughly and then centrifuged at $2000 \times g$ for 5 min to extract LPO into chloroform layer. Then, 500 μl of chloroform extract was mixed with 450 μl of chloroform-methanol solvent and 50 μl of freshly prepared chromogen (containing 4.5 mM ferrous sulfate in 0.2 M hydrochloric acid) in glass tube. Absorbance was measured at 500 nm after 5 min incubation. The LPO levels in sample homogenates were calculated with standard curve of LPO. Each homogenate was assessed in duplicates, and LPO was expressed as nmol/g tissue.

4.6. Enzyme activity assays

4.6.1. GCS and GS activity

Activity of GCS and GS were determined by a fluorescence-based microtiter plate assay originally developed by White et al. (2003) with little modification. Briefly, 50 μl of homogenate was centrifuged in micro-tubes for 20 min at 4°C at $12,000 \times g$ to remove endogenous GSH and other inhibitors (Liu et al., 1998). Then, 0.3 ml of 0.1 M PBS was added, and then the samples were centrifuged for another 20 min to wash and concentrate the protein. Final concentrates were tested for their protein content with Bio-Rad DC protein assay kit. For GCS activity assay, 50 μl of sample was added to 50 μl of GCS reaction cocktail containing 5 mM L-cysteine, 100 mM Tris, 10 mM ATP, 20 mM L-glutamic acid, 2 mM EDTA, 20 mM sodium borate, 2 mM serine, and 40 mM MgCl_2 then was incubated at 37°C . The GCS reaction was initiated by addition of 50 μl of 2 mM cysteine. For GS activity assay, L-glutamic acid was substituted with 30 mM glycine, and L-cysteine was substituted with 3 mM γ -glutamylcysteine (γ -GC). After incubation for 20 min, the GCS and GS reactions were stopped by addition of 50 μl of 200 mM SSA. Following deproteinization, the supernatants were incubated with 180 μl of 10 mM NDA to form NDA- γ -GC and NDA-GSH. Then, NDA- γ -GC or NDA-GSH fluorescence intensity was measured (472 excitation/528 emission) on a fluorescence plate reader (Molecular Devices, Menlo Park, CA). The production of γ -GC and GSH was calculated with standard curves for NDA- γ -GC and NDA-GSH. Each assay was performed in duplicate, and GCS and GS activity were reported as nmol/min/mg protein.

4.6.2. GPx activity

GPx activity was determined using a commercial kit supplied by Cayman Chemical. In this assay system, the oxidation of glutathione (GSH) was coupled to NADPH oxidation by GR (Paglia and Valentine, 1967). Briefly, the reaction mixture (200 μ l) contained 20 μ l of brain homogenate, 5.0 mM GSH, 0.1 mM NADPH, 50 mM Tris-HCl (pH 7.6), 5 mM EDTA, and 0.1 unit of GR. The reaction was initiated by addition of 20 μ l of 0.2 mM cumene hydroperoxide at room temperature. The decrease in absorbance at 340 nm was recorded at 60 s intervals for 6 min. The rate of decrease in the absorbance is directly proportional to the GPx activity in the sample. Each assay was performed in duplicate, and enzyme units were recorded as nmol NADPH oxidized/min/mg protein.

4.6.3. GR activity

GR activity was assayed spectrophotometrically by monitoring the oxidation of NADPH to NADP⁺ by GR at 340 nm with the Cayman's GR assay kit at room temperature (Carlberg and Mannervik, 1985). Briefly, the reaction mixture (200 μ l) contained 50 mM potassium phosphate (pH 7.5), 1 mM EDTA, 1 mM GSSG, and 0.1 mM NADPH. The reaction was initiated by addition of 20 μ l of brain homogenate. The decrease in absorbance at 340 nm was recorded at 60 s intervals for 6 min. Each assay was performed in duplicate, and enzyme units were recorded as nmol NADPH oxidized/min/mg protein.

4.6.4. GST activity

GSTs have been grouped into species-independent classes of isozymes, including both cytosolic and microsomal enzymes (Morgenstern et al., 1979; Mannervik, 1985). Three families of cytosolic soluble GSTs, α (GSTA), μ (GSTM), and π (GSTP), were known in the brain (Theodore et al., 1985; Board et al., 1990). Cayman's GST assay kit measured total GST activity (cytosolic and microsomal) using 1-chloro-2,4-dinitrobenzene (CDNB) as the substrate. Briefly, the reaction mixture (200 μ l) contained 20 μ l of brain homogenate, 100 mM potassium phosphate (pH 6.5), 0.1% (v/v) Triton X-100, 5.0 mM reduced GSH. The reaction was initiated by addition of 10 μ l of 20 mM CDNB at room temperature. The increase in absorbance at 340 nm was recorded at 60 s intervals for 7 min. The rate of increase in the absorbance is directly proportional to the GST activity in the sample. Each assay was performed in duplicate, and enzyme units were recorded as nmol/min/mg protein.

4.6.5. γ -GT activity

γ -GT activity was measured following the procedure of Forman et al. (1995). Briefly, a 0.1 ml of brain homogenates was added to 0.25 ml of a reaction mixture containing 50 mM Tris-HCl (pH 7.6), pH 8.6, 20 mM glycylglycine, 20 μ M γ -glutamyl-7-amino-4-methyl-coumarin (γ -glutamyl-AMC), and 0.1% (v/v) Triton X-100. The reaction was carried out at 37 °C for 30 min and terminated by adding 1.5 ml cold 50 mM glycine. The fluorescence was measured at 440 nm with excitation wavelength of 370 nm. The enzyme activity, represented by product formation, was calculated and compared with a standard curve of AMC. Each assay was performed in duplicate, and enzyme units were recorded as nmol/min/mg protein.

4.7. Western blot for analysis of GCS protein

The GCS heavy subunit (GCS-HS) and light subunit (GCS-LS) proteins were determined by Western blot as described by Liu et al. (1998). Briefly, the homogenates were mixed with a protease inhibitor cocktail, and then the samples were prepared as described for GCS activity measurement. For each sample, 30 μ g of total protein was electrophoresed in 10% sodium dodecyl sulfate-polyacrylamide gel (SDS-PAGE) and blotted onto a nitrocellulose membrane. After blocking with milk, the membrane was incubated with a primary antibody to GCS-HS or GCS-LS. Anti-GCS-HS polyclonal antibody was diluted at 1:1000. Anti-GCS-LS polyclonal antibody was used at 1:2000. Second antibodies to anti-GCS-HS or GCS LS were conjugated with peroxidase. Films were exposed using enhanced chemiluminescence. The X-ray film was scanned, and the density of band was quantified using Scion Image software (Scion Corporation, Frederick, MD). All band densities were compared with that of cerebellum of male rat at 4 months old.

4.8. Statistical analyses

Data are expressed as mean \pm SEM. Differences among groups and regions were analyzed by one-way analysis of variance (ANOVA) followed by Tukey's method. Two-way ANOVA was used to analyze interaction of gender and age. Pearson 2-tailed test was used to detect correlation between GCS activities and GCS protein levels. A probability value of less than 0.05 was considered statistically significant.

Acknowledgments

This study was supported by NINDS NS045316, NIEHS 012307, USARMRA W81XWH-04-01-0365, and grant from the Michael J. Fox Foundation. The authors also thank Dr. Terrance J. Kavanagh at University of Washington for his generosity of providing GCS-LS anti sera.

REFERENCES

- Abbott, L.C., Nejad, H.H., Bottje, W.G., Hassan, A.S., 1990. Glutathione levels in specific brain regions of genetically epileptic (tg/tg) mice. *Brain Res. Bull.* 25, 629–631.
- Ames, B.N., Shigenaga, M.K., Hagen, T.M., 1993. Oxidants, antioxidants, and the degenerative diseases of aging. *Proc. Natl. Acad. Sci. U. S. A.* 90, 7915–7922.
- Baker, M.A., Cerniglia, G.J., Zaman, A., 1990. Microtiter plate assay for the measurement of glutathione and glutathione disulfide in large numbers of biological samples. *Anal. Biochem.* 190, 360–365.
- Board, P., Coggan, M., Johnston, P., Ross, V., Suzuki, T., Webb, G., 1990. Genetic heterogeneity of the human glutathione transferases: a complex of gene families. *Pharmacol. Ther.* 48, 357–369.
- Bottje, W.G., Wang, S., Beers, K.W., Cawthon, D., 1998. Lung lining fluid antioxidants in male broilers: age-related changes under thermoneutral and cold temperature conditions. *Poult. Sci.* 77, 1905–1912.

- Brown, A.M., Deutch, A.Y., Colbran, R.J., 2005. Dopamine depletion alters phosphorylation of striatal proteins in a model of Parkinsonism. *Eur. J. Neurosci.* 22, 247–256.
- Carlberg, I., Mannervik, B., 1985. Glutathione reductase. *Methods Enzymol.* 113, 484–490.
- Carrillo, M.C., Kanai, S., Sato, Y., Kitani, K., 1992. Age-related changes in antioxidant enzyme activities are region and organ, as well as sex, selective in the rat. *Mech. Ageing Dev.* 65, 187–198.
- Chen, T.S., Richie Jr., J.P., Lang, C.A., 1989. The effect of aging on glutathione and cysteine levels in different regions of the mouse brain. *Proc. Soc. Exp. Biol. Med.* 190, 399–402.
- Dickinson, D.A., Forman, H.J., 2002. Cellular glutathione and thiols metabolism. *Biochem. Pharmacol.* 64, 1019–1026.
- Dringen, R., Gutterer, J.M., Hirrlinger, J., 2000. Glutathione metabolism in brain metabolic interaction between astrocytes and neurons in the defense against reactive oxygen species. *Eur. J. Biochem.* 267, 4912–4916.
- Forman, H.J., Shi, M.M., Iwamoto, T., Liu, R.M., Robison, T.W., 1995. Measurement of gamma-glutamyl transpeptidase and gamma-glutamylcysteine synthetase activities in cells. *Methods Enzymol.* 252, 66–71.
- Gayle, D., Ilyin, S.E., Romanovitch, A.E., Peloso, E., Satinoff, E., Plata-Salaman, C.R., 1999. Basal and IL-1 β -stimulated cytokine and neuropeptide mRNA expression in brain regions of young and old Long-Evans rats. *Brain Res. Mol. Brain Res.* 70, 92–100.
- Gipp, J.J., Bailey, H.H., Mulcahy, R.T., 1995. Cloning and sequencing of the cDNA for the light subunit of human liver gamma-glutamylcysteine synthetase and relative mRNA levels for heavy and light subunits in human normal tissues. *Biochem. Biophys. Res. Commun.* 206, 584–589.
- Gray, D.A., Tsigotis, M., Woulfe, J., 2003. Ubiquitin, proteasomes, and the aging brain. *Sci. Aging Knowledge Environ.* RE6.
- Griffith, O.W., Bridges, R.J., Meister, A., 1978. Evidence that the gamma-glutamyl cycle functions in vivo using intracellular glutathione: effects of amino acids and selective inhibition of enzymes. *Proc. Natl. Acad. Sci. U. S. A.* 75, 5405–5408.
- Halliwell, B., 1996. Oxidative stress, nutrition and health. Experimental strategies for optimization of nutritional antioxidant intake in humans. *Free Radical Res.* 25, 57–74.
- Hampton, T., 2005. Study reveals mitochondrial role in aging. *JAMA* 294, 672.
- Huang, C.S., Anderson, M.E., Meister, A., 1993. Amino acid sequence and function of the light subunit of rat kidney gamma-glutamylcysteine synthetase. *J. Biol. Chem.* 268, 20578–20583.
- Hussain, S., Slikker Jr., W., Ali, S.F., 1995. Age-related changes in antioxidant enzymes, superoxide dismutase, catalase, glutathione peroxidase and glutathione in different regions of mouse brain. *Int. J. Dev. Neurosci.* 13, 811–817.
- Kang, Y., Viswanath, V., Jha, N., Qiao, X., Mo, J.Q., Andersen, J.K., 1999. Brain gamma-glutamyl cysteine synthetase (GCS) mRNA expression patterns correlate with regional-specific enzyme activities and glutathione levels. *J. Neurosci. Res.* 58, 436–441.
- Kasapoglu, M., Ozben, T., 2001. Alterations of antioxidant enzymes and oxidative stress markers in aging. *Exp. Gerontol.* 36, 209–220.
- Kim, H.G., Hong, S.M., Kim, S.J., Park, H.J., Jung, H.I., Lee, Y.Y., Moon, J.S., Lim, H.W., Park, E.H., Lim, C.J., 2003. Age-related changes in the activity of antioxidant and redox enzymes in rats. *Mol. Cells* 16, 278–284.
- Lin, A.M., Chen, C.F., Ho, L.T., 2002. Neuroprotective effect of intermittent hypoxia on iron-induced oxidative injury in rat brain. *Exp. Neurol.* 176, 328–335.
- Ling, Z.D., Collier, T.J., Sortwell, C.E., Lipton, J.W., Vu, T.Q., Robie, H.C., Carvey, P.M., 2000. Striatal trophic activity is reduced in the aged rat brain. *Brain Res.* 856, 301–309.
- Ling, Z.D., Chang, Q., Lipton, J.W., Tong, C.W., Landers, T.M., Carvey, P.M., 2004. Combined toxicity of prenatal bacterial endotoxin exposure and postnatal 6-hydroxydopamine in the adult rat midbrain. *Neuroscience* 124, 619–628.
- Lipton, J.W., Gyawali, S., Borys, E.D., Koprich, J.B., Ptaszny, M., McGuire, S.O., 2003. Prenatal cocaine administration increases glutathione and alpha-tocopherol oxidation in fetal rat brain. *Brain Res. Dev. Brain Res.* 147, 77–84.
- Liu, R.M., 2002. Down-regulation of gamma-glutamylcysteine synthetase regulatory subunit gene expression in rat brain tissue during aging. *J. Neurosci. Res.* 68, 344–351.
- Liu, R., Choi, J., 2000. Age-associated decline in gamma-glutamylcysteine synthetase gene expression in rats. *Free Radical Biol. Med.* 28, 566–574.
- Liu, R.M., Gao, L., Choi, J., Forman, H.J., 1998. Gamma-glutamylcysteine synthetase: mRNA stabilization and independent subunit transcription by 4-hydroxy-2-nonenal. *Am. J. Physiol.* 275, L861–L869.
- Maher, P., 2005. The effects of stress and aging on glutathione metabolism. *Ageing Res. Rev.* 4, 288–314.
- Mannervik, B., 1985. The isoenzymes of glutathione transferase. *Adv. Enzymol. Relat. Areas Mol. Biol.* 57, 357–417.
- Meister, A., 1988. Glutathione metabolism and its selective modification. *J. Biol. Chem.* 263, 17205–17208.
- Mihaljevic, B., Katusin-Razem, B., Razem, D., 1996. The reevaluation of the ferric thiocyanate assay for lipid hydroperoxides with special considerations of the mechanistic aspects of the response. *Free Radical Biol. Med.* 21, 53–63.
- Morgenstern, R., DePierre, J.W., Ernster, L., 1979. Activation of microsomal glutathione S-transferase activity by sulphydryl reagents. *Biochem. Biophys. Res. Commun.* 87, 657–663.
- Olanow, C.W., Tatton, W.G., 1999. Etiology and pathogenesis of Parkinson's disease. *Annu. Rev. Neurosci.* 22, 123–144.
- Ossowska, K., Wardas, J., Smialowska, M., Kuter, K., Lenda, T., Wieronska, J.M., Zieba, B., Nowak, P., Dabrowska, J., Bortel, A., Kwieciński, A., Wolfarth, S., 2005. A slowly developing dysfunction of dopaminergic nigrostriatal neurons induced by long-term paraquat administration in rats: an animal model of preclinical stages of Parkinson's disease? *Eur. J. Neurosci.* 22, 1294–1304.
- Paglia, D.E., Valentine, W.N., 1967. Studies on the quantitative and qualitative characterization of erythrocyte glutathione peroxidase. *J. Lab. Clin. Med.* 70, 158–169.
- Porter, N.A., Caldwell, S.E., Mills, K.A., 1995. Mechanisms of free radical oxidation of unsaturated lipids. *Lipids* 30, 277–290.
- Richman, P.G., Meister, A., 1975. Regulation of gamma-glutamyl-cysteine synthetase by nonallosteric feedback inhibition by glutathione. *J. Biol. Chem.* 250, 1422–1426.
- Samuele, A., Mangiagalli, A., Armentero, M.T., Fancello, R., Bazzini, E., Vairetti, M., Ferrigno, A., Richelmi, P., Nappi, G., Blandini, F., 2005. Oxidative stress and pro-apoptotic conditions in a rodent model of Wilson's disease. *Biochim. Biophys. Acta* 1741, 325–330.
- Schulz, J.B., Lindenau, J., Seyfried, J., Dichgans, J., 2000. Glutathione, oxidative stress and neurodegeneration. *Eur. J. Biochem.* 267, 4904–4911.
- Seelig, G.F., Simonsen, R.P., Meister, A., 1984. Reversible dissociation of gamma-glutamylcysteine synthetase into two subunits. *J. Biol. Chem.* 259, 9345–9347.
- Sian, J., Dexter, D.T., Lees, A.J., Daniel, S., Agid, Y., Javoy-Agid, F., Jenner, P., Marsden, C.D., 1994. Alterations in glutathione levels in Parkinson's disease and other neurodegenerative disorders affecting basal ganglia. *Ann. Neurol.* 36, 348–355.
- Sortwell, C.E., Camargo, M.D., Pitzer, M.R., Gyawali, S., Collier, T.J., 2001. Diminished survival of mesencephalic dopamine neurons grafted into aged hosts occurs during the immediate postgrafting interval. *Exp. Neurol.* 169, 23–29.
- Subathra, M., Shila, S., Devi, M.A., Panneerselvam, C., 2005.

- Emerging role of *Centella asiatica* in improving age-related neurological antioxidant status. *Exp. Gerontol.* 40, 707–715.
- Sun, W.M., Huang, Z.Z., Lu, S.C., 1996. Regulation of gamma-glutamylcysteine synthetase by protein phosphorylation. *Biochem. J.* 320 (Pt 1), 321–328.
- Theodore, C., Singh, S.V., Hong, T.D., Awasthi, Y.C., 1985. Glutathione S-transferases of human brain. Evidence for two immunologically distinct types of 26500-Mr subunits. *Biochem. J.* 225, 375–382.
- Vu, T.Q., Ling, Z.D., Ma, S.Y., Robie, H.C., Tong, C.W., Chen, E.Y., Lipton, J.W., Carvey, P.M., 2000. Pramipexole attenuates the dopaminergic cell loss induced by intraventricular 6-hydroxydopamine. *J. Neural Transm.* 107, 159–176.
- Wang, H., Liu, H., Liu, R.M., 2003. Gender difference in glutathione metabolism during aging in mice. *Exp. Gerontol.* 38, 507–517.
- White, C.C., Viernes, H., Krejsa, C.M., Botta, D., Kavanagh, T.J., 2003. Fluorescence-based microtiter plate assay for glutamate-cysteine ligase activity. *Anal. Biochem.* 318, 175–180.
- Yan, N., Meister, A., 1990. Amino acid sequence of rat kidney gamma-glutamylcysteine synthetase. *J. Biol. Chem.* 265, 1588–1593.
- Zeng, B.Y., Medhurst, A.D., Jackson, M., Rose, S., Jenner, P., 2005. Proteasomal activity in brain differs between species and brain regions and changes with age. *Mech. Ageing Dev.* 126, 760–766.

Running Head: BBB Leakage

(Submitted revision 11-04-2006 to Neurobiology of Disease)

**TNF-Alpha Knockout and Minocycline Treatment Attenuates Blood Brain Barrier
Leakage in MPTP-Treated Mice**

Chaohui Zhao¹, Zaodung Ling¹, Mary B. Newman^{1,2}, Ankush Bhatia¹,
and Paul M. Carvey^{1,2}

Department of Pharmacology¹ and Neuroscience Program²,
Rush University Medical Center, Chicago IL USA

Corresponding Author:

Dr. Paul M. Carvey, PhD,
Professor and Chairman of Pharmacology,
Rush University Medical Center,
1735 W Harrison St
Cohn Research Building, Suite 406
Chicago, IL 60612
Phone (312) 563-2563
Fax (312) 563-3552
pcarvey@rush.edu

Abstract

Following intraparenchymal injection of the dopamine (DA) neurotoxin 6-hydroxydopamine, we previously demonstrated passage of fluorescein isothiocyanate labeled albumin (FITC-LA) from blood into the substantia nigra (SN) and striatum suggesting damage to the blood-brain barrier (BBB). The factors contributing to the BBB leakage could have included neuroinflammation, loss of DA neuron control of barrier function, or a combination of both. In order to determine which factor(s) was responsible, we assessed BBB integrity using the FITC-LA technique in wild-type (WT), tumor necrosis factor alpha (TNF- α) knockout (KO), and minocycline (an inhibitor of microglia activation) treated mice 72 hrs following 1-methyl-4-phenyl-1,2,3,6-tetrahydropyridine (MPTP). Compared with WT mice, TNF- α KO mice treated with MPTP, showed reduced FITC-LA leakage, decreased numbers of activated microglia, and reduced pro-inflammatory cytokines (TNF- α and interleukin 1 beta) associated with significant MPTP-induced DA neuron loss. In contrast, minocycline treated animals did not exhibit MPTP-induced DA neuron loss although their FITC-LA leakage, numbers of activated microglia, and MPTP-induced cytokine increases were markedly attenuated. Since both TNF- α KO and minocycline treatment attenuated MPTP-induced BBB dysfunction, microglial activation and cytokine increases, but had differential effects on DA neuron loss, it appears that neuroinflammation and not DA neuron loss was responsible for disrupting barrier integrity.

Keywords: Parkinson's disease; neuroinflammation; microglia; TNF- α ; IL-1 β ; minocycline; endothelial cells.

Introduction

Parkinson's disease (PD) is marked by the progressive loss of dopamine (DA) neurons in the substantia nigra (SN) (Hastings and Zigmond, 1997). While the etiology of PD remains unclear, both genetic factors and environmental toxins have been proposed in its pathogenesis (Ladeby et al., 2005; McGeer and McGeer, 2004). Regardless of the underlying etiology, neuroinflammation is thought to contribute to the loss of DA neurons seen in patients with PD (McGeer and McGeer, 2004; Ladeby et al., 2005). Neuroinflammation is also present in trauma, stroke, multiple sclerosis, epilepsy and bacterial meningitis (Mennicken et al., 1999; Phillis et al., 2006) in which damage to the blood brain barrier (BBB) has been reported (Huber et al., 2001). More recent studies point to microvascular changes in the SN and alterations in several markers of normal BBB integrity in PD patients (Barcia et al., 2004; Faucheux et al., 1999; Kortekaas et al., 2005). Whether actual changes in permeability, functionality, or physical damage of the BBB occur in PD is currently unknown.

We recently demonstrated that the DA neurotoxin, 6-hydroxydopamine (6-OHDA), compromised BBB integrity producing apparent leakage of both fluorescein isothiocyanate-labeled albumin (FITC-LA) and horseradish peroxidase into the SN and striatum. This leakage was accompanied by loss of DA neurons, activation of microglia, up-regulation of p-glycoprotein and β -integrin on the endothelial cells that comprise the BBB, and attenuation of a DA-mediated behavior by domperidone, a DA antagonist that normally does not cross the BBB (Carvey et al., 2005). Since neuroinflammation including microglia activation and increased levels of proinflammatory cytokines including tumor necrosis factor- α (TNF- α) are present in patients with PD and in animal models of the disease (Aschner, 1998; Hirsch et al., 2005; Nagatsu and Sawada, 2005) and both are well known to affect the integrity of the BBB (Ryu and McLarnon, 2006; Tsao et al., 2001; Yenari et al., 2006) it is quite possible that 6-OHDA-induced neuroinflammation was responsible for the breakdown in barrier integrity. However, neurons containing biogenic amines are found in close proximity to brain capillaries (Rennels and Nelson, 1975; DiCarlo, Jr. et al., 1984; Kapadia and de Lanerolle, 1984), endothelial cells express both noradrenergic and serotonergic transporters (Wakayama et al., 2002) and receptors (Wakayama et al., 2002; Kobayashi et

al., 1985), and stimulation of the locus coeruleus increases BBB permeability (Raichle et al., 1975) suggesting that neurotransmitters may regulate BBB function as well. It is therefore possible that the increased BBB leakage we observed in rats treated with 6-OHDA was the result of neuroinflammation, DA neuron loss, or a combination of both. We designed a set of experiments to determine the relative contribution of each to BBB leakage.

Materials and methods

Animals

A total of 88 male mice, 8 weeks of age and weighing 22-25 g at the start of the study were used. The TNF- α KO mice (B6;129S6-Tnf^{tm1Gkl}/J; n=22), WT background control mice (B6;129S6; n=22), and C57BL/6 (n=44) mice were purchased from Jackson Laboratory (Bar Harbor, ME). All mice were acclimated to the animal facility for at least two weeks prior to the start of the study. One day prior to MPTP treatment, the mice were moved to a controlled ventilated room and housed in ventilation chambers until sacrificed. Mice were allowed free access to food and water for the duration of the study. The protocols used in this study were approved by the Rush University Medical Center Institutional Animal Care and Utilization Committee and were compliant with all regulations at the institution, state, and federal levels. 1-methyl-4-phenyl-1,2,3,6-tetrahydropyridine (MPTP)-HCl (Sigma, St. Louis, MO) handling and safety measures followed methods described by Przedborski et al. (Przedborski et al., 2001).

Study Design

Study One: TNF- α KO (n=22) and WT (n=22) mice were randomly assigned to one of two groups (Saline or MPTP) for a total of 4 groups designated as follows: WT/Sal = WT mice treated with saline (n=10); WT/MPTP = WT mice treated with MPTP (n=12); TNF- α KO/Sal = KO mice treated with saline (n=10); and TNF- α KO/MPTP = KO mice treated with MPTP (n=12). TNF- α KO and WT mice were injected (i.p.) with either saline or MPTP and sacrificed 72 hours later. MPTP-HCl (10mg/kg freebase) was injected (i.p.) in a saline vehicle four times at 1-hour intervals for

a total of 40mg/kg over a 4 hour period. Saline treated mice followed the same injection protocol. After their injections, the mice were returned to their home-chambers, and sacrificed after 3 days.

Study Two: C57BL/6 mice received either saline or minocycline followed by either MPTP or saline injection. Mice (n=44) were randomly divided into four groups designated as follows: Sal/Sal = saline injections given in place of minocycline and MPTP (n=10); Sal/MPTP = mice treated with saline in place of minocycline, but treated with MPTP (n=12); Mino/Sal = mice treated with minocycline and given saline in place of MPTP (n=10); and Mino/MPTP = mice treated with minocycline and MPTP (n=12). Minocycline (90mg/kg per day, dissolved in 5% sucrose, Sigma, St. Louis, MO) was injected (i.p) for 3 consecutive days, with the first minocycline injection administered 30 minutes prior to the first MPTP injection and 24 hrs prior to sacrifice. MPTP-HCL (10mg/kg per hour) was injected as described above.

In both studies, 5 mice from each treatment group were processed for immunohistochemistry and 5 mice were processed for biochemical analysis. The dependent measures in each study were identical and consisted of visualization of BBB leakage throughout the brain, DA and microglia cell counts in the SN, and determination of levels of TNF- α and IL-1 β protein in the SN and striatum.

FITC-LA Leakage

The leakage of FITC-LA (MW=69-70 KD, Sigma, St. Louis, MO) from vasculature into brain parenchyma was assessed as described previously (Carvey et al., 2005) to determine BBB integrity. Briefly, three days following the last MPTP or saline injections, the mice were anesthetized with pentobarbital (60mg/kg). Heparin (100 units/kg in Hank's Balanced Salt Solution) was injected intracardially followed immediately by 5 ml FITC-LA [5mg/ml, in 0.1 M Phosphate-buffered saline (PBS) buffer] injected at a rate of 1.5ml/minute with the right atrium open. After perfusion, the brains were removed immediately and immersed into 4% paraformaldehyde. Three days later, the fixative was replaced with three changes of 30% sucrose in 0.1 M PBS buffer. Each brain was sectioned at 40 μ m using a sliding microtome, divided into 6 consecutive series, and stored in cryoprotectant (0.05 M PBS with 30% sucrose and 30% ethylene

glycol). One series of sections from each of the 5 mice from both studies were mounted onto gelatin coated slides, dehydrated, and covered for confocal microscopy (Olympus) analysis of FITC-LA leakage.

Immunohistochemistry

A second series of brain sections from each animal in both studies was used for tyrosine hydroxylase (TH, a DA neuron marker) immunohistochemistry as described previously (Carvey et al., 2005). Briefly, sections were washed (6 x 10 minutes) in Tris buffered saline (TBS, pH 7.4) and incubated for 1 h in 0.05% TBS Triton-X-100 solution. Sections were then incubated 30 min in TBS solution with 2.13% sodium periodate to block endogenous peroxidase activity, and then incubated for 1 h with 3 % normal goat serum in TBS. Tissues were incubated overnight with the primary antibody to TH (rabbit:anti-mouse, Chemicon, 1:1,000 dilution). Immunolabeling was continued using biotinylated secondary antibody (goat:anti-rabbit, Vector Laboratories, 1:200) in TBS with 3% goat serum and incubated for 1 hour at room temperature. The antibody complex was amplified using an avidin-biotin kit (ABC-Elite kit; Vector) and visualized with 3,3'-diaminobenzidine (DAB) with nickel enhancement.

A third series of sections from each animal of both studies was processed for CD_{11b} immunohistochemistry to reveal activated microglial cells. The procedure for CD_{11b} immunohistochemistry was similar to the THir staining except that the primary antibody to CD_{11b} originated in rat (Rat:anti-mouse CD_{11b} 1:200; Serotec) and the second antibody was goat:anti-rat IgG (1:200; Vector Laboratories).

Stereological assessment of THir cell and activated microglia cell counts

The estimation of the total number of THir neurons and activated microglia in the SN was performed using the computerized optical dissector method (MicroBrightField software) as described previously (Vu et al., 2000). Briefly, a 10X objective lens was used to define the contour around the entire SN (Ling et al., 2004) and a 100X lens was used for the tyrosine hydroxylase immunoreactive cells (THir cells) and activated microglia assessments. One series of sections from each animal were analyzed. For THir and a second series for CD_{11b} staining, the total number (N) of THir or activated

microglia in the SN from each animal was estimated using the formula $N = NV \cdot VSN$, where NV is the numerical density and VSN is the volume of the SN, as determined by Cavalieri's principle.

ELISA for determination of TNF- α and IL-1 β concentration in the SN and striatum

Mice were anesthetized with 60mg/kg pentobarbital. The brains were removed and immediately placed in cold 2-methylbutane, and then stored at -80°C. The TNF- α and IL-1 β levels were determined for both studies as previously described (Ling et al., 2004). Briefly, brains were slightly thawed, the SNs and striata dissected out, then submerged in ice-cold 150 μ l homogenate buffer (Trizma/HCl pH 7.2, 0.1 M, sodium chloride 0.9%, protease inhibitor cocktail 1%), and sonicated. The homogenates were centrifuged at 13,000 x g for 30 minute at 4°C. The concentrations of TNF- α and IL-1 β in the supernatants were determined using commercial ELISA kit (BioScour International, Camarillo, CA). Standards, diluent buffers or samples (100 μ l) along with 50 μ l biotinylated anti-TNF- α solutions were pipetted into each well and then incubated for 2 hours at 37°C. After washing, streptavidin-HRP working solution was incubated for 1 hour at room temperature. Following washing, stabilized chromogen was incubated for 1 hour and the reaction was stopped with stop solution. The plates were read in a Dynatech ELISA plate reader (Dynatech Laboratories, Chantilly, VA) and the concentrations of the TNF- α and IL-1 β were determined against a seven-point standard curve. The total protein concentration of each homogenate was determined using the BCA protein assay kit (Pierce, IL) and the quantity of TNF- α and IL-1 β was expressed as pg/mg total protein.

Statistical analyses

All values were expressed as mean \pm S.E.M. Separate Two-way analysis of variance (ANOVA) were used to analyze the THir and activated microglia counts along with TNF- α and IL-1 β level in both studies. TNF- α genotype and MPTP treatment were both factors in the TNF- α KO study. In the study of minocycline treatment, the two factors were minocycline and MPTP treatment. The least significant difference test (LSD) was used as the *post-hoc* test to determine individual group differences with significance set at $p \leq 0.05$.

Results

MPTP increased FITC-LA leakage into the SN and striata

FITC-LA was injected into the common carotid artery 72 hours following treatment with MPTP (a time at which active DA neurodegeneration was occurring (Sugama et al., 2003), and the brains were assessed using confocal microscopy to determine if this large molecular weight marker (MW range = 69-70kD) entered brain parenchyma. FITC-LA was confined exclusively to blood vessels in the SN and striatum in the control animals of both genotypes [WT/Sal (Fig. 1A,C); TNF- α KO/Sal (Fig. 1B,D)] and the C57 BL/6 minocycline study animals [Sal/Sal (Fig. 1I,K); Mino/Sal (Fig. 1J,L)] indicating an intact BBB. FITC-LA was also confined within vessels in the majority of the area within the SN and striata of MPTP-treated animals (Fig. 1E,G,M,O). However, all animals treated with MPTP also exhibited numerous patchy areas of leakage in both structures indicative of disruption of barrier integrity. In some areas, individual vessels were not recognizable because the leakage of the FITC-LA was so intense and wide spread. Interestingly, the locations of the leaks were not the same in every animal, but varied considerably from animal to animal. Moreover, the apparent magnitude of the leaks similarly varied from animal to animal such that in both the SN and striatum, some animals had areas of leakage in almost every section whereas in other animals, the number of leaks was markedly less. Regardless, every control animal exposed to MPTP exhibited leakage in some sections of the SN and striatum. The ability of MPTP to induce FITC-LA leakage did not appear to differ between the wild types of the two genotypes.

If FITC-LA distribution reflects BBB integrity, then areas of the brain not protected by the BBB should also reveal leakage. This was indeed the case. Thus, examination of periventricular structures such as area postrema (Fig. 1S) revealed extensive leakage into brain parenchyma in all animals regardless of treatment. In contrast, leakage was never detected in areas outside the nigro-striatal pathway or periventricular organs in any animal regardless of treatment. Thus, in MPTP treated animals, leakage was not seen in the parietal cortex (Fig. 1Q) or hippocampus (Fig. 1R) even though leakage was detected in the SN, striata and periventricular structures of these animals. This suggests that the perfusion pressure used to deliver the FITC-LA filled the

brain's vascular compartment completely without leakage resulting from excess perfusion pressure.

Both TNF- α KO and Minocycline attenuated BBB leakage

In order to determine if inflammation and/or DA neuron loss was responsible for the apparent BBB dysfunction, FITC-LA leakage was assessed in TNF- α KO animals as well as animals treated with minocycline. MPTP treatment increases TNF- α (Nagatsu et al., 2000) which could, in turn, disrupt BBB integrity given its well documented ability to do so (Farkas et al., 2006; Miller et al., 2005; Wong et al., 2004). MPTP also activates microglia (Sugama et al., 2003; Wu et al., 2002; Du et al., 2001; Orr et al., 2002) which release TNF- α (Hirsch et al., 2005; Huang et al., 2005; Nagatsu et al., 2000) as well as a number of other proinflammatory mediators that could disrupt barrier integrity (e.g., free radicals; (Abbott, 2000; Calingasan et al., 1998; Hirsch et al., 2005; Yenari et al., 2006). Since minocycline prevents microglial activation (Du et al., 2001; Hirsch et al., 2005; Zemke and Majid, 2004) by reducing ED-1 and other transcription factors involved in inflammatory processes (Lai and Todd, 2006) and TNF- α KO prevents release of a key proinflammatory cytokines implicated in barrier integrity, assessment of leakage in these animals would enable us to assess the role of neuroinflammation on the barrier dysfunction produced by MPTP. Of perhaps greater importance, however, is that TNF- α KO and minocycline produce differential effects on MPTP-induced DA neuron loss in the SN. Thus, TNF- α KO animals exhibit nigral DA neuron loss in response to MPTP (Rousselet et al., 2002; Ferger et al., 2004), while minocycline treatment prevents MPTP-induced DA neuron loss (Du et al., 2001; Tikka and Koistinaho, 2001). The use of these two models would therefore enable us to ascertain the relative contributions of neuroinflammation and DA neuron loss to the MPTP-induced BBB dysfunction.

FITC-LA leakages into the SNs and striata were markedly attenuated in both TNF- α KO and minocycline treated animals following MPTP. Thus, in both the SN (Fig. 1F,N) and the striatum (Fig. 1H,P), few areas of FITC-LA leakage were observed, and in many animals, no leakage at all was observed. Examination of the vessels in these animals revealed less distinct borders in many of the vessels suggesting a minor compromise of barrier integrity. However, no areas of overt entry into brain parenchyma

were observed in the SNs or striata. These findings suggest that TNF- α and activated microglia participate in MPTP-induced barrier dysfunction.

Both TNF- α KO and minocycline reduced MPTP-induced inflammation

Although CD_{11b}-immunoreactive (ir) cells (a marker for microglial cells) were detected in all animals, control animals exhibited only several hundred cells in their SNs and striata, the vast majority of which had small rounded cell bodies with few ramified processes typical of resting microglia. In contrast, MPTP treatment not only significantly increased the numbers of CD_{11b}-ir cells in both TNF- α KO ($F_{1,16}=60.317$; $p<0.001$) and minocycline treated animals ($F_{1,16}=62.762$; $p<0.001$), but also induced dramatic changes in their morphology as well, such that the vast majority of the cells had large cell bodies with highly ramified processes typical of activated microglia (Fig. 2A,B). Stereological assessments of the CD_{11b}-ir cell counts revealed that both TNF- α KO and minocycline treatment significantly attenuated the numbers of activated microglia (Fig. 2C). Thus, in the B6;129S6 mice, MPTP treatment increased the numbers of activated microglia 26 fold compared with WT/Sal ($p<0.05$), whereas the TNF- α KO /MPTP mice showed only a 2.6 fold increase ($p<0.05$). Similarly, MPTP induced an 18 fold ($p<0.05$) increase in numbers of CD_{11b}-ir cells compared with saline treated C57 BL/6 controls whereas the minocycline treated animals revealed only a 1.07 fold increase ($p>0.05$) (Fig. 2D). Thus, both TNF- α KO and minocycline treatment markedly attenuated microglial activation as well as FITC-LA leakage suggesting that microglia activation was associated with the barrier dysfunction observed. Moreover, assessment of CD_{11b}-ir cells in the patches of FITC-LA leakage revealed the almost universal presence of activated microglia (Fig. 3) further supporting their involvement in BBB dysfunction.

In addition to microglia, we also assessed the proinflammatory cytokines TNF α and interleukin 1 β (IL-1 β) in these animals (Table I). As expected, TNF- α signal was not detectable in any tissue sample taken from TNF- α KO mice whereas both WT saline treated animals exhibited similar levels of TNF- α in the SNs and striata. MPTP treatment consistently increased levels of TNF- α in both the SNs ($F_{1,8}=6.474$, $p<0.05$) and striata ($F_{1,8}=20.215$, $p<0.05$) of WT/MPTP mice, compared with WT/Sal. Similar increases were seen in the C57 BL/6 animals treated with MPTP in both the SNs ($F_{1,16}=12.611$;

$p < 0.05$) and striata ($F_{1,16} = 14.162$; $p < 0.05$). However, these increases were significantly attenuated by minocycline treatment in both the SN ($F_{1,16} = 15.433$; $p < 0.05$) and the striatum ($F_{1,16} = 18.119$; $p < 0.05$).

Similar findings were seen for IL-1 β (Table I). Normal levels of IL-1 β were seen in both the SNs and striata of the WT, TNF- α KO mice, and C57 BL/6 animals. MPTP treatment consistently increased levels of IL-1 β in both the SN ($F_{1,16} = 12.683$, $p < 0.05$) and striatum ($F_{1,16} = 50.098$, $p < 0.05$) of WT/MPTP mice. TNF- α KO attenuated the release of IL-1 β in the striatum ($F_{1,16} = 15.731$, $p < 0.05$) but not in the SN ($F_{1,16} = 1.859$, $p > 0.05$). Similar increases of IL-1 β were seen in the C57 BL/6 animals treated with MPTP in both the SN ($F_{1,16} = 22.283$, $p < 0.05$) and striatum ($F_{1,16} = 34.885$, $p < 0.05$). However, these increases were significantly attenuated by minocycline treatment in the SN ($F_{1,16} = 7.146$; $p < 0.05$) and the striatum ($F_{1,16} = 6.770$; $p < 0.05$). Thus, MPTP increased the levels of this proinflammatory cytokine whereas TNF- α KO and minocycline treatment markedly attenuated the MPTP-induced increases. These data suggest that the attenuation in FITC-LA leakage seen in the TNF- α KO and minocycline treated animals was also associated with reductions in these pro-inflammatory cytokines.

MPTP-induced DA neuron loss was not associated with BBB leakage

MPTP treatment led to an anticipated loss of THir neurons (a marker for DA neurons). Thus, stereological assessments of THir cells in the SN revealed a 35% reduction ($F_{1,16} = 37.415$; $p < 0.05$) in the B6;129S6 control mice and a 44% reduction in the C57BL/6 controls ($F_{1,16} = 14.856$; $p < 0.05$), which were not significantly different from one another (Fig. 4A; $p > 0.05$). Compared with their wild type controls treated with MPTP, the TNF- α KO mice were equivalently sensitive to MPTP losing 30% of their THir cells (Fig 4B; $F_{1,16} = 0.005$, $p = 0.943$). In contrast, minocycline treatment markedly attenuated the MPTP-induced THir cell loss (Fig. 4C; $F_{1,16} = 4.707$; $p < 0.05$). There was not significantly different in THir cell counts between Mino/MPTP and Mino/Sal ($p > 0.05$). These data confirm the previously reported differential effects on DA neuron loss (Tikka and Koistinaho, 2001;Rousselet et al., 2002;Leng et al., 2005;Ferber et al., 2004;Du et al., 2001). Most importantly, they demonstrate that the attenuation of FITC-LA leakage in these two sets of animals was independent from DA neuron loss

suggesting that inflammatory events and not a DA neuron loss *per se* was responsible for the barrier dysfunction induced by MPTP.

Discussion

The current study confirms and extends our previous work in rats in which injection of the DA neurotoxin 6-hydroxydopamine into the striatum or medial forebrain bundle similarly produced patchy areas of leakage of FITC-LA and horseradish peroxidase as well as increase of $\beta 3$ integrin expression (a marker of angiogenesis) in the SN and striatum (Carvey et al., 2005). In the present study, the DA neurotoxin was injected systemically so that the barrier dysfunction seen could not be a consequence of stereotaxic brain surgery. In addition, two different genotypes of mice exhibited barrier dysfunction using MPTP suggesting that the previous effects observed in rats were neither species nor toxin specific. Finally, the current studies clearly demonstrated the validity of the FITC-LA injection procedure as a marker for barrier integrity because areas devoid of a BBB exhibited leakage, regardless of treatment history, and detailed evaluation of several non-dopaminergic brain areas revealed complete vascular perfusion without evidence of leakage demonstrating specificity while ruling out a perfusion-based epiphenomenon. These data strongly argue that DA neurotoxins induce BBB dysfunction in well-established animal models of PD.

At this time, we do not know if the areas of leakage were static (i.e., an area developed a leak and remained leaky) or dynamic (i.e. an area developed a leak and repaired itself such that after several days, leakage would no longer be detected). Given that activated microglia were associated with areas of leakage and microglia are known to migrate (Cho et al., 2006; Carbonell et al., 2005), it is more likely that the pattern of leaks is dynamic. A dynamic pattern of leakage was further supported by the fact that the areas of leakage were different in every animal. This suggests that a “window” of increased leakage developed in an area of inflammation that could subsequently close. It is also becoming increasingly clear that the BBB dysfunction, although it may be dynamic in nature, is not temporary. We previously showed that FITC-LA leakage was still present 10 and 34 days following 6-OHDA treatment (Carvey et al., 2005). Whether or not barrier dysfunction continues for months after toxin exposure remains to be established. Regardless, these results argue that the BBB is somewhat long-lived and common to two different animal models of PD.

The MPTP-induced barrier dysfunction appeared to be a consequence of neuroinflammation independent of DA neuron loss. Although MPTP produced neuroinflammation as evidenced by increased numbers of activated microglia and increases in TNF- α and IL-1 β in both genotypes, the TNF- α KO animals exhibited significant DA neuron losses whereas the animals treated with minocycline did not. Since TNF- α and minocycline both dramatically attenuated the FITC-LA leakage, there was a clear-cut dissociation between the DA neuron loss and the barrier dysfunction. In addition, in *in vitro* studies of human brain microvascular endothelial cell (HBMEC), the condition mediums of LPS-induced activate microglia directly decreased electric resistance of HBMEC. However, condition mediums of DA neuron degenerative and activated astrocyte cells did not affect the resistance of HBMEC (These data will be published in another paper). Thus, although biogenic amine containing neurons are often seen in close proximity to endothelial cells that also express noradrenergic and serotonergic receptors, and norepinephrine containing locus ceruleus cells have been shown to regulate barrier function (Kobayashi et al., 1985; Raichle et al., 1975; Wakayama et al., 2002), there was no evidence of dopaminergic control of barrier leakage in the SN and striatum in the current study. It therefore appears that inflammatory events are more responsible for the barrier dysfunction observed than DA neuron loss. This does not negate the probability that the DA neuron degeneration led to the inflammation, but rather, that DA neuron loss by itself did not lead to the barrier dysfunction. It is possibility that just because DA neuron loss did produce the neuroinflammation in the nigrostriatal system (Carvey et al., 2005; Dassiou-Plakida, 1992), BBB dysfunction was specific to the nigrostriatal system following MPTP treatment.

TNF- α by itself activates microglia (John et al., 2003) and our results show that TNF- α KO inhibits microglia activation. Minocycline is a semisynthetic tetracycline derivative that exerts anti-inflammatory effects and inhibits microglial activation by decreasing IL-1 β and nitric oxide release (Du et al., 2001; Tikka and Koistinaho, 2001). Moreover, our data showed that minocycline also decreased the TNF- α release. Activated microglia release numerous neuroinflammatory substances that can potentially disrupt barrier function including prostanoids, proteases, nitric oxide (NO), superoxide, and the proinflammatory cytokines TNF α and IL-1 β (Dringen, 2005; Lynch et al., 2004; Tsao et

al., 2001;Wong et al., 2004;Yenari et al., 2006). Although any of these factors could have contributed to the barrier breakdown in the current study, the MPTP-induced increase in TNF- α and IL-1 β in conjunction with FITC-LA leakage and the attenuation in these increases in the TNF- α KO and minocycline treated animals argues for their potential involvement in the barrier disruption. TNF- α and IL-1 β are known to decrease electrical resistance and increase permeability in *in vitro* BBB models (Didier et al., 2003;Miller et al., 2005). TNF- α causes a redistribution of cadherin and junctional adhesion molecule (JAM) leading to a rearrangement of microfilaments, and a down-regulation of occludin expression increasing BBB permeability (Ozaki et al., 1999;Petrache et al., 2003;Kniesel and Wolburg, 2000;Mankertz et al., 2000). IL-1 β also increases BBB permeability by decreasing expression of occludin and zonula occludens-1 proteins leading to apparent redistribution of the adherens junction protein vinculin (Bolton et al., 1998). IL-1 β may also induce cyclooxygenase-2 (COX-2) synthesis in brain endothelial cells (Konsman et al., 2004), activating of NF-kappaB molecules and prostaglandins within brain endothelial cells (Laflamme et al., 1999;Nadjar et al., 2005). However, although the current evidence suggests the involvement of TNF- α and IL-1 β , we cannot, at this time, rule out other inflammogens associated with microglial activation.

Several studies have argued against BBB dysfunction in PD. Haussermann et al. (Haussermann et al., 2001) revealed no changes in blood CSF barrier function by examining CSF/serum ratios and oligoclonal bands in PD patients. If the BBB dysfunction is not universal, but rather punctate as our data suggests, major changes such as these would not be detected. Kurkowska-Jastrzebska et al. in 1999 (Kurkowska-Jastrzebska et al., 1999) similarly argued that the DA neurotoxin MPTP does not disrupt BBB function. Yet, although they showed that IgG was restricted to the inside of the blood vessels, they also reported that mononuclear cells infiltrated the SN and striatum, which would suggest BBB dysfunction. O'Callaghan et al. in 1990 (O'callaghan et al., 1990) used a single small administered dose of MPTP (12.5mg/kg, s.c.) that did not produce DA neuron loss and reported no dysfunction of the BBB. Canudas et al. in 2000 (Canudas et al., 2000) injected MPP⁺ into the left SN of the rat that produced only a small lesion yet assessed BBB integrity in the striatum with a crude index of BBB integrity (albumin staining) that could have easily been missed because of the small size of the SN

injury. It is also important to point out that the animal studies using MPTP or its metabolite MPP⁺ just described, were not designed to assess BBB integrity, but rather focused on other effects of MPTP. Moreover, they used global indices of BBB integrity which could have readily missed the punctuate leakage that seems to characterize the DA neurotoxin exposed BBB. In contrast, the study by Faucheux et al. (Faucheux et al., 1999) showed an increase in vascular density in the SN, but not the VTA of PD patients and Barcia et al., (Barcia et al., 2004) discussed evidence of microangiogenesis in the PD brain which is often associated with barrier dysfunction. Kortekaas et al., (Kortekaas et al., 2005) used [¹¹C]-verapamil imaging, and demonstrated an 18% increase in brain uptake in the mesencephalon of PD patients relative to aged controls. This increase may have reflected alterations in P-gp function or simply increased leakage into brain. Barcia et al., (Barcia et al., 2004) also recently noted an increase in the number of blood vessels indicative microangiogenesis that follows barrier damage in close proximity to degenerating DA neurons in non-human primates. Moreover, the increase in vessels was highly correlated with increases in vascular endothelial growth factor (VEGF) probably caused by neo-microangiogenesis that similarly accompanies barrier breakdown following an inflammatory event. Thus, an emerging literature supports barrier dysfunction in patients with PD and animal models of this disorder.

There are numerous implications to PD if areas of active inflammation lead to focal areas of barrier dysfunction in patients. Areas of leakage in focal neuroinflammatory loci would afford the opportunity to target delivery of anti-inflammatory agents that normally do not cross the BBB or deliver a variety of therapeutics to those areas using nanoparticles. Notwithstanding the effect of these agents on areas of the brain not protected by a BBB, this strategy would target areas ostensibly undergoing active DA neurodegeneration potentially slowing disease progression. On the other hand, BBB dysfunction could allow inhomogeneous entry of antiparkinsonian drugs into the SN and striatum that could contribute to dyskinesias since dopaminergic “hotspots” have been implicated in this DA agonist induced side effect (Bankiewicz et al., 2006). Alternatively, levodopa decarboxylase inhibitors including carbidopa and benserazide, which normally do not cross the BBB, may do so in these areas of leakage. This would inhibit conversion of levodopa to DA in these areas creating hot spots of

increased DA activity in intact areas. In addition, focal BBB dysfunction would increase entry of elements of the peripheral vasculature into the SN and striatum that could similarly contribute to disease progression. Moreover, environmental toxins that may not cross the BBB readily would concentrate in areas of BBB dysfunction. Taken together, these results suggest that detailed imaging assessments of BBB integrity should be performed in patients with PD to determine the role, if any, compromised BBB integrity plays in disease progression and side effects.

Acknowledgments

This work was supported by NINDS NS045316, NIEHS 012307, W81XWH-04-01-0365 and the Michael J. Fox Foundation.

Figure Legends

Figure 1. TNF- α KO and minocycline treatment attenuated the FITC-LA leakage in the SN and striatum after MPTP treatment. FITC-LA was visualized using confocal microscopy in the SN of WT/Sal (A) and TNF- α KO/Sal (B) as well as the striatum of WT/Sal (C) and TNF/Sal animals (D). FITC-LA leakage was evident in the SN of the WT/MPTP (E) and striatum of WT/MPTP (G) treated mice. Areas of leakage were not found in the SN (F) or striata (H) of TNF- α KO/MPTP treated mice. Similar findings were seen in the minocycline treated animals. FITC-LA was confined within vessels in the SN of Sal/Sal (I) and Mino/Sal (J) as well as the striatum of Sal/Sal (K) and Mino/Sal (L) animals. FITC-LA leakage was evident in the SN of the Sal/MPTP (M) and striatum of Sal/MPTP (O) treated mice. Areas of leakage were not found in the SN (N) or striata (P) of Mino/MPTP treated mice. There was no FITC-LA leakage in the parietal cortex (Q) and hippocampus (R), in any of the animals regardless of treatment. However, leakage was always seen in the area postrema (S), areas devoid of a BBB. [* = The fourth ventricle. Arrows indicate areas of FITC-LA leakage. Scale bar = 100um (A-T)].

Figure 2. TNF- α KO and minocycline reduced microglial activation. (A) TNF- α KO inhibited MPTP-induced microglial activation. The shapes of microglia were not different in WT (Lane 1: SN of WT/Sal) and TNF- α KO mice (Lane 2: SN of TNF- α KO/Sal) treated with saline. Three days after the last MPTP administration, microglia became large, amoeboid, and had thick processes (Lane 3: SN of WT/MPTP). However, in TNF- α KO/MPTP mice the morphology of microglia remained small and ramified (Lane 4: SN of TNF- α KO/MPTP) comparable with those in WT/Sal mice. (B) Minocycline treatment inhibited MPTP-induced microglial activation. The shape of microglia showed no difference in the C57BL/6 mice between saline only (Lane 1: SN of Sal/Sal) and minocycline only (Lane 2: SN of Mino/Sal) treatment groups. Numerous activated microglia were present in the SN of mice 3 days after MPTP treatment (Lane 3: SN of Sal/MPTP). Minocycline treatment attenuated the MPTP-induced microglia activation (Lane 4: SN of Mino/MPTP). Microglia in the mice injected with both MPTP and minocycline had small cell bodies with ramified long, thin processes in the SN. (C) Quantification of CD11b-ir cells in the WT and TNF- α KO mice following the MPTP

treatment. After the MPTP treatment, the number of activated microglia increased 26 fold in the SN of WT mice. However, TNF- α KO clearly prevented microglia activation. (Marker A: $p < 0.001$ relative to WT/Sal group; Marker B: $p < 0.001$ relative to WT/MPTP group, but it was undistinguishable from WT/Sal group, $P > 0.05$). (D) Quantification of CD11b-ir cells in C57BL/6 mice with or without minocycline treatment following MPTP administration. MPTP treatment increased the number of activated microglia. Minocycline treatment (90mg/kg X3) attenuate this change. (Marker A: $p < 0.05$ relative to Sal/Sal group; Marker B: $p < 0.05$ relative to Sal/MPTP group, but it was indistinguishable from Sal/Sal group, $P > 0.05$). Left (Scale bar=100 μ m) and right (Scale bar=10 μ m).

Figure 3: Areas of FITC-LA leakage contained activated microglia. Upper images show no FITC-LA leakage in areas of resting microglia whereas the lower row demonstrates FITC-LA leakage associated with marked microglial activation. (Bar=25 μ m).

Figure 4: The loss of dopamine neurons was attenuated by minocycline treatment, not by TNF- α KO following MPTP treatment. (A) Photomicrographs of representative sections of THir staining in the SNs of the mice used to generate the bar graph of (B) and (C). SN of (a) WT/Sal, (b) TNF- α KO/Sal, (c) WT/MPTP, (d) TNF- α KO/MPTP, (e) Sal/Sal, (f) Mino/Sal, (g) MPTP/Sal, and (h) MPTP/Mino. (Magnification bar=0.25mm). (B) Quantification of THir cells in the WT and TNF- α KO mice following MPTP treatment. MPTP similarly reduced the numbers of THir cells in the SN of both WT and TNF- α KO mice. The number of THir cells was not significantly different in WT/MPTP and TNF- α KO/MPTP mice [$p = 0.774$; Marked A and B, separately]. (C) Quantification of THir cells in C57BL/6 mice with or without minocycline treatment following MPTP administration. The number of THir cells was significantly different ($p = 0.044$) between Sal/MPTP (Marker C) and Mino/MPTP mice (Marker D).

Reference List

1. Abbott NJ (2000) Inflammatory mediators and modulation of blood-brain barrier permeability. *Cell Mol Neurobiol* 20: 131-147.
2. Aschner M (1998) Astrocytes as mediators of immune and inflammatory responses in the CNS. *Neurotoxicology* 19: 269-281.
3. Bankiewicz KS, Daadi M, Pivrotto P, Bringas J, Sanftner L, Cunningham J, Forsayeth JR, Eberling JL (2006) Focal striatal dopamine may potentiate dyskinesias in parkinsonian monkeys. *Exp Neurol* 197: 363-372.
4. Barcia C, Emborg ME, Hirsch EC, Herrero MT (2004) Blood vessels and parkinsonism. *Front Biosci* 9: 277-282.
5. Bolton SJ, Anthony DC, Perry VH (1998) Loss of the tight junction proteins occludin and zonula occludens-1 from cerebral vascular endothelium during neutrophil-induced blood-brain barrier breakdown in vivo. *Neuroscience* 86: 1245-1257.
6. Calingasan NY, Park LC, Calo LL, Trifiletti RR, Gandy SE, Gibson GE (1998) Induction of nitric oxide synthase and microglial responses precede selective cell death induced by chronic impairment of oxidative metabolism. *Am J Pathol* 153: 599-610.
7. Canudas AM, Friguls B, Planas AM, Gabriel C, Escubedo E, Camarasa J, Camins A, Pallas M (2000) MPP(+) injection into rat substantia nigra causes secondary glial activation but not cell death in the ipsilateral striatum. *Neurobiol Dis* 7: 343-361.
8. Carbonell WS, Murase S, Horwitz AF, Mandell JW (2005) Migration of perilesional microglia after focal brain injury and modulation by CC chemokine receptor 5: an in situ time-lapse confocal imaging study. *J Neurosci* 25: 7040-7047.
9. Carvey PM, Zhao CH, Hendey B, Lum H, Trachtenberg J, Desai BS, Snyder J, Zhu YG, Ling ZD (2005) 6-Hydroxydopamine-induced alterations in blood-brain barrier permeability. *Eur J Neurosci* 22: 1158-1168.
10. Cho BP, Song DY, Sugama S, Shin DH, Shimizu Y, Kim SS, Kim YS, Joh TH (2006) Pathological dynamics of activated microglia following medial forebrain bundle transection. *Glia* 53: 92-102.
11. Dassiou-Plakida D (1992) Greek Society for Dermatologic Surgery. *J Dermatol Surg Oncol* 18: 642.
12. DiCarlo LA, Jr., Botvinick EH, Canhasi BS, Schwartz AS, Chatterjee K (1984) Value of noninvasive assessment of patients with atypical chest pain and suspected

- coronary spasm using ergonovine infusion and thallium-201 scintigraphy. *Am J Cardiol* 54: 744-748.
13. Didier N, Romero IA, Creminon C, Wijkhuisen A, Grassi J, Mabondzo A (2003) Secretion of interleukin-1beta by astrocytes mediates endothelin-1 and tumour necrosis factor-alpha effects on human brain microvascular endothelial cell permeability. *J Neurochem* 86: 246-254.
 14. Dringen R (2005) Oxidative and antioxidative potential of brain microglial cells. *Antioxid Redox Signal* 7: 1223-1233.
 15. Du Y, Ma Z, Lin S, Dodel RC, Gao F, Bales KR, Triarhou LC, Chernet E, Perry KW, Nelson DL, Luecke S, Phebus LA, Bymaster FP, Paul SM (2001) Minocycline prevents nigrostriatal dopaminergic neurodegeneration in the MPTP model of Parkinson's disease. *Proc Natl Acad Sci U S A* 98: 14669-14674.
 16. Farkas E, Sule Z, Toth-Szuki V, Matyas A, Antal P, Farkas IG, Mihaly A, Bari F (2006) Tumor necrosis factor-alpha increases cerebral blood flow and ultrastructural capillary damage through the release of nitric oxide in the rat brain. *Microvasc Res*.
 17. Faucheux BA, Bonnet AM, Agid Y, Hirsch EC (1999) Blood vessels change in the mesencephalon of patients with Parkinson's disease. *Lancet* 353: 981-982.
 18. Ferger B, Leng A, Mura A, Hengerer B, Feldon J (2004) Genetic ablation of tumor necrosis factor-alpha (TNF-alpha) and pharmacological inhibition of TNF-synthesis attenuates MPTP toxicity in mouse striatum. *J Neurochem* 89: 822-833.
 19. Hastings TG, Zigmond MJ (1997) Loss of dopaminergic neurons in parkinsonism: possible role of reactive dopamine metabolites. *J Neural Transm Suppl* 49: 103-110.
 20. Haussermann P, Kuhn W, Przuntek H, Muller T (2001) Integrity of the blood-cerebrospinal fluid barrier in early Parkinson's disease. *Neurosci Lett* 300: 182-184.
 21. Hirsch EC, Hunot S, Hartmann A (2005) Neuroinflammatory processes in Parkinson's disease. *Parkinsonism Relat Disord* 11 Suppl 1: S9-S15.
 22. Huang Y, Erdmann N, Peng H, Zhao Y, Zheng J (2005) The role of TNF related apoptosis-inducing ligand in neurodegenerative diseases. *Cell Mol Immunol* 2: 113-122.
 23. Huber JD, Egleton RD, Davis TP (2001) Molecular physiology and pathophysiology of tight junctions in the blood-brain barrier. *Trends Neurosci* 24: 719-725.
 24. John GR, Lee SC, Brosnan CF (2003) Cytokines: powerful regulators of glial cell activation. *Neuroscientist* 9: 10-22.

25. Kapadia SE, de Lanerolle NC (1984) Immunohistochemical and electron microscopic demonstration of vascular innervation in the mammalian brainstem. *Brain Res* 292: 33-39.
26. Kniesel U, Wolburg H (2000) Tight junctions of the blood-brain barrier. *Cell Mol Neurobiol* 20: 57-76.
27. Kobayashi I, Osawa M, Ohta K, Maruyama S (1985) L-dopa-induced asterixis. *Folia Psychiatr Neurol Jpn* 39: 507-513.
28. Konsman JP, Vignes S, Mackerlova L, Bristow A, Blomqvist A (2004) Rat brain vascular distribution of interleukin-1 type-1 receptor immunoreactivity: relationship to patterns of inducible cyclooxygenase expression by peripheral inflammatory stimuli. *J Comp Neurol* 472: 113-129.
29. Kortekaas R, Leenders KL, van Oostrom JC, Vaalburg W, Bart J, Willemsen AT, Hendrikse NH (2005) Blood-brain barrier dysfunction in parkinsonian midbrain in vivo. *Ann Neurol* 57: 176-179.
30. Kurkowska-Jastrzebska I, Wronska A, Kohutnicka M, Czlonkowski A, Czlonkowska A (1999) The inflammatory reaction following 1-methyl-4-phenyl-1,2,3, 6-tetrahydropyridine intoxication in mouse. *Exp Neurol* 156: 50-61.
31. Ladeby R, Wirenfeldt M, Garcia-Ovejero D, Fenger C, Dissing-Olesen L, Dalmau I, Finsen B (2005) Microglial cell population dynamics in the injured adult central nervous system. *Brain Res Brain Res Rev* 48: 196-206.
32. Laflamme N, Lacroix S, Rivest S (1999) An essential role of interleukin-1 β in mediating NF- κ B activity and COX-2 transcription in cells of the blood-brain barrier in response to a systemic and localized inflammation but not during endotoxemia. *J Neurosci* 19: 10923-10930.
33. Lai AY, Todd KG (2006) Microglia in cerebral ischemia: molecular actions and interactions. *Can J Physiol Pharmacol* 84: 49-59.
34. Leng A, Mura A, Feldon J, Ferger B (2005) Tumor necrosis factor- α receptor ablation in a chronic MPTP mouse model of Parkinson's disease. *Neurosci Lett* 375: 107-111.
35. Ling Z, Chang QA, Tong CW, Leurgans SE, Lipton JW, Carvey PM (2004) Rotenone potentiates dopamine neuron loss in animals exposed to lipopolysaccharide prenatally. *Exp Neurol* 190: 373-383.
36. Lynch NJ, Willis CL, Nolan CC, Roscher S, Fowler MJ, Weihe E, Ray DE, Schwaebler WJ (2004) Microglial activation and increased synthesis of complement component C1q precedes blood-brain barrier dysfunction in rats. *Mol Immunol* 40: 709-716.

37. Mankertz J, Tavalali S, Schmitz H, Mankertz A, Riecken EO, Fromm M, Schulzke JD (2000) Expression from the human occludin promoter is affected by tumor necrosis factor alpha and interferon gamma. *J Cell Sci* 113 (Pt 11): 2085-2090.
38. McGeer PL, McGeer EG (2004) Inflammation and neurodegeneration in Parkinson's disease. *Parkinsonism Relat Disord* 10 Suppl 1: S3-S7.
39. Mennicken F, Maki R, de Souza EB, Quirion R (1999) Chemokines and chemokine receptors in the CNS: a possible role in neuroinflammation and patterning. *Trends Pharmacol Sci* 20: 73-78.
40. Miller F, Fenart L, Landry V, Coisne C, Cecchelli R, Dehouck MP, Buee-Scherrer V (2005) The MAP kinase pathway mediates transcytosis induced by TNF-alpha in an in vitro blood-brain barrier model. *Eur J Neurosci* 22: 835-844.
41. Nadjar A, Bluth RM, May MJ, Dantzer R, Parnet P (2005) Inactivation of the cerebral NFkappaB pathway inhibits interleukin-1beta-induced sickness behavior and c-Fos expression in various brain nuclei. *Neuropsychopharmacology* 30: 1492-1499.
42. Nagatsu T, Mogi M, Ichinose H, Togari A (2000) Cytokines in Parkinson's disease. *J Neural Transm Suppl* 143-151.
43. Nagatsu T, Sawada M (2005) Inflammatory process in Parkinson's disease: role for cytokines. *Curr Pharm Des* 11: 999-1016.
44. O'callaghan JP, Miller DB, Reinhard JF, Jr. (1990) Characterization of the origins of astrocyte response to injury using the dopaminergic neurotoxicant, 1-methyl-4-phenyl-1,2,3,6-tetrahydropyridine. *Brain Res* 521: 73-80.
45. Orr CF, Rowe DB, Halliday GM (2002) An inflammatory review of Parkinson's disease. *Prog Neurobiol* 68: 325-340.
46. Ozaki H, Ishii K, Horiuchi H, Arai H, Kawamoto T, Okawa K, Iwamatsu A, Kita T (1999) Cutting edge: combined treatment of TNF-alpha and IFN-gamma causes redistribution of junctional adhesion molecule in human endothelial cells. *J Immunol* 163: 553-557.
47. Petrache I, Crow MT, Neuss M, Garcia JG (2003) Central involvement of Rho family GTPases in TNF-alpha-mediated bovine pulmonary endothelial cell apoptosis. *Biochem Biophys Res Commun* 306: 244-249.
48. Phillis JW, Horrocks LA, Farooqui AA (2006) Cyclooxygenases, lipoxygenases, and epoxigenases in CNS: Their role and involvement in neurological disorders. *Brain Res Brain Res Rev* 52: 201-243.
49. Przedborski S, Jackson-Lewis V, Naini AB, Jakowec M, Petzinger G, Miller R, Akram M (2001) The parkinsonian toxin 1-methyl-4-phenyl-1,2,3,6-

tetrahydropyridine (MPTP): a technical review of its utility and safety. *J Neurochem* 76: 1265-1274.

50. Raichle ME, Hartman BK, Eichling JO, Sharpe LG (1975) Central noradrenergic regulation of cerebral blood flow and vascular permeability. *Proc Natl Acad Sci U S A* 72: 3726-3730.
51. Rennels ML, Nelson E (1975) Capillary innervation in the mammalian central nervous system: an electron microscopic demonstration. *Am J Anat* 144: 233-241.
52. Rousselet E, Callebert J, Parain K, Joubert C, Hunot S, Hartmann A, Jacque C, Perez-Diaz F, Cohen-Salmon C, Launay JM, Hirsch EC (2002) Role of TNF-alpha receptors in mice intoxicated with the parkinsonian toxin MPTP. *Exp Neurol* 177: 183-192.
53. Ryu JK, McLarnon JG (2006) Minocycline or iNOS inhibition block 3-nitrotyrosine increases and blood-brain barrier leakiness in amyloid beta-peptide-injected rat hippocampus. *Exp Neurol* 198: 552-557.
54. Sugama S, Yang L, Cho BP, DeGiorgio LA, Lorenzl S, Albers DS, Beal MF, Volpe BT, Joh TH (2003) Age-related microglial activation in 1-methyl-4-phenyl-1,2,3,6-tetrahydropyridine (MPTP)-induced dopaminergic neurodegeneration in C57BL/6 mice. *Brain Res* 964: 288-294.
55. Tikka TM, Koistinaho JE (2001) Minocycline provides neuroprotection against N-methyl-D-aspartate neurotoxicity by inhibiting microglia. *J Immunol* 166: 7527-7533.
56. Tsao N, Hsu HP, Wu CM, Liu CC, Lei HY (2001) Tumour necrosis factor-alpha causes an increase in blood-brain barrier permeability during sepsis. *J Med Microbiol* 50: 812-821.
57. Vu TQ, Ling ZD, Ma SY, Robie HC, Tong CW, Chen EY, Lipton JW, Carvey PM (2000) Pramipexole attenuates the dopaminergic cell loss induced by intraventricular 6-hydroxydopamine. *J Neural Transm* 107: 159-176.
58. Wakayama K, Ohtsuki S, Takanaga H, Hosoya K, Terasaki T (2002) Localization of norepinephrine and serotonin transporter in mouse brain capillary endothelial cells. *Neurosci Res* 44: 173-180.
59. Wong D, Dorovini-Zis K, Vincent SR (2004) Cytokines, nitric oxide, and cGMP modulate the permeability of an in vitro model of the human blood-brain barrier. *Exp Neurol* 190: 446-455.
60. Wu DC, Jackson-Lewis V, Vila M, Tieu K, Teismann P, Vadseth C, Choi DK, Ischiropoulos H, Przedborski S (2002) Blockade of microglial activation is neuroprotective in the 1-methyl-4-phenyl-1,2,3,6-tetrahydropyridine mouse model of Parkinson disease. *J Neurosci* 22: 1763-1771.

61. Yenari MA, Xu L, Tang XN, Qiao Y, Giffard RG (2006) Microglia potentiate damage to blood-brain barrier constituents: improvement by minocycline in vivo and in vitro. *Stroke* 37: 1087-1093.
62. Zemke D, Majid A (2004) The potential of minocycline for neuroprotection in human neurologic disease. *Clin Neuropharmacol* 27: 293-298.